Plasmodium vivax naturally acquired immunity: patterns and influences

Zoe Shih-Jung Liu
ORCID: 0000-0002-0269-0119

Submitted in total fulfilment of the requirements of the degree of
Doctor of Philosophy

August 2020

The Walter and Eliza Hall Institute of Medical Research
Department of Medical Biology
Faculty of Medicine, Dentistry and Health Sciences
University of Melbourne

Abstract

Malaria is caused by *Plasmodium* parasites and *Plasmodium vivax* is the dominant *Plasmodium* spp. in low-transmission regions outside of Africa. Due to the unique biological characteristics of this parasite, such regions often feature asymptomatic patients with sub-microscopic parasitaemia and relapses. Naturally acquired antibody responses are induced after *Plasmodium* infection, providing partial protection against high parasitaemia and clinical episodes. Serology is a promising tool for monitoring transmission levels, estimating past and recent exposure and identifying populations at risk of infections. However, due to key gaps in our knowledge of naturally acquired antibody responses to *P. vivax*, the full potential of serology has not yet been reached. This thesis aimed to establish antibody kinetics against a large panel of *P. vivax* antigens following infections in western Thailand, and investigate the factors potentially associated with the acquisition and development of antibody responses. A multiplexed bead-based assay was first established and antibody measurements against more than 50 antigens were taken in *P. vivax*-infected individuals from western Thailand following symptomatic and asymptomatic infections. I found that most *P. vivax* antigens followed a highly similar post-infection kinetic pattern in the absence of any boosting infections. The magnitude and longevity of antibody responses varied between antigens, antibody subclasses and subtypes. An assay quantifying the antigen-specific memory B cell responses was established and verified to determine the role of memory B cells on antibody kinetics for future experiments. Lastly, I reported that the genetic diversity of an antigen sequence had a significant impact on antigen-specific antibody responses, and such impact increased in individuals with more past exposure and mature immunity. The findings presented in this thesis provide novel insights into naturally acquired immunity development to *P. vivax* and support the decision of taking genetic diversity of antigen sequences into consideration for the development of highly efficacious sero-surveillance tools and vaccines.

Declaration

This is to certify that:

i) this thesis comprises only my original work towards the degree of Doctor of Philosophy, except where indicated in the Preface;

ii) due acknowledgement has been made in the text to all other material used;

iii) this thesis is fewer than 100,000 words in length, exclusive of tables, figures, bibliographies and appendices.

Zoe Shih-Jung Liu

08/08/2020

Preface

The work presented in this thesis was undertaken in Prof Ivo Mueller's laboratory at the Walter and Eliza Hall Institute of Medical Research (WEHI) between June 2016 and September 2019. This PhD project was co-supervised by Dr Rhea Longley.

During my PhD, I was supported by the Melbourne Research Scholarship through the Department of Medical Biology, Faculty of Medicine, Dentistry and Health Sciences at the University of Melbourne. I have also received financial support from the Australian Society for Parasitology Student Conference Travel Grant, the Australian Centre for Research Excellence in Malaria Elimination Travel Awards and the 7th International Conference on *Plasmodium vivax* Research Travel Grant. This study was also funded in part by National Health and Medical Research Council grant ((#1092789 and #1134989), National Institute of Health grant 5R01 AI 104822), Global Health Innovative Technology Fund (T2015-142) and Foundation for Innovative New Diagnostics grant through funding from the Australian and British governments.

The plasma and PBMC samples from western Thailand and Bangkok were collected by the Mahidol Vivax Research Unit (MVRU) at the Mahidol University in Bangkok, Thailand, and the WEHI, led by Dr Jetsumon

Sattabongkot. The plasma samples from Manaus, Brazil, were provided by Prof Marcus Lacerda from the Fundação de Medicina Tropical Doutor Heitor Vieira Dourado. The Papua New Guinea (PNG) hyperimmune pool plasma was provided by Prof Christopher King at Case Western Reserve University in Cleveland, USA, and the PNG Institute of Medical Research.

The wheat-germ cell-free expressed *P. vivax* antigens used in this thesis were expressed in the laboratories of Prof Takafumi Tsuboi and A/Prof Eizo Takashima at Proteo-Science Centre at the Ehime University and Dr Matthias Harbers at CellFree Sciences Co., Ltd. Additional *P. vivax* antigens were provided by Prof Alan Cowman, Dr Julie Healer, A/Prof Wai-Hong Tham, Dr Jakub Gruszczyk at WEHI and Prof Chetan Chitnis at the Institut Pasteur in Paris, France.

The mathematical model (described in Chapters 2 and 4) was developed by Dr Michael White at the Institut Pasteur. The R script used to convert Luminex® raw data into standardised units (described in Chapter 2) was written by Dr Connie SN Li Wai Suen at WEHI.

The R package used to generate the population genetic parameters from isolate amino acid sequences were developed by Elijah Martin and Myo Naung in A/Prof Alyssa Barry's laboratory at WEHI.

The work presented in Chapter 5 was co-supervised by Dr Lisa Ioannidis in the laboratory of Dr Diana Hansen at WEHI, who provided training on the assay and reagents required, intellectual input into experimental designs and assisted with reviewing the chapter draft. The work shown in Chapter 6 was co-supervised by A/Prof Alyssa Barry at WEHI who introduced the techniques, provided guidance in interpretation of the results and direction of the study and assisted with reviewing the chapter draft.

Acknowledgements

This work would not have been possible with the help from the following people.

I am truly grateful for my PhD supervisors Prof Ivo Mueller and Dr Rhea Longley for their support, critique and trust along the way. It has been an absolute pleasure to learn from them and their passion for science and life. I would also like to thank my advisory committee members – Prof Phil Hodgkin, Dr Diana Hansen and Prof James Beeson – for their insights, constant support and advice.

Enormous thanks to the Mueller Lab past and present. For more than 3.5 years, you have successfully kept me fed, sane and alive. I am forever indebted for your generosity and tolerance.

Thank you to the Population Health & Immunity and the Infection & Immunity Divisions and the malaria community. This journey would not have been the same without every single one of you. Thank you for your friendship and support.

To my beloved family – thank you for your unconditional love, support and tolerance even from 7,400 km away. Finally, thank you Roth for going through this journey with me.

Table of Contents

Abstract ii

Declaration iii

Preface iv

Acknowledgements vii

List of Figures xii

List of Tables xvi

List of Abbreviations xvii

Chapter 1. Introduction 20

1.1 Malaria 21
1.1.1 Epidemiology and clinical features 21
1.1.2 *Plasmodium* life cycle 22
1.1.3 The emerging threat – *P. vivax* 27
1.1.4 Unique biological features of *P. vivax* 30
1.1.5 Current strategies for prevention and treatment 35

1.2 Immune responses against malaria 43
1.2.1 Innate Immunity 44
1.2.2 Adaptive Immunity 48

1.3 Factors affecting immunity in human 65
1.3.1 Intrinsic host and demographic factors 66
1.3.2 Environmental factors 70
1.3.3 Antigenic factors 71

1.4 Thesis aims 76

Chapter 2. Materials & Methods 78

2.1 Study populations 79
2.1.1 Thai symptomatic cohort 80
2.1.2 Brazilian symptomatic cohort 81
2.1.3 Thai asymptomatic cohort 81
2.1.4 Negative control panels 84

2.2 PBMC isolation 85

2.3 P. vivax antigen selection and expression 86
2.3.1 Antigen panel 86
2.3.2 Antigen down-selection following antigen discovery study using AlphaScreen® 91
2.3.3 Serological marker targets – protein expression and purification 92
2.3.4 Traditional vaccine targets – protein expression and purification 92

2.4 Antigen conjugation to microspheres *93*
2.4.1 Optimisation 93
2.4.2 Conjugation 94

2.5 Antibody measurement on the Luminex® platform *95*
2.5.1 Total IgG 98
2.5.2 IgM 99
2.5.3 IgG subclasses 99
2.5.4 Unit conversion 100

2.6 Antibody kinetics model *100*
2.6.1 Fitting the model to data 101
2.6.2 Model likelihood 104
2.6.3 Mixed effects likelihood 104
2.6.5 Markov Chain Monte Carlo parameter update 106

2.7 Antigen features – data collection *106*

2.8 Memory B cell ELISpot assay *107*
2.8.1 PBMC re-stimulation 107
2.8.2 Detection of ASC populations 108
2.8.3 Data processing 111

2.9 Population structure of P. vivax antigens *114*
2.9.1 Data collection 114
2.9.2 Population genetics 117

2.10 Statistical analyses *117*

Chapter 3. Establishment and validation of a multiplexed bead-based assay for antibody measurements 118

3.1 Introduction *119*

3.2 Results *123*
3.2.1 Optimisation of *P. vivax* protein amounts for the multiplexed bead-based assay 123
3.2.2 Stability of antigen-conjugated microspheres 131
3.2.3 Validation of alternative incubation condition 135
3.2.4 Reproducibility of the multiplexed bead-based assay 137
3.2.5 Determination of the optimal plasma dilution for the multiplexed bead-based assay 140
3.2.6 Optimisation of the multiplexed bead-based assay for IgM measurements 145
3.2.7 Comparison of IgG responses measured on AlphaScreen® and Luminex® platforms 149

3.3 Discussion *153*

Chapter 4. Determination of antibody kinetic profiles following *P. vivax* infections in Thailand and Brazil 159

4.1 Introduction *160*

4.2 Results *162*
4.2.1 Total IgG longevity following a symptomatic *P. vivax* infection in Thai individuals 162
4.2.2 Evaluation of association between antigenic features and total IgG longevity 175

4.2.3 Association between IgG subclass dominance and IgM immunogenicity with total IgG longevity ... 181
4.2.4 Association between IgM and total IgG kinetic profiles ... 190
4.2.5 Total IgG longevity following an asymptomatic *P. vivax* infection ... 194
4.2.6 Additional results: attempt to establish total IgG kinetics in Brazilian patients ... 198

4.3 Discussion ... *213*

Chapter 5. Establishment of an ELISpot assay for protein-specific memory B cell measurements ... 222

5.1 Introduction ... *223*

5.2 Results ... *228*
5.2.1 Sample recovery rate and the proportion of viable cells remaining ... 228
5.2.2 Optimisation of re-stimulation duration for Thai PBMCs ... 233
5.2.3 Optimisation of antigen concentrations for antigen-specific IgG^+ ASC responses 236
5.2.4 Optimisation of cell concentrations for antigen-specific IgG^+ ASC responses ... 244

5.3 Discussion ... *249*

Chapter 6. Evaluation of the impact of antigen sequence diversity on antibody profiles ... 254

6.1 Introduction ... *255*

6.2 Results ... *260*
6.2.1 Summary statistics of population genetic parameters ... 260
6.2.2 Impact of protein sequence diversity on total IgG and IgG subclass profiles in a symptomatic cohort ... 267
6.2.3 Impact of protein sequence diversity on IgM profile in a symptomatic cohort ... 275
6.2.4 Impact of protein sequence diversity on IgG profile in an asymptomatic cohort ... 282

6.3 Discussion ... *287*

Chapter 7. General discussion and perspectives ... 295

7.1 Overview ... *296*

7.2 Establishment of P. vivax-specific antibody kinetic profiles and MBC ELISpot assay ... *300*
7.2.1 Summary of findings ... 300
7.2.2 Study significance ... 301

7.3 Population genetic analysis on P. vivax antigens and their associations with antibody profiles ... *303*
7.3.1 Summary of findings ... 303
7.3.2 Study significance ... 304

7.4 Future directions ... *306*
7.4.1 Further defining antibody profiles in the asymptomatic Thai cohort ... 306
7.4.2 Determining the role of antigen-specific MBCs in antibody longevity ... 307
7.4.3 Assessing the association of genetic diversity with quantitative measures of antibody responses and further analyses with populations from higher transmission settings ... 308
7.4.4 Examining the association of protein structure with antigen-specific antibody responses ... 310

7.5 Concluding remarks ... *310*

References **312**

List of Figures

Figure 1.1 *Plasmodium* spp. life cycle. 26

Figure 1.2 Estimated number of *P. vivax* clinical cases from 2005 – 2017. 28

Figure 1.3 Development of humoral immunity.. 55

Figure 1.4 Types of antibody molecules. 59

Figure 2.1 Schematic illustration of the Luminex® technology. 97

Figure 2.2 Schematic representation of the relationship between the population-level and individual-level parameters for the half-life of the short-lived ASCs.. 103

Figure 2.3 Detection of IgG-producing ASC on ELISpot. 109

Figure 2.4 Process of population genetic analysis.....116

Figure 3.1 Change in results of standard curve tests against 53 *P. vivax* antigens during and after optimisation. 127

Figure 3.2 Attempts to optimise *P. vivax* antigen PVX_002550.. 128

Figure 3.3 Examples of SDS-PAGE gels for *P. vivax* antigen production by the CFS company. 129

Figure 3.4 Standard curve tests for 52 *P. vivax* antigens.. 133

Figure 3.5 Comparison of standard curves between different incubation conditions. 136

Figure 3.6 Correlation between duplicates per *P. vivax* antigen in 34 Thai symptomatic patients. 139

Figure 3.7 Examples of 'max-out' total IgG antibody responses at early time points of *P. vivax* infection in 34 symptomatic Thai individuals.. 141

Figure 3.8 Comparison of total IgG antibody responses against three *P. vivax* antigens in differentially diluted samples from 33 Brazilian symptomatic patients. 144

Figure 3.9 Comparison of performance between anti-human IgM secondary antibodies from two different manufacturers.. 148
Figure 3.10 Correlation of detected IgG responses between AlphaScreen® and Luminex® platforms. 152
Figure 4.1 Total IgG kinetic profiles against 52 *P. vivax* antigens in the Thai symptomatic cohort.....166
Figure 4.2 Total IgG kinetic profiles at an individual level following symptomatic infections.. 167
Figure 4.3 Relationship between modelled antibody decay rate and the assigned IgG longevity category. 174
Figure 4.4 Adjusted IgG subclass and total IgG kinetics in the Thai symptomatic cohort.....186
Figure 4.5 Comparison of the adjusted peak IgG subclass magnitude between the Thai symptomatic cohort and the PNG hyperimmune pool. 187
Figure 4.6 Comparison of the peak IgM magnitude between the Thai symptomatic cohort and malaria-free individuals. 189
Figure 4.7 Adjusted total IgG and IgM kinetics against *P. vivax* antigens in the Thai symptomatic cohort. 192
Figure 4.8 Unadjusted IgM kinetics against *P. vivax* antigens in the Thai symptomatic cohort.....193
Figure 4.9 Total IgG kinetics and longevity against 27 *P. vivax* antigens in the Thai asymptomatic cohort.....197
Figure 4.10 Total IgG kinetics against 24 *P. vivax* antigens in the Brazilian symptomatic cohort.....200
Figure 4.11 Standard curve tests for 24 *P. vivax* antigens in the Brazilian symptomatic cohort.....202
Figure 4.12 Total IgG kinetics for the Brazilian symptomatic cohort in MFI. 203

Figure 4.13 Correlation between duplicates per *P. vivax* antigen in the Brazilian symptomatic cohort. 205
Figure 4.14 Correlation of data from original and repeated IgG responses...206
Figure 4.15 Antigen-specific IgG responses and timing of potential missed infections in 33 Brazilian symptomatic individuals. 211
Figure 5.1 Percentage of PBMCs recovered after cryopreservation. 229
Figure 5.2 Effect of the re-stimulation cocktail on cell numbers.....232
Figure 5.3 Effect of the re-stimulation duration on retention of viable cells and ASC differentiation from Thai PBMCs. 235
Figure 5.4 Total IgG kinetic profiles against two *P. vivax* antigens in 34 Thai patients with symptomatic *P. vivax* infections.....238
Figure 5.5 Validation of total IgG^+ ASCs responses in four samples used for optimisation of antigen concentration. 240
Figure 5.6 Frequency of antigen-specific ASCs against three antigens at different concentrations. 243
Figure 5.7 Frequency of antigen-specific ASCs against two *P. vivax* antigens with different cell concentrations.....248
Figure 6.1 Frequency distribution of different population genetic parameters amongst the 49 candidate *P. vivax* sero-surveillance antigens.. 266
Figure 6.2 Correlations between protein sequence diversity and total IgG response in a symptomatic Thai cohort. 270
Figure 6.3 Distribution of data for population genetic parameters per IgG subclass category.. 273
Figure 6.4 Distribution of population genetic parameters per IgM immunogenicity category. 277
Figure 6.5 Heatmap for correlations between protein sequence diversity and IgM response in the symptomatic Thai cohort. 279

Figure 6.6 Significant correlations between population genetics and IgM parameters in the symptomatic Thai cohort. 281
Figure 6.7 Heatmap for correlations between protein sequence diversity and total IgG response in the asymptomatic Thai cohort. 284
Figure 6.8 Significant correlations between haplotype diversity, balancing selection and total IgG response variation in the asymptomatic Thai cohort. 286

List of Tables

Table 2.1 Demographic characteristics of the three study populations.....83

Table 2.2 Information on the 52 *P. vivax* antigens selected for this study.....88

Table 2.3 Calculation for the average number of ASCs per 10^6 PBMCs from the anti-IgG positive control. 113

Table 2.4. Standardisation for the number of antigen-specific ASCs per 10^6 PBMCs from antigen-coated wells. 113

Table 4.1 Relative IgG immunogenicity against 52 *P. vivax* antigens in the Thai symptomatic cohort.....168

Table 4.2 Antigenic features of the 52 *P. vivax* antigens selected for this study. 176

Table 4.3 Effects of antigen features on total IgG immunogenicity and longevity categorisations.. 179

Table 4.4 Effects of the increasing number of enzyme domains and LCRs on antibody profile categorisation.. 180

Table 4.5 IgG subclass categories and IgM positivity for IgG immunogenic antigens 1-2 weeks post-infection in the Thai symptomatic cohort. 184

Table 4.6 Distribution and parasite density of the 22 qPCR-positive individuals in the symptomatic Brazilian cohort.....209

Table 5.1 Cell concentrations tested in each Thai PBMC sample for optimisation 246

Table 6.1 Definition and general interpretation of population genetics parameters.....259

Table 6.2 Estimates of genetic diversity in *P. vivax* isolates (n=19) from Thailand for 49 candidate sero-surveillance antigens. 263

List of Abbreviations

ADCC	Antibody-dependent cellular cytotoxicity
AMA1	Apical membrane antigen 1
APC	Antigen-presenting cell
ARC	Australian Red Cross
ASC	Antibody-secreting cell
BCR	B cell receptor
BSA	Bovine serum antigen
CCS	Cosmic calf serum
cDC	Conventional dendritic cell
CFS	CellFree Sciences Co. Ltd.
CpG ODN	CpG oligodeoxynucleotide
CQ	Chloroquine
CyRPA	Cysteine rich protective antigen
D	Tajima's D
DARC	Duffy antigen receptor for chemokine
D-PBS	Dulbecco's phosphate-buffered saline
DBP	Duffy binding proteins
DC	Dendritic cell
E. coli	*Escherichia coli*
EBP	Erythrocyte binding protein
EGF	Epidermal growth factor
ELISA	Enzyme-linked immunosorbent assay
ELISpot	Enzyme-linked immunospot
G6PD	Glucose-6-phosphate dehydrogenase
GAMA	Glycosylphosphatidylinositol-anchored micronemal antigen
GC	Germinal centre
GPI	Glycosylphosphatidylinositol
h	Number of haplotypes
Hd	Haplotype diversity
H_E	Heterozygosity
HI-FCS	Heat-inactivated foetal calf serum
HREC	Human Research Ethics Committee
IFN	Interferon
Ig	Immunoglobulin
IL	Interleukin
InDels	Insertions and deletions
iRBC	Infected red blood cell
IRS	Indoor residual spraying

ITN	Insecticide-treated bed nets
JIR	Jackson ImmunoResearch
LCR	Low-complexity region
LLIN	Long lasting insecticidal nets
MBC	Memory B cell
MCMC	Markov Chain Monte Carlo
MDA	Mass drug administration
MFI	Median fluorescence intensity
MHC	Major histocompatibility complex
MSAT	Mass screening and treatment
MSP	Merozoite surface protein
MSP1	Merozoite surface protein 1
msp3	Merozoite surface protein 3 gene
msp7	Merozoite surface protein 7 gene
NK	Natural Killer
NS (SNP)	Non-synonymous single nucleotide polymorphism
PAMP	Pathogen associated molecule pattern
PBMC	Peripheral blood mononuclear cell
PBS	Phosphate-buffered saline
PC	Plasma cell
PCR	Polymerase chain reaction
pDC	Plasmacytoid dendritic cell
PE	Phycoerythrin
PEXEL	*Plasmodium*-exported element
PNEL	PEXEL-negative exported protein
PNG	Papua New Guinea
PQ	Primaquine
PRR	Pattern recognition receptor
pvrbp	*P. vivax* reticulocyte binding protein gene
PWM	Pokeweed mitogen
RACD	Reactive case detection
RAU	Relative antibody unit
RBC	Red blood cell
RBP	Reticulocyte binding proteins
Ripr	Rh5 interacting protein, putative
ROS	Reactive oxidative species
Rs	Allelic richness
S	Segregating site
SA-ALP	Streptavidin-alkaline phosphatase
SB	Southern Biotech
SD	Standard deviation
SNP	Single nucelotide polymorphism

SP	Signal peptide
SP (SNP)	Synonymous single nucleotide polymorphism
TCR	T cell receptor
T_{FH}	Follicular T helper cell
TLR	Toll-like receptor
TMD	Transmembrane domain
TRAP	Thromospondin-related adhesive protein
TRC	Thai Red Cross
T_{REG}	Regulatory T cell
TT	Tetanus toxoid
VBDR	Volunteer Blood Donor Registry
vir	Virulence genes of *P. vivax*
WEHI	Walter and Eliza Hall Institute of Medical Research
WGCF	Wheat germ cell free
WHO	World Health Organisation
π	Nucleotide diversity

Chapter 1. Introduction

1.1 Malaria

1.1.1 Epidemiology and clinical features

Malaria is an infectious disease caused by parasitic protozoan under the genus of *Plasmodium*. The parasites are transmitted between mosquito vectors and human hosts. There are six *Plasmodium* species – including two sub-species – that can infect humans and cause morbidity or even mortality: *Plasmodium falciparum*, *Plasmodium vivax*, *Plasmodium knowlesi*, *Plasmodium malariae*, *Plasmodium ovale curtisi* and *Plasmodium ovale wallikeri*. Of the *Plasmodium* parasites that infect humans, *P. falciparum* and *P. vivax* are the most prevalent and are responsible for the majority of the morbidity and mortality worldwide [1]. In the year 2018, more than 225 million people were infected with malaria and up to 400,000 people died, most of whom were children under 5 years of age [2].

As one of the acute febrile illnesses, malaria can cause clinical symptoms of varying severity, including high fever, headache, vomiting, breathing difficulty and even death [3]. These symptoms are caused by the blood stage of the infection [4, 5]. For instance, adherence of *Plasmodium* infected red blood cells (iRBCs) to the lining of endothelium (termed as sequestration) leads to microvascular obstruction and hence respiratory distress [6]. Deformity and loss of function in the iRBCs can also lead to anaemia [7]. Other factors associated

with malaria clinical manifestation include parasitaemia, antigenic polymorphisms and antigenic variation [8, 9]. Current evidence shows few clinical differences between *P. falciparum* and *P. vivax* infections [10-13]. This suggests the mechanisms regulating clinical tolerance against various *Plasmodium* species in humans might be similar [13]. Additionally, malaria can be acquired during pregnancy, contributing to severe intrauterine growth restriction, low birth weight and chronic malnutrition in the foetus [14-16]. These symptoms and complications have been reported to link to sequestration of iRBCs on the placenta, also known as placental malaria [9]. Overall, it has been shown that the intensity of malaria transmission is linked to slower population and economic growth, severely damaging the development of a country [17].

1.1.2 *Plasmodium* life cycle

Plasmodium parasites are transmitted between human hosts and insect vectors, specifically female *Anopheles* mosquitoes. This results in a complex life-cycle with stages in both the hosts and vectors. An overview of the *Plasmodium* life cycle is outlined below.

Pre-erythrocytic stage: The parasites in the form of sporozoites are injected into the human host through a blood meal taken by an infected vector (Figure 1.1). The total number of sporozoites injected via a single mosquito bite is highly variable in mice, ranging from zero to more than 1000 (mean = 123, median = 18) [18]. The sporozoites travel through the blood stream and quickly arrive at the liver within an hour after injection, after which the sporozoites invade hepatocytes [19]. Some sporozoites undergo a maturation process in the liver and develop into schizonts. Mature schizonts rupture and release merozoites from the hepatocytes into the blood circulation approximately one week since the initial infection [19]. This marks the end of the pre-erythrocytic or liver stage and the start of the erythrocytic stage of a malaria infection. The pre-erythrocytic stage in the human host is asymptomatic. *P. vivax* is characterised by the formation of hypnozoites, a quiescent form of the parasite that resides in the hepatocyte [20]. This unique feature contributes to several challenges to *P. vivax* elimination and is further discussed in Section 1.1.4.1.

Erythrocytic stage: The blood stage of *Plasmodium* parasites is similar across different species, and can be roughly divided into several asexual sub-stages based on the morphology of the parasite inside the invaded RBCs: ring stage, immature and mature trophozoites, schizonts, and merozoites released from the ruptured schizonts [21]. *P. vivax* has been known to preferably invade immature

RBCs, known as reticulocytes [22]. This observation is potentially due to the fact that reticulocytes produce unique metabolome that can be utilised for the development of the *Plasmodium* parasites [23]. The newly produced merozoites then invade uninfected RBCs, making the erythrocytic stage a cycle that aims to produce more merozoites [21]. It has been demonstrated *in vitro* that *P. falciparum* parasites produce approximately 15- 18 merozoites per mature schizont [24]. In humans, the number of *Plasmodium* parasites grows exponentially from 10^4 – 10^5 in the first cycle to up to 10^8 after 3 – 4 cycles [25]. It has been estimated that the duration of the erythrocytic stage, in the absence of treatment, varies between *Plasmodium* species in naturally infected human populations. The erythrocytic stage of *P. falciparum* has been predicted to last longer (36 – 135 days) than *P. vivax* (24 – 29 days) [26]. Most of the symptoms observed in *Plasmodium*-infected individuals are derived from this life stage due to destruction of RBCs and chronic inflammation [4].

Sexual and mosquito stages: While most merozoites infect red blood cells, some undergo a sexual cycle to form male and female gametocytes [27]. These gametocytes can be taken up by a mosquito upon another blood meal and subsequently complete the other half of their life cycle in the vector [27]. Within a vector, the gametocytes undergo further maturation and fertilisation to form zygotes [28]. Zygotes migrate towards the midgut of the vector and transform

into ookinetes which transverse the gut epithelial layers and enter the lumen [28]. Ookinetes that are successful in transversion and surviving the vector's protective immune mechanisms transform into oocysts [28]. Inside the lumen, oocysts continue to develop extracellularly until maturation and eventually rupture to release sporozoites [29]. Sporozoites travel to the salivary gland and are transmitted into another human host during the next blood meal [29].

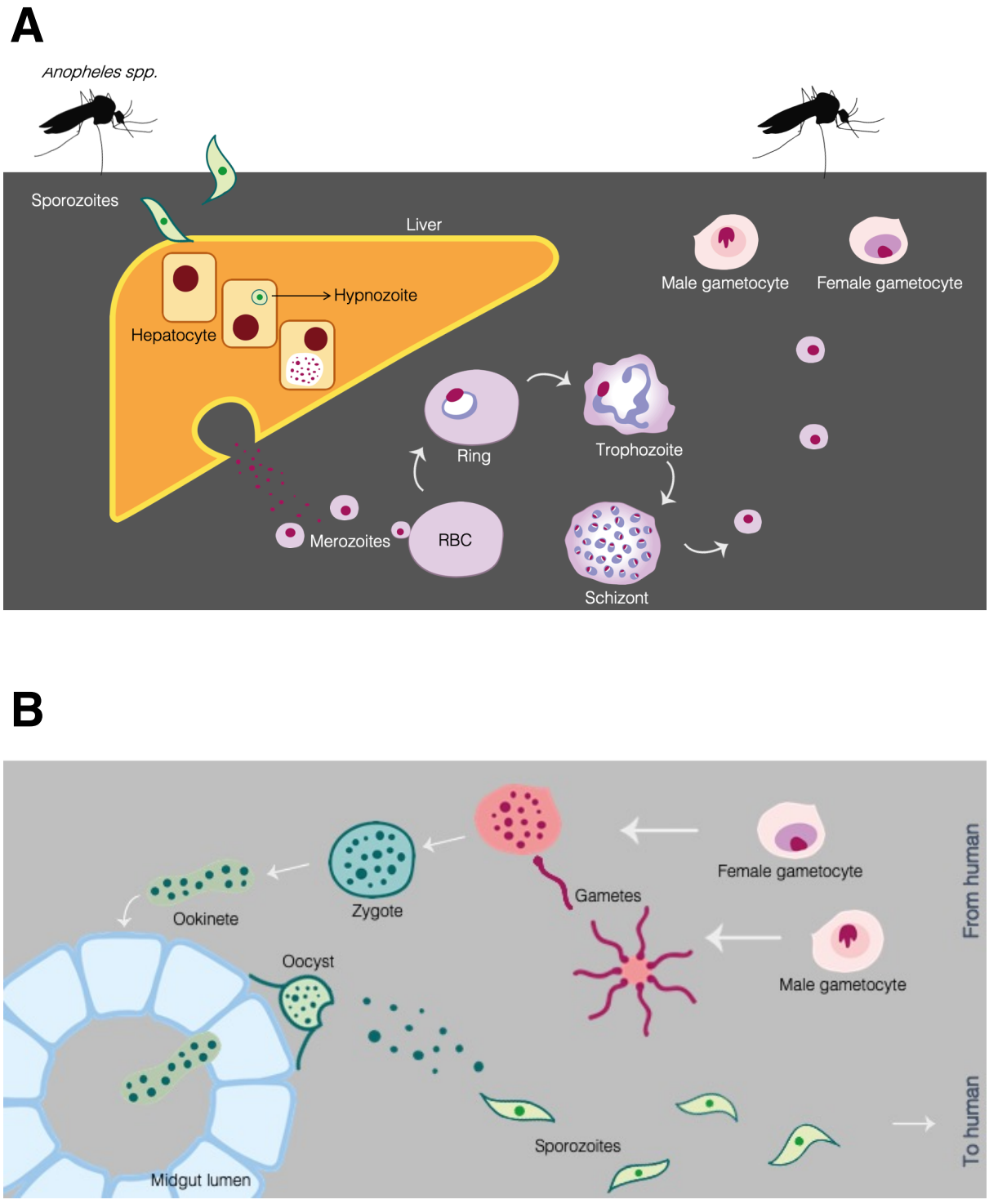


Figure 1.1 *Plasmodium* spp. life cycle. The *Plasmodium* parasites infect **A)** humans and **B)** female *Anopheles* mosquitoes as vectors, and undergo a complex process to achieve sexual development and robust transmission between hosts.

1.1.3 The emerging threat – *P. vivax*

Malaria is prevalent in 87 countries globally with a varying level of risk [1]. Approximately 80% of malaria deaths are found in the World Health Organisation (WHO) African region due to the high incidence and mortality rates caused by *P. falciparum* infections [1]. However, it has been shown that *P. vivax* is the most widely distributed *Plasmodium* spp. outside of sub-Saharan Africa and this species has put an estimated 2.5 billion people at risk of infection [30, 31]. Recently, Battle and colleagues published the change in global *P. vivax* endemicity between 2000 and 2017 [32]. As shown in Figure 1.2, it is clear that in most countries the estimated number of *P. vivax* clinical cases has reduced dramatically since the early 2000s. On the contrary, some countries such as Brazil, Afghanistan and Indonesia actually had significant increases in the estimated number of cases (Figure 1.2). Moreover, the authors reported an increase in the proportion of malaria cases due to *P. vivax* as the overall malaria incidence and transmission have declined [32]. Additionally, it has been demonstrated in Thailand and Solomon Islands that *P. vivax* has become the main source of malaria cases [33, 34]. These findings have highlighted the increasing significance of *P. vivax* as we progress towards elimination.

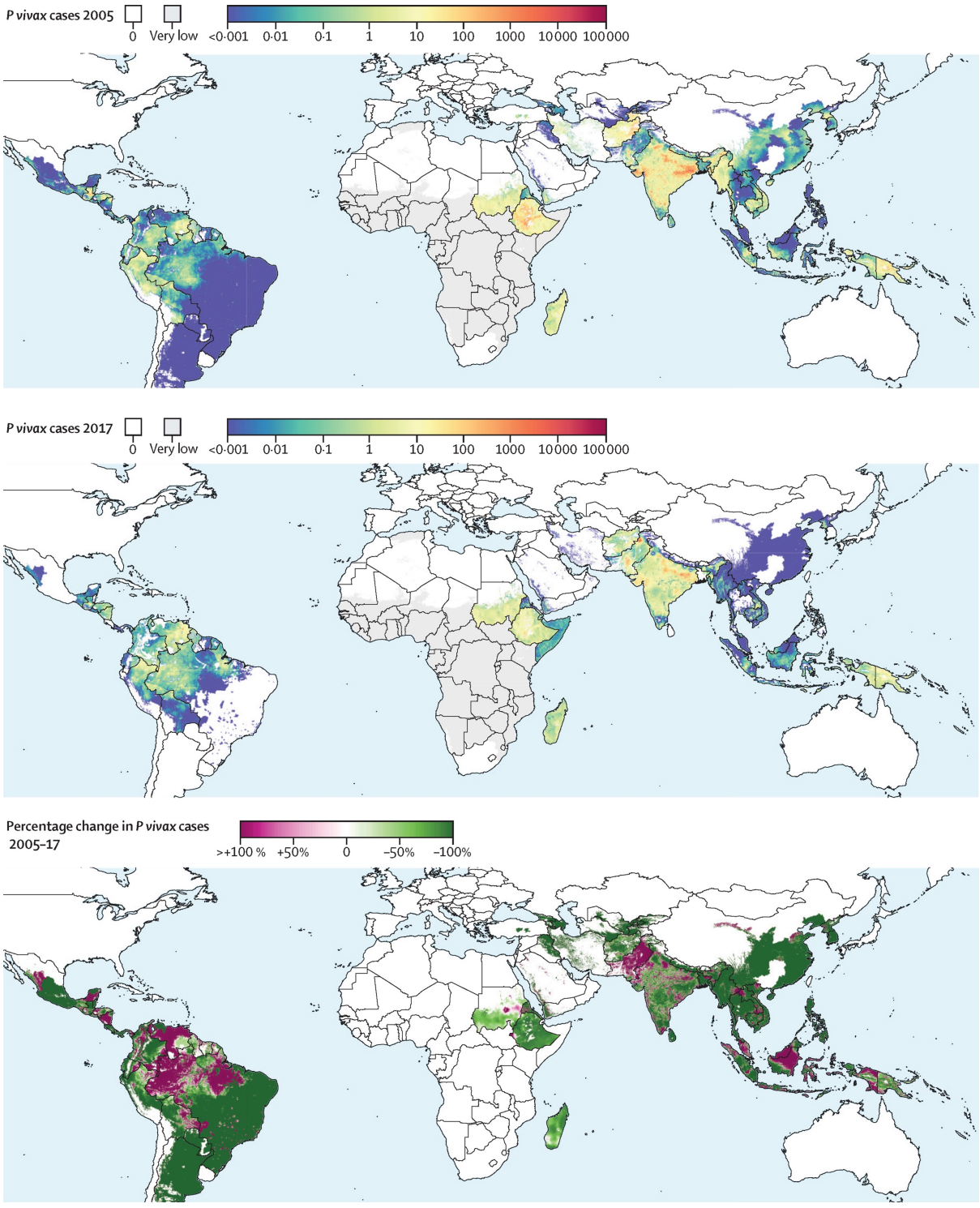


Figure 1.2 Estimated number of *P. vivax* clinical cases from 2005 – 2017. The top and middle panels show the global distribution and estimated number of *P. vivax* cases in the year 2005 and 2017, respectively. The bottom panel shows the change in the number of cases between the two time points: green corresponds to decrease and pink increase. Source: [32]

P. vivax has been long neglected compared to *P. falciparum* by both the healthcare and academic sectors and has come under the spotlight since the early 2000s [35-37]. This was likely due to the higher mortality rate associated with *P. falciparum* infections and the exceptionally large burden of disease in Africa [38, 39], however more recently the severe outcomes that can result from *P. vivax* infections have also been acknowledged [40]. Over the past 15 years there has been an increase in the number of research studies addressing the severe and fatal consequences of *P. vivax* infections [41].

Together, these findings suggest that both *P. falciparum* and *P. vivax* should be taken into consideration in order to advance our current malaria elimination effort. Setting such a goal means new strategies and tools will be required to fight against *P. vivax*, especially given that this *Plasmodium* species seems to be more resistant to existing control measures (indicated by the increasing proportion of infections due to *P. vivax* in co-endemic regions). In the Section below, I discuss the differences between *P. vivax* and other *Plasmodium* species and why it has become a challenge for effective malaria control.

1.1.4 Unique biological features of *P. vivax*

There are a number of distinct biological features of *P. vivax* compared to other *Plasmodium* species, many of which pose a great difficulty for malaria elimination.

1.1.4.1 Hypnozoites

The first is the formation of hypnozoites during its life cycle in humans. During the pre-erythrocytic stage, a fraction of the sporozoites will remain 'dormant' in the hepatocytes in an arrested form termed hypnozoites [42]. Hypnozoites can stay quiescent for months or even years following the initial infection before they are reactivated by unknown signals and undergo maturation, releasing merozoites and causing new infections in the blood [43]. The re-establishment of an erythrocytic infection, demonstrated by an increase in parasitaemia and reappearance of clinical symptoms, is known as relapse [20]. Relapses have been extensively studied and identified as a major challenge in the era of malaria elimination. It was reported that up to 80% of detectable *P. vivax* blood stage infections were caused by relapses in high transmission areas, causing a significant burden on healthcare facilities, economics and education [44].

In temperate areas such as North America, Europe and Russia before elimination, *P. vivax* exhibited an approximately 9-month long incubation period and interval

between relapses [45]. The presence of relapses in *Plasmodium* species was speculated to provide survival advantages. The dormancy allows the parasites to stay inactive until it is the appropriate season for mosquito breeding and transmission [46]. Currently, Korea remains the only temperate region from which *P. vivax* with long dormancy phenotypes has still been reported [47]. It has also been suggested that the incubation period, rate and number of relapses are most likely dependent on the number of sporozoites inoculated: more sporozoites lead to a shorter incubation period and more relapses [48]. Additionally, frequent *P. vivax* relapses were observed in *P. falciparum*-infected individuals post-antimalarial treatment [49]. This demonstrates that antimalarial treatment could potentially weaken host immunity, facilitating the occurrence of symptomatic relapses and hence further complicating our current elimination strategies [45]. Interestingly, Shanks and White have also speculated that other infectious diseases, including *P. falciparum* infections, can stimulate reactivation of *P. vivax* hypnozoites [43].

Hypnozoites and the relapses they cause are a major challenge for elimination. Being an intracellular and quiescent form of the parasite, hypnozoites are shielded from the detection of host immune surveillance and hence are less likely to be removed from the host naturally [50]. Moreover, hypnozoites are shown to be irresponsive to most antimalarial treatments as the majority of them aim

to reduce symptoms by targeting the blood-stage parasites [51]. The only licensed anti-malarial treatments that clear hypnozoites are 8-aminoquinolines which are contraindicated in patients with glucose-6-phosphate dehydrogenase (G6PD) deficiency [52, 53], thus hindering their applications in many malaria endemic countries. Further limitations of anti-malarial treatments are discussed in more detail in Section 1.1.5.4. Additionally, hypnozoites accounted for up to 80% of the clinical episodes experienced by infected children [44] and currently there are no detection or surveillance tools being used by malaria control programs that can identify these individuals [54].

1.1.4.2 Invasion of reticulocytes

During the blood stage of its life cycle, *P. vivax* targets young RBCs known as reticulocytes [22]. It is generally accepted that the invasion of reticulocytes by *P. vivax* requires the expression of Duffy antigens [55-57]. This suggests that Duffy blood group negative populations, mostly located in African regions, are highly resistant to *P. vivax* infections, providing an explanation of the low prevalence of *P. vivax* infections in Africa [58]. However, recent evidence has reported that *P. vivax* was found specifically in Duffy negative individuals, challenging the paradigm that Duffy negativity confers complete protection against the parasite [59, 60]. Besides Duffy antigens, other ligands for invasion have now also been

identified, such as the reticulocyte binding proteins (RBPs), encoded by the *rbp* gene family, some of which are involved in the recognition of reticulocytes in the binding process [61, 62].

The finding that *P. vivax* preferably invades reticulocytes and erythroblasts has significant implications for elimination. Erythroblasts are restricted to the bone marrow [22], suggesting that *P. vivax*-infected cells could also be present in the bone marrow. Based on evidence in a single *P. vivax*-infected patient and *Aotus lemurinus* monkeys, it has been suggested that there is a large biomass of *P. vivax* that remains undetectable in the bone marrow [63, 64]. Secondly, it has been postulated that *P. vivax*'s preference for invading reticulocytes leads to the comparably low parasitaemia seen during blood stage infections [37, 65], as reticulocytes account for a small proportion in the periphery [65]. Nevertheless, this postulation remains debatable as Lim et al. demonstrated that the *P. vivax* parasitaemia exceeded the number of reticulocytes [66]. The authors have proposed that parasitaemia might not be mediated only by the availability of peripheral reticulocytes. In several recent reports, the association of splenic complications and splenectomy with high risk of *P. vivax* infections have strongly indicated the importance of splenic reservoirs for *P. vivax* parasites [67-72].

1.1.4.3 Wide geographic distribution

Thirdly, *P. vivax* is known for its adaptability in areas of higher latitude and lower temperature compared to other *Plasmodium* species. Generally, malaria is identified as a disease sensitive to climate and temperature [73]. This is largely due to its mosquito vectors and their preferable condition for growth and maturation [74]. It has been shown that *P. vivax* can be transmitted via its vectors at a minimum of 15°C whilst *P. falciparum* transmission requires 19°C [75]. This feature potentially explains the presence of *P. vivax* cases in temperate areas and the wider geographic distribution compared to *P. falciparum*. Being able to transmit at a lower temperature also translates to decreased sensitivity to seasonal changes and therefore a longer transmission window each year.

1.1.4.4 Sexual development

P. vivax also differs from *P. falciparum* with regards to its sexual development. Firstly, it is well established that *P. vivax* demonstrates earlier gametocytogenesis than *P. falciparum* [76], resulting in the appearance of gametocytes at the beginning of the first cycle of blood stage infection [77], even before the manifestation of clinical symptoms [78]. This is a challenge for elimination as infectious gametocytes are more likely to be ingested by new

mosquitoes before anti-malarial treatments have been given. Additionally, *P. vivax* shows a shorter duration of sporogony (the formation of sporozoites inside an *Anopheles* vector). Studies reported the presence of *P. vivax* sporozoites in the salivary gland as early as six days after the primary blood meal [79, 80], compared to 14 to 16 days for *P. falciparum* [81], meaning they are able to transmit *P. vivax* parasites to new hosts sooner.

Taken together, these biological characteristics of *P. vivax* are beneficial for the parasites to be transmitted between hosts more efficiently with less interference from host immunity and geographic factors. At the same time, they also highlight the need to revisit our current control and elimination strategies.

1.1.5 Current strategies for prevention and treatment

As lower transmission rates of *Plasmodium* spp have been observed in more malaria-endemic countries and we move towards elimination, changes in our current malaria control strategies should be expected. Given the pivotal role of *P. vivax* in maintaining the residual transmission level, interruption of *P. vivax* transmission has gradually come into focus of elimination programs in many countries. However, elimination of *P. vivax* will be difficult and dependent on multiple factors, such as geography, climate, parasite biology, political, financial

and cultural situations. Several approaches have been implemented to facilitate the progress of controlling and eliminating *P. vivax*. In this Section, I will discuss the tools currently available in the context of prevention, diagnosis and treatment, and their corresponding complications.

1.1.5.1 Preventative measures: vector-control

The primary aim of the preventive measures in the field of malaria is to interrupt disease transmission via vector control. Conventional interventions include indoor residual spraying (IRS), insecticide-treated bed nets (ITNs) and long-lasting insecticidal nets (LLINs) which are all effective by limiting the human's exposure to mosquitoes and/or decreasing the population of mosquitoes [82]. The insecticides used for these interventions often contain the key molecule pyrethroid which interferes with voltage-gated sodium channels in mosquitoes [83]. The protective efficacy and public health impact of these interventions have been extensively reviewed, which shows that they are highly effective in reducing the incidence and mortality rates in several *P. falciparum*-endemic countries [84-87]. It is worth noting that their implementation is strongly dependent on a high level of community engagement, knowledge and acceptance, which can potentially hinder the overall efficacy without the support and commitment from local government. Recently, resistance to pyrethroid have been reported in

multiple regions and this is likely to jeopardise preventive efforts [88-90]. Additionally, *P. vivax* may be less affected by vector control due to its faster developmental process [82]. In this case, parasites are more likely to finish their full life cycle and are further transmitted before the vectors are killed upon contact with insecticide-treated materials.

The use of ITS and IRS has been shown to be less effective in *P. vivax*-endemic areas outside Africa in comparison to *P. falciparum* in Africa. This is due to differences in biting behaviours of the primary mosquito vectors in Asia and the Americas. For instance, in southeast Asia the dominant vector species are *Anopheles dirus* and *Anopheles minimus* which exhibit both indoor and outdoor biting activity [91], limiting the effectiveness of indoor vector control measures such as ITS and IRS. Similarly, evidence has shown in Indonesia that most *Anopheles* vectors bite at dusk before the inhabitants return from outdoor activities [92]. Furthermore, *P. vivax* vectors in India such as *Anopheles culicifacies* show outdoor-resting behaviours, indicating that they avoid contact with insecticide-treated surfaces and can contribute to transmission despite high coverage of ITN and IRS [93]. Therefore, the WHO has called for a new approach in order to address the challenges presented for targeting *P. vivax* through vector control.

1.1.5.2 Preventative measures: vaccines

Vaccines are another option for the prevention of malaria. Currently, a number of *P. vivax* vaccines targeting the liver or blood stage have entered pre-clinical or clinical trials, but are still at the early stage of development [94]. Only two *P. vivax* vaccines have entered human clinical trials. PvCSP is a pre-erythrocytic candidate based on *P. vivax*-derived circumsporozoite antigen and has shown promising effects in eliciting cell-mediated and antibody immune responses [95]. The second candidate is Pvs25 based on the surface proteins of *P. vivax* during the mosquito stage [96]. Pvs25 aims to induce antibody responses to block cellular invasion by the parasites and hence is often referred to as a transmission blocking vaccine candidate [96, 97]. However, these *P. vivax* vaccine candidates still require significant amount of further investigations to prove their efficacy and application. On the other hand, RTS,S is the most advanced malaria vaccine, and it targets pre-erythrocytic *P. falciparum* infection [98, 99]. It consists of circumsporozoite proteins fused with human Hepatitis B virus antigens and formulated with various adjuvants [98]. RTS,S achieved an efficacy of 30 – 40% during a phase III clinical trial and has recently entered pilot implementation in children in three African countries [100, 101]. This again highlights the imbalance of resource distribution between *P. vivax* and *P. falciparum*. To assist

further development of vaccines, identifying antigens associated with protection and understanding naturally acquired immunity against malaria will be crucial.

1.1.5.3 Diagnosis and surveillance

Diagnosis is another pivotal component in the control programme. Not only does it enable efficient screening of the current burden of disease, it also allows detection of malaria-infected individuals with precision and enables an appropriate treatment (or elimination) regime to be implemented. The use of traditional diagnostic tools such as rapid diagnostic tests and light microscopy is well established in remote malaria endemic regions. This is due to their user-friendly nature and the fact that they require minimal facilities and medically trained labour [102]. For *P. vivax*, however, the quiescent liver stage hypnozoites and low-density parasite load during the blood stage mean many infected individuals remain undetected due to the limited sensitivity of these tools [103]. Molecular diagnostic tools such as the polymerase chain reaction (PCR) and loop-mediated isothermal amplification can provide much higher sensitivity to capture low parasitaemia, but are less feasible and accessible in the field [102]. Furthermore, there are not yet any tools for the successful detection of hypnozoites.

More recently, the idea of sero-surveillance has become popular and has shown great potential in estimating transmission levels and identifying populations at risk [104]. This technique works by measuring antibody levels against a panel of *Plasmodium* antigens (or biomarkers) in the serum or plasma samples of the participants exposed to the parasites, providing information on anti-malarial immunity [105] and potentially the time since the individual was last infected. One of the two main uses of such information is to reflect current or past exposure to the parasite in a population, and therefore inform timely interventions [106]. The other use is to evaluate the presence of protective immunity [104]. Several studies have attempted to use this approach to address *P. vivax* infections. This includes comparing transmission levels across different geographic regions [107, 108], identifying asymptomatic individuals [109, 110], and monitoring recent *P. vivax* exposure to potentially predict hypnozoite-carriers [111, 112]. In order to further optimise and promote the application of sero-surveillance, it has been suggested antibody responses against *P. vivax* be better characterised with more longitudinal studies [113]. Additionally, a larger panel of biomarkers with more antigenic candidates should be developed to capture the highly polymorphic nature of *P. vivax* [104].

1.1.5.4 Treatment

Lastly, an effective elimination programme is not complete without antimalarial treatment. For *P. vivax*, chloroquine (CQ) remains the first-line treatment and works by disrupting parasitic growth during the blood stage of infection [1, 114]. It has been widely used due to its low cost and minimal adverse effects in most people [102]. Following the discovery of CQ-resistant *P. vivax* strains, artemisinin-based combination therapy that also targets blood stage infection has been recommended by the WHO for treating uncomplicated *P. vivax* cases in endemic areas with high CQ treatment failure rates [1, 115, 116]. To eliminate liver stage hypnozoites, countries with high *P. vivax* transmission are encouraged to include primaquine (PQ) in their treatment regimens [1]. Currently, PQ is the only commonly used antimalarial drug targeting liver stage hypnozoites and is known as the 'radical cure' for *P. vivax* [117]. Unfortunately, PQ has an adverse effect that provides a major challenge in its application.

PQ is known to induce dose-dependent haemolysis and potentially lethal anaemia in individuals with G6PD deficiency [52, 53]. G6PD deficiency is the most common form of hereditary enzyme deficiency in humans, affecting 400 million people worldwide [118]. This restricts the applications of PQ. Furthermore, there are only two point-of-care G6PD diagnostic tests available

on the market, both of which are yet to be registered by the WHO for regular use with PQ treatment [119]. It has become clear that more advanced and accessible G6PD diagnostic tests will greatly improve the public health impact of PQ treatment. Lastly, tafenoquine has emerged as a new radical cure in the early 2000s and has shown similar efficacy in lowering the risk of relapse in *P. vivax*-infected individuals [120, 121]. The major difference between PQ and tafenoquine is PQ requires multiple doses over 14 days whilst tafenoquine is effective with a single dose, which allows much better patient compliance to treatment and a higher success rate [122, 123]. So far tafenoquine is only recommended to individuals with G6PD activity >70% and further investigations are required for it to be used safely [124].

In addition to using anti-malarial drugs to treat individuals with clinical symptoms, there are other strategies to maximise the application of treatment for elimination. A major focus is the treatment of whole at-risk populations with anti-malarial drugs, which can be performed in a number of approaches. Mass drug administration (MDA) in response to malaria transmission is referred to as administration of anti-malarial drugs to the entire target population regardless of infection status or symptoms [125]. Another approach is mass screening and treatment (MSAT) that aims to treat individuals identified as infected [126]. Similar to MSAT, another widely used method in the malaria field is reactive

case detection (RACD), which screens individuals living in close proximity to the clinical cases for treatment [127]. However, *P. vivax* still poses a great challenge for these methods. Firstly, the potentially severe implication of using PQ for clearing hypnozoites in G6PD deficient individuals suggests that MDA is too risky to conduct [102]. Secondly, MSAT and RACD rely on precise diagnostic screening for *P. vivax* infection, which remains problematic due to the presence of hypnozoites and high frequency of parasitaemia below the detection limit [54, 128].

Overall, in our current *P. vivax*-targeting elimination toolkit, there are a number of well-established and innovative interventions. However, some gaps still need to be addressed urgently. These include effective vaccines, accurate identification of hypnozoite-carriers and precise yet accessible diagnosis of G6PD deficiency. Combining current resources and exploring next-generation tools will be the utmost priority in order to sustain the current momentum and maximise public health impact.

1.2 Immune responses against malaria

The protective effects conferred by naturally acquired malaria-specific immune responses have been well demonstrated in animal models and clinical and

epidemiological studies. The current knowledge on immunity against malaria has been applied in multiple aspects of elimination and control programmes, including surveillance, diagnosis and vaccine development. In this Section, I will discuss in detail how different arms of human immunity provide protection against symptoms and further infections. Due to the fact that there is a longstanding lack of a *in vitro* culturing system for *P. vivax*, most studies addressing the immune responses against malaria focus on *P. falciparum* instead of *P. vivax*. Hence, findings presented here are derived from *P. falciparum* unless specified.

1.2.1 Innate Immunity

The innate immune responses are the first line of protection and play a pivotal role in modulating the adaptive immune responses. Several immune cell types are known to contribute to innate immunity and are generally derived from the myeloid cell lineage. These include neutrophils, macrophages, natural killer (NK), γδ T cells and dendritic cells (DCs). As the primary focus of this thesis is adaptive immunity, innate immunity is covered briefly in the Sections below.

Neutrophils: Neutrophils are naturally abundant in healthy individuals and are first responders to the site of parasite sequestration during the blood stage of an infection [129, 130]. Neutrophils contribute to parasite clearance through phagocytic activity, which is heavily dependent on the presence of opsonising antibodies and/or components from the complement pathways [131]. Besides iRBCs, *Plasmodium* merozoites [132] and gametes [129] are also typical targets of neutrophil phagocytosis. The reactive oxidative species (ROS) produced by neutrophils are capable of killing the phagocytosed parasite or inhibiting its growth [129]. There is evidence that neutrophil responses are impaired during *P. vivax* infections via reduced expression of chemokine receptors and therefore disruption of neutrophil recruitment [132]. The weakened neutrophil responses during a *P. vivax* infection is potentially linked with the increased risk of bacterial infections and respiratory distress [133, 134].

Macrophages: Similar to neutrophils, macrophages are one of the early responders to merozoites and asexual iRBCs [135]. The phagocytic capacity of macrophages can be activated by opsonising or non-opsonising interactions. Opsonising activation involves opsonising antibodies or complement components attached on the surface of iRBCs [136], which leads to further macrophage recruitment and production of inflammatory cytokines mediated by Fcγ receptors [136] [137]. Macrophages also express pattern recognition

receptors (PRRs), such as toll-like receptors (TLRs), which are involved in non-opsonising activation and the recognition of various pathogen-associated molecule patterns (PAMPs) [138]. It has been shown that macrophages are efficient phagocytic cells and potent producer of inflammatory cytokines [132, 139, 140]. However, macrophages can be a double-edged sword in the context of malaria, resulting in tissue damage from excessive inflammation [136] and suppression of macrophage activation via anti-inflammatory cytokine production [141].

Dendritic cells: DCs are a crucial component of the bridge between innate and adaptive immunity due to their exceptional antigen-presenting capacity. In humans, DCs can be found in blood and both lymphoid and non-lymphoid tissues [142]. They can be further categorised into two major subsets: conventional DCs (cDCs; $CD11c^{+}$ $CD123^{-}$) and plasmacytoid DCs (pDCs; $CD11c^{-}$ $CD123^{+}$) based on the expression of surface markers [143]. cDCs are professional antigen-presenting cells (APCs) and cytokine-producing cells [142], whilst pDCs specialise in the production of interferon (IFN)-α. *Plasmodium* infection can affect the size and composition of the DC population. However, very few human studies have specifically assessed the impact of *P. vivax* infections. Some evidence suggests *P. vivax* infections result in a decreased number of total DCs and cDCs [144-146]. In contrast, there is conflicting

evidence on the impact for pDCs where both decrease [144, 146] and increase have been reported [145]. It was also demonstrated that *P. vivax* infections could hinder the effector functions of pDCs ([147].

Natural killer cells: Similar to DCs, NK cells also assist in strengthening the link between innate and adaptive immune responses against malaria. NK cells contribute to more than 10% of PBMCs and are characterised by the expression of NK cell receptor (CD161), multiple cytokine receptors, Fc receptors and a wide range of unique ligands [148-150]. These phenotypical features mediate NK cells' activation by the distressed iRBCs [151] and pro-inflammatory cytokines produced by other immune cell types [152]. Most importantly, activated NK cells contribute to rapid cytokine production and direct killing of iRBCs via antibody-dependent cellular cytotoxicity (ADCC) [152, 153]. IFN-γ and interleukin (IL)-10 secreted by NK cells are important players in immunoregulation. IFN-γ promotes macrophage activation, DC maturation and T cell-mediated responses [153] whilst IL-10 enhances NK-mediated cytotoxicity and dampens $CD8^+$ T cell responses which can be potentially pathological [154]. However, the role of NK cells in *P. vivax* infections and their association with clinical outcomes remain unclear [155] as the total number of NK cells was found to be uncorrelated with parasitaemia in *P. vivax*-infected individuals [156, 157].

To summarise, a wide variety of innate immune components induce early responses against *P. vivax* infections. Such responses are usually in the form of phagocytic activities and cytokine secretion, facilitating the clearance of blood stage parasites or iRBCs. Additionally, the production of cytokines is also essential for enhancing antigen-presenting capacity of APCs, promoting the activation of downstream adaptive immune responses. Despite this, it remains unclear if the effector activities of these cells can be harnessed for clinical treatment. More studies will be required to address the significance of innate immunity against *P. vivax* in naturally exposed populations.

1.2.2 Adaptive Immunity

Compared to innate immunity, adaptive immunity against *Plasmodium* infections has drawn more attention in research. Adaptive immunity has two arms: cell-mediated and humoral immune responses. The cell-mediated response is centred around several types of T cells whilst the humoral response is mediated by B cells. Both arms can develop immunological memory defined as the capacity to respond more rapidly at a higher magnitude upon second or repeated exposure to a pathogen [158]. In this Section, I will outline the specific roles of cell-mediated and humoral responses against *Plasmodium* infections in human, with a focus on humoral immunity given its relevance to the aims of my PhD.

1.2.2.1 Cell-mediated Immunity

It is well-established that T cells expressing surface markers CD8 and CD4 are the two main types of T cells receiving stimulation signals from APCs in the context of the major histocompatibility complex (MHC) molecules class I and II, respectively [159]. Such signals are received via the T cell receptor (TCR), consisting of α and β chains and are associated with the T cell-specific co-receptor CD3 [159].

$CD8^+$ T cells: Upon presentation of *Plasmodium* antigenic peptides, $CD8^+$ T cells (or cytotoxic T cells) are activated and begin differentiation into effector $CD8^+$ T cells [160]. Following activation, a fraction of the $CD8^+$ T cells differentiate into memory cells which can initiate faster and more effective effector functions during recall infection [161]. The primary effector function of $CD8^+$ T cells is to release perforin, granulysin and/or granzyme to induce lysis in target cells and hence inhibit the growth of intracellular parasites [162]. $CD8^+$ T cells also contribute to protection against parasitic development through the secretion of IFN-γ [163-165]. $CD8^+$ T cells have been shown to provide protection against *P. vivax* infections by inducing lysis in *P. vivax*-infected reticulocytes [166], suggesting a role in controlling parasitaemia and disease outcome. In contrast,

P. vivax has also been shown to impair $CD8^+$ T cell responses in naturally infected Brazilian individuals [157].

$CD4^+$ T cells: Compared to $CD8^+$ T cells, $CD4^+$ T cells and their role in immunoregulation during *Plasmodium* infections has been more extensively documented. $CD4^+$ T cells, also known as T helper cells, can be further divided into multiple subtypes (T_H1, T_H2, T_H17, regulatory T (T_{REG}) cells and follicular T helper (T_{FH}) cells), each of which plays a distinct role in regulating malaria disease. A primary role of $CD4^+$ T cells in supressing *Plasmodiu*m infections is to assist the development of antigen-specific antibody responses via direct contact with their cognate antigen and other immune cell types [167]. The presence of $CD4^+$ T cells and the resultant production of antibody responses were shown to be pivotal in controlling blood stage infections in mice [168]. Additionally, Boyle et al. further demonstrated the importance of $CD4^+$ T cells in their study of humans where a higher frequency of $CD4^+$ T cells was significantly correlated with reduced risk of *P. falciparum* malaria clinical symptoms [169]. On the other hand, multiple studies provide evidence suggesting that *P. vivax* can impair overall $CD4^+$ T cell responses to achieve effective immune evasion. It was demonstrated that *P. vivax* infections disrupted the proliferation of $CD4^+$ T cells [146] and resulted in a significant reduction in the $CD4^+$ T cell population [145]. More specifically, Ourives and colleagues have recently shown in Brazil that T_H1,

T_H2, T_H17 and T_{REG} responses were significantly reduced following *P. vivax* infections [157, 170, 171]. These findings can be potentially explained by the prior observation that *P. vivax* induced apoptosis in human $CD4^+$ T cell population via the suppression of anti-apoptotic protein expression and the activation of death receptors [172]. Alternatively, the reduction of $CD4^+$ T cell population could also be due to an increase in cell sequestration in lymph nodes [173].

Follicular T helper cells: T_{FH} cells are specialised $CD4^+$ T cells that play a distinct role in the generation of high-affinity antibodies. T_{FH} cells co-localise with proliferated B cells in the light zone of the germinal centre (GC) following somatic hypermutation of immunoglobulin genes [174]. The primary function of T_{FH} is to provide survival signals to B cells that are efficient in the capture, processing and presentation of cognate antigens [175]. Additionally, the interaction between CD40 (on B cells) and CD40 ligand (on T_{FH}) also induces the secretion of IL-21 by T_{FH} [176], resulting in B cell clonal expansion and differentiation into long-lived plasma cells and GC-dependent memory B cells [174]. In the absence of T_{FH}, B cells can still undergo proliferation and differentiation by cognate antigen activation and receiving T cell help [174], but can only generate short-lived plasmablasts involved in rapid secretion of low-affinity antibodies and GC-independent B cell memory [174]. These findings

also highlight the importance of T_{FH} cells in the generation of B cell memory. There has been a lack of human studies assessing the role of T_{FH} in the context of either *P. falciparum* or *P. vivax* infections, with those published having conflicting results [177]. Whilst more research is needed, the general consensus so far suggests that *P. vivax* infections are associated with specific T_{FH} populations skewing immunity towards T_H1 and therefore impaired antibody responses resulting in ineffective parasite clearance [177, 178].

Natural killer and γδ T cells: NKT and γδ T cells are known as unconventional T cells due to the unique phenotypic expression. For γδ T cells, the TCRs are composed of γ and δ chains instead of the conventional α and β chains [179]. NKT cells are characterised by the expression of both classic αβ TCRs and NK cell receptor CD161 which are specific for lipid-based antigens presented by APCs [180, 181]. NKT cells are most abundant in the liver whilst γδ T cells are mostly found in the gut mucosa [182, 183]. These two types of cells can be stimulated by blood stage *Plasmodium* infection (via different mechanisms), resulting in parasite growth inhibition [184] and killing of iRBCs via either perforin/granzyme-mediated cytotoxicity or ADCC [185, 186]. These effector functions are mediated by the secretion of cytokines from NKT cells (IFN-γ) [187] and γδ T cells (IFN-γ, IL-3, GM-CSF) [186, 188]. Despite clear effector functions against infections, whether or not NKT cells contribute to protection against

malaria remains unclear. One study reported a significantly higher number of NKT cells in Chinese individuals acutely infected with *P. vivax* compared to malaria-free individuals living in the same region, but significantly lower than individuals from non-malaria-endemic regions [171]. This suggested that NKT cell frequency was susceptible to immune status and transmission level. However, another study found no association between the NKT cell and the level of past exposure [157]. Given that NKT cells are most abundant in the liver, it would be of interest to investigate the possible role of NKT cells against liver stage *P. vivax* infection. For γδ T cells, multiple studies have demonstrated that P. *vivax* infections increase the number of γδ T cells [189], however it remains unclear whether or not γδ T cells plays a protective role in *P. vivax* infection in humans [190].

1.2.2.2 Humoral Immunity

Humoral immunity, or B cell-mediated immunity, has been the focus of most research assessing protection against malaria. This notion stemmed from a study conducted by Cohen et al. in 1961 where the authors observed a significant reduction in parasitaemia and clinical symptoms in *P. falciparum*-infected children passively transferred with sera from exposed adults [191]. Figure 1.3 shows the process via which humoral immunity is developed. B cells are the core

of humoral immune responses. Naïve B cells residing in secondary lymphoid organs [192] are activated upon contact with their cognate antigens via B cell receptors (BCRs) [193, 194]. Activated B cells subsequently migrate towards the T cell zone to receive help from cognate $CD4^+$ T cells, resulting in proliferation and differentiation of the B cells [195, 196]. A fraction of the proliferated B cells differentiates into short-lived plasmablasts/plasma cells [197] and GC-independent memory B cells [198]. Other proliferated B cells differentiate into GC B cells, aggregating into B cell follicles to form the GC [199]. Within the GC, proliferated B cells undergo somatic hypermutation in the dark zone of the B cell follicle and multiple rounds of selection by follicular DC and T_{FH} cells in the light zone [200, 201]. Upon their encounter with B cells, follicular DCs provide survival signals to B cells with BCRs capable of capturing cognate antigens available [202], facilitating the retention of these B cells in the GC [203]. Once captured, the antigens are endocytosed, processed and subsequently presented by B cells through MHC class II to T_{FH} cells [204, 205]. During this process, B cells again compete for the limited number of T_{FH} cells based on their efficiency of antigen presentation [204]. Successful B cells will be induced to proliferate and differentiate, leading to the generation of long-lived plasma cells and GC-dependent memory B cells (MBCs) [204]. This process, known as the GC reaction, is regulated by CD40/CD40 ligand interaction [206] and cytokine secretion [207].

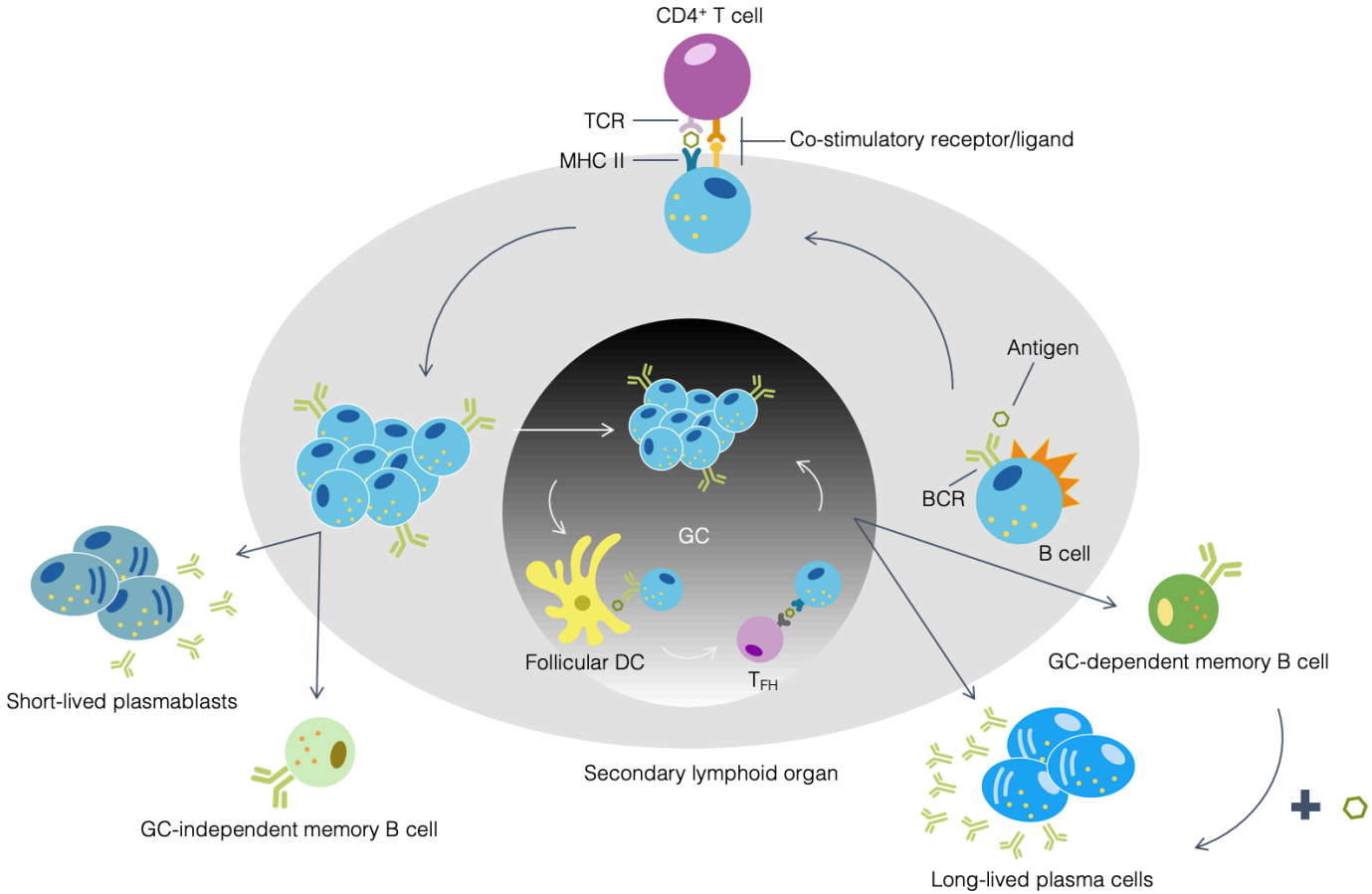


Figure 1.3 Development of humoral immunity. B cells play a pivotal role in the development of humoral responses. With T cell help and the correct molecular signals, B cells are activated to proliferate and differentiate into various B cell subsets that aim to produce antibodies. Abbreviations: BCR=B cell receptor; TCR=T cell receptor; MHC II=major histocompatibility molecule class II; GC=germinal centre; DC=dendritic cell; T_{FH}=follicular T helper cell.

The production of antibody or immunoglobulin (Ig) occurs following the activation and differentiation of naïve B cells into plasma cells. There are different types of antibody that can be produced as part of the humoral immune responses that are functionally and structurally variable (Figure 1.4). Naïve B cells express two isotypes of surface antibody, IgM and IgD, which differ in their heavy chains [208, 209]. After B cells receive T cell help via the binding of co-stimulatory molecules such as CD40 ligand/CD40, isotype switching is initiated and genes encoding for the antibody molecules are cleaved and recombined to produce other isotypes [206, 209]. These include IgG, IgA and IgE (Figure 1.4), which vary in their distribution, molecular structure and effector function, as reviewed by Irani et al [210]. Being the most abundant isotype in humans, IgG also has four subclasses: IgG1, IgG2, IgG3 and IgG4 [210]. These IgG subclasses exhibit specific molecular properties that can influence the development of humoral immunity in a particular manner. This topic is discussed further in the Section below.

IgG subclasses: It has been well documented that *P. vivax* antigen-specific antibody responses are associated with protection against clinical symptoms and prediction of risk of infection [211-213]. Specifically, antibody isotypes IgG1 and IgG3 have been described as the major players in conferring protection and were observed in elevated levels following *P. falciparum* and *P. vivax* infections [214-

220]. This is due to the fact that IgG1 and IgG3 are cytophilic antibodies (in contrast to non-cytophilic antibodies IgG2 and IgG4) that engage Fc receptors and are involved in facilitating opsonic phagocytosis and killing of blood stage merozoites by monocytes [221-225]. Additionally, IgG1 and IgG3 have been shown to promote complement fixation and therefore complement-mediated lysis and invasion inhibition [226]. The induction of complement was also found to be associated with protection against malaria [226, 227].

Antigenic targets of immunity: As antibodies contribute to *Plasmodium* parasite clearance as outlined above, all the studies to-date correlate antibody reactivity or magnitude with the presence or absence of clinical symptoms in naturally infected populations to infer protective immunity. Two studies have reported that antibody responses against *P. vivax* Duffy binding proteins (DBPs) were associated with clinical protection [213, 228]. More specifically, He et al. have highlighted the significance of IgG1 and IgG3, instead of total IgG or other subclasses, in mediating protective immunity [213]. Similar to this finding, Matos et al. also demonstrated that IgG3 played a critical role in the recognition of thrombospondin-related adhesive protein (TRAP) [229]. Additionally, the titre of anti-TRAP IgG3 in *P. vivax*-infected Brazilians was significantly association with a reduction in symptoms [229]. Besides DBPs and TRAP, the level of antibodies specific for the erythrocyte binding protein (EBP) and RBPs

have also been found to be associated with protection in cohorts from Papua New Guinea (PNG), Thailand and Brazil [213, 230]. These results are in line with the observations that naturally acquired antibodies specific for RBP and DBP exhibited inhibitory properties against RBC invasion by *P. vivax* [231, 232]. The use of multiplex assays such as protein microarray and Luminex® in the past few years has accelerated the process of measuring antibody responses against many proteins and therefore has greatly facilitated the identification of possible key targets of immunity. Novel *P. vivax* antigenic targets associated with protection have been discovered by the use of Luminex® [220], suggesting that multiplex assays can be beneficial in expanding our current scope of research.

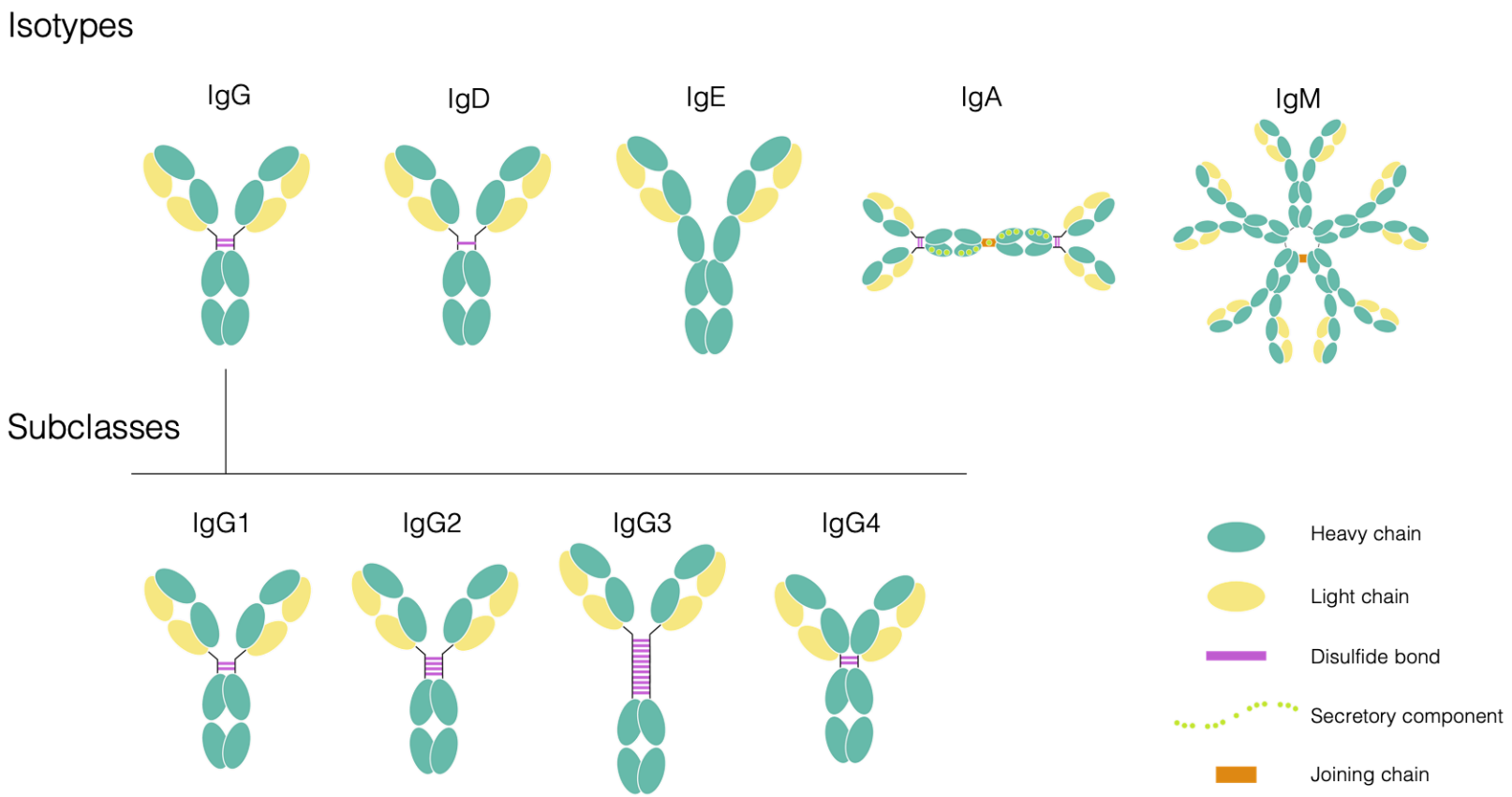


Figure 1.4 Types of antibody molecules. IgD and IgM are expressed on the surface naïve B cells whilst other isotypes are produced via 'isotype switching' following antigen-activated B cell's contact with a $CD4^+$ T helper cell. IgG is further divided into four subclasses, IgG1, 2, 3 and 4, which differ both structurally and functionally.

Antibody longevity: Plasma cells ($CD19^{+}$ $CD27^{hi}$ $CD38^{hi}$) are capable of rapidly producing large amounts of antigen-specific antibodies following contact with pathogens [233]. Based on their localisation and longevity, plasma cells can be further divided into short-lived plasma cells (present in extrafollicular sites of secondary lymphoid organs) and long-lived plasma cells (present in the bone marrow) [234]. For *P. falciparum*, the longevity of short- and long-lived plasma cell compartments in naturally exposed populations has been well documented since the 2000s [235-237]. Additionally, with the help of mathematical modelling, researchers were able to show that in response to *P. falciparum* infection the estimated half-lives for short- and long-lived plasma cells ranged from 2-10 days and 3-9 years, respectively [238]. The progress has been slightly slower for *P. vivax*. Longevity of naturally acquired antibody responses against specific *P. vivax* antigens has been reported since 2009 [211, 232, 239-242]. More detailed investigations are needed to determine the contribution of short- and long-lived plasma cells in modulating *P. vivax*-specific antibody response longevity. A better understanding of the key elements required to induce long-lived antibody responses would be highly valuable for designing the next generation of malaria vaccines.

MBCs are potent and fast antibody producers upon re-encounter with cognate antigens. Long-lived MBC responses against *P. vivax* have been observed in

different regions of Thailand [239, 243, 244]. On the contrary, evidence on the induction of long-lived MBC responses against *P. falciparum* antigens has been scarce. Dorfman et al. reported that no *P. falciparum*-specific MBCs were found in a Kenyan population [245]. Weiss et al. showed a gradual expansion of B cell populations following repeated *P. falciparum* infections in Mali, but could not confirm that this was due to the presence of long-lived MBCs [246]. Nevertheless, Wipasa et al. were able to demonstrate that Thai adults acquired long-lived *P. falciparum*-specific MBCs despite the low transmission in this region [239]. These findings indicate that *Plasmodium*-specific MBC responses could be reflective of *Plasmodium* species (i.e. longer lived responses following *P. vivax* infections) and the transmission level of a region, as discussed below.

It has been suggested that high intensity infections, as seen in regions with high transmission, are likely to impair long-lived *Plasmodium*-specific antibody and MBC responses [243]. This can potentially explain the lack of evidence on long-lived *P. falciparum*-specific MBC responses to-date. Such impairment to humoral immunity is often demonstrated by the expansion of atypical MBCs (commonly defined as $CD19^+$ $CD20^+$ $CD21^-$ $CD27^-$ in oppose to $CD19^+$ $CD20^+$ $CD21^+$ $CD27^+$ for conventional MBCs) following *Plasmodium* infections [177, 243, 247-250]. It has been hypothesised that atypical MBCs can negatively influence antibody responses and hence could be an approach utilised by *Plasmodium*

parasites to evade immune surveillance [243]. Studies have shown that atypical MBCs exhibit differential surface marker expression and reduced responses against *P. falciparum* compared to conventional MBCs [248, 250]. This indicates that atypical MBCs are still capable of antibody production but to a lesser extent. It has also been observed in *P. falciparum*-infected individuals that these atypical MBCs express high levels of pro-apoptotic markers [250], which most likely explains their short-lived nature [251]. On the contrary, results have been shown where *P. falciparum*-specific atypical MBCs were described as active antibody-producers [252]. Nevertheless, more detailed investigations are needed to demonstrate the underlying mechanisms by which this atypical MBC population affects the efficiency or maintenance of *Plasmodium*-specific antibody responses.

IgM memory: Whilst IgG-producing MBCs have been the primary focus of recent research, the presence of IgM-producing MBCs has also been reported following *Plasmodium* infections. Using a *P. chabaudi*-infected mouse model, it was revealed that IgM^+ MBCs were somatically hypermutated, meaning that they generated high-affinity antibodies [253]. Furthermore, these IgM^+ MBCs were shown to proliferate and differentiate into IgM^+ plasma cells, which are critical contributors of an early response, upon rechallenge with *Plasmodium* infection [253]. In humans, naturally acquired merozoite-specific IgM antibodies can

persist for at least a year following a primary *P. falciparum* infection [212]. The source of the long-lived IgM antibodies identified is likely either IgM^+ memory B cells or long-lived IgM^+ plasma cells [212]. Importantly, the authors demonstrated that the boost of IgM responses at the early stage of infection elicited complement fixation and therefore the inhibition of invasion and were associated with clinical protection [212]. These results indicate that IgM antibodies could play an important yet so far largely unrecognised role in anti-malarial immunity.

Sero-surveillance: In addition to contributing towards protection against clinical malaria (either naturally or in the form of vaccine-induced responses), the strong association between antibody responses and the immune status of infected individuals has formed the basis for using serology to measure *P. vivax* transmission and monitor exposure on a population scale. Numerous studies have been published to demonstrate the use of serology in a variety of malaria-endemic countries to infer the change in transmission pattern [107, 108, 254-258] and level of past exposure [112, 259-262]. One of the benefits of measuring exposure using serology is that it can potentially overcome the current challenge of MSAT (as discussed in Section 1.1.5.4), where individuals with low-density infections fail to be detected in low transmission regions [54, 106, 128]. Additionally, serology has been used to estimate time since last *P. vivax* exposure

and therefore provide information on how likely an exposed individual is harbouring hypnozoites [112]. This shows that serology can be used to cross the hurdle of overtreatment in MDA [52, 53, 106] and undertreatment in MSAT [126, 263]. Collectively, these applications have indicated that serology can be a useful method in the toolkit for *P. vivax* surveillance and control and deserves more attention. However, our current progress of using serology for this purpose has been primarily reported in the context of research [106]. To ensure the implementation and to maximise the advantage of this approach, there is still a strong need for the identification of *P. vivax* antigens as reliable serological markers and standardisation of analytical and technical strategies [106]. Additionally, determination of antibody longevity in response to *P. vivax* will also provide important insights into the development of antibody responses and the long-term impacts on immune status following exposure or intervention, which remains largely understudied [264, 265].

Overall, it can be concluded that immune responses elicited in response to *Plasmodium* infections facilitate parasite clearance by targeting primarily the blood stage of the infection. Additionally, it has been indicated that this immunity can be dampened by *Plasmodium* parasites as a strategy to escape immune recognition. Despite this, adaptive immunity, including immunological memory responses, has been the focus of research to promote clinical protection

(through vaccination). In addition, *Plasmodium*-specific antibody responses can be utilised as a promising tool to overcome current surveillance and diagnostic challenges. Further research is required to establish a standardised and valid application of this tool in order to achieve significant impact in malaria control and elimination.

1.3 Factors affecting immunity in human

As established in the previous Section, *Plasmodium*-specific naturally acquired immunity plays a pivotal role in protection against clinical symptoms. It has also been of major interest for potential application in the optimisation and development of current vaccines and surveillance tools. To be used for these applications, it is important to identify determinants of immune responses. Therefore, in this Section, I have reviewed multiple prior studies focussing on potential factors that can influence immunity in humans, including the longevity of responses. These factors can be roughly divided into three categories: intrinsic, environmental and antigenic factors.

1.3.1 Intrinsic host and demographic factors

Determining the effect of intrinsic factors on immunity is challenging as they are closely inter-related to each other. Intrinsic factors include age, sex, ethnicity, physical conditions and genetics. For *Plasmodium* infections, age is strongly associated with the risk of morbidity [266]. This is due to the fact that age reflects the level of past exposure to malaria; older individuals have more past exposure and hence are more likely to gradually develop immunity against clinical malaria [267]. *P. vivax*-infected children have also been shown to be more susceptible to relapses [30]. This can be partially explained by the under-dosed anti-malarial treatment for children as medications are given based on age group in most malaria endemic settings [268], but could also be due to lower levels of immunity. These scenarios highlight the difficulty in determining whether differences in naturally acquired immunity are due to age or the level of past exposure. This has been partially resolved through studies of travellers to endemic areas. For instance, it has been reported that young travellers returning from malaria-endemic countries under the age of six had the highest risk of malaria infections compared to those who were older [269]. Additionally, adult transmigrants in Indonesia were shown to have higher risk of developing severe malaria than their children after acute *P. falciparum* infection [270]. However, the adults also acquired immunity faster (indicated by a more rapid reduction in

parasitaemia) than the children. These findings indicate the presence of an intrinsic age effect on immune acquisition that is independent of lifetime exposure.

The impact of sex and ethnicity on immunity against *Plasmodium* infections is poorly understood due to the fact that they can vary greatly between different demographics. For many malaria-endemic countries in Southeast Asia, the link between sex and *Plasmodium* infection is strong. Being male has been described as a major risk factor for infection as the majority of workers involved in outdoor labour and travelling are male and thus have exposure to parasite-carrying mosquitoes [271]. Biologically, it was found that sex-associated hormones led to differential B cell subsets and serum Ig levels in healthy male and female individuals, which potentially affects the immune responses after an infection [272]. Despite this, this concept has not been validated in the context of *Plasmodium* infections. Ethnicity, on the other hand, is heavily confounded by geographical regions with varying levels of transmission, engagement in outdoor activities and socio-economic status [271]. However, Torcia et al. reported unique expression profile of immune-related genes between two ethnically distinct populations in West Africa which explains the differences in susceptibility for *P. falciparum [273]*. This shows that immune responses against

Plasmodium infections can vary between ethnic groups due to differences in host genetics.

Several physical conditions have been shown to affect the capacity of an individual to react to an infection. Pregnancy (including gravidity) in women as a specific physical condition affects immunity against infections dramatically [274, 275]. More recently, it has also been reported that obesity and diabetes are significant risk factors for severe *P. falciparum* symptoms in adults [276]. Similarly, obese children after treatment exhibited a higher likelihood of new infections than children with normal body weight and below [277]. However, sub-optimal nutritional status was associated with more severe malaria-related symptoms in children [278] and infant mortality [279]. These observations demonstrate the complexity of malaria elimination, as it requires strong commitment to cultural and behavioural changes in local communities.

The effect of genetics on immunity has been highly debatable. Several prior twin studies report significant contributions from heritable factors to the variability observed in vaccine responses [280], plasma cytokine levels [281] and the proportion of major immune cell populations [282]. Some studies have identified specific genetic loci that were associated with multiple aspects of immune responses [272, 283]. Additionally, genetic components were described to be the major hurdle to achieve effective vaccines against common infectious

diseases [284]. For example, results represented from multiple genome-wide association studies show that specific variations in genes encoding for the human leukocyte antigen, calcium pumps on RBCs, signal-regulatory proteins and tight junction proteins were associated with variable vaccine responses against Epstein-Barr virus, rubella, Hepatitis B, influenza [285], tetanus [286] and severe malaria [287].

Some other studies, however, showed that the difference in early humoral responses, immune cell populations and serum protein levels were consequences of predominantly non-heritable, environmental factors [288, 289]. An example is the expression of Duffy antigen receptor for chemokine (DARC). It has been well established that DARC expressed on RBCs is utilised by *P. vivax* parasites for invasion via DBP [290]. Maestre et al. showed evidence that individuals who expressed higher level of DARC were more susceptible to *P. vivax* infections [291]. However, the cumulative level of exposure to the parasites was shown to shape the polymorphisms in DARC [292], further resulting in differences in the risk of contracting *P. vivax* malaria [293]. To date, no studies focussing on the comparison between heritable and non-heritable factors on protection against malaria have been published, making it difficult to draw appropriate conclusions.

1.3.2 Environmental factors

In the context of malaria, the most identified environmental factors associated with exposure and hence anti-malarial immunity [294] are geographical location, climate and the use of mosquito-targeted interventions and treatments [295]. As the transmission capacity of *Anopheles* mosquitoes is dependent on their breeding conditions and habitats [296, 297], geographical locations and other relevant variations (including level of exposure, terrain and seasonal changes in temperature and rainfall, the use of anti-malarial chemicals and the presence of strains resistant to interventions and treatments) are all critical contributory factors in the development of immunity [75, 89, 298, 299].

Secondly, the presence of other pathogens in the environment can have significant impact on the immune responses in humans. The cross-reactivity between *Plasmodium* and other infectious pathogens has been well documented. These include dengue virus, *Leishmania infantum*, *Nippostrongylus brasiliensis*, *Litomosoides sigmodontis*, human immunodeficiency virus and *Schistosoma* parasites [300-304]. In the above cases, the presence of cross-reactivity was defined as the *Plasmodium*-specific antibody responses elicited by other infectious organisms. Furthermore, antibody inter-species cross-reactivity was also shown in a number of studies and has been presented in two ways. The first is the cross-reactivity

in the same antigens or their homologues between different *Plasmodium* species. Specifically, evidence has shown that antibodies targeting MSP5 [305], apical asparagine-rich protein [306], AMA1 [307], sexual stage [308] and sporozoite proteins [309] were cross-reactive between a wide range of *Plasmodium* species, including *P. vivax, P. falciparum, P. knowlesi, P. cynomolgi* and *P. berghei*. On the other hand, cross-reactivity was also observed between different antigens derived from different *Plasmodium* species. For instance, anti-PvDBP antibodies were recently found to recognise the VAR2CSA protein derived from *P. falciparum* which is involved in regulating cytoadherence of RBCs to the placenta [310], although this finding has been controversial [311].

Together these results show that multiple environmental factors contribute to the transmission level of malaria and the potential presence of cross-reactivity, and therefore partially control the immune responses in *Plasmodium*-infected individuals.

1.3.3 Antigenic factors

The notion that antigenic factors may contribute to host immune response modulation has only been extensively explored in recent years. Antigenic

variation, antigen-specific features and genetic diversity in antigens are the three key focuses of research in this field.

Antigenic variation refers to the expression of variant proteins on the surface of iRBCs by *Plasmodium* parasites [312]. The best-known example of this is *var* and *vir* gene families of *P. falciparum* and *P. vivax*, respectively. The *vir* gene family of *P. vivax* is the largest multigene family in the *Plasmodium* species, containing 600 to 1000 copies of genes [313, 314]. Similar to their *P. falciparum* counterpart, *vir* genes undergo frequent recombination and subsequent transcription [315], contributing to antigenic variation and cytoadherence of iRBCs on host endothelial cells [316, 317]. These features ultimately promote immune evasion and parasite survival [316]. More importantly, Requena et al. have shown that proteins encoded by *vir* genes are targeted by naturally acquired antibody and T cell responses [318]. Given that the *vir* gene family directly contributes to the generation of multiple variants to evade immunity, it has been proposed that the level of past exposure could be critical for the development of immunological responses [289]. This is because an individual could have a greater chance of developing immunity against multiple variants if they have more past exposure.

Some antigenic features have been reported to link to immune responses against pathogens, but research in this field has been scarce. The current studies primarily focus on two main areas: the presence of extracellular elements in an

antigen and the production of secreted proteins by a pathogen. In the study published by Liu et al., *P. falciparum*-derived antigens with extracellular components were more likely to induce stronger total IgG reactivity compared to intracellular antigens [319]. Similarly, Guy et al. observed in *P. falciparum* that antigens with amino acid residues exposed on the surface were major targets of host humoral immunity [320]. However, whether or not the same observation can be made in *P. vivax* remains undetermined. Additionally, there is still a lack of evidence to inform whether or not extracellular antigens are the targets of cellular immunological responses. Similar to the extracellular elements, the production of secretory proteins has been shown to influence host immunity. Lucas et al. and Hewits et al. have reviewed multiple secretory proteins produced by viruses and helminths, respectively, that are involved in activating or dampening immune responses [321, 322]. This suggests that secretory proteins, like extracellular elements, can potentially be good immunological targets due to their accessibility to the immune system. From this brief review, it is evident that there is a severe lack of research that aims to identify specific antigenic features associated with *Plasmodium* parasites that will be likely to be recognised by human immune responses. This topic is further explored in Chapter 3 of this thesis.

Lastly, genetic diversity in an antigen has been the most well reported factor associated with modulation of host immunity. It is defined by the presence of allelic polymorphisms within any *Plasmodium* gene and can vary greatly between geographical regions [316, 323]. Such polymorphisms are known to be introduced by mutations and genetic recombination [316] and have been described as the major hurdle against developing effective vaccines against malaria [324, 325]. For *Plasmodium* antigens, it has been reported that they are often found in the form of single nucleotide polymorphisms (SNP) within coding sequences of T or B cell epitopes [316]. It has been proposed that such polymorphisms may allow *Plasmodium* parasites to escape immune surveillance [316]. In line with this concept, it has been demonstrated that the presence of highly polymorphic tandem repeats can mask immune responses against functionally critical epitopes [326, 327]. However, more recent studies have shown evidence that proves otherwise. Multiple studies have demonstrated that *Plasmodium* antigens with higher levels of polymorphisms are stronger targets for human host immunity and are able to induce stronger total IgG responses [319, 320]. Specifically, the number of non-synonymous SNPs was observed to be positively correlated with antigen-specific total IgG reactivity [319].

It was proposed that the high level of genetic variability in antigens could be the product of unique selection pressures exerted by the host immunity during the

process of evolution [328]. However, this concept has not been further verified in *Plasmodium* antigens. According to prior studies, *P. vivax* has a greater level of genetic diversity compared to *P. falciparum* [329-331]. These findings suggest higher level of inter-breeding between *P. vivax* strains carrying different allelic polymorphisms [331], resulting in higher intra-population variation than *P. falciparum*. Additionally, the fact that *P. vivax* has been described as a species older than *P. falciparum* [332] means *P. vivax* has more genetically differentiated populations and higher inter-population variation. Together, these results indicate that *P. vivax* is more likely to rapidly adapt to newly introduced environmental changes [331].

Nevertheless, very little is known about the potential association between genetic polymorphisms and immune responses against *P. vivax*. To date, as the need of an efficacious malaria vaccine has become clear, identification of immunological relevant polymorphisms in antigenic candidates will be critical for the selection of potential new targets and understanding the performance of multivalent or chimeric vaccines [333].

1.4 Thesis aims

From the review above, it shows the urgent need to eliminate *P. vivax* in the era of declining transmission. It is equally crucial to develop innovative control measures to overcome major challenges unique to this parasite, particularly the detection and treatment of asymptomatic populations and individuals harbouring hypnozoites. Serological measurement has been considered as an approach to monitor individual immune status, past and recent exposure to *Plasmodium* parasites and local transmission level. However, the lack of longitudinal studies with intensive follow-up makes it difficult to harness the antibody responses for clinical applications. Additionally, majority of the current studies have only focussed on a limited number of traditional antigens, posing significant challenge to explore new targets.

To address these key knowledge gaps, the present study endeavours to characterise naturally acquired antibody responses, and their longevity, against a large panel of *P. vivax* antigens in both symptomatic and asymptomatic longitudinal cohorts in western Thailand with low malaria transmission. Furthermore, I aim to explore the association between antigenic diversity and *P. vivax*-specific antibody responses. Together these aims will provide deeper understandings of the development and maintenance of antibody responses,

which will ultimately guide control and intervention strategies that are based on harnessing the immune system.

Aim 1: To optimise a multiplexed bead-based assay for antibody measurements against 52 *P. vivax* antigens (Chapter 3)

Aim 2: To define antigen-specific total IgG, IgG subclasses and IgM kinetics following a *P. vivax* infection and to identify relevant antigenic features (Chapter 4)

Aim 3: To determine the impact of sequence genetic diversity on *P. vivax*-specific antibody kinetics (Chapter 6)

Aim 4: To establish an antigen-specific memory B cell ELISpot (Chapter 5)

Chapter 2. Materials & Methods

2.1 Study populations

In this thesis, blood samples have been used from multiple different sources. Plasma samples were used from three cohort studies conducted in malaria-endemic areas (Thai symptomatic, Brazilian symptomatic, Thai asymptomatic), as detailed below. Peripheral blood mononuclear cells (PBMCs) were also sourced from a sub-set of volunteers in the Thai symptomatic study. In addition, plasma samples were also used from three panels of malaria-naïve negative controls. Two of these panels were sourced locally from Melbourne, Australia (from the Red Cross and the Volunteer Blood Donor Registry (VBDR)) and one from Bangkok, a non-malaria endemic area of Thailand. PBMCs were also obtained from a sub-set of the VBDR donors. Plasma samples from all sources and PBMCs from the Thai symptomatic cohort were already collected prior to the start of this thesis by colleagues and collaborators. PBMCs from the VBDR were collected as part of this thesis.

The Thai symptomatic longitudinal study in Tha Song Yang, Tak Province, was approved by The Ethics Committee of the Faculty of Tropical Medicine, Mahidol University, Thailand (MUTM 2014-025-01 and -02). For the Thai asymptomatic cohort study in the Kanchanaburi and Ratchaburi provinces, collection of samples was approved by The Ethics Committee of the Faculty of Tropical

Medicine, Mahidol University, Thailand (MUTM 2013-027-01). The Human Research Ethics Committee (HREC) at the Walter and Eliza Hall Institute of Medical Research (WEHI) approved the use of these samples in Melbourne (#14/02). The collection and/or use of the three malaria-free control panels in Melbourne were approved by the HREC at WEHI (#14/02).

2.1.1 Thai symptomatic cohort

34 Thai patients with confirmed *P. vivax* infection (see Table 2.1) were enrolled in a nine-month longitudinal study in Tha Song Yang, Tak Province, Thailand, as previously described [112]. These individuals were a sub-set from a larger study [334], and selected due to the absence of recurrent *Plasmodium* infections during follow-up. Chloroquine and primaquine were administered according to Thai national guidelines upon confirmation of infection. Blood samples were collected via finger prick at 17 time points during follow-up: time of infection (week 0), week 1, week 2, then every fortnight for 6 months, then every month until nine months. Samples were processed into red blood cell pellets and plasma at the field-site. Whether or not the study participants had an infection was determined by regular assessment via light microscopy and *Plasmodium* species-specific qPCR (QMAL) whenever blood samples were taken [335]. An estimate

of past malaria history was obtained by self-reported questionnaire. PBMCs were collected at weeks 1, 12, 24 and 36 only.

2.1.2 Brazilian symptomatic cohort

Blood samples from 33 volunteers were used from a longitudinal study conducted in Manaus, Brazil (see Table 2.1), with the same study design as the Thai symptomatic cohort, as previously described [108]. The individuals had a symptomatic *P. vivax* infection at enrolment and were followed up for nine months at 17 time points and had no recurrent infections during the study, with infection status determined by PCR as per the Thai study. No PBMCs were available for this cohort. These volunteers were also a sub-set of a larger longitudinal study as described previously [108].

2.1.3 Thai asymptomatic cohort

30 individuals with asymptomatic *P. vivax* infections were selected from a larger longitudinal observational cohort study conducted in the Kanchanaburi and Ratchaburi Provinces of western Thailand between 2013 and 2014 [265]. Blood samples were collected via finger prick at enrolment and approximately every month for 14 months (a total of 14 visits). The 30 participants (see Table 2.1)

were detected as *P. vivax*-positive by PCR at early time-points (between enrolment and 6 months) of this yearlong study, and each volunteer had at least six samples available post-infection. The infections were classified as asymptomatic as the individuals had no self-reported fever or other malaria symptoms at the time of infection.

Table 2.1 Demographic characteristics of the three study populations

Cohort	Thai symptomatics (n=34)	Brazilian symptomatics (n=33)	Thai asymptomatics (n=30)
Symptoms	Symptomatic	Symptomatic	Asymptomatic
Age (years)[a]	29 (7-71)	37 (16-56)	26.5 (4-72)[b]
Proportion male	58.8%	78.8%	63.3% [b]
Study duration	9 months	9 months	14 months
Time points with antibody measurements	17	17	10 - 14
P. vivax infection[c]	Enrolment (w0)	Enrolment (w0)	Enrolment – 6 months
Recurrent infection	No	No	No
Parasite density at enrolment (copies/μL) [a, c]	2.5×10^5 (2.85×10^4 – 6.84×10^6)	3.74×10^2 (1.01×10^1 – 3.04×10^5)	1.03×10^2 (2.44×10^{-1} –9.58×10^5)

[a] Data are shown as median and range

[b] No age or gender data available for four asymptomatic individuals (N219006, N254001, N398003 and N402007)

[c] Indicated by positive *P. vivax*-specific qPCR or PCR results.

2.1.4 Negative control panels

Plasma samples of 274 malaria-naïve volunteers from the Australian Red Cross (ARC, n=100) in Melbourne, Australia, the Thai Red Cross (TRC, n=72) in Bangkok, Thailand and VBDR (n=102) in Melbourne, Australia, were collected. PBMCs were also collected from a sub-set of the VBDR donors (n = 23). These malaria-naïve individuals have very little chance of having had a past malaria infection as there is no malaria transmission in Australia or Bangkok, Thailand. Specifically, blood donors from Melbourne with travel history to malaria-endemic countries and any autoimmune-related conditions were excluded from the panel based on self-reported questionnaires. To be eligible as a blood donor in Australia, the individual is required to be aged between 18 – 75 years and with no recent tattoos, operations, pregnancy, specific health conditions and use of medication. Any overseas travel history in the past four months and with a risk of contracting infectious diseases is also investigated prior to donation [336, 337]. Blood donation guidelines in Thailand are similar to Australia, with the exception where individuals aged between 17 – 70 years can donate. In addition, people with no recent piercings or vaccinations are also allowed to donate blood to the TRC [338].

2.2 PBMC isolation

Blood samples donated to the VBDR at WEHI were regularly collected and processed into plasma and PBMC samples, which were stored until used as controls in various assays. For collection of PBMCs, approximately 9mL of whole venous blood was centrifuged at 300×g for 10 minutes after which the top layer consisting of plasma was transferred to microcentrifuge tubes for storage at -80°C. The remaining blood was diluted in 1:1 ratio with D-PBS. The diluted blood was then carefully layered on top of 10mL of lymphoprep. Subsequently the tube was centrifuged for 30 minutes at 800×g during which mononuclear cells were separated from granulocytes and erythrocytes due to the lower density. The PBMCs formed a white band of precipitate between the sample and medium, and were collected and further diluted with D-PBS. The mixture was then centrifuged at 300×g for 10 minutes and the supernatant removed to complete the 1st washing step. PBMCs were washed twice before incubation with 2mL of RBC lysis buffer for two minutes. After incubation, the mixture was diluted with PBS before centrifugation, which was followed by another wash. The PBMC pellet was then resuspended in 1mL PBS and cell counting performed via haemocytometer. PBMCs were again pelleted and resuspended in half a cryovial of 100% cosmic calf serum (CCS). An equal volume of 20% dimethyl sulfoxide in CCS was then added to the mixture dropwise. The cells were then transferred

to cryovials, 1mL per vial, which were immediately placed in a pre-cooled freezing module and kept at -80°C overnight. Afterwards the cells were transferred to liquid nitrogen for long-term storage.

2.3 *P. vivax* antigen selection and expression

2.3.1 Antigen panel

A total of 53 *P. vivax* antigens were used to capture *P. vivax*-specific antibody responses. These antigens were selected as they are either serological marker or vaccine candidates. Among them, 40 antigens were produced by CellFree Sciences Co., Ltd. (CFS) in Tokyo, Japan, and 13 additional *P. vivax* antigens were given as a gift from A/Prof Wai-Hong Tham, Prof Alan Cowman at WEHI, Melbourne, Australia, and Prof Chetan Chitnis at Institut Pasteur, Paris, France. The 40 CFS antigens were down-selected from a preliminary 'antigen discovery' study in which antigen-specific antibody responses were measured using a bead-based high-throughput assay known as AlphaScreen®. These antigens were selected based on their ability to accurately classify recent exposure. The Section below briefly outlines the down-selection process. The remaining 13 antigens are vaccine candidates described in the literature, for either *P. vivax* or *P.*

falciparum (with the *P. vivax* orthologs used in this thesis). The full list of the 53 *P. vivax* antigens is shown in Table 2.2.

Table 2.2 Information on the 52 *P. vivax* antigens selected for this study.

Antigen ID[a]	Gene Annotation	Stage of Expression	Protein Length (aa)	Construct, aa (size)	Expression System	Purification Method	Amount (μg)[d]
PVX_099980	merozoite surface protein 1 (MSP1) $MSP1_{19}$	Blood	1751	1622-1729 (108)	WGCF	AC	0.76
PVX_096995	tryptophan-rich antigen (Pv-fam-a)	Blood	480	61-end (420)	WGCF	AC	0.85
PVX_088860	sporozoite invasion-associated protein 2 (SIAP2)	Blood, Liver	412	33-end (380)	WGCF	AC	0.95
PVX_101530	*Plasmodium* exported protein, unknown function	Blood	367	38-end (330)	WGCF	AC	0.025
PVX_112680	tryptophan/threonine-rich antigen	Blood	313	33-end (281)	WGCF	AC	1.2
PVX_097715	hypothetical protein	Blood	450	20-end (431)	WGCF	AC	0.35
PVX_094830	hypothetical protein, conserved	Blood	250	19-end (232)	WGCF	AC	0.69
PVX_112675	tryptophan-rich antigen (Pv-fam-a)	Blood	312	33-end (280)	WGCF	AC	0.47
PVX_112670	tryptophan-rich antigen (Pv-fam-a)	Blood	335	34-end (302)	WGCF	AC	1.13
PVX_090970	hypothetical protein, conserved	Unknown	266	20-254 (235)	WGCF	AC	2
PVX_084720	translocon component PTEX150 (PTEX150)	Blood	908	24-908 (885)	WGCF	AC	0.12
PVX_003770	merozoite surface protein 5	Blood	387	23-365 (343)	WGCF	AC	0.025
PVX_092990	tryptophan-rich antigen (Pv-fam-a)	Blood	1414	1126-1414 (289)	WGCF	AC	2.6
PVX_091710	hypothetical protein, conserved	Blood	1689	26-884 (859)	WGCF	AC	0.22
PVX_087885	rhoptry associated membrane antigen, putative	Blood	730	462-730 (269)	WGCF	AC	0.15
PVX_003555	*Plasmodium* exported protein, unknown function	Blood	1122	434-1075 (642)	WGCF	AC	0.025
PVX_117385	phosphatidylinositol-4-phosphate-5-kinase	Blood	326	1-326 (326)	WGCF	AC	1

Antigen ID[a]	Gene Annotation	Stage of Expression	Protein Length (aa)	Construct, aa (size)	Expression System	Purification Method	Amount (μg)[d]
PVX_090265	tryptophan-rich antigen (Pv-fam-a)	Blood	326	1-326 (326)	WGCF	AC	0.5
PVX_082700	merozoite surface protein 7	Blood	420	23-end (397)	WGCF	AC	0.5
PVX_082650	merozoite surface protein 7	Blood	453	24-end (429)	WGCF	AC	0.35
PVX_094255A[c]	reticulocyte binding protein 2b (RBP2b)	Blood	2806	1986-2653 (667)	WGCF	AC	0.7
PVX_097680	merozoite surface protein 3β	Blood	1016	21-end (996)	WGCF	AC	0.15
PVX_001000	hypothetical protein	Unknown	668	20-end (650)	WGCF	AC	0.5
PVX_097625	merozoite surface protein 8	Blood	487	24-463 (440)	WGCF	AC	0.175
PVX_082670	merozoite surface protein 7	Blood	411	24-end (388)	WGCF	AC	0.5
PVX_099930	high molecular weight rhoptry protein-2	Blood	1369	23-387 (365)	WGCF	AC	0.5
PVX_084340	IMP-specific 5'-nucleotidase	Unknown	444	1-444 (444)	WGCF	AC	0.65
PVX_098915	subpellicular microtubule protein 1 (SPM1)	Unknown	521	1-521 (521)	WGCF	AC	1
PVX_088820	tryptophan-rich antigen (Pv-fam-a)	Blood	316	58-end (259)	WGCF	AC	8
PVX_082735	PvTRAP/SSP2	Liver	556	26-493 (468)	WGCF	AC	0.5
PVX_082645	merozoite surface protein 7	Blood	377	23-end (355)	WGCF	AC	0.46
PVX_117880	rhoptry neck protein 2, putative (RON2)	Blood, Liver	2203	21-198 (178)	WGCF	AC	0.75
PVX_121897	tryptophan-rich antigen (Pv-fam-a)	Unknown	275	24-end (252)	WGCF	AC	4
PVX_125728	tryptophan-rich antigen (Pv-fam-a)	Unknown	279	30-end (250)	WGCF	AC	16
PVX_090330	reticulocyte binding protein 2 precursor (PvRBP-2)	Blood	623	31-141 (111)	WGCF	AC	0.4
PVX_123685	histone-lysine N-methyltransferase	Blood	1963	1320-end (644)	WGCF	AC	0.65
PVX_125738	reticulocyte binding protein 1 precursor	Blood	786	1-786 (786)	WGCF	AC	0.5

Antigen ID[a]	Gene Annotation	Stage of Expression	Protein Length (aa)	Construct, aa (size)	Expression System	Purification Method	Amount (µg)[d]
PVX_097720	merozoite surface protein 3α	Blood	852	25-end (828)	WGCF	AC	0.125
PVX_000930	sexual stage antigen s16	Blood, Sexual	140	31-end (110)	WGCF	AC	0.25
PVX_098585	reticulocyte binding protein 1a (RBP1a)	Blood	2833	160-1170 (1011)	*E. coli*	AC ×2, SEC	0.6
PVX_098582	reticulocyte binding protein 1b (RBP1b)	Blood	2608	140-1275 (1136)	*E. coli*	AC ×2, SEC	0.8
PVX_121920	reticulocyte binding protein 2a (RBP2a)	Blood	2487	160-1135 (976)	*E. coli*	AC ×2, SEC	0.9
PVX_094255B[c]	reticulocyte binding protein 2b (RBP2b)	Blood	2806	161-1454 (1294)	*E. coli*	AC ×2, SEC	0.1
PVX_090325	reticulocyte binding protein 2c (RBP2c non-binding region)	Blood	2824	501-1300 (800)	*E. coli*	AC ×2, SEC	0.3
PVX_101590	reticulocyte-binding protein 2 (RBP2), like (RBP2-P2)	Blood	641	161-641 (481)	*E. coli*	AC ×2, SEC	1
PVX_110810A[c]	Duffy binding protein (DBP, region 3-5, Sal1 strain)	Blood	1070	193-521 (329)	*E. coli*	AC	0.2
PVX_090240	cysteine-rich protective antigen, putative (CyRPA)	Blood	366	27-366 (340)	Baculovirus	AC, SEC	0.5
PVX_088910	GPI-anchored micronemal antigen, putative (GAMA)	Blood	771	22-551 (530)	*E. coli*	AC ×2	0.6
PVX_095055	Rh5 interacting protein, putative (Ripr)	Blood	1075	552-1075 (524)	*E. coli*	AC ×2, SEC	0.5
PVX_110810B[c]	Duffy binding protein (DBP, region 2, Sal-1 strain)	Blood	1070	193-521 (329)	*E. coli*	AC, IEC, SEC	0.36
AAY34130.1[b]	Duffy binding protein (DBP, region 2, AH strain)	Blood	237	1-237 (237)	*E. coli*	AC, IEC, SEC	0.45
KMZ83376.1[b]	PvEBPII	Blood	786	109-432 (324)	*E. coli*	AC, IEC, SEC	0.1

[a] PlasmoDB codes (http://plasmodb.org/plasmo/), [b] GenBank codes, [c] A and B represent two distinct antigen fragments derived from one full-length antigen sequence and hence are expressed by identical PlasmoDB code, [d] Amount refers to the amount of antigen coupled to non-magnetic microspheres

Abbreviations: WGCF = wheat germ cell-free; AC = affinity chromatography; SEC = Size exclusion chromatography; IEC = ion exchange chromatography

2.3.2 Antigen down-selection following antigen discovery study using AlphaScreen®

The preliminary antigen discovery study has been previously described [112] and was used to down-select *P. vivax* antigens for this antibody kinetics project. In brief, antibody responses over time in Thai and Brazilian symptomatic cohorts were measured against a large panel of 307 *P. vivax* antigens on the automated AlphaScreen® platform. This panel consisted of traditional vaccine candidates, *P. falciparum* orthologues and novel targets containing transmembrane domains and/or signal peptides. These constructs were expressed as crude proteins using the wheat-germ cell-free (WGCF) system [108, 339]. Crude proteins are defined as proteins that did not undergo affinity purification process. Antibody responses were measured at four time points: w0 (enrolment), w12, w24 and w36 and the antigen-specific half-lives for both cohorts were estimated using mixed-effect linear regression models. Down-selection was performed based on seropositivity and the similarity of estimated half-lives between the cohorts, as well as the level of accuracy in predicting the time since last infection (w0). 60 candidates were selected, with 40 successfully expressed as purified antigens using the WGCF.

2.3.3 Serological marker targets – protein expression and purification

The 40 serological marker targets produced by CFS were expressed using a WGCF system as previously described [112]. Following expression, a one-time purification step was performed using a His-tag, after which an estimation of protein yield and solubility was made. One protein, PVX_002550 (annotated as liver-stage antigen 3), was unable to be expressed at a high yield and hence was excluded from further experiments and analyses. All antigens were prepared in 10% v/v glycerol (20mM Na-phosphate at pH 7.5, 0.3M NaCl and 500mM imidazole) and delivered in four separate batches (approximately 13 antigens per batch) to WEHI, and hence were optimised in batches at WEHI. Most constructs included the full-length of the protein, as detailed in Table 2.2.

2.3.4 Traditional vaccine targets – protein expression and purification

In addition to the candidate serological marker antigens, a total of 13 *P. vivax* antigens (potential vaccine candidates) were kindly provided for this study as previously mentioned. These included six RBPs (RBP1a, RBP1b, RBP2a, RBP2b, RBP2c-NB and RBP2-P2), three DBPs (DBP region 3-5, DBP region II AH strain, DBP region II Sal-I strain), glycosylphosphatidylinositosl-anchored micronemal

antigen (GAMA), Rh5-interacting protein (Ripr), cysteine-rich protective antigen (CyRPA) and EBP. Antigens were expressed with Baculovirus or *Escherichia coli* (*E. coli*) expression systems, followed by purification with hexa-histidine tags (see Table 2.2 for detail). RBP2c fragment was expressed without the erythrocyte–binding domain and hence was referred to as RBP2c-NB (NB for non-binding domain). 50-100µg of all antigens, except for Ripr and DBP R3-5, was supplied in 10% glycerol and kept at -80°C. Ripr was supplied in PBS and DBP R3-5 in 2mM Tris-NaCl, pH8.

2.4 Antigen conjugation to microspheres

In this thesis, antibody responses were detected using a multiplexed bead-based assay, which first required conjugation of antigen to microspheres.

2.4.1 Optimisation

Due to the varying stability, concentration and immunoreactivity of different *P. vivax* proteins, optimisations were performed in which the amount of protein coupled to the microspheres was adjusted individually. For optimisation, the amount of microspheres and all reagents were reduced to a trial volume compared

to the bulk volume used for the final preparation. All other steps were the same as for bulk conjugations, as detailed below. The microspheres were kept in the dark at all times to avoid bleaching.

2.4.2 Conjugation

The protocol for protein coupling to microspheres has been described previously [219]. In brief, for day 1 of the protocol, the COOH microspheres (Bio-Rad Laboratories, Inc.) were first sonicated and vortexed before being transferred into microcentrifuge tubes. The microspheres were then centrifuged at 14000×g for 2 minutes to allow supernatant removal. The pellets were well resuspended in Milli-Q H2O and were again centrifuged for a minute to wash off buffer. Subsequently, to activate the microspheres, 100mM monobasic sodium phosphate was added to resuspend the pellet, followed by thorough vortexing. 50mg/mL N-hydroxysulfosuccinimide (sulfo-NHS) and 50mg/mL N-Ethyl-N'-(3-dimethylaminopropyl)carbodiimide hydrochloride (EDC) were added separately into the mixture, each followed by gentle vortex. The microspheres were then incubated on rotator at room temperature for 20 minutes in the dark. After incubation, the microspheres were pelleted by centrifuged, followed by two washes with 1×PBS and resuspension with 1×PBS. For optimisation, 0.5µg of each protein

as a starting amount was added to the mixture in PBS (total volume 250µL), after which the mixture was incubated either at 4°C overnight or at room temperature for 2 hours.

On day 2 (or after 2-hour incubation), the microspheres coupled with target proteins were washed three times with PBS-TBN (phosphate-buffered saline (PBS), 0.1% bovine serum antigen (BSA), 0.02% Tween-20, 0.05% azide, pH 7.4, store at 4°C). After the final removal of supernatant, microspheres were resuspended in PBS-TBN (112.5µL for trial and 500µL for bulk), vortexed well and kept at 4°C until use. Protein-coupled microspheres were finally tested for their ability to detect a positive control pool of plasma, as detailed in Section 4.1 below. The amount of antigen coupled to the microspheres was finely adjusted based on whether or not a log-linear standard curve was achieved. The final optimised amount of each *P. vivax* antigens used for the subsequent experiments is recorded in Table 2.2.

2.5 Antibody measurement on the Luminex® platform

The Luminex® was used to measure antibody levels in a multiplex format by incubating plasma samples with various *P. vivax* antigens (previously conjugated to microspheres, see 2.4.2). A schematic representation of this assay is shown in

Figure 2.1. Prior to commencing experiments with plasma samples, the standard curve of each type of antigen-coupled microspheres was checked using pooled plasma from hyper-immune PNG individuals as a positive control to ensure log-linearity.

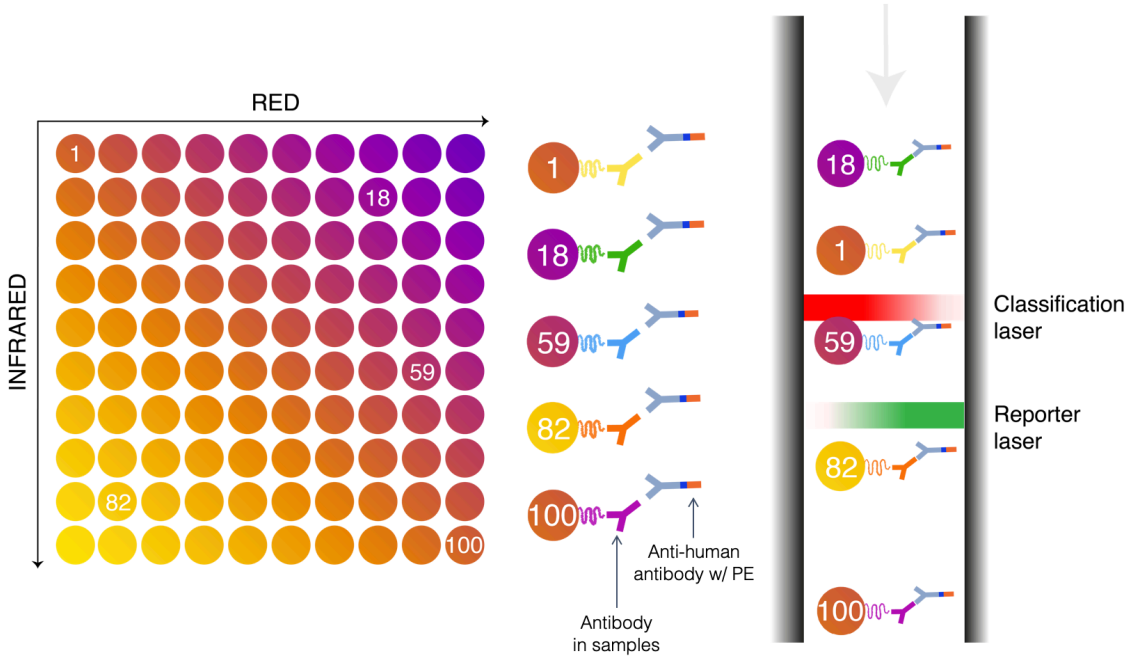


Figure 2.1 Schematic illustration of the Luminex® technology. Polystyrene microspheres that are differentially coloured with two fluorescent dyes are conjugated with different proteins. Conjugated microspheres are passed through the channel and excited by the reporter (525nm) and classification (635nm) lasers which quantifies the signals of fluorochrome attached on the detection secondary antibodies and allocates the signals to specific colours of microspheres, respectively.

2.5.1 Total IgG

IgG antibody measurements were performed at all 17 time points. Total IgG was measured as previously described [340]. Briefly, a plate-specific standard curve was prepared by 2-fold serial dilution with PNG pooled plasma from 1:50 to 1:25,600 on a 96-well plate. For test plasma samples, 1µL was individually transferred to one well and diluted 1:100 with PBT (1×PBS, 1% BSA, 0.05% Tween-20). An equal volume of microsphere mixture consisting of 0.1µL of each type of bead for each well was added to the diluted plasma and was incubated for 30 minutes at room temperature in the dark on a shaker. Following incubation, supernatant was removed and microspheres were washed with PBT three times. Microspheres were subsequently resuspended in phycoerythrin (PE)-conjugated donkey F(ab')2 anti-human IgG secondary antibody (1mg/mL, Jackson Immunoresearch) solution at a 1:100 ratio, followed by incubation for 15 minutes. Afterwards, microspheres were again washed three times and resuspended in PBT for sample acquisition on a BioPlex-200® or Luminex-200® instrument. The same sample preparation procedure as above was followed for each plate of samples, which were run in duplicate. Samples collected at the same timepoint were run on the same plate.

2.5.2 IgM

IgM antibody measurements were performed at all 17 time points and positivity was determined at the peak of response (1-week post-infection). The same multiplexed assay was used as described above for total IgG, with the following modifications: samples were diluted at 1:200 and donkey F(ab')2 anti-human IgM $Fc_{5\mu}$ at 1:400 dilution (1 mg/ml, Jackson ImmunoResearch Laboratories, Inc.) was used as the secondary antibody for detection. Samples were run in singlet. This assay was optimised as part of this thesis.

2.5.3 IgG subclasses

To investigate the IgG subclass profile, measurements were performed at 7 time points: w0, w2, w4, and then every 8 weeks until 9 months. Week 2, rather than peak responses at week 1, was selected due to plasma availability. Again, the multiplexed assay was used, with the following modifications. To maximise signals and minimise non-specific background, samples were diluted at 1:50 and antigen-coupled microspheres were incubated with secondary antibody diluted at 1:100: mouse anti-human IgG1 hinge (0.1 mg/mL, clone 4E3, SouthernBiotech); IgG2 Fc (0.1 mg/mL, clone HP6002, SouthernBiotech); IgG3 hinge (0.1 mg/mL clone HP6050,

SouthernBiotech); IgG4 Fc (0.1 mg/mL, clone HP6025, SouthernBiotech) [219]. Samples were run in singlet.

2.5.4 Unit conversion

The results of antibody measurements on the Luminex-200® platform were expressed in median fluorescence intensity (MFI). For each independent experiment, results in MFI were converted into relative antibody units (RAU) for standardisation against the positive control. Conversion was performed based on 5-parameter logistic regression model established by Dr Connie SN Li Wai Suen run in the program R [219].

2.6 Antibody kinetics model

The mathematical modelling that described the decay of antibody responses following infections was developed by Dr Michael White at the Institut Pasteur. The process of model development is outlined below.

Following infection, we assume that the proliferation and differentiation of B cells leads to a boost in antibody secreting cells (ASC) of size β, commencing at a time δ before the first sample. A proportion ρ of these ASCs are assumed to be short-lived

with half-life d_s, with a proportion $1-\rho$ being long-lived with half-life d_l. It is assumed that all ASCs secrete IgG molecules which decay with a half-life d_a. The antibody level of an individual at time t after first sample is given by:

$$Ab_j(t) = Ab_0 e^{-r_l t} + \beta_j \left(\rho_j \frac{e^{-r_s(t-\delta)} - e^{-r_a(t-\delta)}}{r_a - r_s} + (1-\rho_j) \frac{e^{-r_l(t-\delta)} - e^{-r_a(t-\delta)}}{r_a - r_l} \right)$$

where $r_a = \log(2)/d_a$ is the rate of decay of IgG molecules, $r_s = \log(2)/d_s$ is the rate of decay of short-lived plasma B cells, and $r_l = \log(2)/d_l$ is the rate of decay of long-lived plasma B cells. It is assumed that the measured antibody level before vaccination was Ab_0 which decays exponentially at rate r_l.

2.6.1 Fitting the model to data

The model was fitted to longitudinal antibody level measurements from all participants. Mixed effects methods were used to capture the natural variation in antibody kinetics between individual participants, whilst estimating the average value and variance of the immune parameters across the entire population of individuals. The models were fitted in a Bayesian framework using Markov Chain Monte Carlo (MCMC) methods. Mixed effects methods allow individual-level parameters to be estimated for each participant separately, with these individual-level (or mixed effects) parameters being drawn from global distributions. For example, for each participant

n the half-life of the short-lived ASCs may be estimated as d_s^n (an individual-level parameter). These N estimates of the local parameters d_s^n will be drawn from a probability distribution. A log-Normal distribution is suitable as it has positive support on $[0, \infty)$. Thus we have $log(d_s^n) \sim N(\mu_s, \sigma_s^2)$. The mean d_s and the variance Σ_s^2 of the estimates of d_s^n are given by $d_s = e^{\mu_s + \frac{\sigma_s^2}{2}}$ and $\Sigma_s^2 = \left(e^{\sigma_s^2} - 1\right) e^{2\mu_s + \sigma_s^2}$. The relationship between the parameters describing the population-level distribution and the parameters for each individual in the population are depicted in the schematic diagram in Figure 2.2.

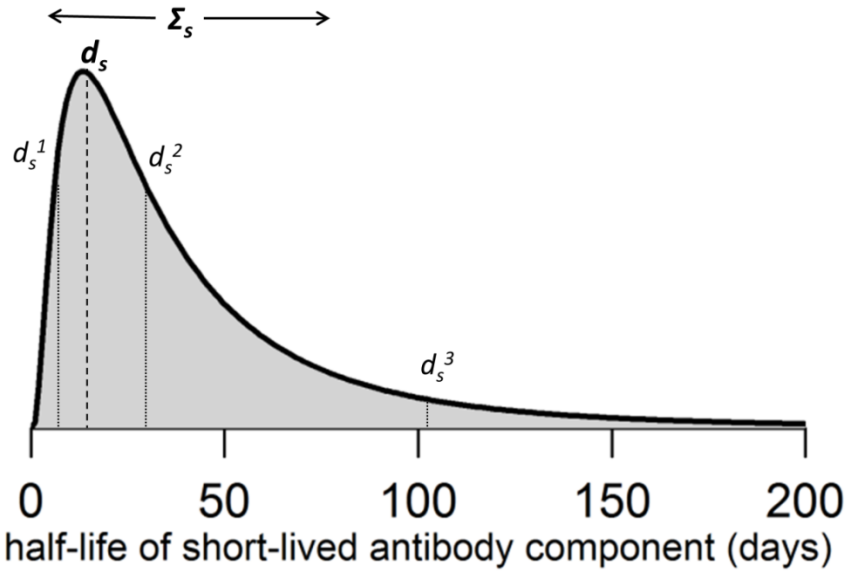


Figure 2.2 Schematic representation of the relationship between the population-level and individual-level parameters for the half-life of the short-lived ASCs. It is assumed that half-lives are log-Normally distributed throughout the population. The population-level parameters define the mean d_s and standard deviation Σ_s of this distribution. The individual-level parameters d_s^n for each of the n participants follow the log-Normal distribution defined by the population-level parameters. Three representative individual-level parameters are shown for illustration.

2.6.2 Model likelihood

For individual n we have data on observed antibody levels $A^n = \{a_1, \dots, a_K\}$ at times $T^n = \{t_1, \dots, t_K\}$. We denote $D^n = (A^n, T^n)$ to be the vector of data for individual n. For individual n, the parameters Ab_0^n, β^n, δ^n, d_s^n , d_l^n , d_a^n and ρ^n are estimated. These parameters are denoted $\theta^n = \{Ab_0^n, \beta^n, \delta^n, d_s^n, d_l^n, d_a^n, \rho^n\}$. The model predicted antibody levels will be $\{A(t_1), A(t_2), \dots, A(t_K)\}$. We assume log-Normally distributed measurement error such that the difference between $\log(a_j)$ and $\log(Ab(t_j))$ is Normally distributed with variance σ_{obs}^2. For model predicted antibody levels $Ab(t_j)$ the data likelihood for individual n is given by

$$L_{mod}^n(\theta^n|D^n) = \prod_{k \in K} \frac{e^{-\frac{\left(log(a_j) - log\left(Ab(t_j)\right)\right)^2}{2\sigma_{obs}^2}}}{a_k \sigma_{obs}\sqrt{2\pi}}$$

2.6.3 Mixed effects likelihood

As described above, for each individual there are 7 parameters to be estimated: $\theta^n = \{Ab_0^n, \beta^n, \delta^n, d_s^n, d_l^n, d_a^n, \rho^n\}$. The mixed effects likelihood can be written as follows:

$$L^n_{mix}(\theta^n|D^n) = \left(\frac{e^{-\frac{\left(log(Ab_0^n)-\mu_{Ab,0}\right)^2}{2\sigma^2_{Ab,0}}}}{\sqrt{2\pi}Ab_0^n\sigma_{Ab,0}}\right)\left(\frac{e^{-\frac{\left(log(\beta^n)-\mu_{\beta}\right)^2}{2\sigma^2_{\beta}}}}{\sqrt{2\pi}\beta^n\sigma_{\beta}}\right)$$

$$\left(\frac{e^{-\frac{\left(log(d_s^n)-\mu_{d,s}\right)^2}{2\sigma^2_{d,s}}}}{\sqrt{2\pi}d_s^n\sigma_{d,s}}\right)\left(\frac{e^{-\frac{\left(log(d_l^n)-\mu_{d,l}\right)^2}{2\sigma^2_{d,l}}}}{\sqrt{2\pi}d_l^n\sigma_{d,l}}\right)\left(\frac{e^{-\frac{\left(log(d_a^n)-\mu_{d,a}\right)^2}{2\sigma^2_{d,a}}}}{\sqrt{2\pi}d_a^n\sigma_{d,a}}\right)\left(\frac{e^{-\frac{\left(log\left(\frac{\rho^n}{1-\rho^n}\right)-\mu_{\rho}\right)^2}{2\sigma^2_{\rho}}}}{\sqrt{2\pi}\rho^n(1-\rho^n)\sigma_{\rho}}\right)$$

As the proportion of the ASCs that are long-lived must be bounded by 0 and 1, the individual-level parameters ρ^n are assumed to be drawn from logit-Normal distributions. Note that the pre-existing antibody level Ab_0^n will be variable, depending on a large number of covariates such as age and past exposure. We therefore do not attempt to constrain pre-existing antibody levels using mixed effects.

2.6.4 Total model likelihood

Denote $D = \{D^1, \dots, D^N\}$ to be the vector of data for all *N* participants. We denote θ to be the combined vector of population-level parameters and individual-level parameters to be estimated. The total likelihood is obtained by multiplying the likelihood for each participant

$$L_{total}(\theta|D) = \prod_{n\epsilon N} L^n_{mix}(\theta^n|D^n)L^n_{mod}(\theta^n|D^n)$$

2.6.5 Markov Chain Monte Carlo parameter update

The model was fitted to the data using MCMC methods using software for Bayesian statistical inference of non-linear mixed-effects models developed and implemented by Dr Michael White. This utilises a Metropolis-within-Gibbs sampler, whereby population-level parameters are updated using a Gibbs sampler, and individual-level and observational parameters are updated using a Metropolis-Hastings sampler.

2.7 Antigen features – data collection

To explore the potential factors defining IgG longevity and immunogenicity, six antigen features were selected for analysis: signal peptide (SP), transmembrane domain (TMD), glycosylphosphatidylinositol (GPI) anchor, *Plasmodium* exported element (PEXEL) motifs, enzyme domain and low-complexity region (LCR). The presence of these features in an amino acid sequence was predicted by Transmembrane Helices Hidden Markov Model Server version 2.0 [341], PredGPI [342], InterPro [343], PlasmoDB [344] and SEG [345].

2.8 Memory B cell ELISpot assay

I used an enzyme-linked immunospot (ELISpot) assay to examine MBC responses by quantifying the number of antigen-specific ASCs following induced differentiation of resting MBCs. Herein, ASCs were defined as IgG-producing cells present in the cell culture following re-stimulation. This assay was optimised as part of this thesis (see Chapter 5).

2.8.1 PBMC re-stimulation

An ELISpot assay was used to detect antigen-specific IgG-producing ASC populations. A schematic representation of this assay is shown in Figure 2.3. In brief, PBMCs were thawed from liquid nitrogen prior to use and resuspended in human B cell medium (RPMI 1640 with penicillin and streptomycin). For the purpose of re-stimulation of MBCs, the cell concentration was adjusted to $2x10^6$ cells/mL after cell count and distributed into 24-well culture plates (Greiner Bio-One). The re-stimulation cocktail containing human B cell medium and immunological stimulants was prepared (see list of buffers for detail recipe). The PBMC suspension and a re-stimulation cocktail were mixed in 1:1 ratio before incubation at 37°C with 5% CO_2. Due to the differences in process and storage conditions (namely, Thai PBMCs collected under field conditions and initially stored on dry ice, before being

transferred to liquid nitrogen), PBMC samples from the Thai symptomatic cohort and the VBDR were re-stimulated for 9 and 6 days, respectively.

2.8.2 Detection of ASC populations

Prior to the end of re-stimulation, 96-well ELISpot plates with 0.45um protein-binding immobilon-P membrane (Merck Millipore) were activated with 70% ethanol, washed with D-PBS and coated with appropriate reagents: D-PBS as blank background, 10µg/mL anti-human monoclonal IgG capture antibody MT91/145 (MabTech) as a positive control, 10µg/mL tetanus toxin from *Clostridium tetani* (Sigma-Aldrich) as an antigen-specific positive control, and 10 or 15µg/mL *P. vivax* antigens of interest. The process of optimising the concentration of each *P. vivax* antigen has been described in detail in Section 5.2.3, Chapter 5. Anti-human IgG capture antibody was diluted in D-PBS and tetanus toxin and *P. vivax* antigens in human B cell medium. After coating, activated ELISpot plates were incubated at 4°C for at least 18 hours in dark until use.

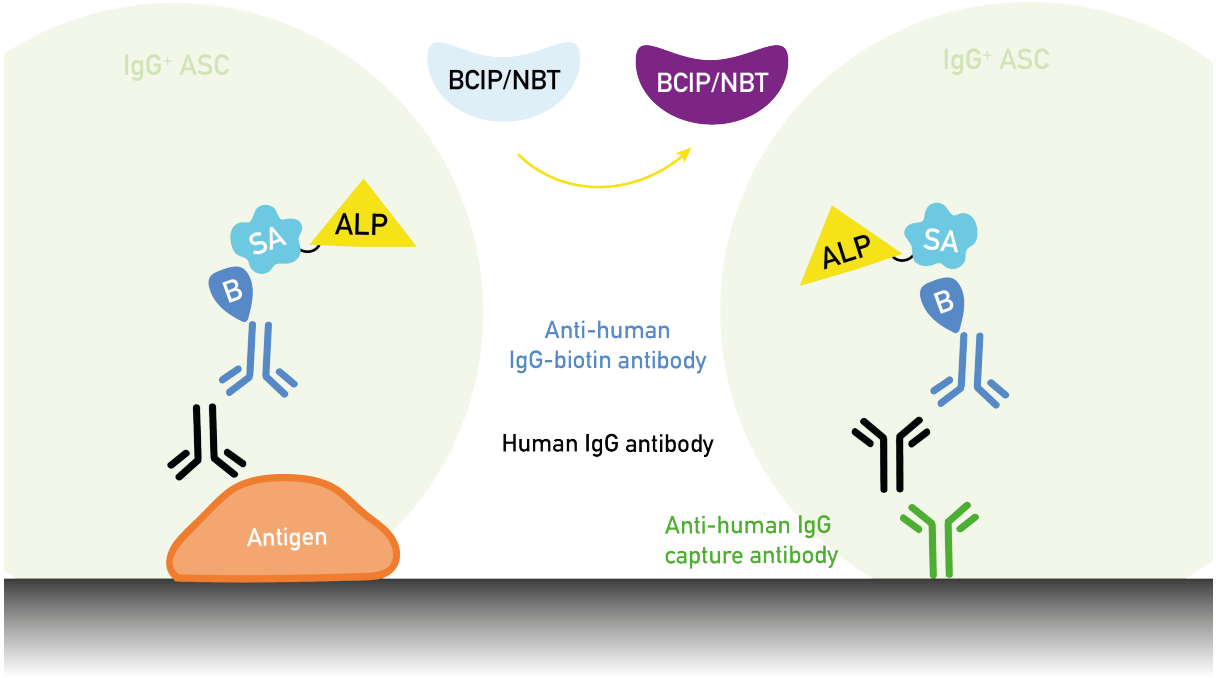


Figure 2.3 Detection of IgG-producing ASC on ELISpot. ELISpot was performed to quantify the number of IgG-producing ASC populations following re-stimulation of resting MBCs. Both antigen-specific (left) and total ASCs (right) were detected.

Abbreviations: IgG⁺ = IgG-producing; ASC = antibody-secreting cell; B = biotin; SA = streptavidin; ALP = alkaline phosphatase; BCIP = 5-Bromo-4-chloro-3-indolyl phosphate; NBT = nitro blue tetrazolium.

After re-stimulation, the ELISpot plate was first washed with D-PBST (D-PBS with 0.05% Tween-20) and D-PBS, and subsequently blocked with blocking buffer (RPMI 1640 with penicillin and streptomycin, 1% BSA) for at least two hours. Contents were discarded at the end of incubation. Before transferring to the ELISpot plate, cells were harvested and adjusted to the following concentrations with human B cell medium: 4×10^4, 1×10^4 and 2.5×10^3 cells/well for anti-IgG positive control; 4×10^4 cells/well for blank (D-PBS only); 5×10^5 and/or 2.5×10^5 cells/well for tetanus toxin and *P. vivax* antigens. Cell suspensions at appropriate dilutions were distributed across the ELISpot plate depending on the plate layout, and were subsequently incubated at 37°C with 5% CO_2 overnight. Following incubation, content of the ELISpot plate was discarded and cells were washed away with both D-PBS and D-PBST in separate steps. Secondary biotinylated anti-IgG detection antibody MT78/145 (MabTech) was diluted to 1µg/mL with D-PBST with 1% heat-inactivated foetal calf serum (HI-FCS) and was added to all wells. Plates were wrapped in cling wrap and incubated in the dark at 4°C overnight. Afterwards, detection antibody was washed away from the plate. Streptavidin-Alkaline (SA-ALP, MabTech) solution was prepared by diluting the stock SA-ALP with D-PBST with 1% HI-FCS in 1:1000 ratio. 100µl of SA-ALP solution was then added to all wells and the plate was incubated at room temperature for one hour. After incubation, SA-ALP was washed away from the plate and 100µl of the substrate mixture was added to all wells and incubated for another 45 minutes in dark at room temperature. Substrate mixture consisted of BCIP and NBT in 0.2M

Tris buffer and was prepared according to manufacturer's instruction (SeraCare Life Sciences Inc.). After developing, the plate was washed with Milli-Q water and left to completely dry in the dark overnight before reading.

2.8.3 Data processing

ELISpot plate reading was performed on an AID ELISpot plate reader and the compatible software EliSpot 7.0iSpot. Camera settings used were as follows: Brightness, 761; Sharpness, 4; White Balance (R), 372; White Balance (B), 284; Hue, 167; Saturation, 0; Shutter (Exposure), 194; Gain, 184. Count settings were set at default: Intensity, 30-255; Size ,10-5000; Gradient, 1-90; Emphasis, small. During counting, spots or stains caused by the presence of artefacts were excluded.

Following spot counting, the number of spots obtained from the positive control was adjusted to the total number of IgG^+ ASCs per 10^6 PBMCs and subsequently averaged (see Table 2.3 for calculation). The three 4-fold serial dilutions served as the replicates of the positive control due to limited number of PBMCs available. The averaged result obtained following the calculation represented the number of IgG^+ ASCs per 10^6 PBMCs.

Similar process of standardisation was performed for the spots counted in the antigen-coated wells. The cells were diluted in one or two of the four dilutions (5×10^4,

1×10^5, 2.5×10^5 or 5×10^5 cells/well) depending on the availability of the PBMCs per sample. The number of spots per well was converted into the number of antigen-specific ASCs per 10^6 PBMCs using the formulas outlined in Table 2.4 below. The purpose of having lower cell concentrations is further discussed in Section 5.2.4, Chapter 5.

Table 2.3 Calculation for the average number of ASCs per 10^6 PBMCs from the anti-IgG positive control.

	4-fold serial dilution		
Cell dilution	4×10^4 cells/well	1×10^4 cells/well	2.5×10^3 cells/well
Spot count in sample	Count 1	Count 2	Count 3
Per 10^6 PBMCs	$\frac{\text{Count 1} \times 10^6}{40\,000} = \text{A}$	$\frac{\text{Count 2} \times 10^6}{10\,000} = \text{B}$	$\frac{\text{Count 3} \times 10^6}{2\,500} = \text{C}$
Average	$\frac{\text{A+B+C}}{3}$ = __x__ ASCs per 10^6 PBMCs		

Table 2.4. Standardisation for the number of antigen-specific ASCs per 10^6 PBMCs from antigen-coated wells.

Cell dilution	5×10^4 cells/well	1×10^5 cells/well	2.5×10^5 cells/well	5×10^5 cells/well
Sample	Count 4	Count 5	Count 6	Count 7
Per 10^6 PBMCs	$\frac{\text{Count 4} \times 10^6}{50\,000} = \text{D}$	$\frac{\text{Count 5} \times 10^6}{100\,000} = \text{E}$	$\frac{\text{Count 6} \times 10^6}{250\,000} = \text{F}$	$\frac{\text{Count 7} \times 10^6}{500\,000} = \text{G}$
Final result	___D, E, F or G___ antigen-specific ASCs per 10^6 PBMCs			

* Samples were run in singlets or duplicates if the remaining amount allowed. For duplicated results, the final numbers were divided by two.

2.9 Population structure of *P. vivax* antigens

To quantify genetic diversity in antigen sequences, 19 isolate sequences from Thailand were down-selected from a global dataset and used along with a specifically developed R package.

2.9.1 Data collection

A previously published global dataset [346] with a total of 325 *P. vivax* isolates was used for population genetic analyses and the *P. vivax* P01 strain was used as the reference. The sequence data were generated by the Wellcome Trust Sanger Institute as part of the *P. vivax* Genome Variation project consisting of data obtained from various independent research groups. Figure 2.4 is a flow chart that outlines the steps involved for sample processing and analysis. Briefly, isolate sequences originated from 13 malaria-endemic countries, and were first mapped to reference strain PvP01 [347] and filtered based on various parameters. The processing step was performed by Jacob Munro from Prof Melanie Bahlo's Laboratory at WEHI. The processing step resulted in isolates that were subsequently analysed for nucleotide and haplotype diversity and global population structure. As our intention was to compare the sequence diversity

with antibody responses measured in the Thai cohorts, we only used sequence data from the 19 isolates from Thailand.

For the sample sequences to be analysed with the R package, insertions and deletions (InDels) and additional singletons were removed from the DNA sequences in Geneious version 9.1.8 (Biomatters, Ltd.). The region of each sample sequence was also trimmed in Geneious to match the antigen constructs used for antibody measurement.

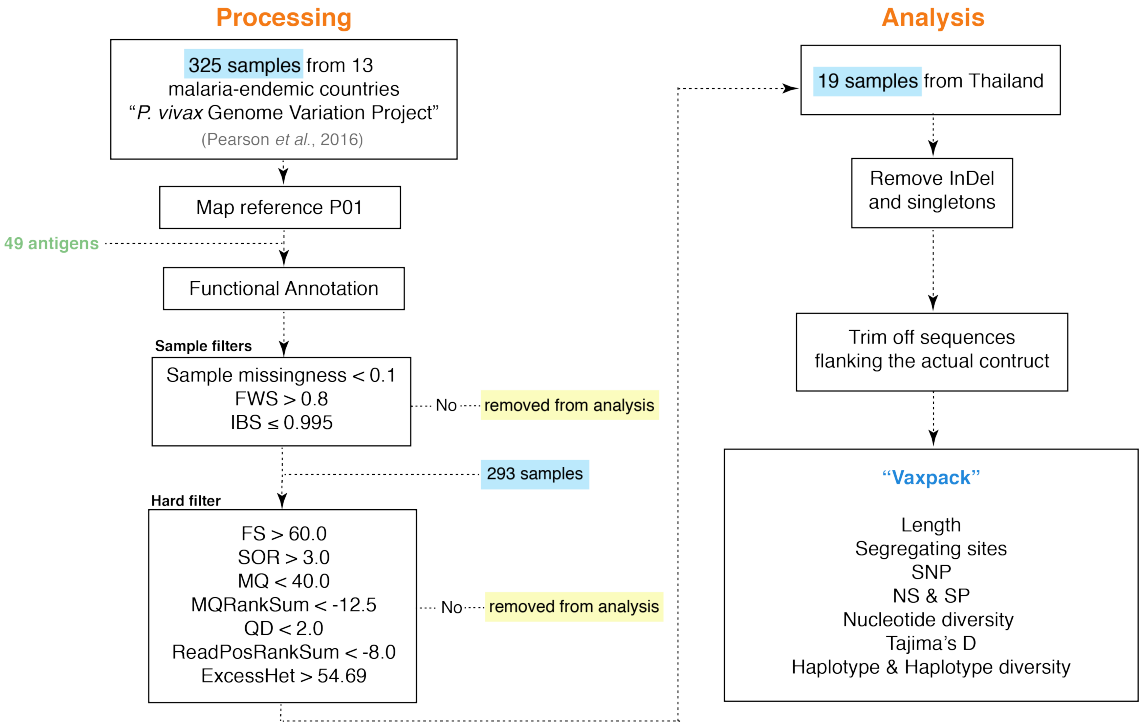


Figure 2.4 Process of population genetic analysis. Prior to population genetic analysis, parasitic DNA sequence data were collected in 13 malaria-endemic countries as part of the MalariaGEN *P. vivax* Genome project [346]. In the processing step, DNA sequences were mapped to the latest *P. vivax* reference strain PvP01 from Indonesia [347] and annotated based on functions. Subsequently, quality of the antigenic sequences was assessed in two steps and the ones with low quality were excluded from further analyses. From the down-selected high-quality sequences, 19 were sourced from Thailand and were therefore selected for cleaning. The R package Vaxpack was used to produce multiple population genetic parameters from a sequence alignment per antigen.

Abbreviations: F_{WS} = inbreeding rate indicator; IBS = identity-by-state; FS = strand bias; SOR = strand odd ratio; MQ = mapping quality; QD = quality by depth; ExcessHet = excess heterozygosity; InDel = insertion/deletion; SNP = single nucleotide polymorphism; NS = non-synonymous SNP; SP = synonymous SNP.

2.9.2 Population genetics

Isolate and reference strain sequences were submitted to and processed by the R package 'Vaxpack' from which all population genetic parameters were generated. The package was developed by Elijah Martin and Myo Naung in A/Prof Alyssa Barry's laboratory at WEHI (details of this package are available on GitHub at https://github.com/BarryLab01/vaxpack). Parameters of interest are shown in Table 6.1, many of which are commonly used for population genetic analysis by studies on malaria and other disease models. The definitions and interpretations of these parameters will be further discussed in Chapter 6.

2.10 Statistical analyses

All statistical analyses were performed using GraphPad Prism version 7, Stata version 12.1 or R version 3.5.3 for Macintosh. These included student t test, Fisher's exact test, chi-square test, Mann-Whitney's U test, Kruskal-Wallis H test, Pearson's and Spearman's correlation tests. To indicate the degree of statistical significance on graphs, symbols were used as follows: ns not significant, * $p < 0.05$, ** $p < 0.01$, *** $p < 0.001$, **** $p < 0.0001$.

Chapter 3. Establishment and validation of a multiplexed bead-based assay for antibody measurements

3.1 Introduction

Luminex® is an established technology platform available for running multiplexed bead-based assays that has been frequently used to quantitate targets of interest in different types of samples due to its cost-saving, labour-efficient and sample-conservative properties. The aim of the procedure is to establish an assay, based on the principle of enzyme-linked immunosorbent assay (ELISA), on colour-coded polystyrene microspheres. As illustrated in Figure 2.1, the microspheres are internally infused with two dyes, red and infrared, which create a gradient of spectrally distinct colours, emitting specific wavelengths when they are excited by lasers [348]. A standard Luminex® assay allows up to 100 differentially coloured microspheres to be used simultaneously. By covalently conjugating protein-capturing or protein-specific molecules onto differentially coloured microspheres and adding fluorochrome-tagged secondary antibody, we are able to allocate signals of different intensity to multiple analytes in one sample. Depending on the research question, the Luminex® assay can be set up in two ways: a) Capture Sandwich where the microspheres are conjugated with capture antibodies that are specific to the analytes of interest in the samples, or b) Indirect Serological Assay where the antibodies are target analytes and hence the antigens are conjugated onto the microspheres [349]. The Indirect Serological Assay has been used in this thesis and the setup is illustrated in Figure 2.1.

The Luminex® assay is well suited to the field of immunological research, particularly research utilising field-based studies where sample volumes are often very small and thus the multiplexing capacity is highly advantageous. The Luminex® assay has been used since the late 1990s, primarily for quantifying cytokine levels in plasma or sera samples (i.e. the Capture Sandwich assay) [350]. The assay was shown to correlate well with data generated by ELISA, the gold standard for immunoassays, but was also more accurate, sensitive and reproducible [351]. In the context of malaria research, the Luminex® platform has been used extensively to measure cytokine levels in the context of both *P. falciparum* and *P. vivax* infections [352-354]. More recently, the platform has been used to measure parasite-specific antibody responses. For *P. falciparum*, the Luminex® platform has been used to monitor antibody acquisition and to infer local transmission of malaria [355-357]. The use of this assay in *P. vivax* malaria serological surveillance was first described by Fernandez-Becerra et al., confirming that the Luminex® platform could detect reproducible IgG antibody levels with good sensitivity, that highly correlated with ELISA, in individuals naturally infected with *P. vivax* [358]. Following this study, several other authors have reported the use of the Indirect Serological Assay on the Luminex® platform for the purpose of evaluation of immune status in various settings [112, 220, 359]. The number of antigens multiplexed ranged from 11 to up to 38 and antibody responses were successfully determined using minimal volumes of plasma from field samples from geographically distinct regions with varying transmission levels (eg. Cambodia,

Thailand, PNG, Brazil and the Solomon Islands). These studies have highlighted the power of the Luminex® platform in serological surveillance for field-based studies where samples are often precious.

A common yet critical piece of information gathered from the past literature about the Luminex® assay is that it requires an extensive process of optimisation to yield the best results and needs to be adapted for specific uses. For instance, the type of sample used determines the ratio in which they should be diluted as pathogen load and antibody concentration can differ. For instance, it was shown that serum samples were best run on the Luminex® platform at a lower dilution (1:50) compared to mucosal samples at a higher dilution (1:10) [360]. Additionally, some laboratories optimised the number of microspheres per antigen per well to balance low background signal and good detection range [359, 361]. Other factors such as inclusion of BSA in the assay buffer have also been shown to reduce background signals [361]. Furthermore, it was demonstrated that the choice and concentration of anti-human secondary antibody could affect the reproducibility of the assay [362]. More recently, Wu et al. conducted an in-depth investigation and found several key determinants of variability, including storage condition of the antigens and antigen-conjugated microspheres in addition to serum dilution [357]. Additionally, for those studies that used 'in-house' recipes to conjugate protein-capturing molecules onto the microspheres, optimisation processes were further extended as the stability of

conjugation was shown to vary between molecules [359, 363, 364]. These scenarios highlight the challenges and importance of optimising the Luminex® assay prior to analyte quantification.

The purpose of this Chapter is to outline the process in which each of 52 *P. vivax* antigens were optimised on the Luminex® platform to enable measurement of *P. vivax*-specific Ig. Several aspects of this assay were already established for IgG measurements, including the general protocol, number of microspheres per antigen per well, serial dilution of a positive control, composition of buffers and storage of antigen-conjugated microspheres. Other factors that are critical for the sensitivity and reliability of the assay but are beyond our control were not further optimised, including the sample collection and storage conditions. Therefore, the results described here focus on: a) optimising the amount of an antigen used for coupling to microspheres, b) trialling a shorter incubation time during microsphere conjugation, c) trialling different dilutions of sample plasma, d) assessing the stability and repeatability of the assay and d) optimising the protocol for IgM measurements. A comparison was also made between IgG data generated using this assay compared to another assay known as the AlphaScreen®. The purpose of each step will be further described in detail below.

3.2 Results

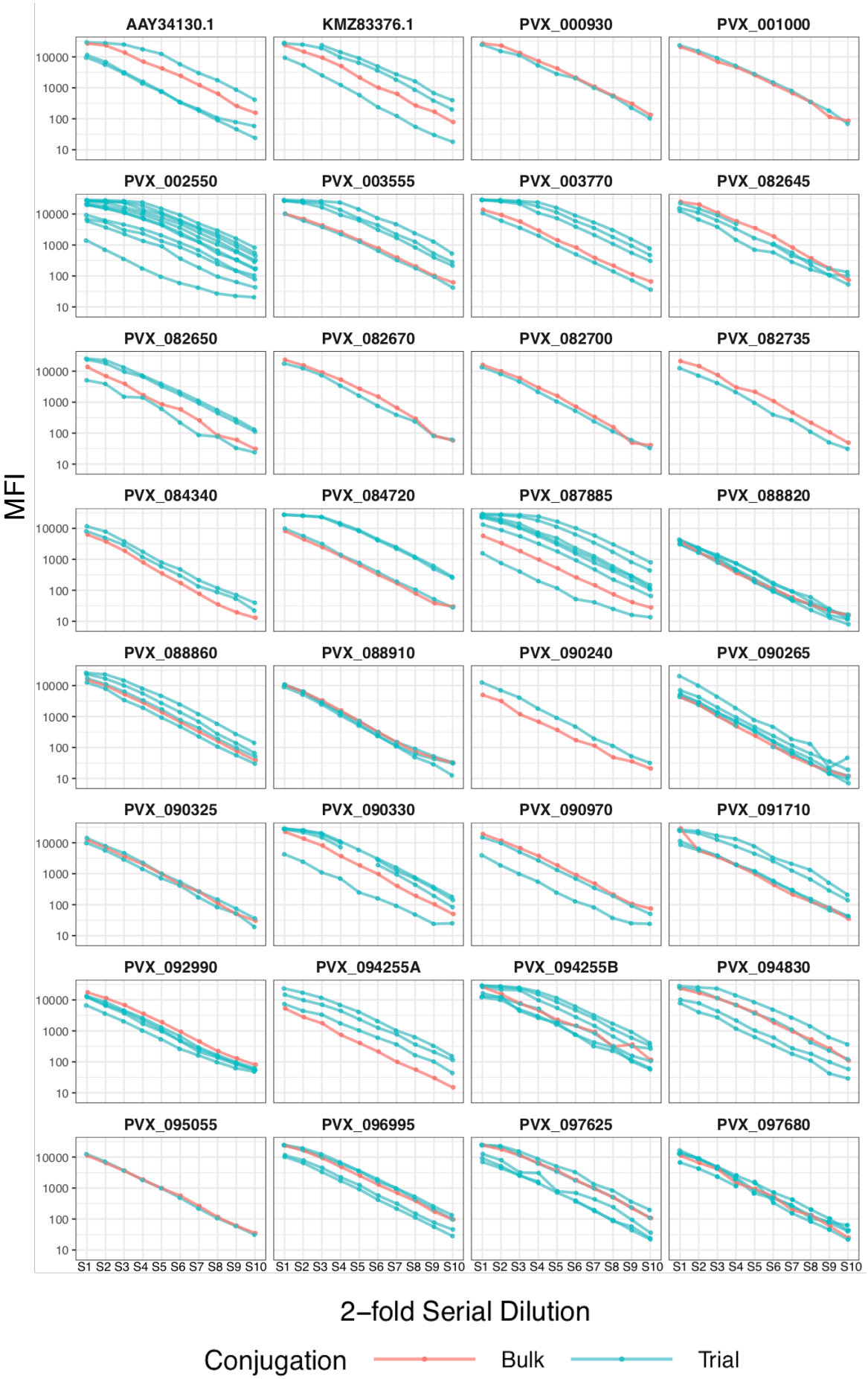
3.2.1 Optimisation of *P. vivax* protein amounts for the multiplexed bead-based assay

Multiple approaches have been used for determining the optimal amount of protein to conjugate to microspheres for Luminex®-based assays. The major choice is whether to conjugate a set amount of protein for each antigen of interest [365], or to optimise all individually [219]. The benefit of optimising all antigens individually is that plasma samples can be run at one dilution. This was preferential for the current project given the limited availability of plasma. For a specific amount of *P. vivax* antigen to be considered optimal, we aimed for a log-linear standard curve generated with a 2-fold serial dilution of a positive control plasma pool from PNG. As all target antigens were produced with varying concentrations (ranging from 0.03 mg/mL to 7.42 mg/mL), it was determined that the amount per antigen for optimisation was to begin with 1 μg in a trial volume. The amount could be further adjusted based on the appearance of the standard curve before achieving log-linearity. If a plateau was observed at higher dilutions, it could indicate saturation - the amount of antigen may be too much and needed to be reduced. On the other hand, a plateau near lower dilutions with lower starting MFI suggested more antigen was required. Once the optimal amount of antigen was determined in a trial coupling, a bulk conjugation was performed.

Figure 3.1 shows the standard curves of each *P. vivax* antigen before and after optimisation. It was observed that most antigens required a few rounds of optimisation before achieving log-linear standard curves. The optimised amount for each antigen is recorded in Table 2.2.

However, for one antigen (PVX_002550) the optimal amount of protein was not finalised during this process despite multiple conjugation attempts and troubleshooting, including re-testing the conjugated microspheres with the same concentration ("Retest") and trialling with microspheres of a different colour and fresh vials of the antigen ("New") (Figure 3.2). Two concentrations did achieve close to log-linear standard curves with a similar dynamic range; however, one was established using 0.02μg of the antigen (magenta) and another 0.5μg (coral). By retesting the pre-existing conjugation with 0.5μg of antigen within a week's time, the starting MFI had dropped significantly ("0.5μg retest", olive). This was also observed in conjugation with 1μg of antigen. Furthermore, the new conjugation with 0.5μg of antigen ("0.5μg new", pink) produced much higher starting MFI – similar to that of "1μg retest" (moss) – than the pre-existing one (coral). For PVX_002550, the amount of antigen conjugated onto the microspheres was not proportional to the magnitude of starting MFI (eg. more antigen used should give stronger signals), which was observed for all other antigens in the panel. In the interests of time, this antigen was excluded from bulk conjugation and any further experiments. SDS-PAGE gels

generated by CFS during the production of four representative antigens are shown in Figure 3.3 as examples to showcase the significant reduction in protein yields for PVX_002550 compared to the other three antigens in our panel.


AAY34130.1
KMZ83376.1
PVX_000930
PVX_001000
PVX_002550
PVX_003555
PVX_003770
PVX_082645
PVX_082650
PVX_082670
PVX_082700
PVX_082735
PVX_084340
PVX_084720
PVX_087885
PVX_088820
PVX_088860
PVX_088910
PVX_090240
PVX_090265
PVX_090325
PVX_090330
PVX_090970
PVX_091710
PVX_092990
PVX_094255A
PVX_094255B
PVX_094830
PVX_095055
PVX_096995
PVX_097625
PVX_097680
MFI
10000
1000
100
10
S1 S2 S3 S4 S5 S6 S7 S8 S9 S10
2−fold Serial Dilution
Conjugation
Bulk
Trial

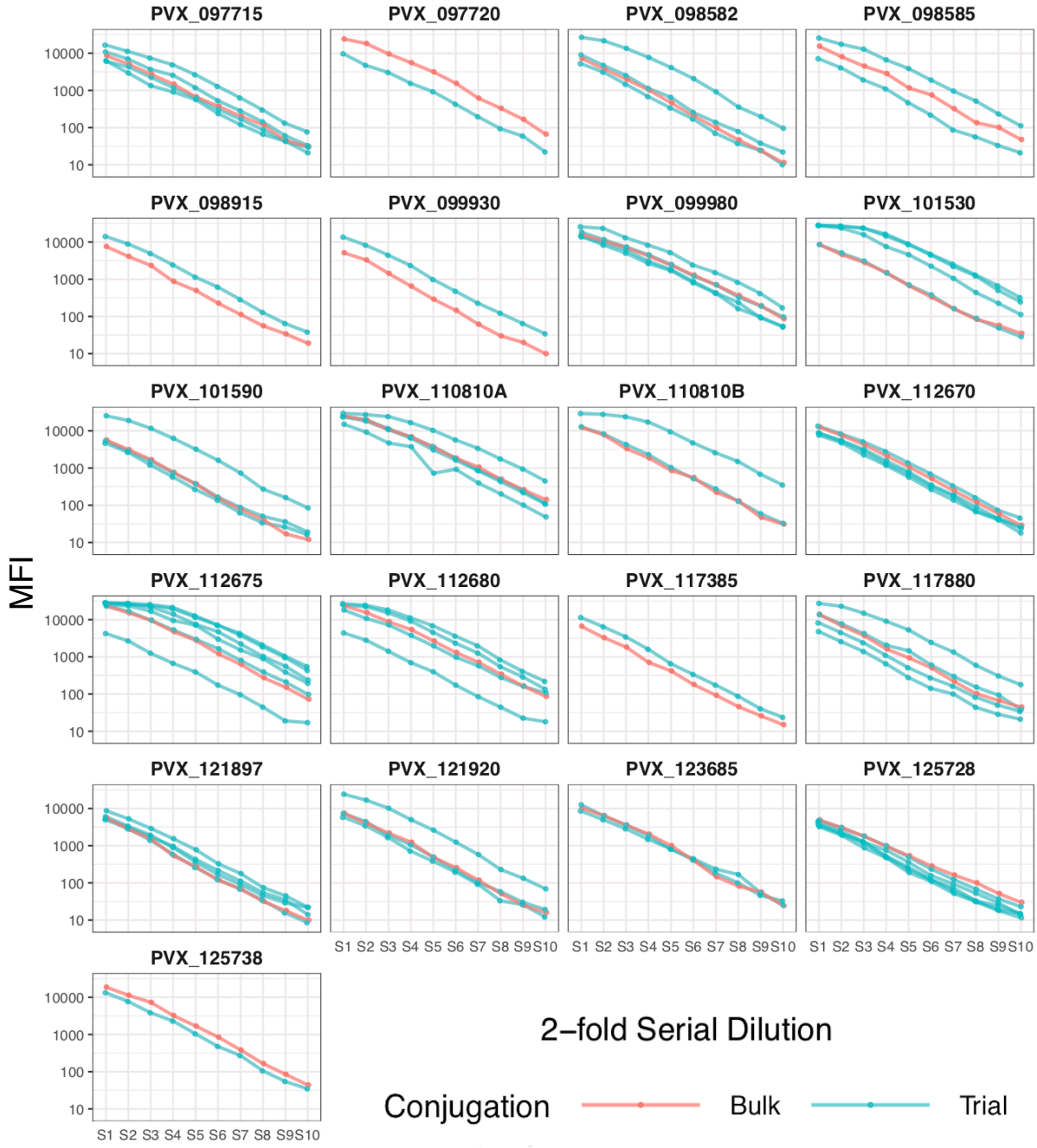


Figure 3.1 Change in results of standard curve tests against 53 *P. vivax* antigens during and after optimisation. A standard curve was established by 2-fold serial dilutions of the positive control, the pooled plasma from PNG hyper-immune adults, starting from 1:50 (S1) to 1:25,600 (S10). A 'trial' volume (teal) of antigen-conjugated microspheres was set up for optimisation. Once the optimal antigen concentration was determined a 'bulk' volume was conjugated and the standard curve confirmed (coral). Antigen-conjugated microspheres in bulk volume were then used in all further experiments. The final amounts of antigen used for conjugation are listed in Table 2.2.

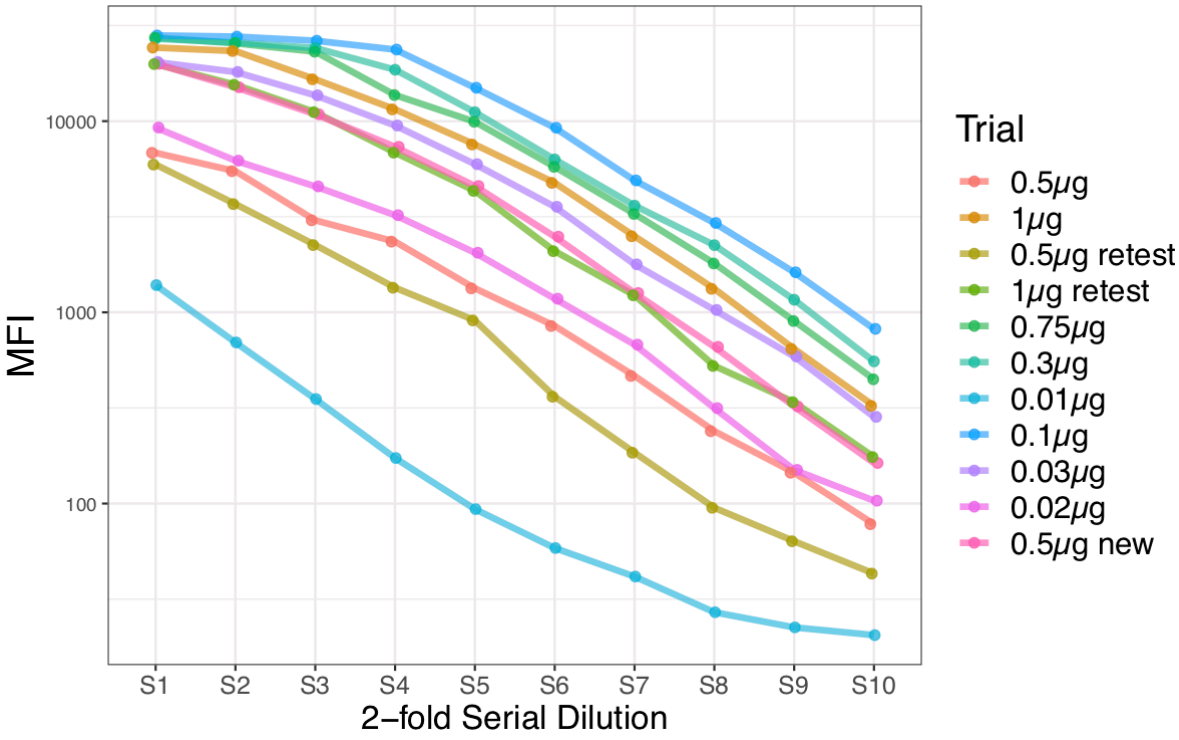


Figure 3.2 Attempts to optimise *P. vivax* antigen PVX_002550. We attempted to optimise PVX_002550 by monitoring the linearity of the standard curves with various antigen concentrations. The standard curves were established by 2-fold serial dilutions of the positive control, the pooled plasma from PNG hyper-immune adults, starting from 1:50 (S1) to 1:25,600 (S10). During the optimisation process, the magnitude of starting MFI failed to change proportionally to the antigen concentration. The order of the trials as depicted in the legend represents the order of the experiments conducted (ie. first experiment with 0.5μg of antigen and second with 1μg). 'Retest' refers to results obtained by performing standard curve tests on pre-existing conjugations and 'new' refers to new conjugation.

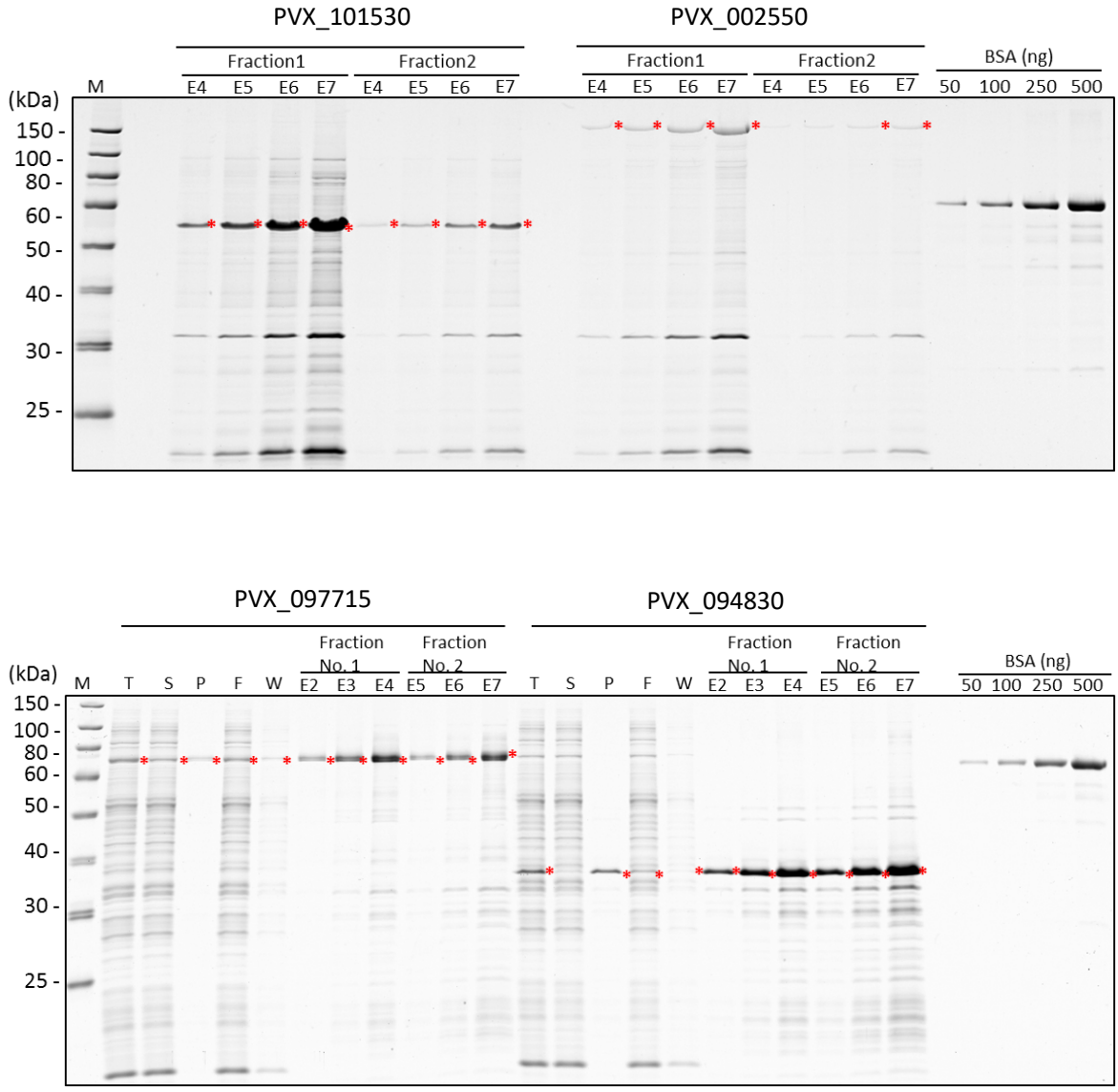


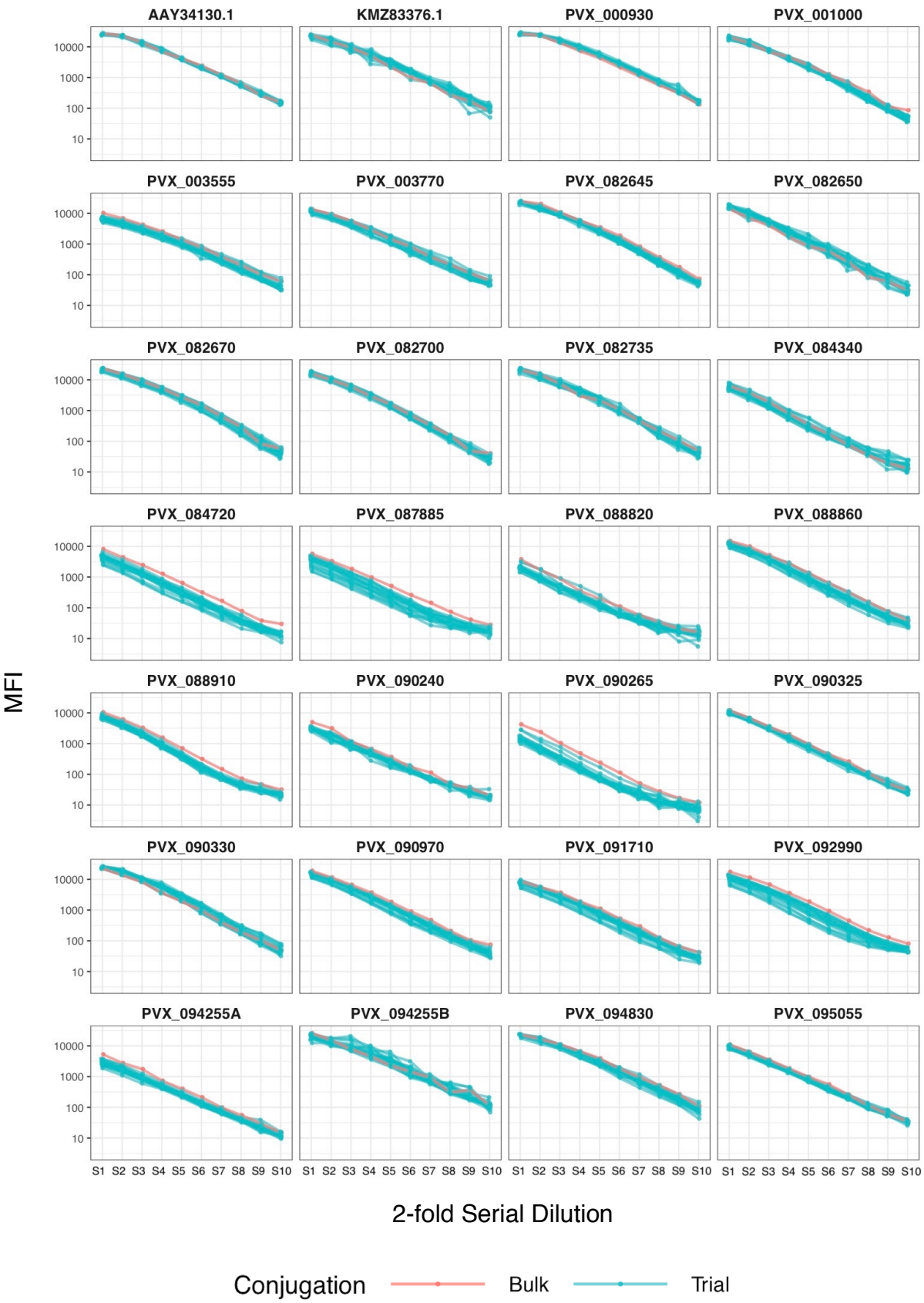
Figure 3.3 Examples of SDS-PAGE gels for *P. vivax* antigen production by the CFS company. The 40 CFS *P. vivax* antigens were expressed in the WGCF system and purified using a His-tag. The proteins were later analysed on 15% SDS-PAGE gels to determine their yields as a quality control step. Four *P. vivax* antigens (PVX_101530, PVX_002550, PVX_097715 and PVX_094830) are shown here as representative examples, showing the difference in protein yields between PVX_002550 (top right) and the other antigens. The asterisks in red mark the presence of the target proteins.

Abbreviations: M = molecular weight marker; T = total fraction crude protein (1μL loaded); S = soluble fraction crude protein (1μL loaded); P = pellet fraction crude protein (1μL loaded); F = flow

through purification (1μL loaded); W = wash purification (1μL loaded); E2 – 7 = total fraction eluted protein (0.156, 0.313, 0.625, 1.25, 2.5 and 5μL loaded); BSA = bovine serum albumin (as reference for quantification).

3.2.2 Stability of antigen-conjugated microspheres

As mentioned previously in Chapter 2, the stability of conjugation was also monitored by regularly performing standard curve tests with the conjugated microspheres during the experiments. Figure 3.4 shows the change of standard curves per antigen over time during the course of total IgG experiments performed. The results indicate that the log-linear property of the standard curves was maintained for at least 2 weeks. However, some degree of inter-plate variability was observed between antigens. For instance, several of the antigens, such as PVX_099930, PVX_110810B and PVX_121920, exhibited reduction in starting MFI as the experiment progressed, indicating less stable conjugation and shorter shelf-life. Additionally, we noticed that antigens with starting MFI (1/50 dilution) above 10,000 were more likely to maintain log-linearity for a prolonged period of time.


AAY34130.1
KMZ83376.1
PVX_000930
PVX_001000
PVX_003555
PVX_003770
PVX_082645
PVX_082650
PVX_082670
PVX_082700
PVX_082735
PVX_084340
PVX_084720
PVX_087885
PVX_088820
PVX_088860
PVX_088910
PVX_090240
PVX_090265
PVX_090325
PVX_090330
PVX_090970
PVX_091710
PVX_092990
PVX_094255A
PVX_094255B
PVX_094830
PVX_095055
MFI
10000
1000
100
10
S1 S2 S3 S4 S5 S6 S7 S8 S9 S10
2-fold Serial Dilution
Conjugation
Bulk
Trial

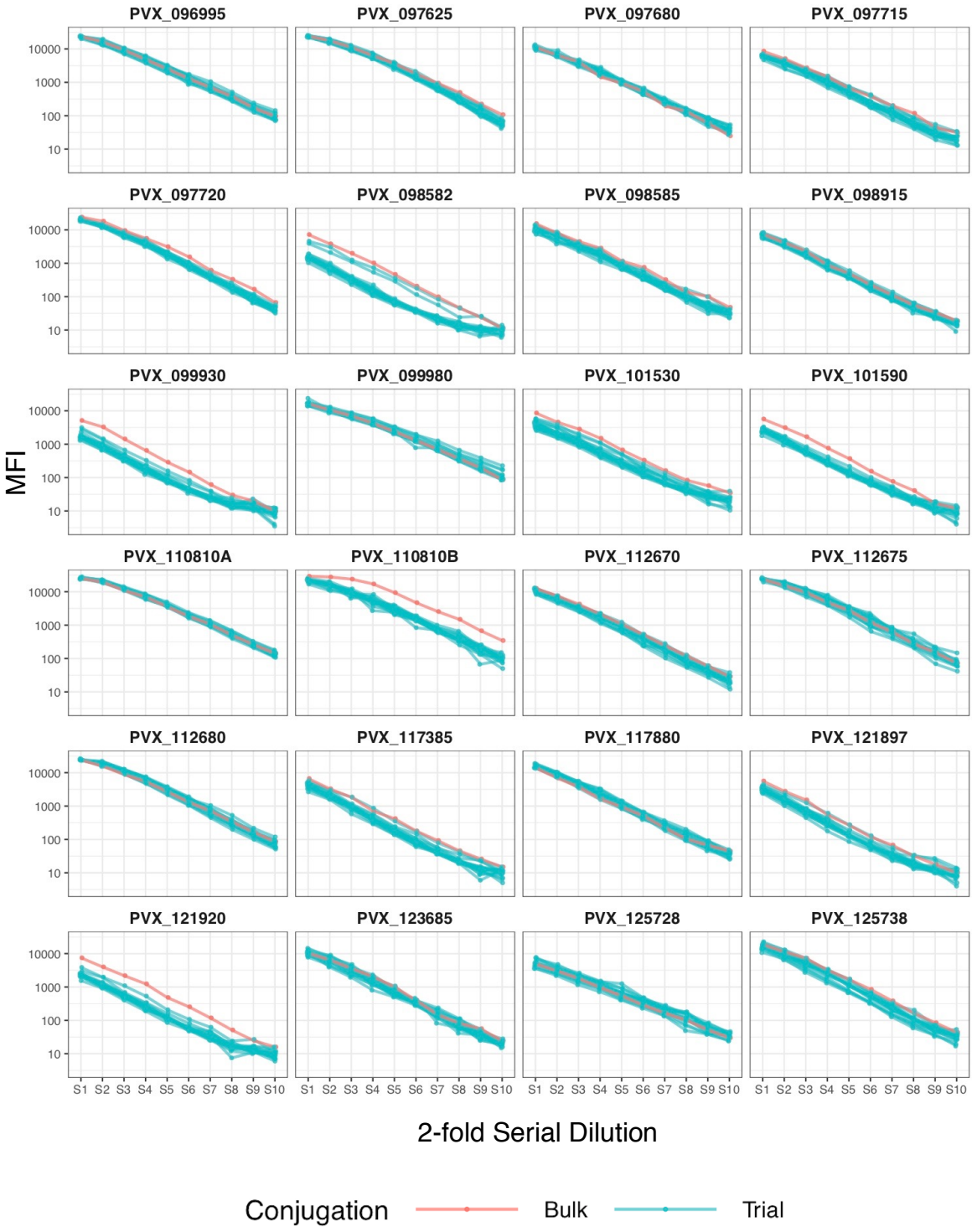


Figure 3.4 Standard curve tests for 52 *P. vivax* antigens. Antigen-specific standard curves were included in each plate of experiments described in Chapter 4 as a measure of inter-plate and/or inter-day variability. This also allowed the stability and shelf-life of each antigen-conjugated Luminex® microsphere to be monitored. The standard curves were established by 2-fold serial dilutions of the

positive control, the pooled plasma from PNG hyper-immune adults, starting from 1:50 (S1) to 1:25,600 (S10). The 'bulk' in coral represents the freshly conjugated Luminex® microspheres whilst the 'plate' in teal represents the standard curve per plate. For the detection of IgG antibody kinetics in duplicates, a total of 16-17 plates of samples were run which took approximately two weeks to complete.

3.2.3 Validation of alternative incubation condition

The original protocol for antigen conjugation to non-magnetic microspheres was established and used by Prof Christopher King's laboratory at Case Western Reserve University in Cleveland, USA, and subsequently adapted by a former PhD student in the Mueller Laboratory, Dr Camila T. França. The protocol was optimised for overnight incubation of the microspheres at 4°C following the addition of the designated antigen of a specific amount. However, the manufacturers stated that either overnight conjugation at 4°C or a 2-hour conjugation at room temperature could be performed. In order to facilitate the progress of future experiments, we validated the shorter incubation time at this particular step.

For this purpose, PVX_112670 (blood stage tryptophan-rich antigen) was selected due to consistent conjugation stability between optimising attempts. PVX_112670 was conjugated to microspheres and incubated for only 2 hours but at room temperature. The standard curve test was performed three times to monitor the conjugation stability: immediately after conjugation and one and two weeks after. It is shown that the conjugation of PVX_112670 to the microspheres remained stable over two weeks following the alternative incubation condition (Figure 3.5).

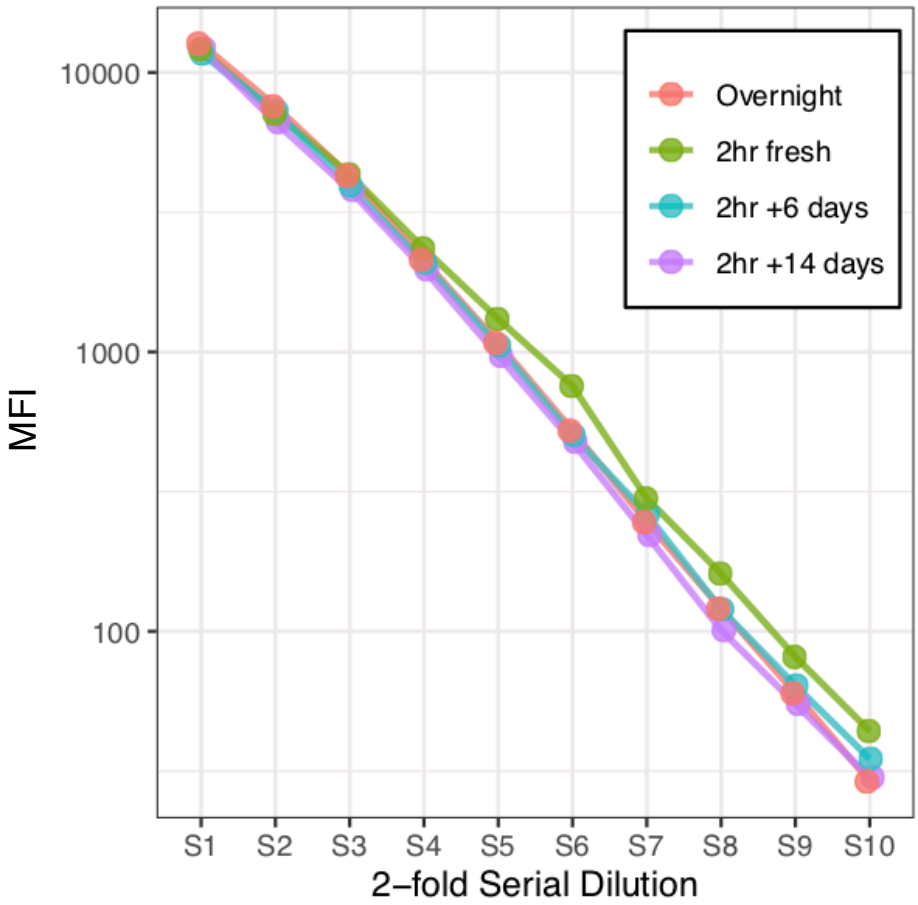
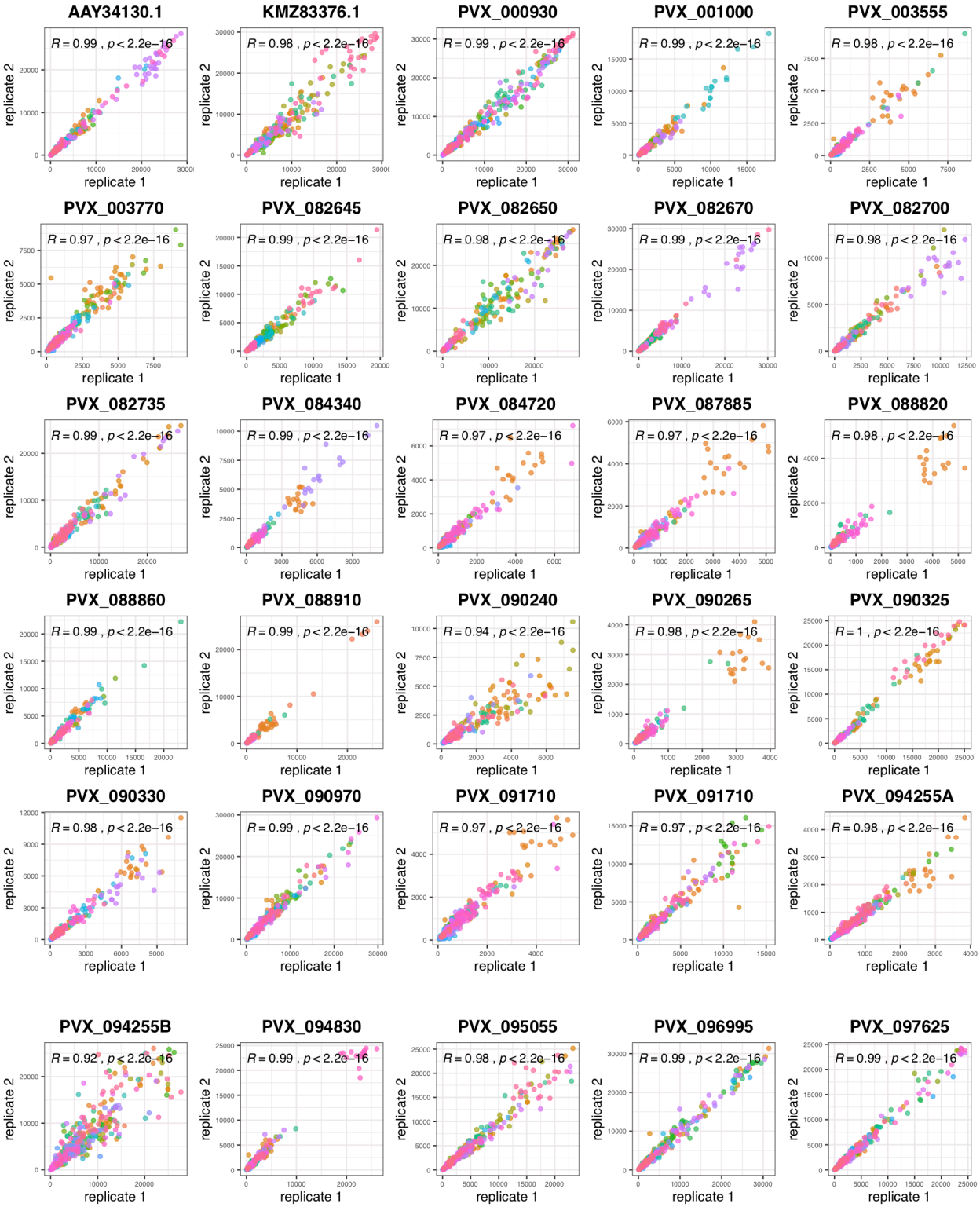


Figure 3.5 Comparison of standard curves between different incubation conditions. To examine the effect of an alternative incubation condition (2-hours incubation at room temperature instead of overnight at 4°C) on the stability of antigen-conjugated Luminex® microspheres, a *P. vivax* antigen PVX_112670 was conjugated under both conditions and the change in signal magnitude and standard curve linearity was monitored for two weeks and subsequently compared to curves produced according to original protocol. The standard curves were established by 2-fold serial dilutions of the positive control, the pooled plasma from PNG hyper-immune adults, starting from 1:50 (S1) to 1:25,600 (S10).

3.2.4 Reproducibility of the multiplexed bead-based assay

In order to examine the reproducibility of the Luminex® assay, plasma samples from symptomatic individuals in western Thailand were run in duplicates for 52 *P. vivax* antigens. Each colour corresponds to one of the 34 Thai symptomatic individuals. There was a strong correlation between duplicates for all *P. vivax* antigens tested (Pearson's $R = 0.87 - 1$, $p<0.0001$) (Figure 3.6)


AAY34130.1
R = 0.99 , p < 2.2e−16
KMZ83376.1
R = 0.98 , p < 2.2e−16
PVX_000930
R = 0.99 , p < 2.2e−16
PVX_001000
R = 0.99 , p < 2.2e−16
PVX_003555
R = 0.98 , p < 2.2e−16
PVX_003770
R = 0.97 , p < 2.2e−16
PVX_082645
R = 0.99 , p < 2.2e−16
PVX_082650
R = 0.98 , p < 2.2e−16
PVX_082670
R = 0.99 , p < 2.2e−16
PVX_082700
R = 0.98 , p < 2.2e−16
PVX_082735
R = 0.99 , p < 2.2e−16
PVX_084340
R = 0.99 , p < 2.2e−16
PVX_084720
R = 0.97 , p < 2.2e−16
PVX_087885
R = 0.97 , p < 2.2e−16
PVX_088820
R = 0.98 , p < 2.2e−16
PVX_088860
R = 0.99 , p < 2.2e−16
PVX_088910
R = 0.99 , p < 2.2e−16
PVX_090240
R = 0.94 , p < 2.2e−16
PVX_090265
R = 0.98 , p < 2.2e−16
PVX_090325
R = 1 , p < 2.2e−16
PVX_090330
R = 0.98 , p < 2.2e−16
PVX_090970
R = 0.99 , p < 2.2e−16
PVX_091710
R = 0.97 , p < 2.2e−16
PVX_091710
R = 0.97 , p < 2.2e−16
PVX_094255A
R = 0.98 , p < 2.2e−16
PVX_094255B
R = 0.92 , p < 2.2e−16
PVX_094830
R = 0.99 , p < 2.2e−16
PVX_095055
R = 0.98 , p < 2.2e−16
PVX_096995
R = 0.99 , p < 2.2e−16
PVX_097625
R = 0.99 , p < 2.2e−16
replicate 1
replicate 2

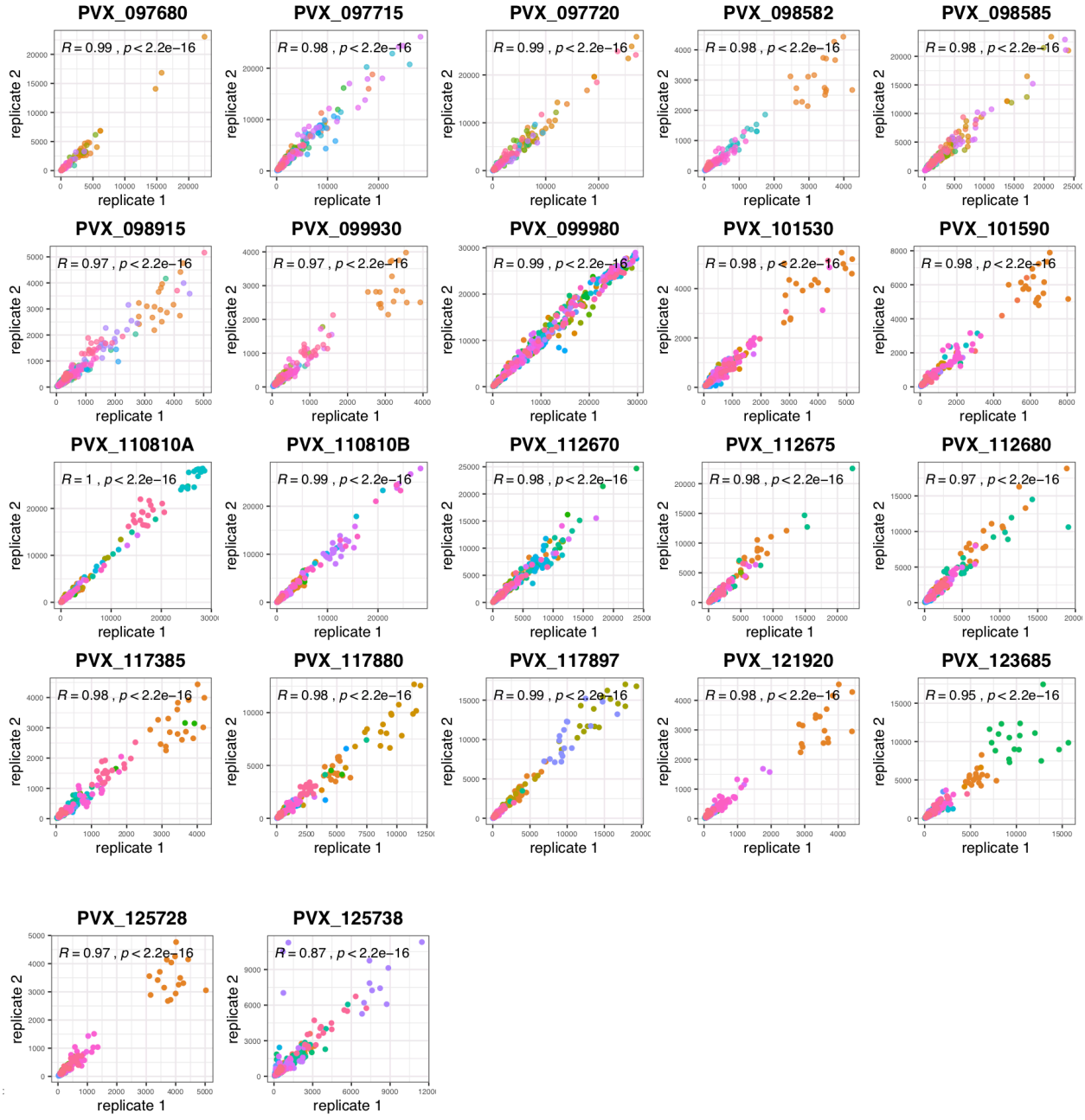


Figure 3.6 Correlation between duplicates per *P. vivax* antigen in 34 Thai symptomatic patients. For the measurement of total IgG kinetics against 52 *P. vivax* antigens in the symptomatic Thai cohort (n=34), all plasma samples were run in duplicates. This plot shows the correlation between the duplicated results in $\log_{10}$ MFI (a total of 578 pairs of duplicates from 34 participants with plasma samples collected at 17 time points). Correlation analysis was performed using Pearson's correlation test, indicated by R and p values.

3.2.5 Determination of the optimal plasma dilution for the multiplexed bead-based assay

Whilst running plasma samples from the symptomatic Thai and Brazilian individuals to establish total IgG kinetics (Chapter 4), exceptionally high MFI signals within the first few weeks of an infection to a subset of the *P. vivax* proteins were observed. As the raw MFI data was converted into antigen-specific RAU based on standard curves as an approach of standardisation, the high MFI signals at the early stage of infection were observed to 'max out' at 0.02 RAU – the maximum of the positive control serial dilution at 1:50, and appeared as a flat line. Figure 3.7 shows representative examples of this observation for two *P. vivax* antigens (PVX_082650 and PVX_094255A) in Thai symptomatic individuals. As depicted in the figure, this observation was only seen in a small number of individuals whilst most remained below the upper detection limit with a clear peak of IgG response.

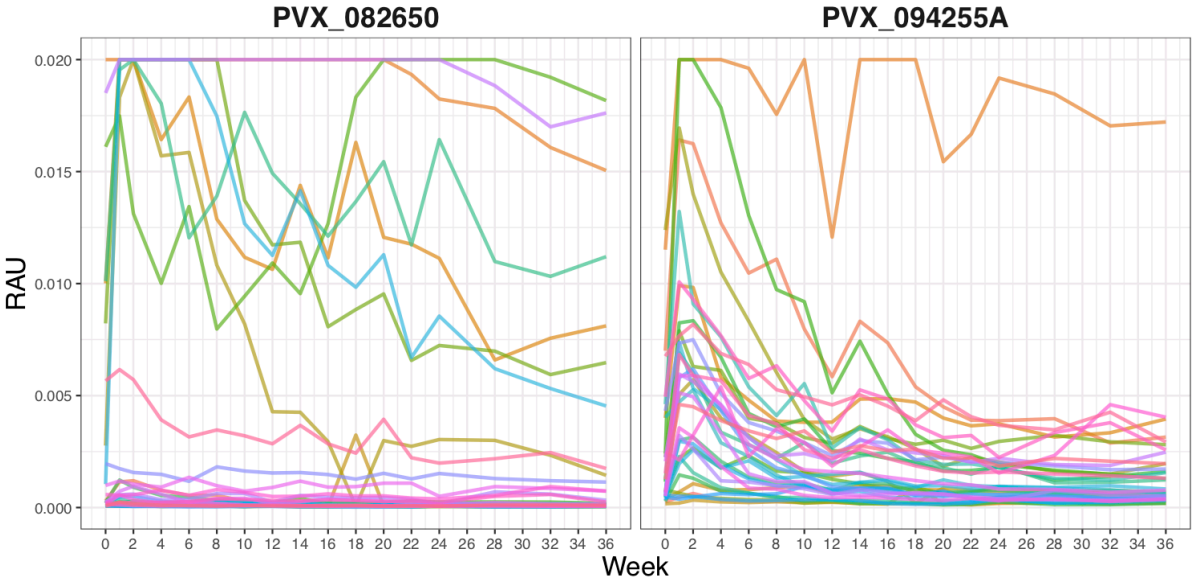


Figure 3.7 Examples of 'max-out' total IgG antibody responses at early time points of *P. vivax* infection in 34 symptomatic Thai individuals. It was observed that total IgG antibody responses stronger than the positive control at 1:50 dilution were lost after unit data normalisation based on antigen-specific standard curves. This was shown in some Thai symptomatic patients and for some *P. vivax* antigens, typically at the early stage of *P. vivax* infection where antibody responses were the strongest. Two *P. vivax* antigens PVX_082650 and PVX_094255A are shown here as representative examples of such an observation. Each line graph (each colour) corresponds to one of the 34 individuals.

An increase in dilution factor, from 100 to 1,000, was trialled as a possible solution to this issue of saturation. Due to sample availability, this was tested using plasma samples from Brazilian individuals with symptomatic *P. vivax* infections at the time of infection and 8 weeks later. IgG levels were measured against three *P. vivax* antigens (PVX_082650, PVX_094255A, PVX_098915). MFI and RAU results after logarithmic transformation produced by plasma samples diluted at 1:100 and 1:1,000 ratios were compared for 33 individuals in the cohort. As expected, plasma samples diluted at 1:1,000 produced lower antigen-specific total IgG responses in MFI (Figure 3.8). This suggests that it could be possible to lower high titre antibody levels and hence to obtain antibody kinetic profiles of higher resolution at the early stage of infection. However, the extent of titre reduction was inconsistent across the 33 Brazilian individuals tested.

Furthermore, when the dilution factor was changed from 100 to 1,000, the reduction in antibody level was not necessarily 10 times lower due to the fact that the background signal (represented by black dotted lines) remained unchanged. This observation was particularly obvious in individuals with relatively low antibody titres when samples were diluted at 1:100, as antibody titres could not be reduced beyond background when samples were diluted at 1:1,000. This shows that increasing the dilution factor of the samples would most likely restore resolution at the peak of total IgG responses but at the expense of losing resolution at lower IgG levels. Additionally,

it was observed that individuals who ‘max-out’ after unit conversion when samples were diluted at a 1:100 ratio were relatively uncommon (Figure 3.7). It was therefore decided to measure all samples at a 1:100 dilution only.

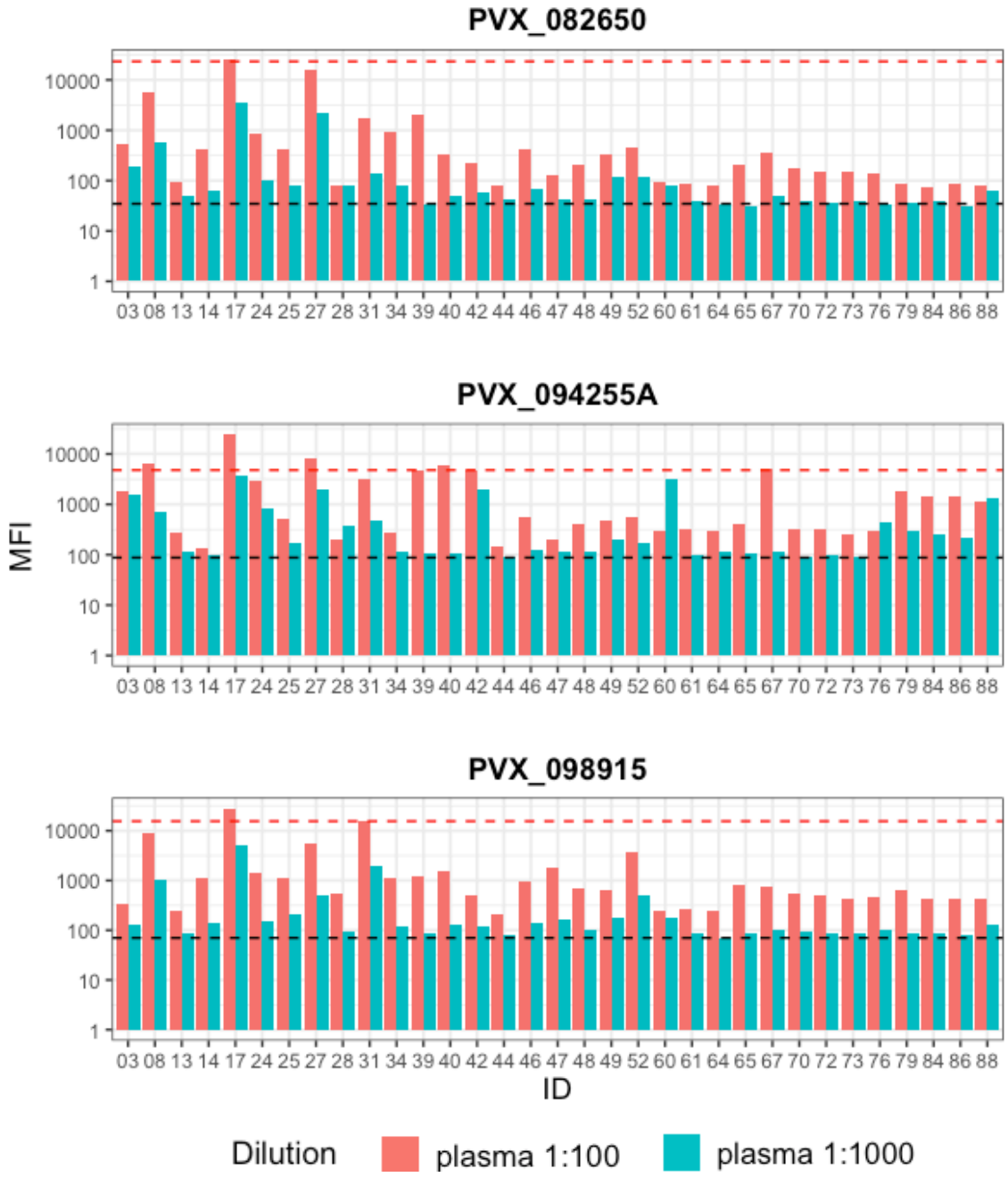


Figure 3.8 Comparison of total IgG antibody responses against three *P. vivax* antigens in differentially diluted samples from 33 Brazilian symptomatic patients. Plasma samples from 33 Brazilians 8-week post-symptomatic *P. vivax* infection were diluted at 1:100 (coral) and 1:1,000 (teal). IgG responses were measured against PVX_082650, PVX_094255A and PVX_098915. Black and red dotted lines represent the blank and maximum levels for each *P. vivax* antigen.

3.2.6 Optimisation of the multiplexed bead-based assay for IgM measurements

Whilst there was a working protocol for measuring IgG antibodies using the Luminex® assay in the Mueller laboratory at the start of my PhD, the assay had not yet been fully adapted to measure IgM antibody responses. Previous work by a short-term visiting student had established the following conditions: plasma samples to be run at 1:200 and the secondary antibody to be diluted at 1:400. The assay was established using a secondary anti-IgM antibody manufactured by Jackson ImmunoResearch (JIR). Subsequently, this secondary antibody was used to run the three negative control panels to explore the baseline level of IgM in malaria-naïve individuals. Whilst running the samples, consistently high background was observed. This prompted me to test an alternative secondary anti-IgM antibody manufactured by Southern Biotech (SB). The process and results of comparing the two antibodies are shown in this Section.

I first assessed the log-linearity of the positive control standard curves created using the JIR and SB anti-human IgM secondary antibodies in six randomly selected *P. vivax* antigens from our panel. Both secondary antibodies were diluted at a 1:400 ratio, as this had been previously optimised for the JIR antibody. From the magnitude of the starting MFI, it was evident that for any given *P. vivax* antigen the JIR secondary in coral induced stronger responses than SB in green (Figure 3.9). Additionally, the standard curves established using the JIR

secondary antibodies were more log-linear and exhibited less plateau towards the lower dilutions than SB. IgM levels were also measured against these proteins in plasma samples from the Thai symptomatic cohort and in one negative control Melbourne donor (Figure 3.9). By comparing the IgM level measured in the negative control, JIR showed higher background signals than SB. This suggested that SB was more preferable than JIR as the former elicited lower background signals.

The lower MFI signal produced using the SB antibody likely relates to its lower overall concentration (0.1mg/ml compared to 0.5mg/ml for the JIR antibody). Hence, I performed another standard curve test with the SB antibody at a 1:80 dilution and compared the results with JIR at 1:400 (Figure 3.9). Interestingly, the SB antibody at 1:80 was able to produce a range of detection similar to JIR at 1:400, but with a much lower background signal. This demonstrated that SB at 1:80 was more ideal than JIR at 1:400 for the IgM assay on the Luminex® platform. However, the negative control panels were already run with JIR at 1:400 at this point. Cost was also taken into consideration. JIR was priced at AUD 450 and SB at AUD 335 for 1mL of products. Since the usage of JIR antibody was less (1:400 dilution) than SB (1:80 dilution) per 96-well plate of experiment, the cost per sample for JIR (AUD 0.13) was almost four times less than SB (AUD 0.47). It was therefore decided to continue the use of JIR antibody

for IgM measurement in the future, with the background in malaria-naïve negative controls taken into consideration during the data analysis.

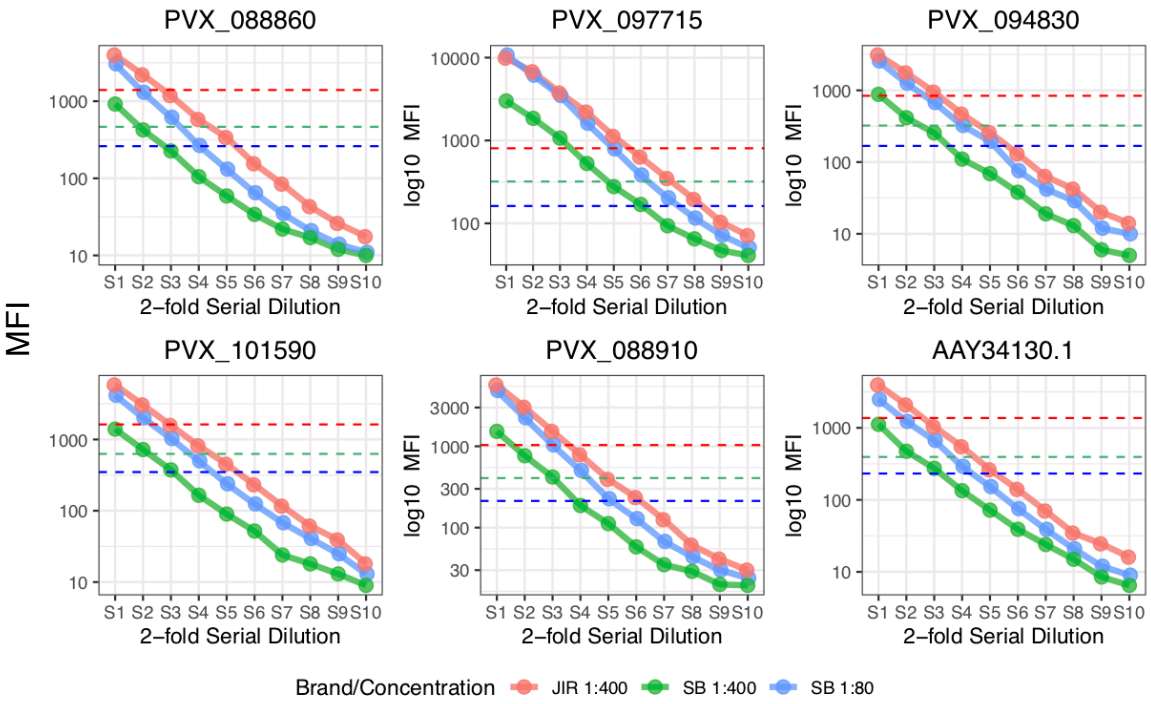


Figure 3.9 Comparison of performance between anti-human IgM secondary antibodies from two different manufacturers. Standard curve test was performed for two anti-IgM antibodies at two different dilutions (JIR diluted in 1:400 and SB diluted in 1:400 and 1:80) and were compared for six *P. vivax* antigens. Dotted lines represent the level of IgM signals in Melbourne donor plasma (n=1) in each trial. The standard curves were established by 2-fold serial dilutions of the positive control, the pooled plasma from PNG hyper-immune adults, starting from 1:50 (S1) to 1:25,600 (S10).

3.2.7 Comparison of IgG responses measured on AlphaScreen® and Luminex® platforms

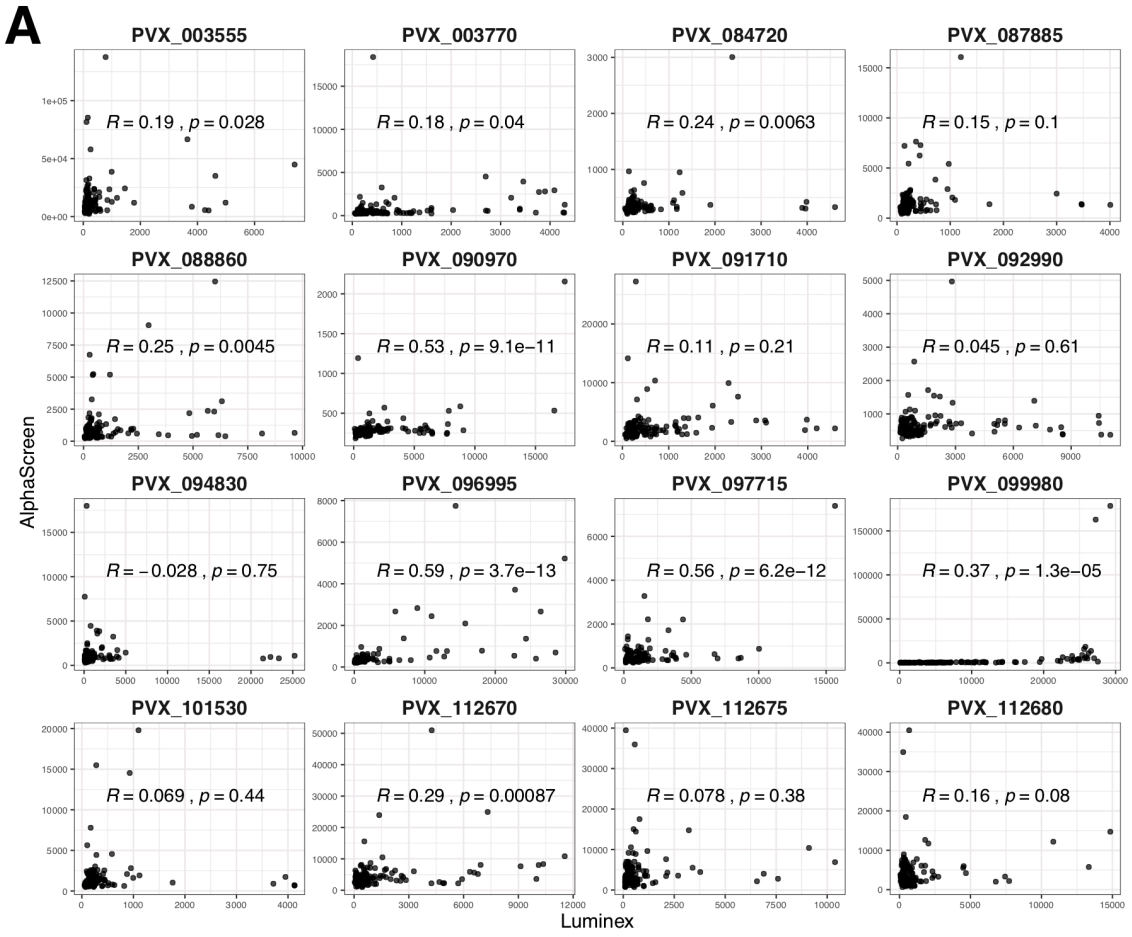
During the preliminary antigen discovery phase of the study (outlined in Chapter 2 Section 2.3.2) [108], antigen-specific total IgG responses were measured using the bead-based high-throughput assay AlphaScreen® at 4 of the 17 time points: weeks 0 (enrolment), 12, 24 and 36. The *P. vivax* antigens used were crude proteins. Subsequently, I measured total IgG responses against a subset of down-selected antigens – produced as purified proteins (the 51 described above) – using the Luminex® platform at 17 time points in 34 patients (data and results described in Chapter 4). In order to examine the potential effect of using crude versus purified proteins in IgG level measurements on the two platforms, I performed correlation tests between the raw data of the first 16 *P. vivax* antigens run as a preliminary investigation. Correlation coefficients and p values were generated for all four-time points to understand the general trend and for each time point to visualise potential differences (Figure 3.10).

In Figure 3.10A where data from the four time points were combined, it is shown that the degree and strength of correlation in IgG levels detected by AlphaScreen® and Luminex® assays differed greatly between *P. vivax* antigens. The range of R values varied between 0.028 and 0.59. For 56.3% of the antigens,

the correlations appeared to be statistically significant ($p < 0.05$). Generally, the correlation between AlphaScreen® (with crude antigens) and Luminex® (with purified antigens) platforms was weak to moderate.

After stratification based on the four time points, a varying degree of impact was observed for different antigens (Figure 3.10B). R and p values remained similar for seven antigens (PVX_087885, PVX_091710, PVX_092990, PVX_094830, PVX_101530, PVX_112675 and PVX_112680) whilst correlations became insignificant for two antigens (PVX_003555 and PVX_112670) following stratification. For the remaining seven antigens, five displayed a strong correlation in the early stage of infection (PVX_084720, PVX_088860, PVX_090970, PVX_096995 and PVX_097715). On the other hand, PVX_003770 and PVX_099980 showed the strongest correlation towards the end of the study.

Taken together, data correlations between AlphaScreen® and Luminex® platforms and between crude and purified proteins depended on the antigen and time point since infection.


A
PVX_003555
R = 0.19 , p = 0.028
PVX_003770
R = 0.18 , p = 0.04
PVX_084720
R = 0.24 , p = 0.0063
PVX_087885
R = 0.15 , p = 0.1
PVX_088860
R = 0.25 , p = 0.0045
PVX_090970
R = 0.53 , p = 9.1e−11
PVX_091710
R = 0.11 , p = 0.21
PVX_092990
R = 0.045 , p = 0.61
PVX_094830
R = −0.028 , p = 0.75
PVX_096995
R = 0.59 , p = 3.7e−13
PVX_097715
R = 0.56 , p = 6.2e−12
PVX_099980
R = 0.37 , p = 1.3e−05
PVX_101530
R = 0.069 , p = 0.44
PVX_112670
R = 0.29 , p = 0.00087
PVX_112675
R = 0.078 , p = 0.38
PVX_112680
R = 0.16 , p = 0.08
AlphaScreen
Luminex

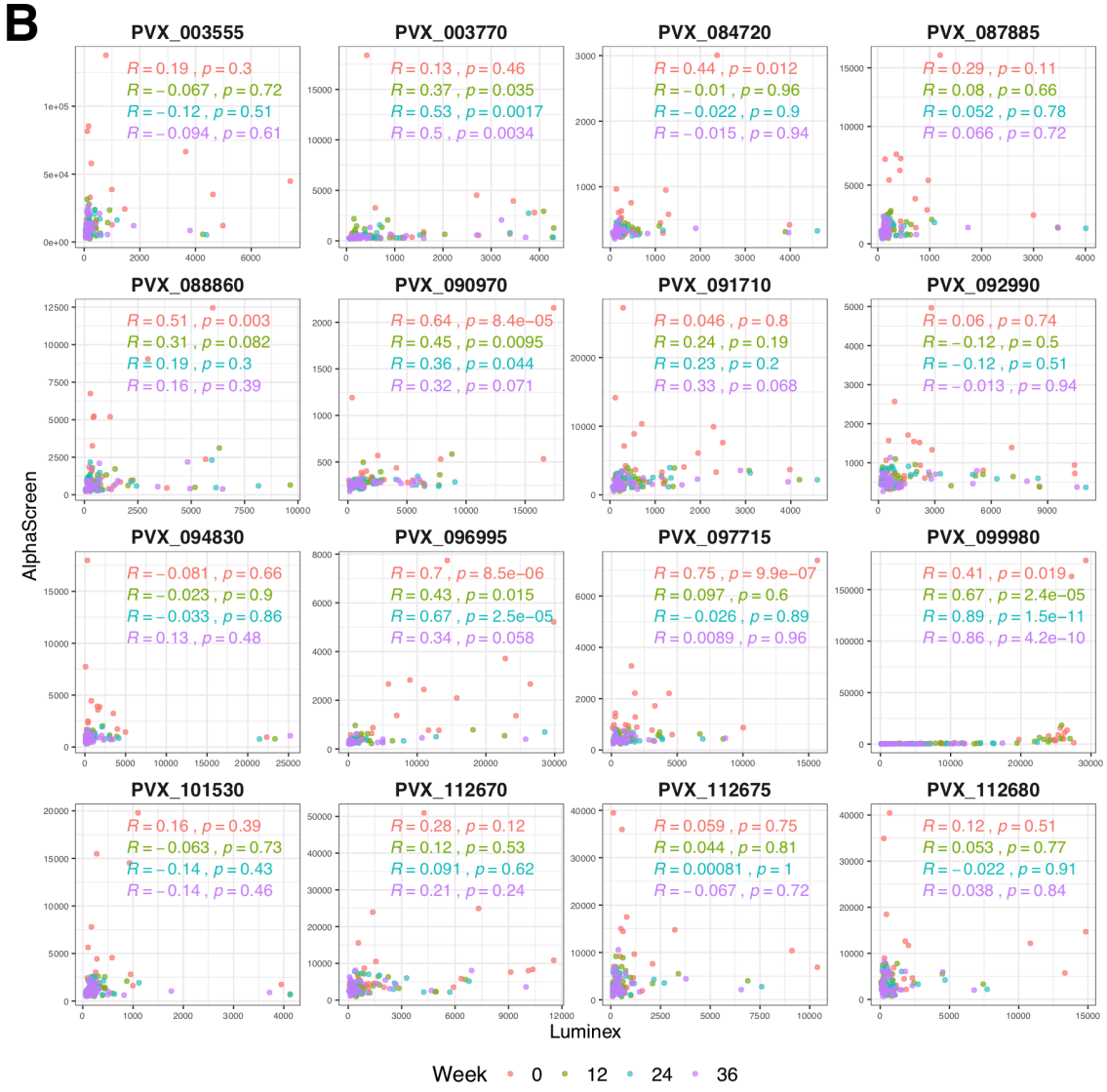


Figure 3.10 Correlation of detected IgG responses between AlphaScreen® and Luminex® platforms. To assess the difference in performance between the two platforms and between crude and purified proteins, antigen-specific total IgG responses detected were correlated **A)** at all four time points (weeks 0, 12, 24 and 36) combined and **B)** at each time point individually. Pearson's correlation tests were performed between the averages of duplicated AlphaScreen® and Luminex® results from 34 participants with plasma samples collected at four time points.

3.3 Discussion

The Luminex® assay has been used extensively in prior research due to its multiplexed nature, especially in addressing immunological research questions in a wide range of disease systems [366]. In order to achieve an optimal dynamic range and reproducibility before establishing antigen-specific antibody kinetic profiles against 52 *P. vivax* antigens, I conducted several trials to optimise protein concentration for conjugation, duration of incubation, plasma dilution and the use of secondary antibodies. Additionally, correlation tests were performed on data obtained by AlphaScreen® and Luminex® platforms to validate the results.

I found that the concentration of each *P. vivax* antigen needed for conjugation differed between *P. vivax* antigens, and that the stability of conjugation also varied from antigen to antigen. This observation is consistent with other previously published studies [359, 363, 364] and was the primary reason behind the optimisation process. Several authors have demonstrated the use of a similar optimisation approach for the Luminex® assay to maximise assay sensitivity and dynamic range [357, 360, 367] and have observed that such sensitivity and linear dynamic range can vary between different antigenic targets. In our case, such an optimal concentration was never found for one antigenic target. I was unable to

produce consistent log-linear standard curves for PVX_002550 despite multiple attempts.

It is likely that the quality of antigens (or other protein-capturing molecules) could influence the stability and also the 'shelf-life' of conjugated microspheres, which may be reflected on the differential dynamic range between antigens. Firstly, the size of a protein fragment may affect the quality of the end product during protein expression. For instance, larger protein products (those > 30 kDa) can be more difficult to express, resulting in lower protein yields [368]. Furthermore, larger protein products can also be more likely to form aggregates with reduced solubility [369]. Interestingly, PVX_002550 is one of the largest antigenic protein fragments in our panel with a size of 102 kDa (the size and further information of each antigenic construct are listed in Table 2.2), and a lower estimated yield of this antigen (as shown in Figure 3.3) was produced compared to the others used in this Thesis (total quantity of 0.44 mg compared to average of 1.20 mg). However, no evidence of increased aggregation or reduced solubility was found for PVX_002550.

Secondly, the purity of a protein product is likely to have a significant impact on its downstream applications. In the context of the Luminex® assay, low protein purity may enhance non-specific binding of irrelevant molecules on the

microspheres and limit the exposure to specific IgG in the samples, potentially contributing to destabilising microsphere conjugation (stability) and the detection limits of the Luminex® assay. The purity of the antigenic proteins used in this work was estimated by CFS based on the resolution and intensity of protein bands on the SDS-PAGE gels (representative examples are shown in Figure 3.3). The average purity of the 40 *P. vivax* antigens produced by CFS was assessed and reported as 79%. This is significantly higher than the purity of PVX_002550 at 19% (also produced by CFS), which most likely explains why we failed to optimise this antigen despite multiple attempts. Some possible reasons for low purity could stem from experimental set-ups, including sub-optimal elution conditions (eg. gradient and flow rate), precipitation of protein in the column during affinity chromatography due to inappropriate buffers and/or size of tubing [370, 371]. Nevertheless, I have shown that the majority of proteins were successfully conjugated to microspheres and established in the Luminex® assay. As most proteins were expressed using the WGCF system, this validates the use and performance of antigens produced by the WGCF system on the Luminex® platform. The WGCF system is reported to achieve the best yield in eukaryotic expression systems [372], and has been used extensively in the production of malarial antigens due to its lack of post-translational modifications (identical to antigens produced by *Plasmodium* parasites), capacity to yield structurally correct and potentially biologically active antigens, and the

ease for large-scale production to meet the demand of serological surveillance and diagnostics [339, 372, 373]. By comparing the WGCF system to the commonly used *E. coli*, Rui and colleagues have also reported that the WGCF system produced more soluble and structurally intact antigens, inducing stronger antigen-specific total IgG responses [374], further highlighting the use of WGCF in antigen production for immunological studies.

Additionally, I demonstrated that a shorter incubation condition can also produce antigen-conjugated microspheres with similar stability and antibody robustness as compared to the original conjugation protocol, which facilitates faster production of antigen-coupled microspheres. I found that plasma diluted at 1:100 could lead to 'maxed-out' total IgG responses in a small number of individuals and hence loss of resolution at the early stage of *P. vivax* infections. However, a lower plasma dilution at 1:1,000 also resulted in loss of resolution in samples with weak responses, and thus 1:100 was selected as the final dilution for all further experiments. It is possible to trial other dilutions (between 1:1,000 and 1:100) to further optimise plasma dilution for the Luminex® assay in the future. Finally, based on results I observed in Chapter 4 of relatively high background in IgM assays, I further optimised this assay with use of a new secondary antibody for IgM that could be used in subsequent research projects if the higher cost is not a limiting factor.

I also performed a correlation analysis of IgG data generated against the same antigens in the same individuals from a cohort in Thailand. Initially, I undertook this analysis in part to validate the results I had generated with my established Luminex® assay. However, the results clearly indicated that whilst there was a significant correlation between the data generated for most proteins, that this was only a weak-moderate correlation and the strength partly depended on the time-point post-infection. This is likely because IgG responses are higher 1-2 weeks post-infection than later time points, and that both assays lose some resolution when measuring low-level IgG responses. Importantly, the AlphaScreen® assay relied on use of crude proteins, as the overall strategy was to efficiently measure IgG responses to a large panel of proteins (>300). Conversely, I have used purified proteins to a smaller sub-set of proteins of interest. This is therefore the most likely reason for the differences in the data generated (rather than the different use of platform) as the crude proteins may contain more non-specific binding sites than the purified, potentially leading to variation in the IgG responses detected. In addition, the number of samples tested was relatively small (n=34 individuals) and better correlations may be observed with a larger data set. To explore this further, it will be of great interest to acquire and compare data generated from crude (or purified) proteins on both the AlphaScreen® and the Luminex® platforms.

In summary, I successfully established the Luminex® assay for 52 *P. vivax* antigens and demonstrated its high reproducibility.

Chapter 4. Determination of antibody kinetic profiles following *P. vivax* infections in Thailand and Brazil

4.1 Introduction

Naturally acquired immunity is elicited upon natural exposure to pathogens and can provide significant insights into the immune status of populations [266]. In the case of infectious diseases, naturally acquired immunity is often correlated with partial protection against clinical symptoms and/or associated with past levels of exposure to the pathogen [264, 375]. Multiple factors are shown to affect the immunity of an individual in response to the threat from a pathogen, including genetics, age, lifestyle, environment, previous vaccinations, nutrition and illnesses [312, 376-378]. This highlights the highly variable and diverse nature of naturally acquired immunity even within populations or sub-populations. In the context of *P. vivax* malaria, studies of naturally acquired immunity have provided novel insights relevant for the development of vaccines and sero-diagnostics [379].

Whilst the acquisition of naturally acquired antibody responses against *P. vivax* has been relatively well studied (albeit to a small number of antigens), there have been only limited studies assessing the longevity of these responses. It has been generally assumed that *Plasmodium*-specific antibody responses are short-lived in the absence of new infections [264], with evidence primarily from individuals with *P. falciparum* infections. However, recent studies have suggested

that the duration of the *P. vivax*-specific antibody response is highly dependent on the age of subjects, transmission level and the intrinsic properties of antigens [236, 380]. Multiple studies have now reported the presence of long-lived *P. vivax*-specific antibody responses, even in the absence of ongoing exposure [239, 265, 381, 382]. Nevertheless, significant variations in study design and the focus on only a limited number of *P. vivax* antigens have impeded the gain of a complete scope of *P. vivax*-specific antibody longevity.

To further our understandings of naturally acquired immunity and to explore its translational implications, I studied the acquisition and maintenance of antibody responses against a panel of 52 *P. vivax* antigens following both symptomatic and asymptomatic *P. vivax* infections. Factors potentially associated with the persistence of antibody responses were also investigated.

4.2 Results

4.2.1 Total IgG longevity following a symptomatic *P. vivax* infection in Thai individuals

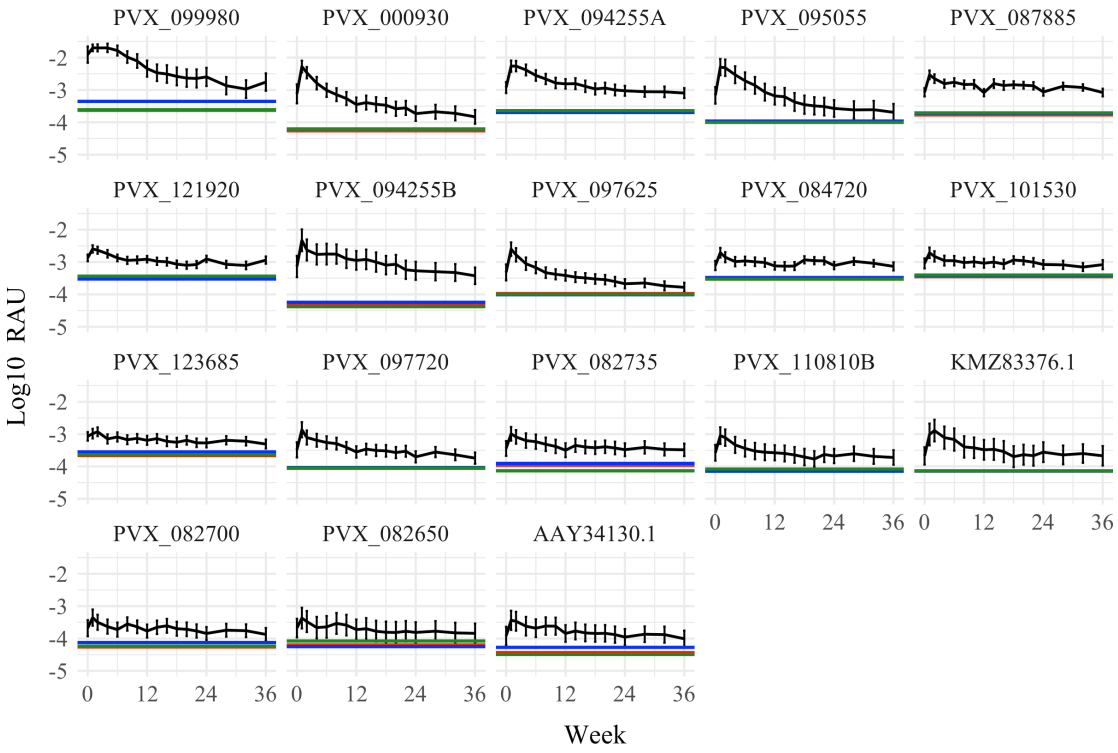
I first determined the levels of antigen-specific total IgG antibody in Thai symptomatic patients (n=34) at the time of infection and throughout 9 months of follow-up in comparison to antibody measurements in three large malaria-naïve control panels (n=274). Antibody responses to the 52 *P. vivax* antigens (detailed information is listed in Table 2.2) were measured at baseline (w0), w1, w2, then every 2 weeks for 6 months, then every month until 9 months (total of 17 measurements) (Figure 4.1). These individuals had no recurrent malaria infections during follow-up (as determined by PCR, regularly performed when blood was collected from the participants)[108]. We observed that IgG antibody responses to most *P. vivax* antigens followed a general pattern consisting of an initial peak in total IgG within the first two weeks post-infection and a subsequent decay of varying rates towards the baseline. 25 of the *P. vivax* antigens were non-immunogenic, with median responses less than 1 standard deviation (SD) above the median of the negative control baseline (calculated using data from the three malaria-naïve control panels). I categorised the remaining 27 immunogenic *P. vivax* antigens into two longevity profiles based

on an arbitrary cut-off of six months: long-lived (median maintained 0.5 SD above the baseline for more than six months; n=18) and short-lived (less than six months; n=9). Total IgG responses were also assessed at an individual level, with variation evident between study participants (Figure 4.2). These observations could be due to differing effects of age, past exposure and daily activities. However, the sample size was not designed for detecting individual-level differences in IgG acquisition and maintenance. In addition, outliers in total IgG responses can be seen in individuals HP09 and HP08, which could be the results of mislabelled samples.

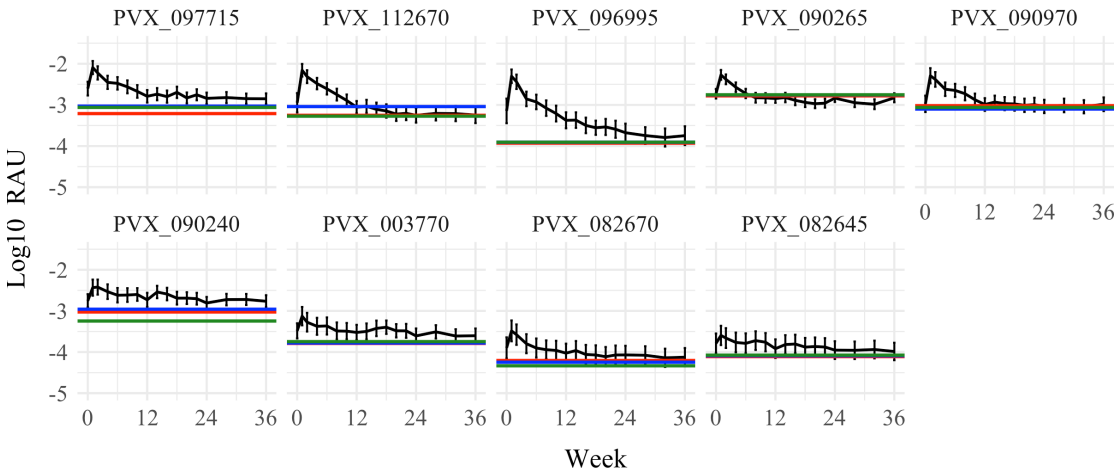
For all antigens, I determined the relative immunogenicity at week 1 post-infection by comparing the strength of the total IgG antibody response to that of the positive control, a hyperimmune plasma pool of PNG donors. The proportion of the Thai individuals reaching 1, 5, 10, 25 and 50% of the antibody response in the 1:50 diluted hyperimmune PNG pool were calculated (Table 4.1). This methodology has previously been used to describe the immunogenicity of antibody responses when using data from the multiplexed bead array where the total amounts of protein coupled to beads differ between antigen [219, 220, 340]. 70-100% of individuals reach 1% of the antibody response in the hyperimmune PNG pool, whereas only 0-70% reach 50% (dependent on antigen). When comparing the proportion of individuals reaching these set levels of the

hyperimmune PNG pool, the median rates against antigens that follow a short-lived longevity profile are consistently higher than against antigens with a long-lived longevity profile (i.e. 100, 100, 90, 70 and 50% of Thai participants reaching 1, 5, 10, 25 and 50% of the antibody response in 1:50 PNG pool, respectively, compared to 100, 85, 70, 40 and 30%). This suggests that antigens with a short-lived profile tend to be more immunogenic in this Thai symptomatic cohort.

A) Long-lived



B) Short-lived



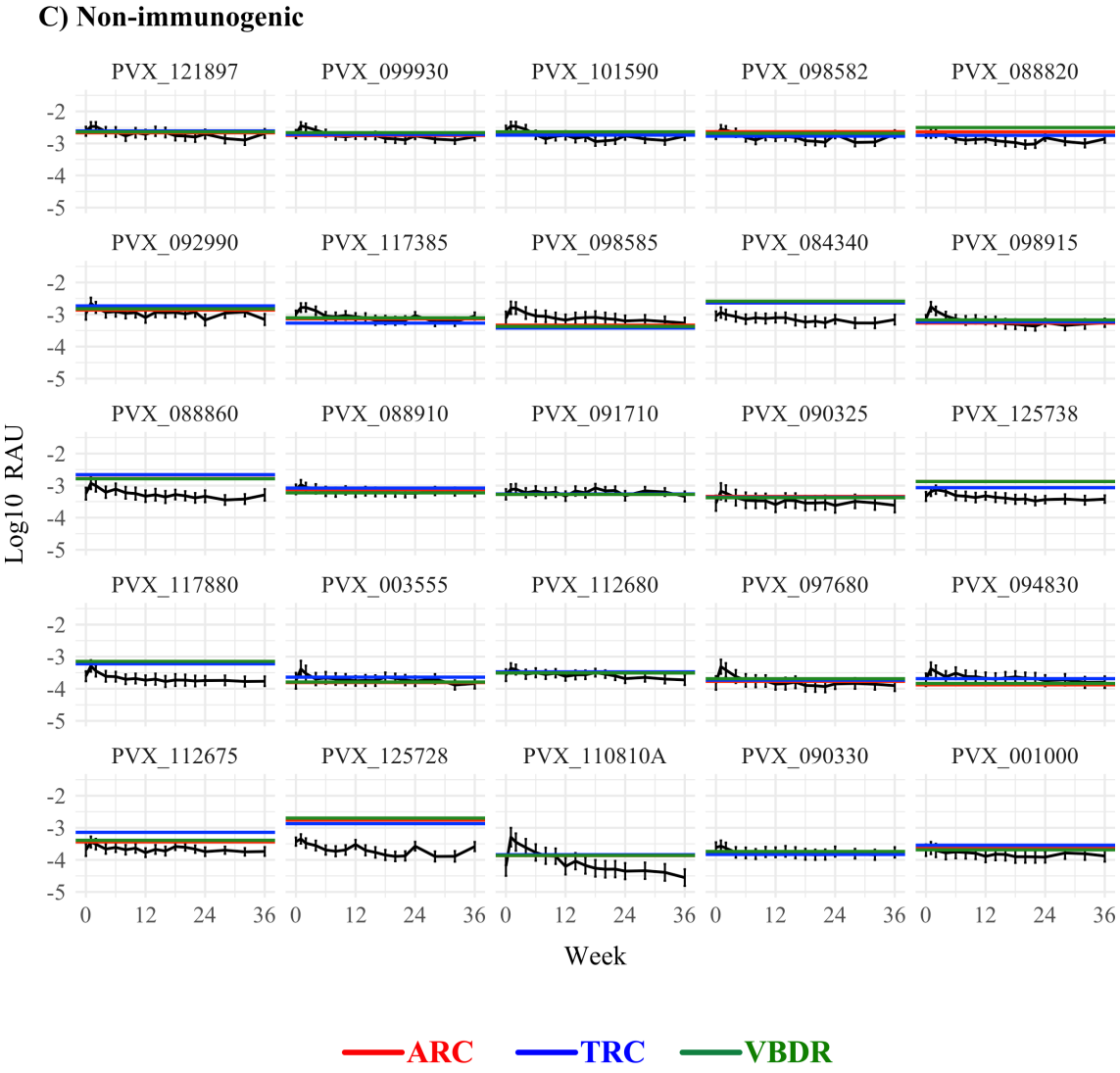


Figure 4.1 Total IgG kinetic profiles against 52 *P. vivax* antigens in the Thai symptomatic cohort. Antigen-specific IgG antibody responses were measured for 9 months following a symptomatic *P. vivax* infection among 34 patients from western Thailand. The observed kinetics profiles were categorised into A) long-lived (> 1 SD at 1-week and > 0.5 SD at 24-week post-infection above negative control baseline); B) short-lived (> 1 SD at 1-week but < 0.5 SD at 24-week post-infection) and C) non-immunogenic (< 1 SD at 1-week post-infection). Negative control panels consisted of malaria-free individuals from 3 sources: ARC (n = 100), TRC (n = 72) and VBDR (n = 102). Data are expressed as median ± 95% CI.

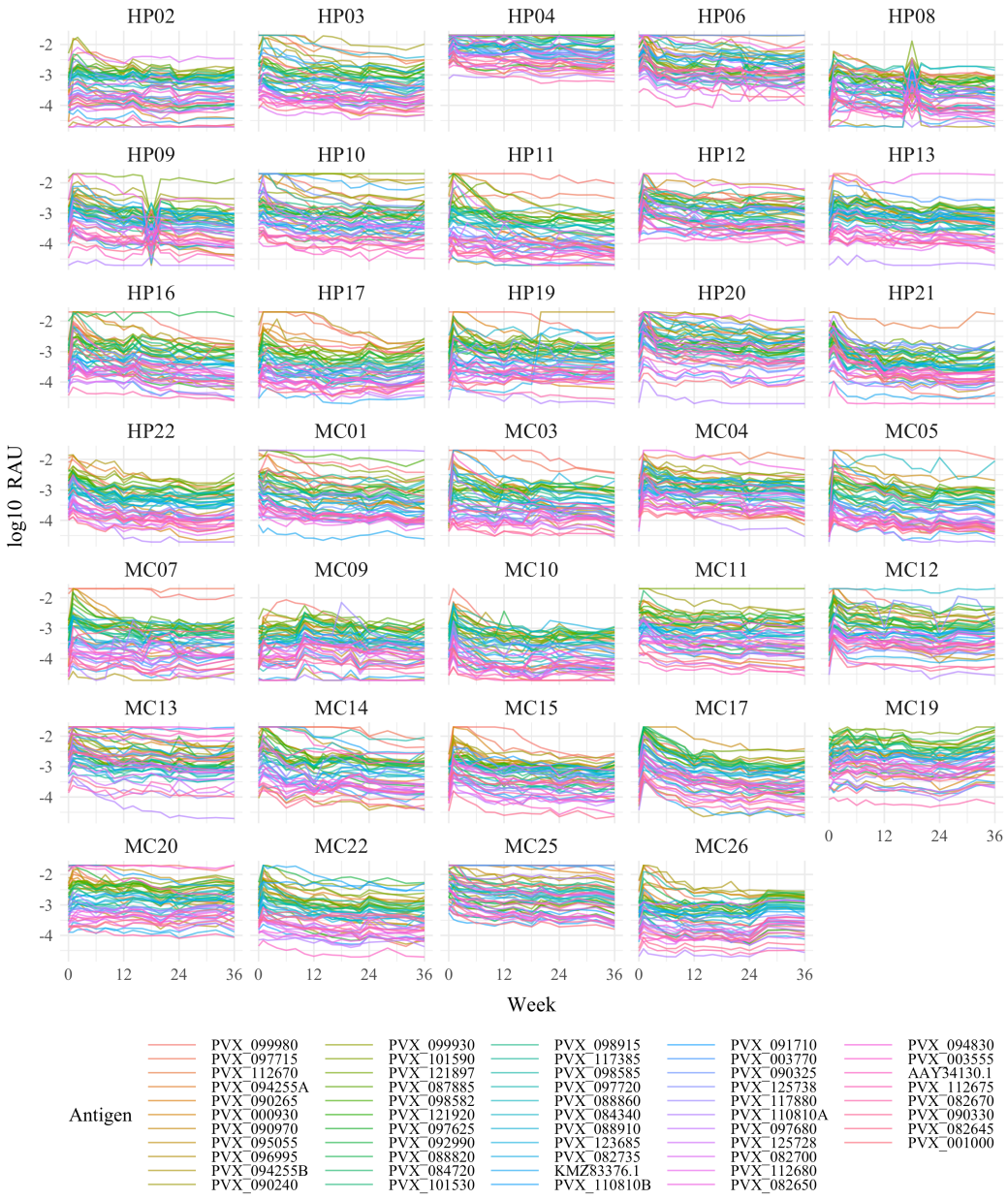


Figure 4.2 Total IgG kinetic profiles at an individual level following symptomatic infections. Antigen-specific IgG antibody responses were measured for 9 months following a symptomatic *P. vivax* infection among 34 patients from western Thailand. The responses of each of the 34 participants were plotted per *P. vivax* antigen. The 52 antigens were ordered based on the magnitude of the peak IgG response, from greatest to smallest, estimated using mathematical modelling.

Table 4.1 Relative IgG immunogenicity against 52 *P. vivax* antigens in the Thai symptomatic cohort. The longevity category of each antigen, level of antigen-specific total IgG antibodies at 1-week post-infection and the proportion of the 34 individuals who reached 1, 5, 10, 25 and 50% of the 1:50 diluted PNG hyperimmune pool are shown.

Protein ID[a]	Longevity category[d]	Total IgG titre (RAU×10³)[e]			Number of volunteers (Proportion)				
		Median	95% CI		1% of PNG levels	5% of PNG levels	10% of PNG levels	25% of PNG levels	50% of PNG levels
PVX_099980	Long	20.00	9.15	20.00	34 (1.0)	34 (1.0)	34 (1.0)	34 (1.0)	17 (0.5)
PVX_096995	Short	4.99	2.40	15.29	34 (1.0)	34 (1.0)	33 (1.0)	27 (0.8)	20 (0.6)
PVX_088860	Non-immunogenic	1.18	0.63	15.29	34 (1.0)	28 (0.8)	19 (0.6)	8 (0.2)	7 (0.2)
PVX_101530	Long	1.95	0.84	3.28	34 (1.0)	32 (0.9)	23 (0.7)	15 (0.4)	8 (0.2)
PVX_112680	Non-immunogenic	0.43	0.26	0.97	34 (1.0)	20 (0.6)	11 (0.3)	5 (0.1)	3 (0.1)
PVX_097715	Short	8.13	3.37	19.14	34 (1.0)	34 (1.0)	32 (0.9)	29 (0.9)	22 (0.6)
PVX_094830	Non-immunogenic	0.42	0.20	1.41	34 (1.0)	18 (0.5)	13 (0.4)	8 (0.2)	2 (0.1)
PVX_112675	Non-immunogenic	0.36	0.25	0.52	32 (0.9)	15 (0.4)	8 (0.2)	5 (0.1)	2 (0.1)
PVX_112670	Short	6.97	2.50	15.91	34 (1.0)	34 (1.0)	32 (0.9)	28 (0.8)	23 (0.7)
PVX_090970	Short	5.14	1.61	13.60	34 (1.0)	32 (0.9)	29 (0.9)	24 (0.7)	18 (0.5)
PVX_084720	Long	1.94	1.04	4.07	34 (1.0)	33 (1.0)	25 (0.7)	12 (0.4)	7 (0.2)
PVX_003770	Short	0.75	0.27	2.94	34 (1.0)	24 (0.7)	18 (0.5)	12 (0.4)	8 (0.2)
PVX_092990	Non-immunogenic	2.27	1.06	5.70	34 (1.0)	33 (1.0)	29 (0.9)	22 (0.6)	11 (0.3)
PVX_091710	Non-immunogenic	0.76	0.59	2.29	34 (1.0)	26 (0.8)	17 (0.5)	9 (0.3)	7 (0.2)
PVX_087885	Long	2.93	1.51	5.22	34 (1.0)	33 (1.0)	29 (0.9	19 (0.6)	9 (0.3)

Protein ID[a]	Longevity category[d]	Total IgG titre (RAU×10³)[e]			Number of volunteers (Proportion)				
		Median	95% CI		1% of PNG levels	5% of PNG levels	10% of PNG levels	25% of PNG levels	50% of PNG levels
PVX_003555	Non-immunogenic	0.41	0.16	1.37	34 (1.0)	20 (0.6)	15 (0.4)	9 (0.3)	6 (0.2)
PVX_117385	Non-immunogenic	1.65	1.08	3.88	34 (1.0)	31 (0.9)	22 (0.6)	11 (0.3)	5 (0.1)
PVX_090265	Short	5.37	2.59	7.43	34 (1.0)	34 (1.0)	31 (0.9)	25 (0.7)	17 (0.5)
PVX_082700	Long	0.44	0.19	2.39	27 (0.8)	15 (0.4)	12 (0.4)	10 (0.3)	7 (0.2)
PVX_082650	Long	0.43	0.12	5.06	27 (0.8)	17 (0.5)	12 (0.4)	9 (0.3)	9 (0.3)
PVX_094255A[c]	Long	5.46	2.45	7.84	34 (1.0)	34 (1.0)	29 (0.9)	29 (0.9)	21 (0.6)
PVX_097680	Non-immunogenic	0.49	0.16	1.39	33 (1.0)	19 (0.6)	10 (0.3)	7 (0.2)	5 (0.1)
PVX_001000	Non-immunogenic	0.23	0.14	0.80	29 (0.9)	14 (0.4)	8 (0.2)	5 (0.1)	2 (0.1)
PVX_097625	Long	2.52	0.85	5.16	34 (1.0)	30 (0.9)	28 (0.8)	19 (0.6)	12 (0.4)
PVX_082670	Short	0.33	0.14	1.69	25 (0.7)	12 (0.4)	10 (0.3)	8 (0.2)	6 (0.2)
PVX_099930	Non-immunogenic	3.53	2.40	6.53	34 (1.0)	34 (1.0)	33 (1.0)	19 (0.6)	9 (0.3)
PVX_084340	Non-immunogenic	1.15	0.78	4.09	34 (1.0)	27 (0.8)	17 (0.5)	10 (0.3)	7 (0.2)
PVX_098915	Non-immunogenic	1.75	0.89	2.24	34 (1.0)	29 (0.9)	23 (0.7)	8 (0.2)	6 (0.2)
PVX_088820	Non-immunogenic	2.01	1.55	3.47	34 (1.0)	34 (1.0)	31 (0.9)	13 (0.4)	7 (0.2)
PVX_082735	Long	1.02	0.41	2.20	32 (0.9)	21 (0.6)	16 (0.5)	10 (0.3)	7 (0.2)
PVX_082645	Short	0.25	0.15	1.69	28 (0.8)	13 (0.4)	10 (0.3)	7 (0.2)	3 (0.1)
PVX_117880	Non-immunogenic	0.52	0.27	1.85	33 (1.0)	17 (0.5)	14 (0.4)	7 (0.2)	3 (0.1)
PVX_121897	Non-immunogenic	3.37	2.03	7.57	34 (1.0)	34 (1.0)	30 (0.9)	20 (0.6)	13 (0.4)
PVX_125728	Non-immunogenic	0.45	0.25	0.71	34 (1.0)	21 (0.6)	10 (0.3)	2 (0.1)	1 (0.0)
PVX_090330	Non-immunogenic	0.27	0.17	0.92	27 (0.8)	12 (0.4)	9 (0.3)	4 (0.1)	1 (0.0)
PVX_123685	Long	1.03	0.54	2.29	34 (1.0)	24 (0.7)	13 (0.4)	9 (0.3)	3 (0.1)
PVX_125738	Non-immunogenic	0.65	0.41	1.83	34 (1.0)	13 (0.4)	10 (0.3)	4 (0.1)	2 (0.1)
PVX_097720	Long	1.37	0.31	3.50	31 (0.9)	22 (0.6)	19 (0.6)	13 (0.4)	7 (0.2)

Protein ID[a]	Longevity category[d]	Total IgG titre (RAU×10³)[e]			Number of volunteers (Proportion)				
		Median	95% CI		1% of PNG levels	5% of PNG levels	10% of PNG levels	25% of PNG levels	50% of PNG levels
PVX_000930	Long	5.29	1.66	11.96	34 (1.0)	34 (1.0)	32 (0.9)	25 (0.7)	20 (0.6)
PVX_098585	Non-immunogenic	1.62	0.78	4.39	34 (1.0)	30 (0.9)	25 (0.7)	15 (0.4)	10 (0.3)
PVX_098582	Non-immunogenic	2.81	1.91	4.56	34 (1.0)	34 (1.0)	31 (0.9)	14 (0.4)	7 (0.2)
PVX_121920	Long	2.54	1.69	3.55	34 (1.0)	34 (1.0)	30 (0.9)	15 (0.4)	4 (0.1)
PVX_094255B[c]	Long	4.72	1.20	14.10	29 (0.9)	28 (0.8)	26 (0.8)	25 (0.7)	22 (0.6)
PVX_090325	Non-immunogenic	0.67	0.21	2.82	34 (1.0)	19 (0.6)	15 (0.4)	9 (0.3)	6 (0.2)
PVX_101590	Non-immunogenic	3.47	2.09	8.45	34 (1.0)	34 (1.0)	30 (0.9)	20 (0.6)	12 (0.4)
PVX_110810A[c]	Non-immunogenic	0.51	0.11	1.46	29 (0.9)	21 (0.6)	15 (0.4)	9 (0.3)	6 (0.2)
PVX_090240	Short	3.70	1.10	15.50	34 (1.0)	34 (1.0)	29 (0.9)	19 (0.6)	15 (0.4)
PVX_088910	Non-immunogenic	1.07	0.67	1.62	34 (1.0)	21 (0.6)	15 (0.4)	5 (0.1)	3 (0.1)
PVX_095055	Long	5.10	1.18	17.45	34 (1.0)	30 (0.9)	28 (0.8)	21 (0.6)	18 (0.5)
PVX_110810B[c]	Long	0.90	0.35	3.18	33 (1.0)	25 (0.7)	19 (0.6)	11 (0.3)	8 (0.2)
AAY34130.1[b]	Long	0.37	0.15	2.49	30 (0.9)	19 (0.6)	12 (0.4)	10 (0.3)	5 (0.1)
KMZ83376.1[b]	Long	0.97	0.11	5.04	28 (0.8)	21 (0.6)	18 (0.5)	16 (0.5)	11 (0.3)

[a] PlasmoDB codes (http://plasmodb.org/plasmo/), [b] GenBank codes (http://www.ncbi.nlm.nih.gov/genbank/), [c] A and B represent two distinct protein fragments derived from one full-length protein sequence and hence are expressed by identical PlasmoDB code, [d] Longevity category is defined by the magnitude of antigen-specific total IgG at 1- and 24-week post-infection in comparison to the malaria-naïve baseline: non-immunogenic (< 1SD above baseline at week 1), short-lived (> 1SD above baseline at week 1 but <

0.5 SD above baseline at week 24) and long-lived (> 1SD above baseline at week 1 and > 0.5 SD above baseline at week 24), [e] Total IgG levels are expressed in RAU interpolated from standard curves using a 5PL logistic regression model. Values were multiplied by 1000 for easy interpretation.

Abbreviations: 95% CI = 95% confidence interval; SD = standard deviation.

In an attempt to generate a quantitative measure of the IgG longevity, rather than the binary categories of short and long, we used mathematical modelling to estimate both the peak magnitude and the decay rate per antigen. The longevity of antibody decay is assessed by calculating the predicted proportion of the peak response remaining at 6, 12 and 24 months. Mathematical modelling has previously been applied to antibody data following infections [26, 108, 123, 238]; however, the current data set is the largest and richest (in terms of number of measurements and number of antigens) and thus the analysis was highly complex. Presented here are modelling results obtained by Dr Michael White (mathematical modeller at the Institut Pasteur, France). An important limitation to this modelling is that antigen-specific background signals measured in malaria-naïve negative control panels were not taken into consideration. Further improvements and refinements will be made, as noted in the Chapter 7.

Interestingly, there was little difference in the proportion of the peak response remaining at 6, 12 and 24 months between the antigens with short-lived (25%, 22% and 18%) and long-lived profiles (26%, 22% and 14%) (Figure 4.3A). As indicated by the interquartile range, antigens with a long-lived profile tend to show greater variation than the short-lived (Figure 4.3A). Figure 4.3B shows the estimated magnitude of IgG responses up to 24 months by multiplying the peak response with the remaining proportion of the peak predicted over time. The

decay was estimated to remain similar throughout the 24 months regardless of an antigen's IgG longevity profile. Additionally, all antigens exhibited bi-phasic characteristics, with a steeper decay initially until 6 months when the decay rate reduced significantly. These results suggest that all immunogenic antigens had similar decay profiles and that the binary categorisation based on longevity was dominated by immunogenicity compared to the negative controls instead of longevity. At this stage, we therefore do not yet have a robust quantitative measure of antibody decay that takes into account the differing levels of background reactivity between antigens, and thus further analysis in the below Sections was performed using the binary longevity categories only.

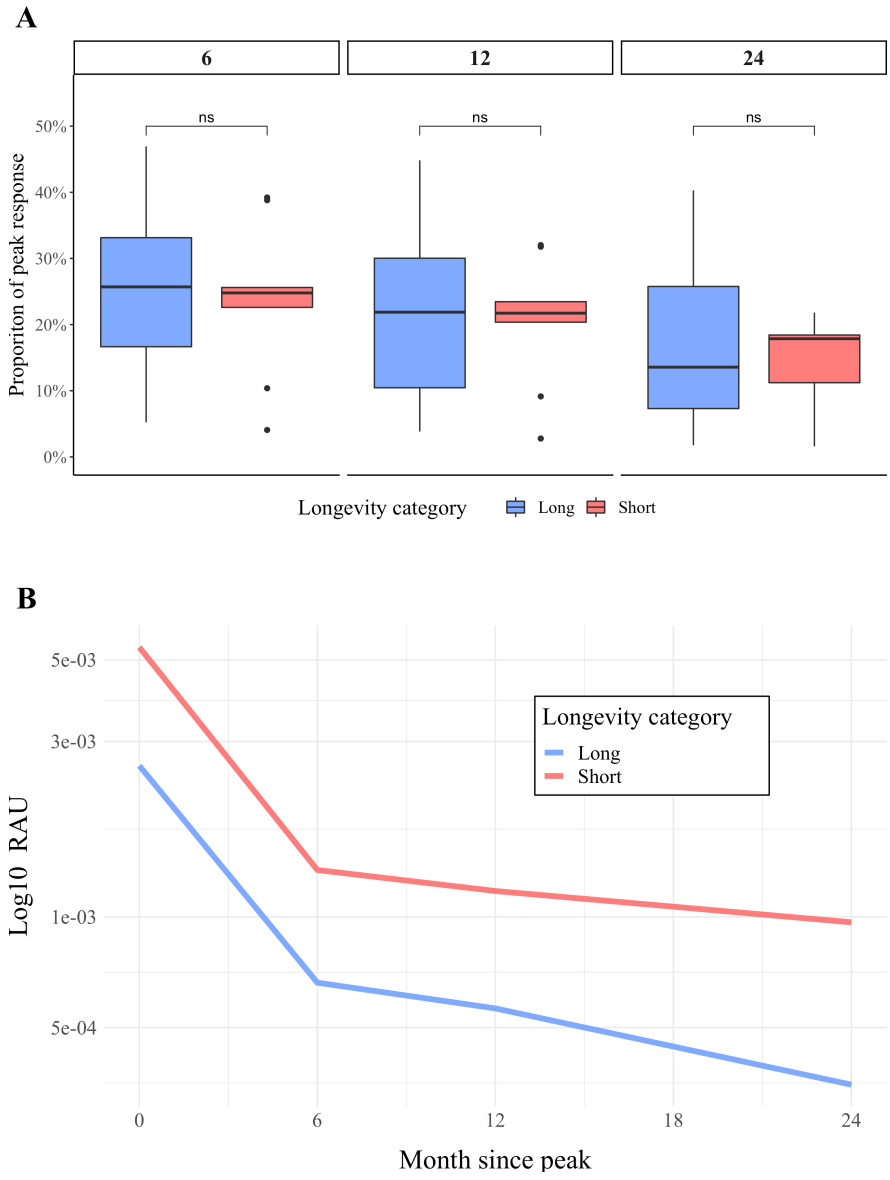


Figure 4.3 Relationship between modelled antibody decay rate and the assigned IgG longevity category. The IgG antibody kinetic profiles of 52 *P. vivax* antigens were obtained on the Luminex® platform and were classified into two longevity categories in comparison to the negative control panels. Mathematical modelling was used to produce **A)** estimated proportion of remaining peak response at 6-, 12- and 24-months post-peak. **B)** Antibody magnitude (log_{10} RAU) post-peak was calculated from peak magnitude multiplied by estimated proportion of remaining peak at the 3 time points. Mann-Whitney's (non-parametric) test was performed to determine statistical significance ($p > 0.05$ ns).

4.2.2 Evaluation of association between antigenic features and total IgG longevity

To explore the potential sources that could account for the acquisition and maintenance of IgG responses against *P. vivax* antigens, I examined the impact of several antigen features that could potentially play a role. These included the presence or absence of predicted SP, TMD, GPI anchors, PEXEL, enzyme domains and the number of LCRs (Table 4.2). SP sequences and PEXEL motifs are responsible for trafficking and secretion of several *Plasmodium* surface antigens capable of inducing robust immune responses [383-386]. The presence of TMDs and GPI anchors suggests the antigens are membrane-bound, and could be targeted by functional antibodies [384, 387, 388]. The presence of enzyme domains is a key indication of conversed protein domains that are often associated with several surface antigens, for instance, merozoite surface proteins (MSPs) [389-391]. LCRs are identified as highly conserved short or single repeats of sequences with limited diversity in protein composition [392]. Multiple studies have demonstrated LCRs can be crucial epitopes for antibody responses [393, 394]. However, no clear associations have been established between these antigen characteristics and maintenance of antibody responses.

Table 4.2 Antigenic features of the 52 *P. vivax* antigens selected for this study.

Antigen ID[a]	SP	TMD	GPI	PEXEL/ PNEP	Enzyme Domains	LCR
PVX_099980	Yes	Yes	Yes	PNEP	1	12
PVX_096995	No	Yes	No	PNEP	1	7
PVX_088860	Yes	Yes	No	PNEP	NP	5
PVX_101530	Yes	Yes	No	PEXEL	NP	3
PVX_112680	Yes	No	No	PNEP	1	1
PVX_097715	Yes	Yes	No	PNEP	NP	6
PVX_094830	Yes	No	No	PNEP	NP	1
PVX_112675	Yes	Yes	No	PNEP	2	1
PVX_112670	Yes	No	No	PNEP	1	4
PVX_090970	Yes	Yes	No	PNEP	NP	3
PVX_084720	Yes	No	No	PNEP	NP	11
PVX_003770	Yes	Yes	Yes	PNEP	NP	2
PVX_092990	Yes	Yes	No	PNEP	1	17
PVX_091710	Yes	No	No	PNEP	1	8
PVX_087885	Yes	No	No	PNEP	NP	11
PVX_003555	No	Yes	No	PEXEL	1	7
PVX_117385	No	No	No	PNEP	NP	2
PVX_090265	No	Yes	No	PNEP	1	3
PVX_082700	Yes	No	No	PNEP	1	2
PVX_082650	Yes	No	No	PNEP	1	4
PVX_094255A[c]	Yes	No	No	PNEP	NP	10
PVX_097680	Yes	No	No	PNEP	NP	17
PVX_001000	Yes	No	No	PEXEL	NP	3
PVX_097625	Yes	Yes	Yes	PNEP	2	4
PVX_082670	Yes	No	No	PEXEL	1	5
PVX_099930	Yes	No	No	PNEP	NP	3
PVX_084340	No	No	No	PNEP	NP	1
PVX_098915	No	No	No	PNEP	NP	0
PVX_088820	No	Yes	No	PNEP	1	2
PVX_082735	Yes	Yes	No	PNEP	1	5
PVX_082645	Yes	No	No	PNEP	1	4
PVX_117880	Yes	Yes	No	PNEP	NP	13
PVX_121897	Yes	No	No	PNEP	1	1
PVX_125728	Yes	No	No	PNEP	1	2
PVX_090330	Yes	No	No	PNEP	NP	4
PVX_123685	No	No	No	PNEP	3	12
PVX_125738	No	Yes	No	PNEP	NP	3

Antigen ID[a]	SP	TMD	GPI	PEXEL/ PNEP	Enzyme Domains	LCR
PVX_097720	Yes	Yes	No	PNEP	NP	14
PVX_000930	Yes	Yes	No	PNEP	NP	2
PVX_098585	Yes	No	No	PNEP	NP	12
PVX_098582	Yes	No	No	PNEP	NP	14
PVX_121920	Yes	No	No	PNEP	1	9
PVX_094255B[c]	Yes	No	No	PNEP	1	10
PVX_090325	Yes	Yes	No	PNEP	NP	16
PVX_101590	Yes	No	No	PNEP	NP	4
PVX_110810A[c]	Yes	Yes	No	PNEP	4	8
PVX_090240	Yes	No	No	PNEP	NP	1
PVX_088910	Yes	No	Yes	PNEP	NP	8
PVX_095055	Yes	No	No	PNEP	9	1
PVX_110810B[c]	Yes	Yes	No	PNEP	4	8
AAY34130.1[b]	No	No	No	PNEP	1	2
KMZ83376.1[b]	No	Yes	No	PNEP	1	3

[a] PlasmoDB codes (http://plasmodb.org/plasmo/), [b] GenBank codes, [c] A and B represent two distinct antigen fragments derived from one full-length antigen sequence and hence are expressed by identical PlasmoDB code.

Abbreviations: SP = signal peptide; TMD = transmembrane domain; GPI = glycosylphosphatidylinisotol; PEXEL =*Plasmodium* exported element motif; PNEP = PEXEL-negative exported protein; NP = none predicted; LCR = low-complexity region.

The majority of the 52 *P. vivax* antigens are predicted to contain signal peptides (79%), no transmembrane domains (58%), no GPI anchor (92%) and no PEXEL motif (92%). Half of the antigens are predicted to have enzyme domains. On average, these antigens had one enzyme domain which tended to be an epidermal growth factor (EGF) or Tryptophan-Threonine-rich *Plasmodium* antigen (Pfam) domains at the C-terminus. All antigens were predicted to contain LCRs (range=1-17, mean=5.98; median=4), except for PVX_098915, which had none. No statistically significant association was found between all of these characteristics with either immunogenicity (27 immunogenic versus 25 non-immunogenic antigens) or the IgG longevity profile (18 long-lived versus 9 short-lived) (Table 4.3, Fisher's exact test, $p>0.05$). The impact of an increasing number of LCRs and enzyme domains was also assessed with logistic regression as continuous variables, but no associations were found (Table 4.4).

Table 4.3 Effects of antigen features on total IgG immunogenicity and longevity categorisations. Fisher's exact tests were performed between immunogenic and non-immunogenic categories, and long- and short-lived categories. p value less than 0.05 was considered significant.

Antigen feature[a]	Immunogenicity			Longevity		
Category	Immunogenic (n=27)	Non-immunogenic (n=25)	p value	Long-lived (n=18)	Short-lived (n=9)	p value
PEXEL	2	2	> 0.99	1	1	> 0.99
Signal Peptide	22	19	0.74	15	7	> 0.99
GPI Anchor	3	1	0.61	2	1	> 0.99
Transmembrane Domain	13	9	0.41	8	5	0.69
Enzyme Domain	17	9	0.09	12	5	0.68

[a]Numbers of antigens expressing the features are indicated

Table 4.4 Effects of the increasing number of enzyme domains and LCRs on antibody profile categorisation. Logistic regression analysis was performed and estimates were adjusted for the presence of signal peptide, transmembrane domain, GPI anchor, PEXEL, LCR and/or enzyme domain.

Category	Enzyme Domain		LCR	
	Unadjusted	Adjusted	Unadjusted	Adjusted
Immunogenicity				
Odds ratio	1.60	1.55	0.99	0.98
p value	0.13	0.17	0.84	0.80
95% CI	0.88 – 2.92	0.83 – 2.87	0.88 - 1.11	0.86 - 1.12
Longevity				
Odds ratio	2.00	2.32	1.28	1.27
p value	0.20	0.31	0.08	0.09
95% CI	0.69 – 5.80	0.45 – 11.92	0.97 - 1.69	0.97 - 1.68

4.2.3 Association between IgG subclass dominance and IgM immunogenicity with total IgG longevity

The distribution of IgG subclasses is known to change from IgG1 dominance to IgG1 and IgG3 co-dominance with increasing exposure in the context of malaria infections [224, 294]. Therefore, it is plausible that differences in IgG subclass responses could be present to antigens with differing longevity profiles, for example, antigens with long-lived IgG responses might have both IgG1 and IgG3. In addition, IgM is elicited upon first encounter with most pathogens [395], so I was interested to address whether IgM immunogenicity was associated with IgG immunogenicity and/or longevity profiles. The hypothesis was that high IgM levels, potentially reflective of an early immune response, would be associated with low levels of IgG immunogenicity and short-lived IgG responses.

IgG subclass responses to 26 IgG-immunogenic antigens (PVX_123685 was excluded from the panel by mistake) were measured at week 2 post-infection and IgM levels to all 52 antigens were measured at week 1 post-infection. Dominance of IgG subclass responses and IgM positivity were compared between antigens with long-lived (n=17) and short-lived (n=9) IgG profiles.

For IgG subclass, IgG1 was identified as the predominant response whilst no IgG4 was detected in the symptomatic Thai individuals at 2 weeks post-infection. I also observed consistently less robust IgG3 signals and very weak IgG2 compared to IgG1. Among the 26 IgG-immunogenic antigens, four types of IgG subclass reactivity profiles were evident: i) IgG1 only (n=13); ii) predominant IgG1 with sub-dominant IgG3 (n=9); iii) predominant IgG1 with subdominant IgG2 and IgG3 (n=2); and iv) IgG1, 2 and 3 with no obvious dominance (n=2) (Table 4.5). Fisher's exact test showed no significant difference in the complexity of IgG subclass profile (comparing IgG1 only, n=13, with mixed IgG subclass responses, n=13) between antigens with long- and short-lived total IgG profiles ($p>0.99$).

IgG subclass kinetics were also measured every 2 weeks throughout the study follow-up. Figure 4.4 shows that, after adjustment with the negative control baseline, IgG1 was acquired more rapidly than other subclasses and its predominance was maintained throughout the study. It was also evident that the magnitude of IgG1 most strongly mirrored that of total IgG over time. Additionally, antigen-specific baseline signals were found to vary significantly. IgG1 tended to induce lower baseline responses among malaria-free individuals compared to total IgG, resulting in more robust signals after adjustment. This suggested that the difference in antibody response magnitude between infected

and infection-free volunteers was more prominent for IgG1 than total IgG. I also found that hyper-immune adults from PNG (used as the positive control) had an elevated level of IgG3 to most *P. vivax* antigens compared to that of the Thai symptomatic patients who have had lower levels of lifetime exposure (Figure 4.5), confirming previously reported observations of subclass switch in higher transmission regions [294].

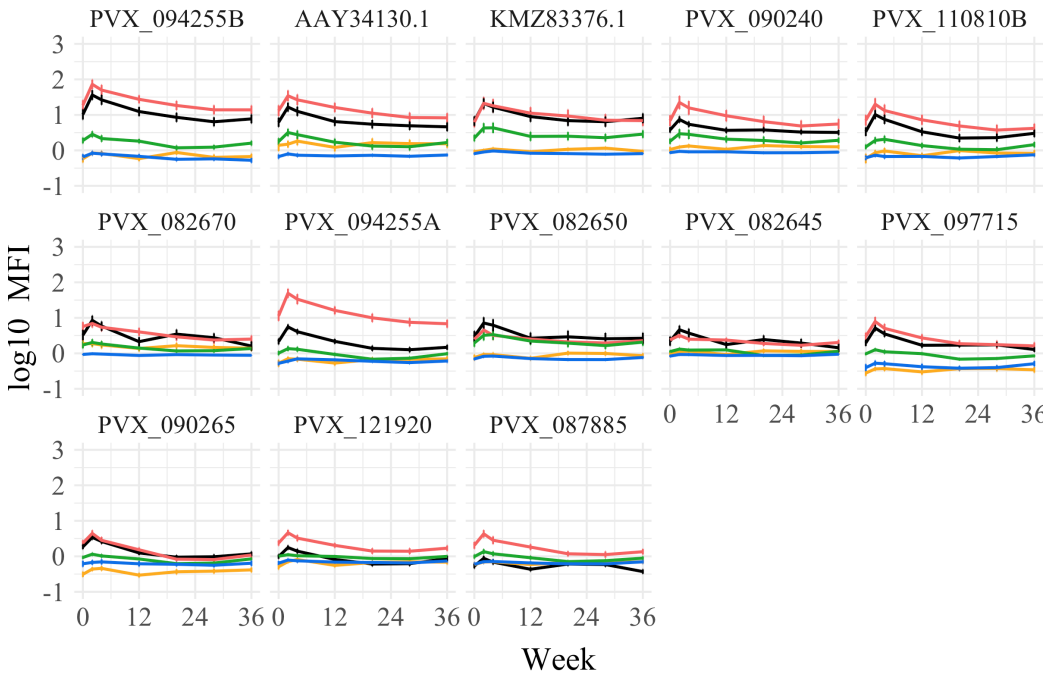
The level of antigen-specific IgM antibodies against 52 antigens was measured in the Thai symptomatic cohort at 1-week post-infection and subsequently compared to the malaria-free panels (Figure 4.6). It was found that only 15 *P. vivax* antigens induced positive IgM responses 2 SD above the median of the negative control panels (Figure 4.6A), although most antigens had a significantly higher IgM level. 2 SD was chosen as the cut-off for classifying responses as IgM immunogenic or not due to the fact that this threshold has been frequently used in multiple previous studies focussing on antibody responses against malaria [396-400]. Interestingly, 7 IgG-non-immunogenic antigens also elicited positive IgM responses. Similar proportions of IgM-positive antigens exhibited long- (n=5, 29.4%) and short-lived (n=3, 33.3%) total IgG profiles (Table 4.5). There was no difference in the likelihood of exhibiting IgM positivity at 1-week post-infection between IgG-immunogenic and non-immunogenic antigens (Fisher's exact test, $p>0.99$).

Table 4.5 IgG subclass categories and IgM positivity for IgG immunogenic antigens 1-2 weeks post-infection in the Thai symptomatic cohort.

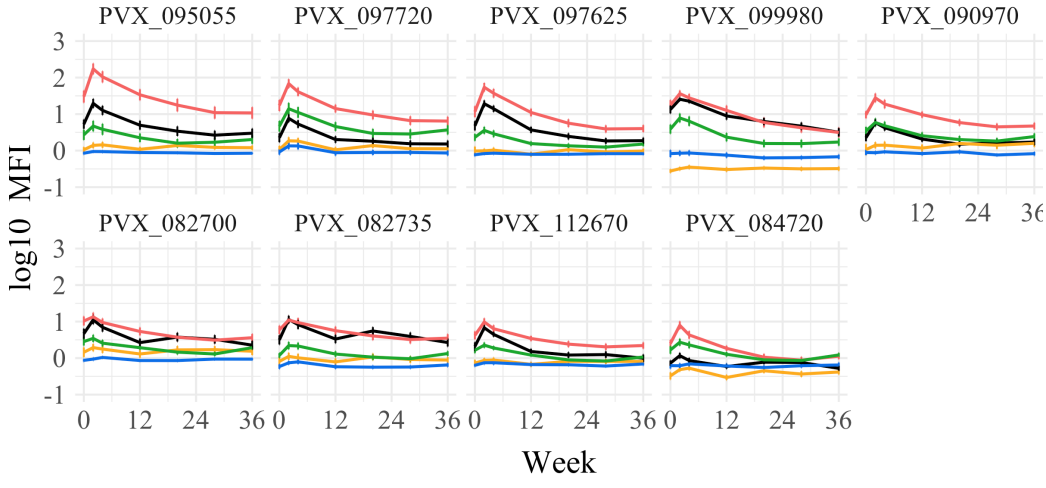
Longevity Category	Long-lived (n=17, 100%)	Short-lived (n=9, 100%)
IgG1	8 (47.1%)	5 (55.6%)
Predominant IgG1 Subdominant IgG3	7 (41.0%)	2 (22.2%)
Predominant IgG1 Subdominant IgG2 & IgG3	1 (5.9%)	1 (11.1%)
IgG1, 2 & 3 (no obvious dominance)	1 (5.9%)	1 (11.1%)
IgM positivity[a]	5 (29.4%)	3 (33.3%)

[a] Cut-offs for IgM positivity were set at + 2 SD from negative control in $\log_{10}$ Relative Antibody Unit (RAU) at 1-week post-infection

A) IgG1 only



B) Predominant IgG1, subdominant IgG3



Total IgG IgG1 IgG2 IgG3 IgG4

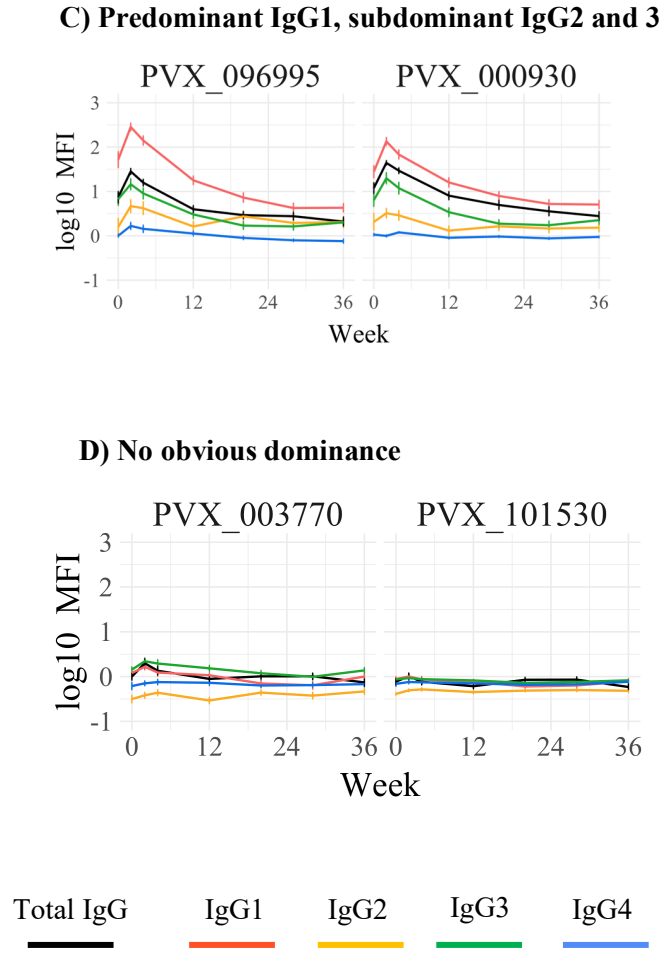


Figure 4.4 Adjusted IgG subclass and total IgG kinetics in the Thai symptomatic cohort. The levels of 4 IgG subclass responses against 26 total-IgG-immunogenic *P. vivax* antigens (PVX_123685 was excluded) were measured every 2-8 weeks for 9 months. Data was adjusted by subtracting the median of pooled negative control panels (n=274). Kinetic profiles are arranged based on IgG subclass profile: **A)** IgG1 only, **B)** predominant IgG1 and subdominant IgG3, **C)** predominant IgG1 and subdominant IgG2 and IgG3 and **D)** no obvious dominance. Data are expressed as median ± 95% CI.

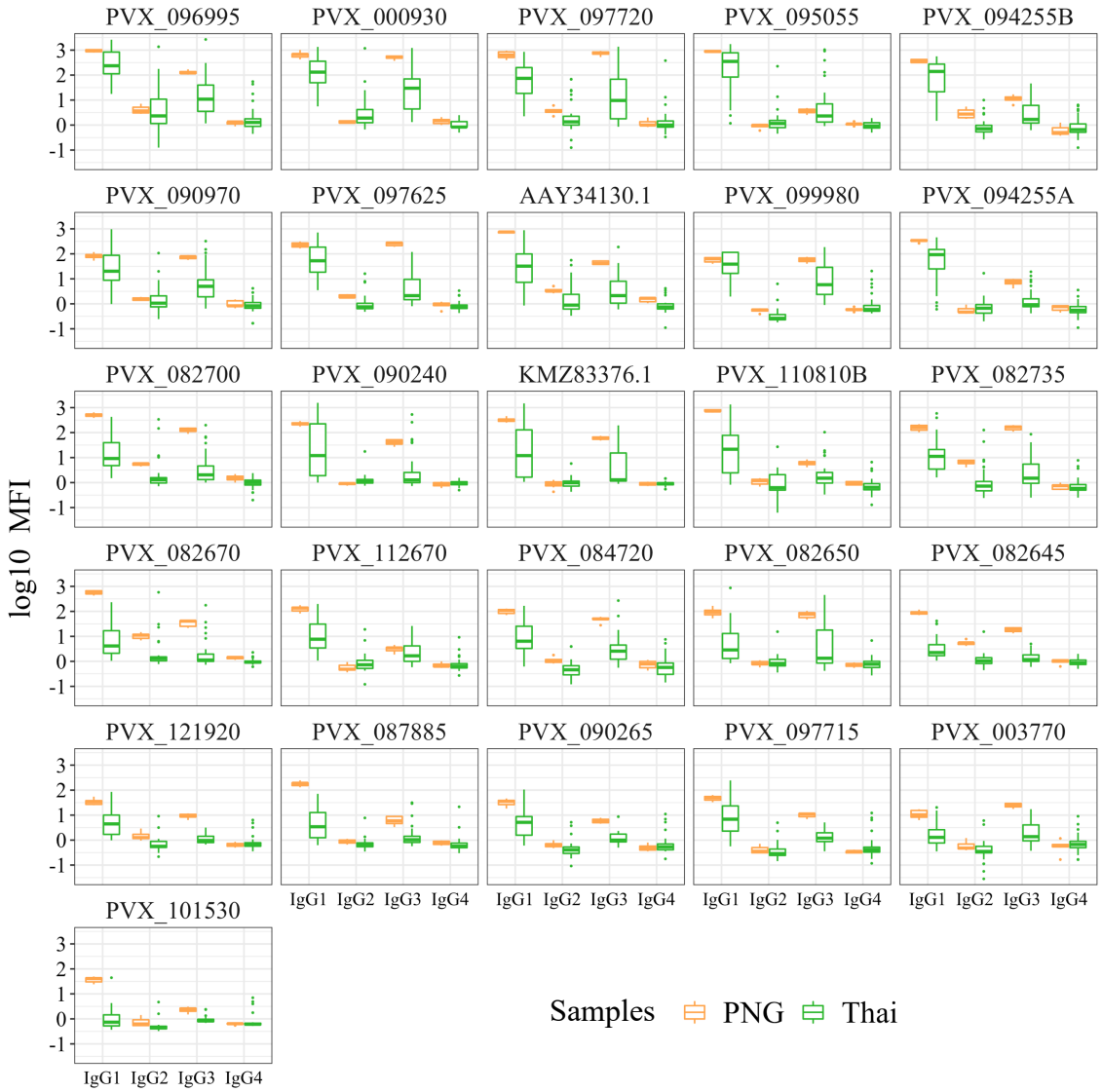
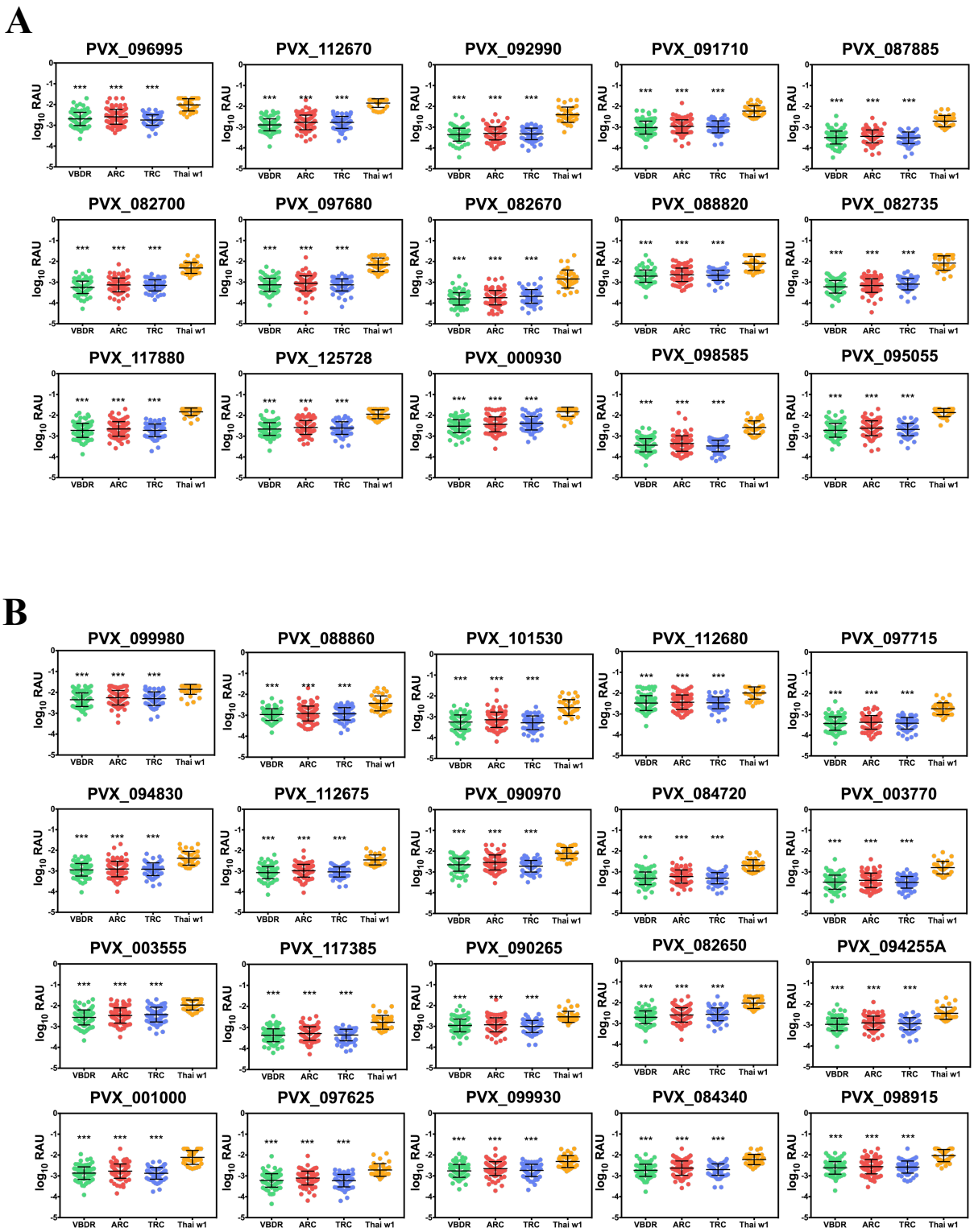


Figure 4.5 Comparison of the adjusted peak IgG subclass magnitude between the Thai symptomatic cohort and the PNG hyperimmune pool. Antigen-specific IgG subclass responses against 26 IgG-immunogenic (PVX_123685 was excluded) antigens were measured for 9 months, and the peak of responses (2-week post-infection) was compared between symptomatic Thai patients and the positive control, hyper-immune pooled plasma of infected PNG individuals. PNG results were collected from the standard curves included in each independent experiment of IgG subclass measurement (n=7). Data was adjusted by subtracting the median of pooled negative control panels (n=274).


A
PVX_096995
PVX_112670
PVX_092990
PVX_091710
PVX_087885
PVX_082700
PVX_097680
PVX_082670
PVX_088820
PVX_082735
PVX_117880
PVX_125728
PVX_000930
PVX_098585
PVX_095055
B
PVX_099980
PVX_088860
PVX_101530
PVX_112680
PVX_097715
PVX_094830
PVX_112675
PVX_090970
PVX_084720
PVX_003770
PVX_003555
PVX_117385
PVX_090265
PVX_082650
PVX_094255A
PVX_001000
PVX_097625
PVX_099930
PVX_084340
PVX_098915
log10 RAU
VBDR
ARC
TRC
Thai w1
***

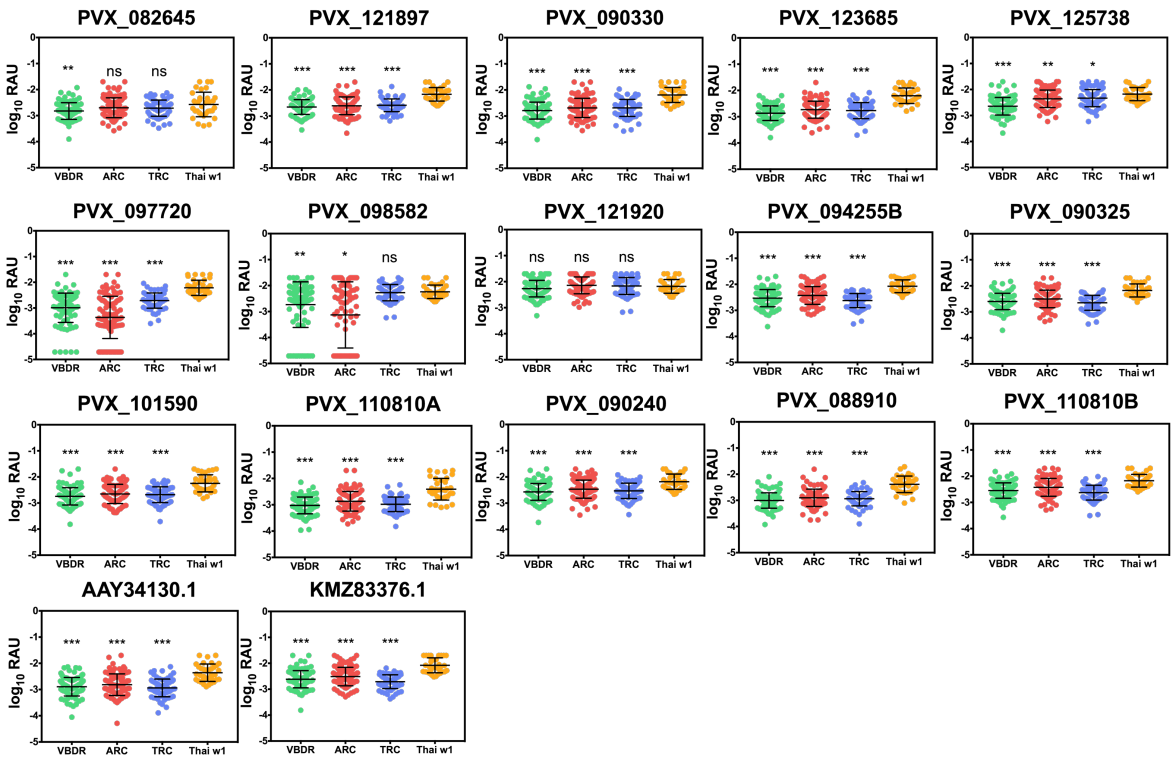


Figure 4.6 Comparison of the peak IgM magnitude between the Thai symptomatic cohort and malaria-free individuals. IgM levels were measured at the peak of responses (1 week following a symptomatic *P. vivax* infection) among 34 Thai patients and were compared to the ARC (n = 100), TRC (n = 72) and VBDR (n = 102) malaria-naïve control panels. Mann-Whitney's (non-parametric) test was performed (p > 0.05 ns, < 0.05 *, < 0.01 **, < 0.001 ***). To down-select IgM-positive antigens, medians and SD were calculated and plotted to identify **A)** antigens with medians more than 2 SD above the pooled negative control panels (n=15) and **B)** those without (n=37).

4.2.4 Association between IgM and total IgG kinetic profiles

To further examine the relationship between IgG and IgM responses, detailed IgM kinetics of the 15 IgM-positive antigens were obtained. These antigens were down-selected based on IgM positivity at 1-week post-infection (more than 2 SD above baseline), including both IgG-immunogenic (n=8; 5 long-lived and 3 short-lived) and IgG-non-immunogenic (n=7) antigens. Figure 4.7 shows IgM kinetics along with total IgG, both adjusted against corresponding baseline signals of the negative control panels. Unadjusted kinetic profiles of IgM responses are shown in Figure 4.8.

All antigens exhibited IgM kinetic patterns similar to total IgG, consisting of an initial peak at week 1 post-infection and gradual decay over the 9 months of study follow-up (Figure 4.7). However, the decay of IgM responses was less distinctive than total IgG. In contrast to popular belief, IgM signals against all 15 antigens were maintained above the median of negative control panels for more than 6 months. In comparison with total IgG, variations in responses between volunteers were also less prominent in IgM (Figure 4.7).

Among 8 IgG-immunogenic antigens, PVX_000930, PVX_096995 and PVX_095055 exhibited a peak total IgG magnitude that was approximately twice

that of IgM before decaying and converging with the IgM level at 18-24 weeks post-infection (Figure 4.7A and B). The level of IgG response against PVX_087885, on the other hand, was maintained above IgM throughout the study. PVX_082700, PVX_082735 and PVX_082670 showed IgM immunogenicity comparable to total IgG for 36 weeks (Figure 4.7A and B). IgM levels against PVX_112670, in particular, remained higher than total IgG since 12-week post-infection (Figure 4.7B). For all 7 IgG-non-immunogenic antigens, IgM responses were stronger than total IgG throughout the study since infection (Figure 4.7C).

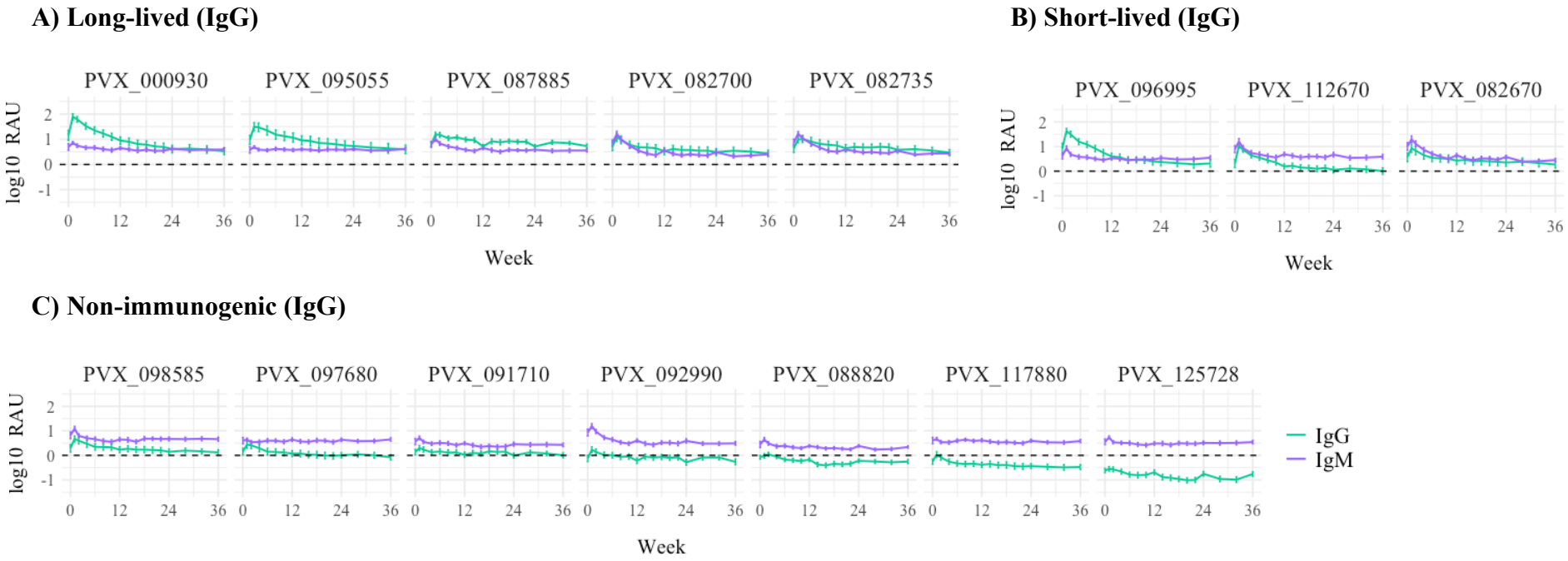


Figure 4.7 Adjusted total IgG and IgM kinetics against *P. vivax* antigens in the Thai symptomatic cohort. 15 antigens with IgM positivity at 1-week post-infection (> 2SD above baseline median) were selected and their IgM responses over a 9-month period were measured and compared to total IgG. Data was adjusted by subtracting the median of pooled negative control panels (n=274). The *P. vivax* antigens are arranged based on total IgG longevity: **A)** long-lived (> 1 SD at 1-week and > 0.5 SD at 24-week post-infection above negative control baseline); **B)** short-lived (> 1 SD at 1-week but < 0.5 SD at 24-week post-infection) and **C)** non-immunogenic (< 1 SD at 1-week post-infection). Data are expressed as the median ± 95% CI. Black dotted lines represent the malaria-naïve baseline.

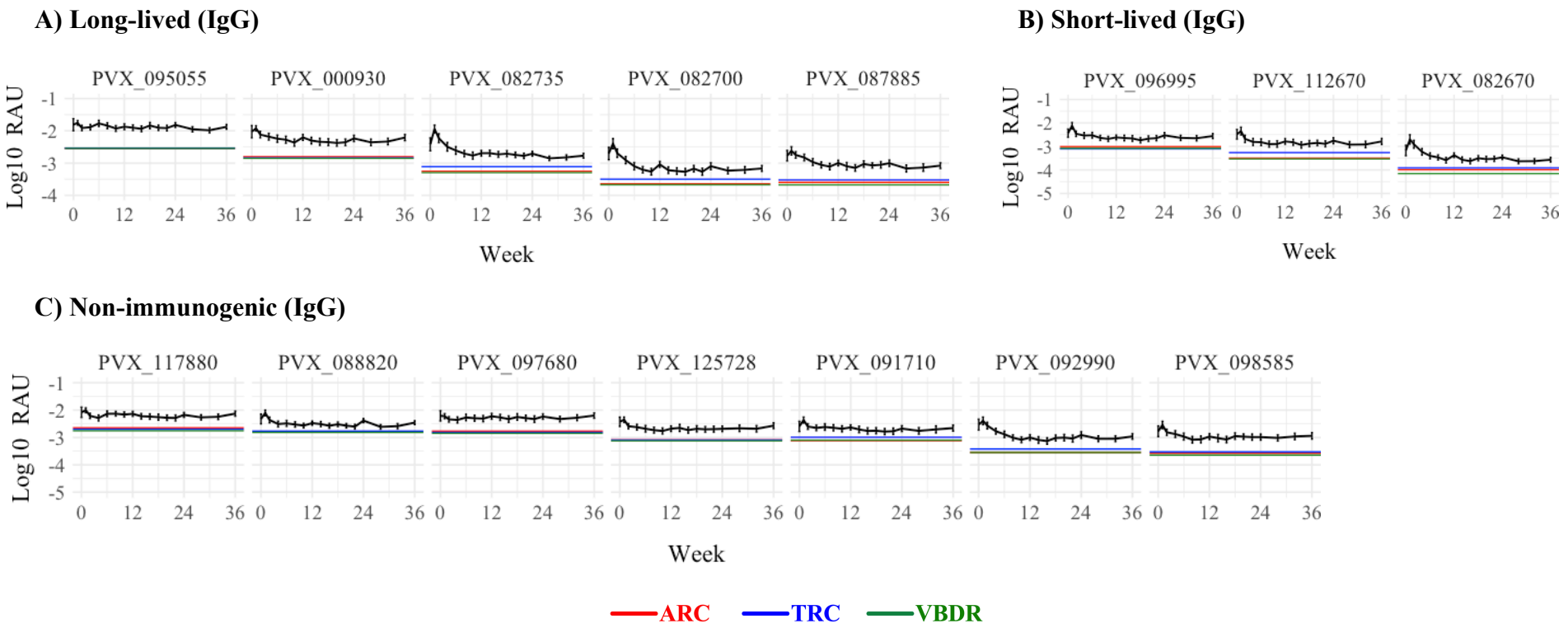


Figure 4.8 Unadjusted IgM kinetics against *P. vivax* antigens in the Thai symptomatic cohort. 8 *P. vivax* antigens that were IgG-immunogenic with IgM positivity (> 2SD above baseline median) at 1-week post-infection were selected and IgM responses over a 9-month period were measured in symptomatic Thai individuals (n=17 timepoints). Horizontal solid lines represent the baseline responses measured in malaria-naïve individuals from 3 different sources (n=274). Data are expressed as the median ± 95% CI.

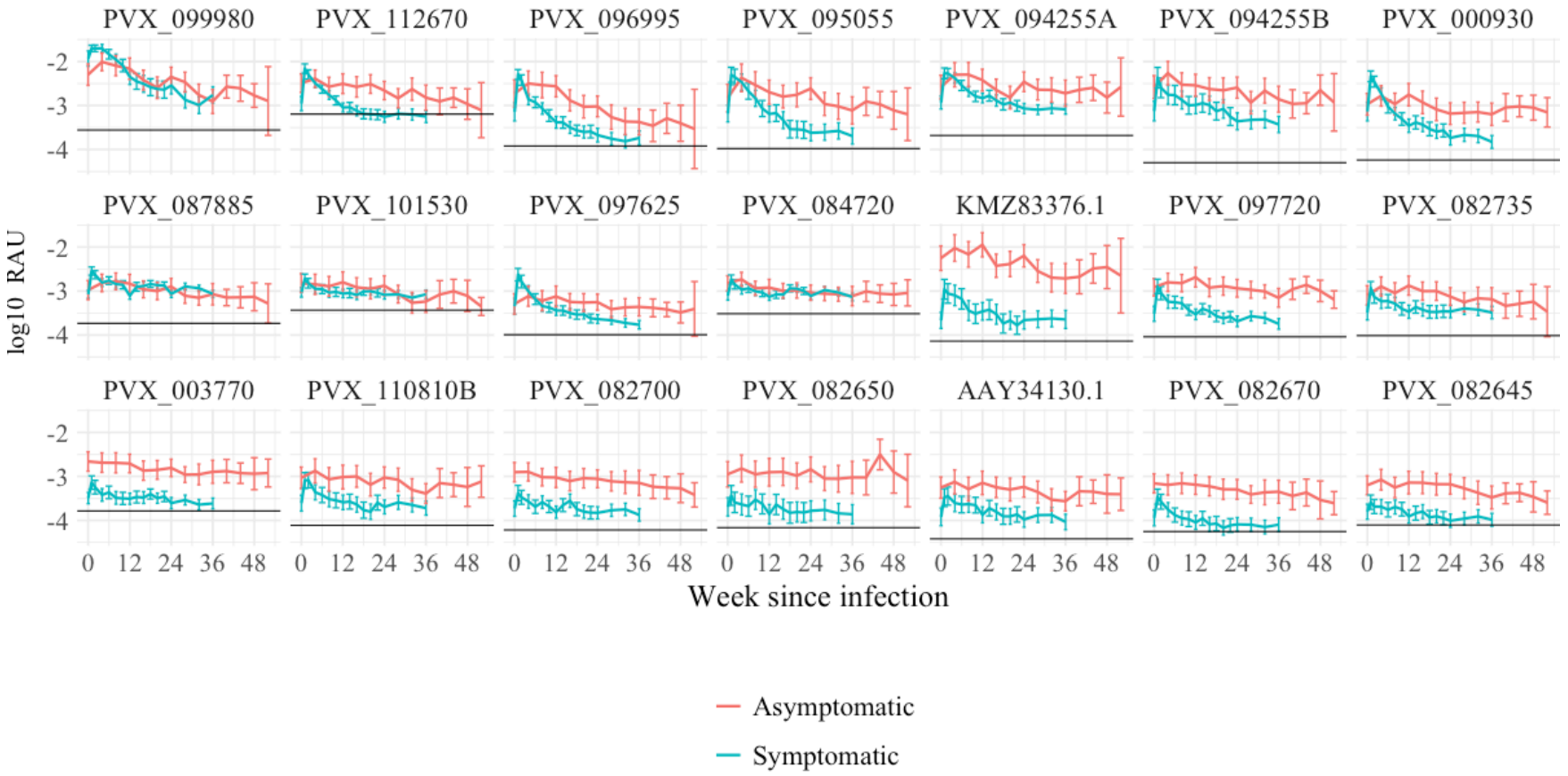
4.2.5 Total IgG longevity following an asymptomatic *P. vivax* infection

Total IgG, IgG subclass and IgM measurements were made in Thai individuals following symptomatic *P. vivax* infections. As these individuals were symptomatic, they have not yet gained sufficient immunity to clinical disease. We were therefore interested to determine whether total IgG kinetics differed in individuals from a similar region of western Thailand who had already acquired immunity to symptomatic disease. 30 individuals were selected from an existing cohort [265] who had an asymptomatic *P. vivax* infection with data available from 14 visits in total. IgG was measured in plasma samples from the time of asymptomatic *P. vivax* infection and all subsequent time-points (i.e. 6 - 13 visits); as per the symptomatic cohort, these individuals were infection-free following the initial detected infection. Total IgG responses were measured against the 27 *P. vivax* antigens found to be IgG immunogenic in the symptomatic cohort. Kinetic profiles against all 27 antigens are shown in Figure 4.9.

21 of 27 *P. vivax* antigens were found to be IgG-immunogenic (more than 1 SD above baseline at the time of infection) following an asymptomatic *P. vivax* infection, all of which showed a long-lived total IgG profile (more than 0.5 SD above baseline at 6-month post-infection) compared to only 18 of the same antigens following symptomatic infection. Individual variation in responses to

antigens was larger than observed in the symptomatic patients, indicated by the longer error bars in Figure 4.9. This is likely related to greater differences in levels of past exposure in these individuals, compared to most symptomatic patients having 0 or 1 past infections (self-reported history)[334]. For *P. vivax* antigens that were non-immunogenic in the asymptomatic *P. vivax* infected individuals (n=6), 4 were classified as short-lived in the symptomatic Thai patients. The lack of response in the asymptomatic individuals might be due to the reduced parasite load; the median parasite density in the asymptomatic individuals (median = 1.0×10^{2}) was 2.5×10^{3} times lower than the symptomatic (median = 2.5×10^{5}) (Table 2.1).

A) Long-lived


PVX_099980
PVX_112670
PVX_096995
PVX_095055
PVX_094255A
PVX_094255B
PVX_000930
PVX_087885
PVX_101530
PVX_097625
PVX_084720
KMZ83376.1
PVX_097720
PVX_082735
PVX_003770
PVX_110810B
PVX_082700
PVX_082650
AAY34130.1
PVX_082670
PVX_082645
log10 RAU
-2
-3
-4
0 12 24 36 48
Week since infection
Asymptomatic
Symptomatic

B) Non-immunogenic

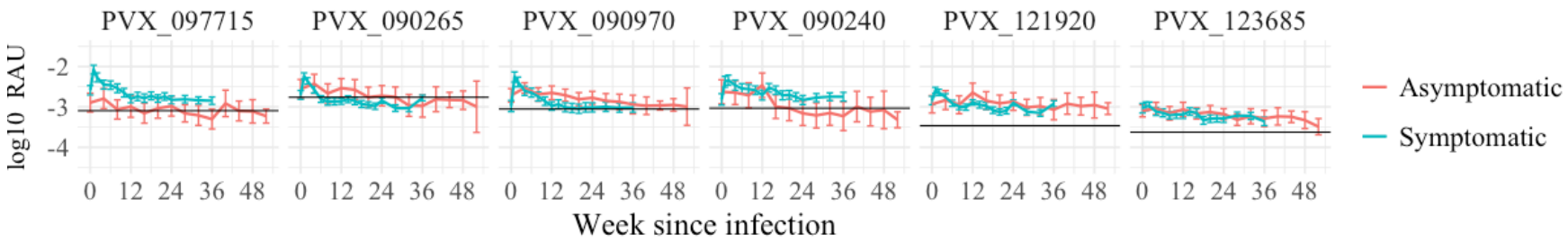


Figure 4.9 Total IgG kinetics and longevity against 27 *P. vivax* antigens in the Thai asymptomatic cohort. The kinetics of total IgG antibody against 27 *P. vivax* antigens were determined following both asymptomatic (for a year) and symptomatic (for 9 months) *P. vivax* infections in Thai individuals in the absence of recurrent infections. Antibody data after asymptomatic infection were aligned to the time of infection, and thus sample size diminishes at later time points. Longevity of the antibody responses is categorised into **A)** long-lived (n=21, > 1 SD at time of infection and > 0.5 SD at 6-month post-infection above negative control baseline) and **B)** non-immunogenic (n=6, < 1 SD at time of infection), based on the responses in the asymptomatic individuals. Horizontal solid line represents the baseline responses measured in malaria-naïve individuals from 3 different sources (n=274). Data are expressed as the median ± 95% CI.

4.2.6 Additional results: attempt to establish total IgG kinetics in Brazilian patients

Following the characterisation of antibody kinetics in the Thai symptomatic cohort, it was of interest to examine, compare and potentially validate the results in another malaria-endemic country with low transmission but a distinct geographical location. Therefore, samples from another longitudinal study on symptomatic *P. vivax*-infected individuals from Manaus, Brazil, were obtained [108]. The design of the Brazilian longitudinal study was identical to the Thai study and is described in detail in Chapter 2 Sections 2.1.1 and 2.1.2. In this Section, I report the initial findings of IgG kinetics in this cohort and results of multiple attempts to troubleshoot various issues encountered.

As per the Thai cohort, total IgG responses were measured in a subset of Brazilian individuals (n=33) at all time points that plasma samples were collected (time of infection, week 1, week 2, then every 2 weeks until week 24, then every 4 weeks until the end of the study at 9 months). IgG responses were measured against a panel of 24 *P. vivax* proteins. At the time of the experiment, only 24 antigens had arrived at WEHI and completed optimisation, and hence were used for IgG measurement. As shown in Figure 4.10, in contrast to the Thai cohort, total IgG antibody responses against all 24 antigens in the Brazilian

cohort were shown to peak and drop randomly throughout the study across all participants. For most antigens, the noisy responses mostly occurred above the malaria-naïve baseline.

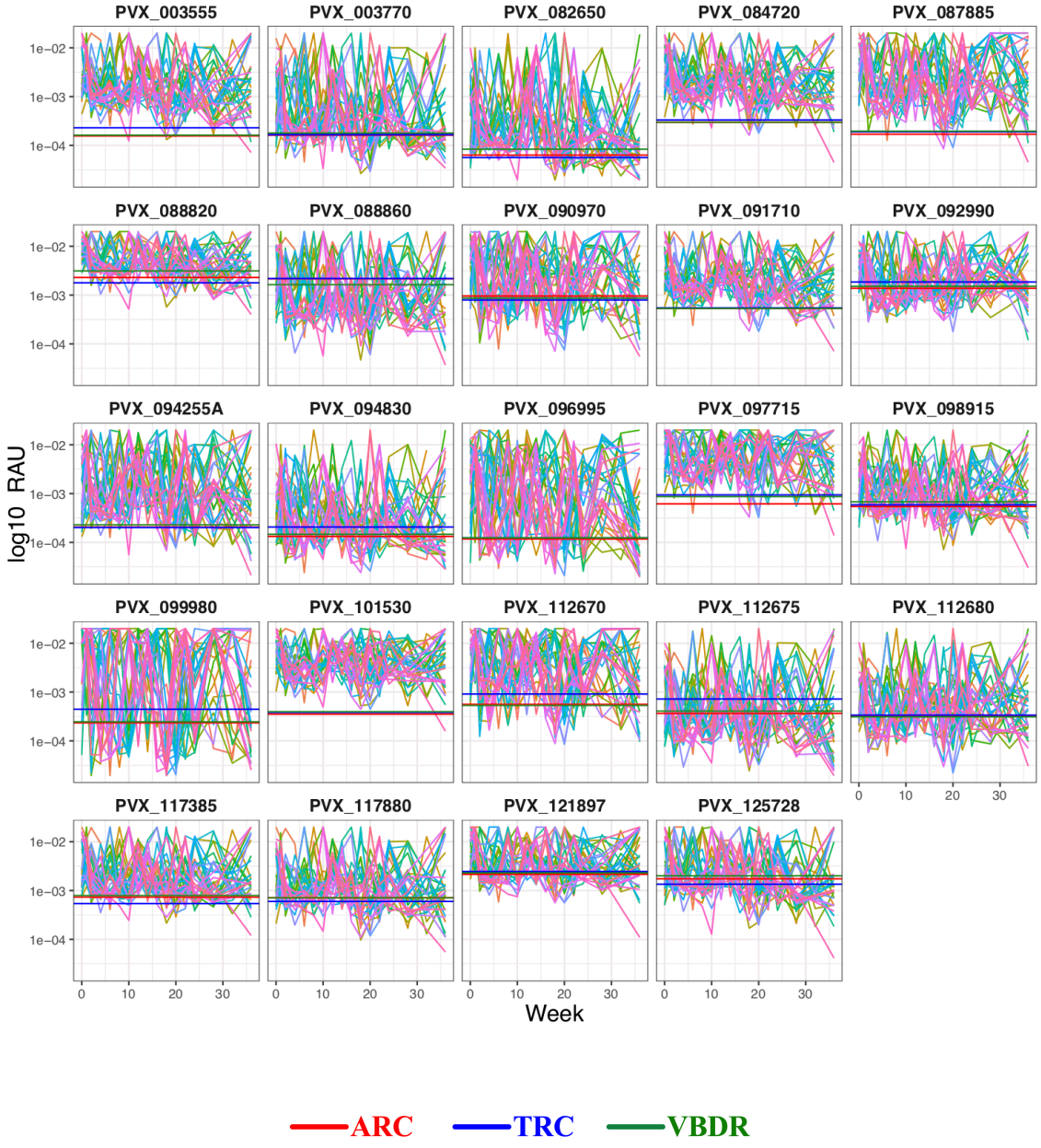


Figure 4.10 Total IgG kinetics against 24 *P. vivax* antigens in the Brazilian symptomatic cohort. The kinetics of antigen-specific total IgG antibody were determined for 9 months following a symptomatic *P. vivax* infection in Brazilian individuals in the supposed absence of recurrent infections. Each line graph (each colour) corresponds to one of the 33 individuals. Negative control panels consist of malaria-free individuals from three different sources.

From the above observation, I performed a series of analyses to assess different aspects of the experiment and to explore the potential source of the highly variable antibody signals in this longitudinal cohort. This included: a) stability of standard curves, b) correlation between replicates and c) presence of potentially missed infections per participant.

Firstly, I found that the standard curves for the bulk conjugation and each plate of experiment had remained log-linear throughout the 2-week experiment (Figure 4.11). This confirms the consistency and reliability of unit conversion. Additionally, this result was supported by the fact that IgG responses in MFI before conversion also exhibited an identical pattern as the RAU (Figure 4.12).

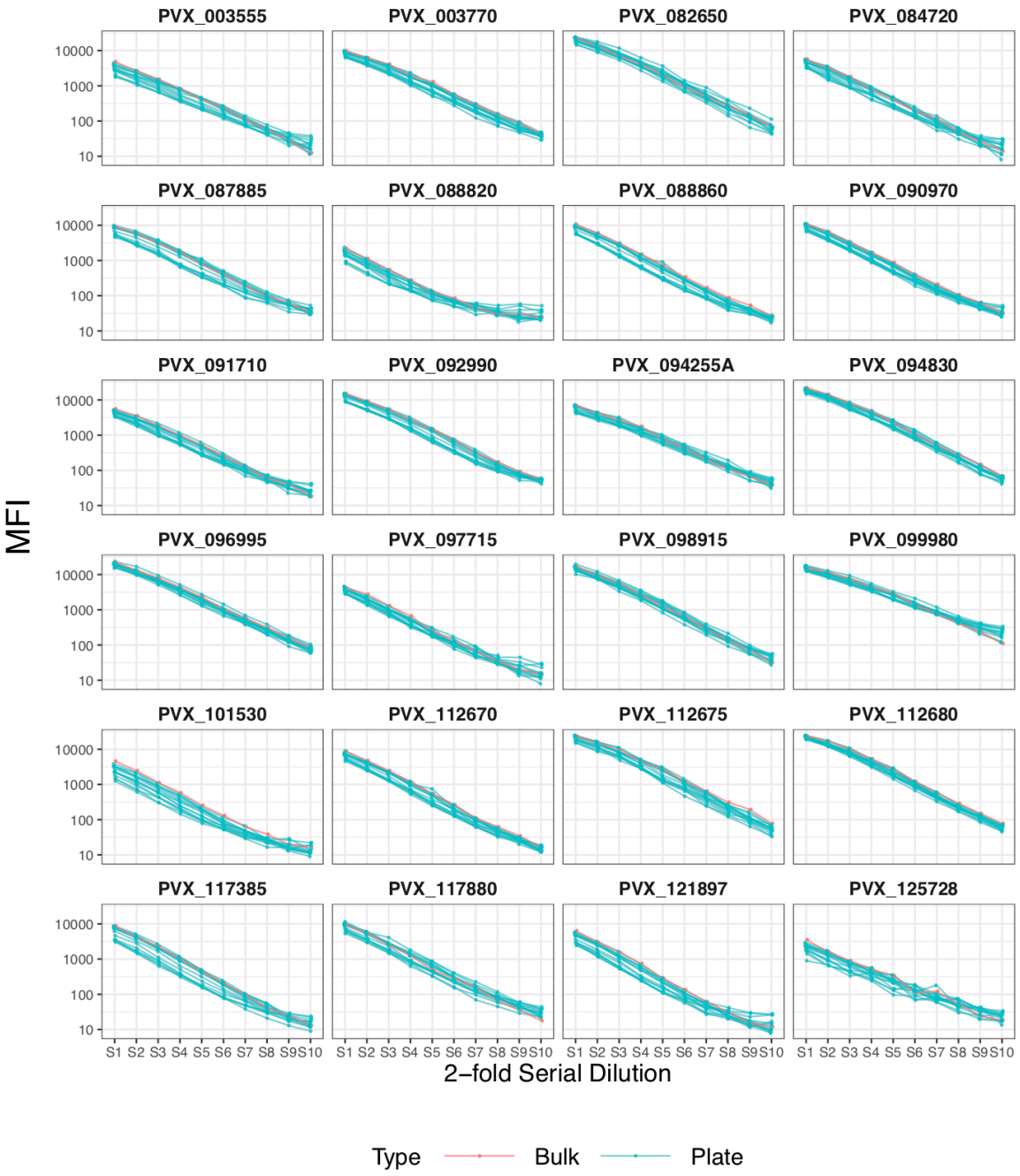


Figure 4.11 Standard curve tests for 24 *P. vivax* antigens in the Brazilian symptomatic cohort. Antigen-specific standard curves were included in each plate of experiments as a measure of inter-plate and/or inter-day variability. The 'Bulk' in coral represents the freshly conjugated Luminex® microspheres whilst the 'Plate' in teal represents the standard curve per plate. For the detection of IgG antibody kinetics in duplicates, a total of 16-17 plates of samples were run which took approximately two weeks to complete.

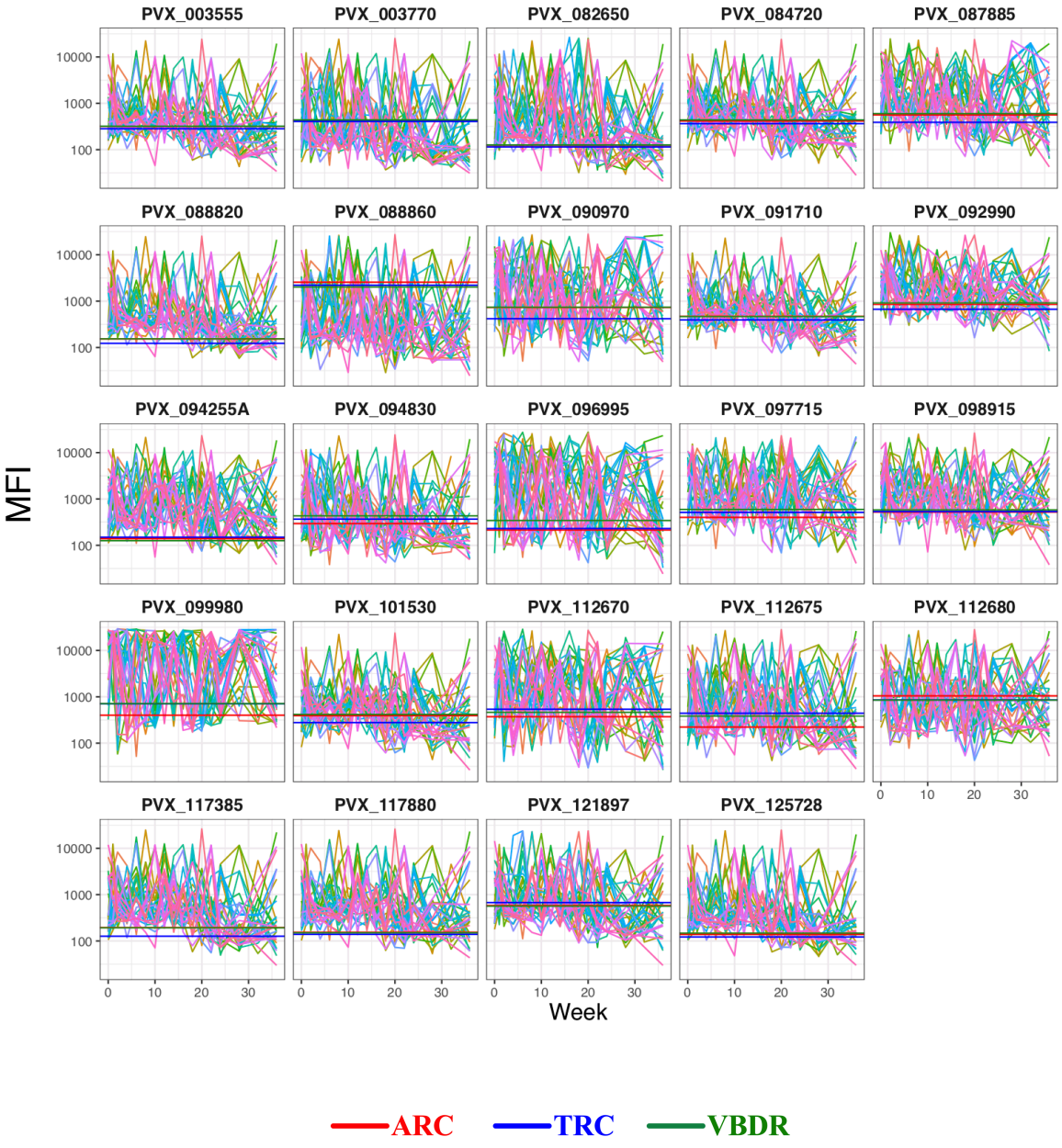


Figure 4.12 Total IgG kinetics for the Brazilian symptomatic cohort in MFI. The kinetics of antigen-specific total IgG antibody shown here are in MFI before unit conversion into RAU. Each line graph (each colour) corresponds to one of the 33 individuals. Three horizontal lines corresponds to the three negative control panels.

Secondly, correlation tests were performed between duplicates per sample (Figure 4.13). Pearson's R values in the Brazilian cohort were moderate, ranging from 0.32 – 0.71, with p values <0.0001 indicating statistical significance. The strength of correlations between duplicates in this cohort was lower than the Thai (0.87 – 1, p <0.0001) (Figure 3.6). Due to this, I further repeated this experiment using samples from a random time point (ie. 8-week post-infection). Three *P. vivax* antigens (PVX_082650, PVX_094255A and PVX_098915) with stable antigen-conjugated microspheres were selected to measure IgG responses. The results were then correlated to the original data. For the three antigens, data obtained from the repeat and original experiments were strongly correlated (Pearson's R=0.97 – 1, p<0.0001) (Figure 4.14). This suggests that despite the moderate correlation values for some antigens, overall there was unlikely to be any laboratory issue related to the IgG measurements accounting for the highly variable and inconsistent IgG kinetics compared to the Thai cohort.

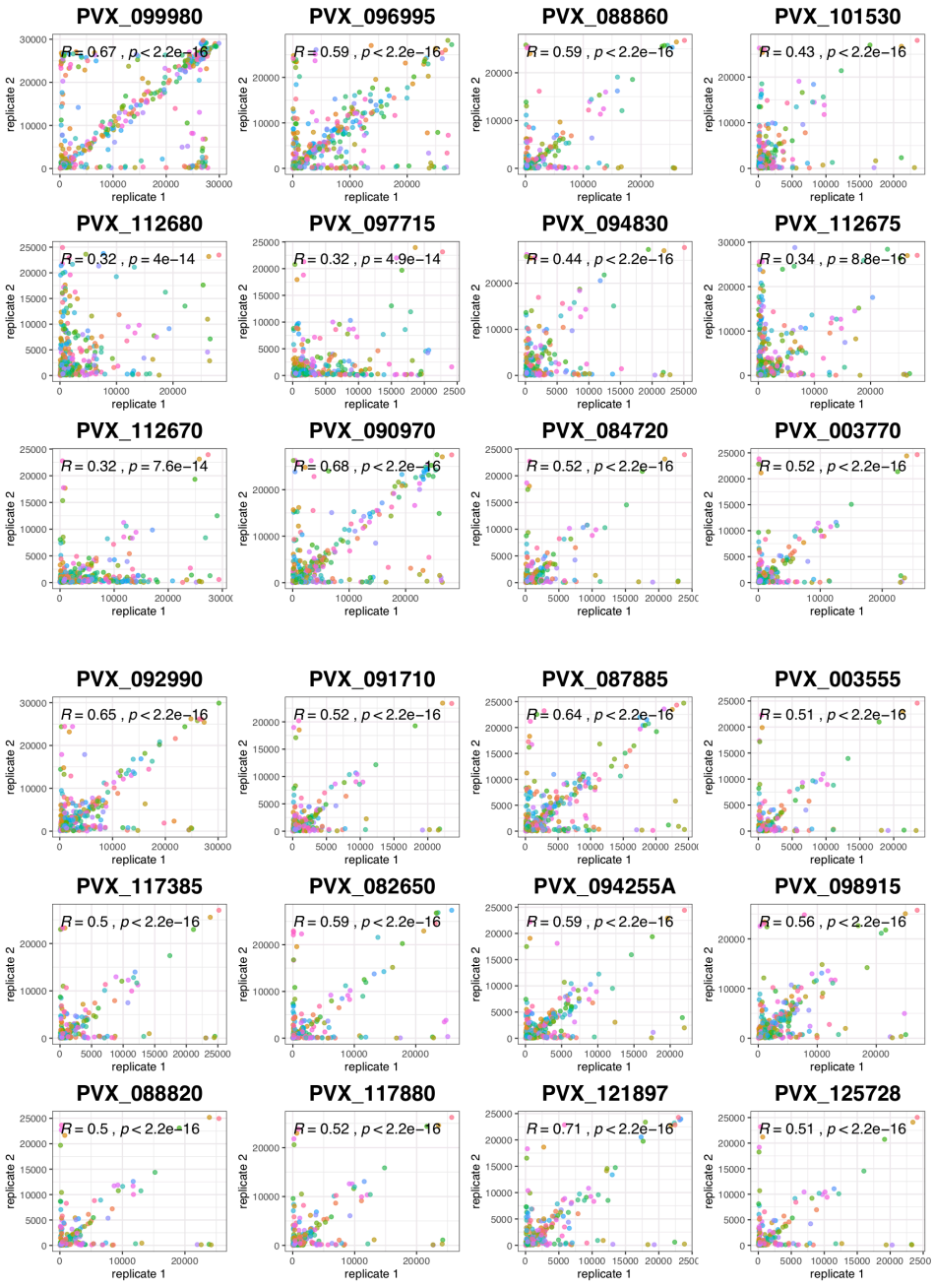


Figure 4.13 Correlation between duplicates per *P. vivax* antigen in the Brazilian symptomatic cohort. For the measurement of total IgG kinetics against 24 *P. vivax* antigens in the symptomatic Brazilian cohort (n=33), all plasma samples were run in duplicates. This plot shows the correlation between the duplicates (a total of 561 pairs of duplicates from 33 participants with plasma samples collected at 17 time points). Correlation analysis was performed using Pearson's correlation test, indicated by R and p values. Dots of the same colour correspond to a single participant at different time points across the study.

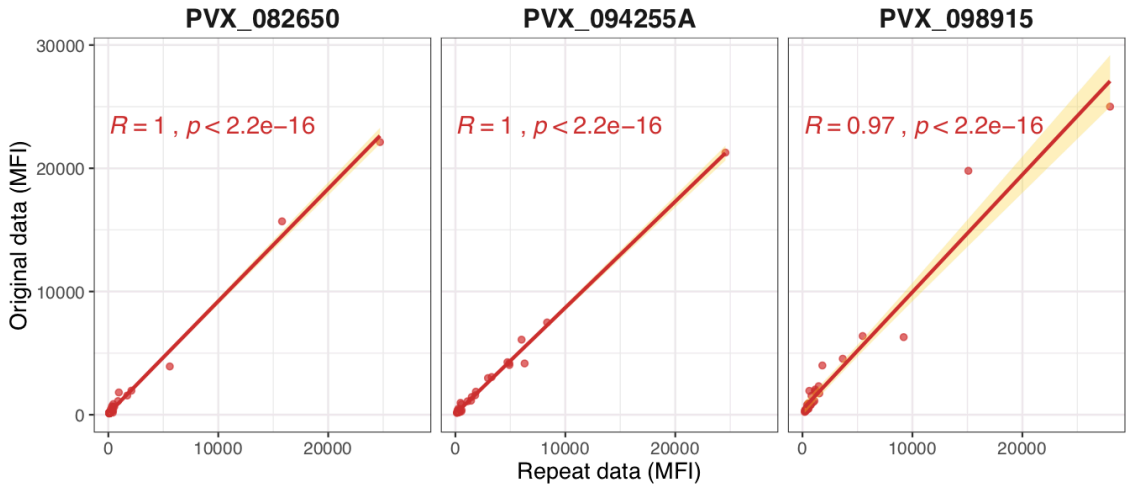


Figure 4.14 Correlation of data from original and repeated IgG responses. To validate the results, total IgG responses against three *P. vivax* antigens were measured for the second time, using plasma samples from 33 symptomatic Brazilians 8-week post-infection. Data obtained were correlated to the data from the original experiment.

After examination of the quality of the antibody experiment and finding no obvious issues, it was speculated that there may be missed infections that led to noisy IgG signals. During the 9-month study, the 33 Brazilian symptomatic individuals were screened at each time point by *Plasmodium*-specific qPCR (QMAL) to confirm the absence of recurrent *P. vivax* infections, as per the Thai cohort. QMAL results indicate parasite density and are expressed as copies per μL of samples. Strong readings with great numbers of copies allow the differentiation between *P. vivax* (*Pv*$^+$) and *P. falciparum* (*Pf*$^+$) infections in an individual, using a further species-specific assay [335].

According to the original record QMAL results for the Brazilian cohort (document not shown), all 33 participants were QMAL$^+$ and *Pv*$^+$ at enrolment. However, it was found that some individuals showed QMAL and/or *Pv* positivity during the study, conflicting with the intended study design. A total of 22 individuals show qPCR positivity between week 1 to week 36, amongst which six individuals (participant ID 028, 040, 052, 061, 067 and 088) showed positivity twice. The time points at which QMAL$^+$ and *Pv*$^+$ results were found during the study and the respective number of participants and the parasite density are recorded in Table 4.6. Initially, these infections were presumed to be due to PCR contamination or error (given most were either QMAL or Pv positive

but not both); however, given the sporadic peaks in antibody responses, I further investigated whether they could be true infections.

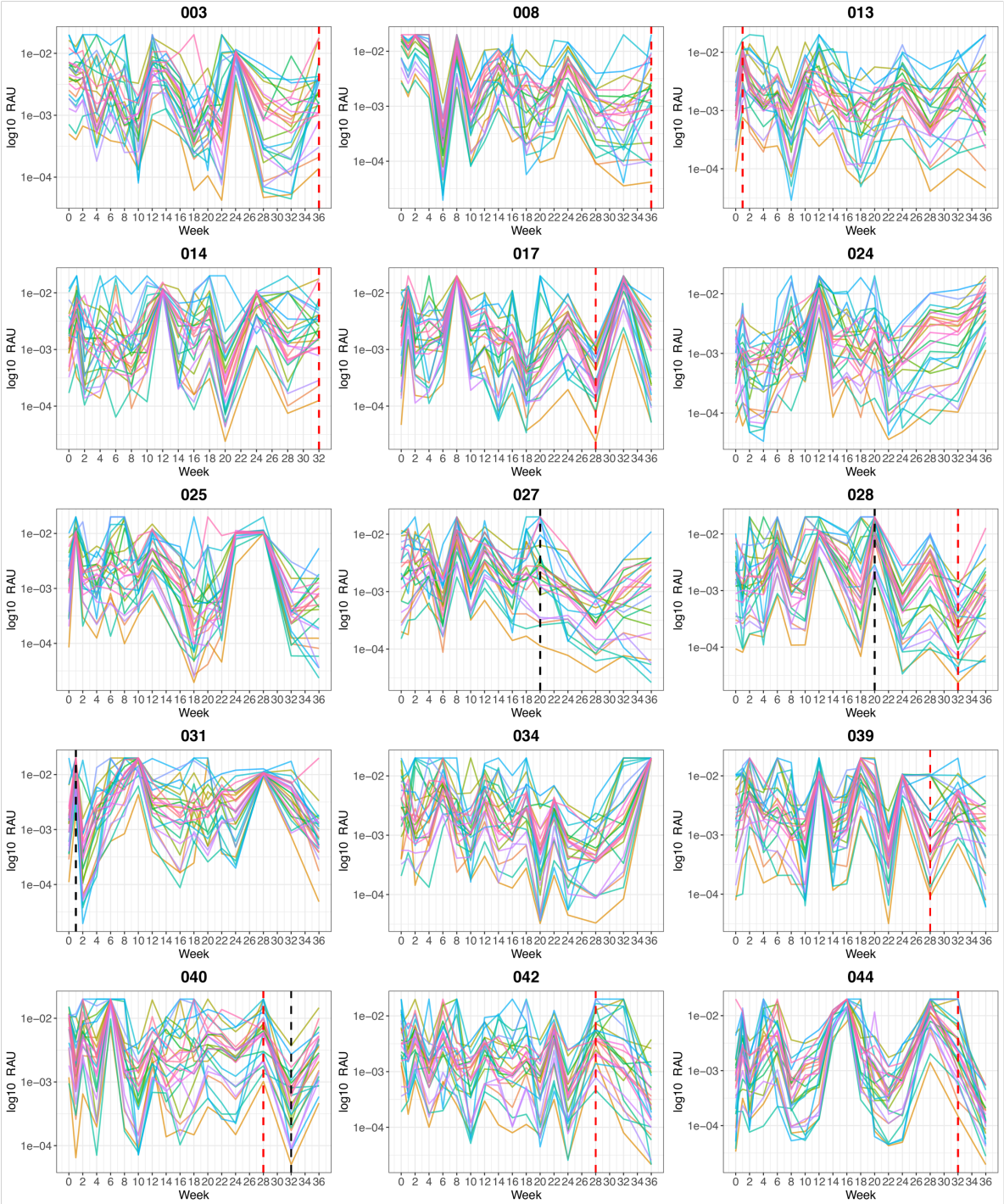
Most positive qPCR results were found at week 1 and between weeks 28 and 32 (Table 4.6). Infections detected at week 1 are likely just remaining parasites from the initial infection, and are not of concern. The sporadic and relatively rare cases of QMAL$^+$ individuals found between weeks 4 and 28 and at week 36 could potentially be missed true infections.

To determine if qPCR positivity was the causative factor of the irregular IgG responses, time points where QMAL$^+$ and *Pv*$^+$ were found were indicated on the IgG antibody kinetic profiles. In Figure 4.15, IgG responses against almost all antigens in some participants were shown to peak the time when they were detected as QMAL$^+$ (eg. participants 028, 031 and 047). The timing of some *Pv* positivity was also in line with an IgG peak (eg. participants 013, 042 and 065). Despite this, numerous other peaks and drops could still not be explained by the QMAL results.

Table 4.6 Distribution and parasite density of the 22 qPCR-positive individuals in the symptomatic Brazilian cohort.

	Week 1	Week 4	Week 10	Week 20	Week 22	Week 28	Week 32	Week 36
Total number of qPCR positive individuals	6	1	1	2	1	7	9	2
Number of QMAL$^+$	2	1	1	2	1	0	5	0
QMAL$^+$ results (copies/μL)[a]	4.4	8.7×10^{-1}	4.3×10^{-1}	7.3	2.9×10^{4}	NA	7.5	NA
Number of *Pv*$^+$	4	0	0	0	0	7	4	2
Pv$^+$ results (copies/μL)[a]	1.6×10^{4}	NA	NA	NA	NA	9.4×10^{1}	3.9×10^{2}	1.1×10^{1}

[a] The median of parasite density was shown.


003
008
013
014
017
024
025
027
028
031
034
039
040
042
044
log10 RAU
1e−02
1e−03
1e−04
Week
0 2 4 6 8 10 12 14 16 18 20 22 24 26 28 30 32 34 36

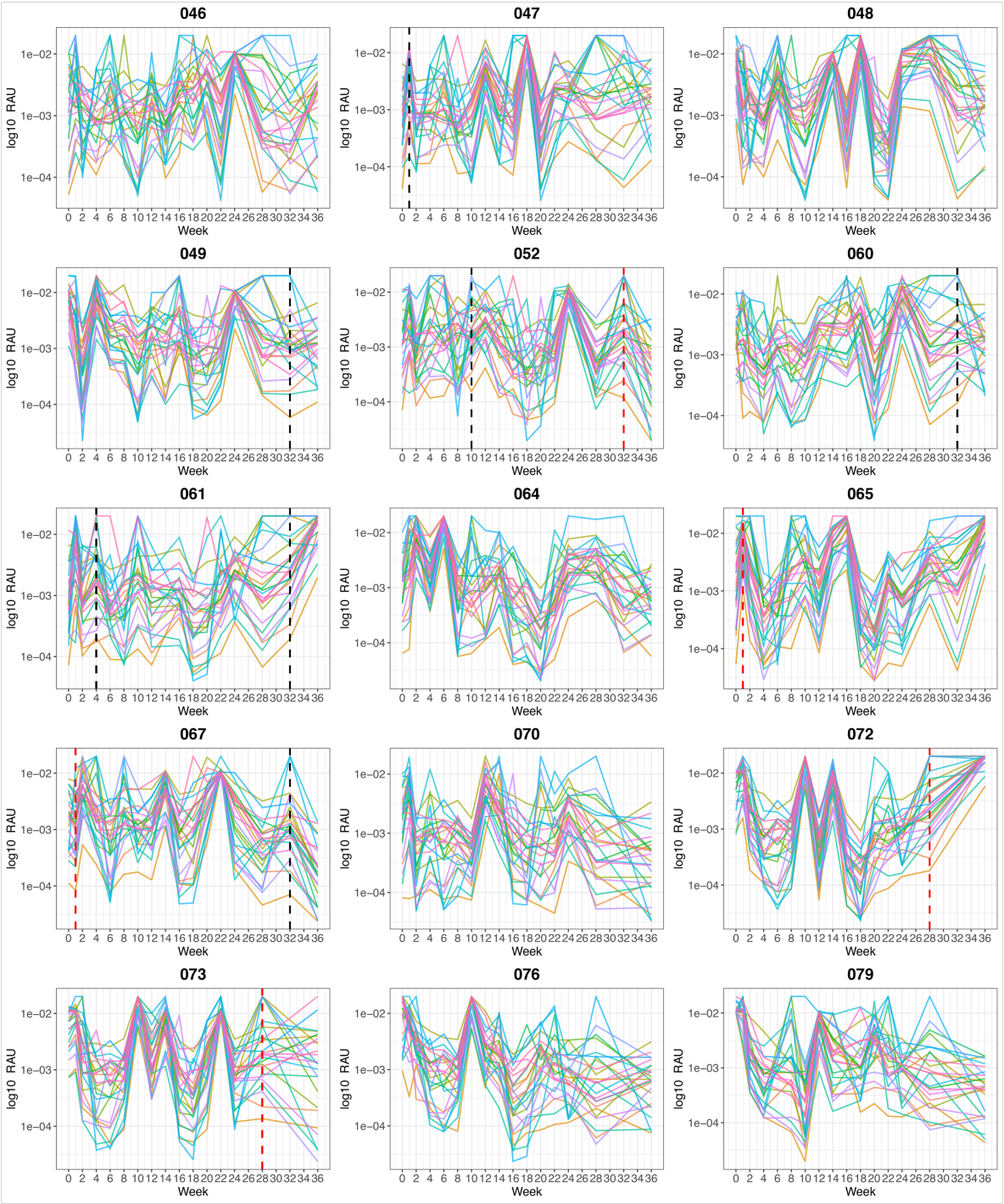


Figure 4.15 Antigen-specific IgG responses and timing of potential missed infections in 33 Brazilian symptomatic individuals. The IgG antibody responses against 24 *P. vivax* antigens in 33 Brazilians were measured for 9 months post-infection. Each line graph (each colour) corresponds to one of the 33 individuals. QMAL^{+} and *Pv*$^{+}$ are recognised as potential missed infections, and are represented as vertical black and red dotted lines, respectively.

Taking our findings together, the reason behind the noisy IgG responses in the Brazilian symptomatic cohort remain inconclusive. However, the strong peaks in IgG levels at various time-points throughout the study do suggest that either there were infections that were misclassified by PCR or that there were issues in performing the PCR assays in Brazil, leading to false results. Other potential factors that are beyond our control include sample collection, aliquoting, storage and shipping conditions. In the interest of time, no further investigation was conducted and the Brazilian symptomatic cohort was excluded from future analyses.

4.3 Discussion

P. vivax is known for its high genetic diversity compared to *P. falciparum* [329] and its capacity to evade immune surveillance whilst hiding in the liver as hypnozoites. It is such characteristics that make naturally acquired immunity against *P. vivax* more challenging to define than *P. falciparum*. In the present study, I used human samples from a low transmission region in Thailand to develop a model of the dynamics of naturally acquired antibody responses against more than 50 *P. vivax* antigens, including well-studied vaccine candidates and novel targets, following both symptomatic and asymptomatic *P. vivax* infections. I show that *P. vivax* antigens are able to induce total IgG responses of varying longevities, dependent on the *P. vivax* antigen target, with a general pattern of bi-phasic decay. Of the 27 IgG immunogenic antigens, it was found that 18 had a relatively long-lived antibody kinetic profile (responses lasting more than 6 months), whilst 9 had a short-lived profile (responses lasting less than 6 months). It was observed that for most antigens IgG1 was the dominant subclass, and that the decay of IgG1 mirrored that of total IgG. Of interest, I also detected long-lived antigen-specific IgM responses with a similar kinetic pattern after symptomatic infections. When comparing antibody kinetics following symptomatic or asymptomatic *P. vivax* infections, I show that responses following asymptomatic infections are longer-lived, in line with previous

observations that antibody longevity increases in individuals with higher levels of past exposure [108].

To investigate the source of variation in IgG antibody longevity against different *P. vivax* antigens, the impact of the presence of several major characteristics and the presence of IgG subclass and IgM antibody responses was assessed. It was found that there was no significant association between defined IgG longevity categories (short or long, based on the presence of IgG at 6 months) with all antigen features, IgG subclass or IgM responses. However, our findings suggested that immunogenic antigens tended to contain enzyme domains such as Pfam and EGF (Table 4.2.3). *P. vivax* is known to contain a greater number of tryptophan-rich protein-coding genes compared to other *Plasmodium* species [315]. Several studies have reported antigen-specific antibody responses induced by enzyme domains of *P. vivax* antigens, particularly the tryptophan-rich domain found in tryptophan-rich antigens [401-403]. On the other hand, the C-terminal EGF-like domains in the *P. vivax* merozoite surface protein 1 ($MSP1_{19}$) were found to be the most immunogenic region of the antigen and humoral responses against this region were protective against clinical symptoms in a rodent model [242, 319, 404, 405]. Despite the weak association observed, our results indicate enzyme domains could potentially play a role in the immunogenicity of *P. vivax* antigens. A larger antigen panel will be required for future assessment to

confirm such associations are true. Additionally, a quantitative instead of binary categorising system for the kinetic profiles would be ideal for comparing features relating to immunogenicity or longevity of antibody responses.

Interestingly, whilst it was expected that the 52 *P. vivax* antigens to be mostly immunogenic [108, 112], based on our prior studies, I found that only 27 induced IgG and 15 induced IgM seropositive responses at week 1 following infection. This was beneficial in enabling analysis of factors impacting immunogenicity, such as the presence of enzyme domains, but the reasons for these differences should be explored. Potential reasons are that I have used purified antigens compared to our large-scale analysis of more than 300 *P. vivax* antigens [108], and that our sample size is much smaller than our analysis of 829 individuals from malaria-endemic regions using identical purified antigens [112]. Previous studies have reported the immunogenicity of numerous *P. vivax* antigens in regions with various transmission settings. Among the 25 antigens categorised as non-immunogenic in the present study, some have been commonly studied as potential vaccine candidates due to their involvement in reticulocyte invasion, including RBPs, DBP, MSP3β, SIAP-2, RON2 and GAMA. Whilst antibody responses against these *P. vivax* antigens often indicates incidence of infection or clinical protection, their immunogenicity in low-transmission regions has rarely been addressed [220, 340, 406-409]. Among the

six *P. vivax* RBPs investigated in this Chapter, it was demonstrated that RBP2b (PVX_094255B) is the only immunogenic RBP. This result is line with the findings reported by Hietanen et al. who investigated antibody responses in individuals from Thai-Myanmar border [410]. In contrast, He et al. reported significant IgG antibody responses against *P. vivax* RBP2b, RBP1a and RBP2c-NB in infected Thai and Brazilian individuals from low-transmission regions [213]. The differences observed between studies could be the results of having much larger sample size (n>1000) and also the fact that immunogenicity was defined differently in the He study. Similarly, whilst GAMA is categorised as non-immunogenic in our study, Changrob et al. have reported high seroprevalence of more than 55% even a year after recovery from acute infection in southern Thailand [411]. This could be due to inclusion of mixed-species malaria infection cases, potential presence of boosting infections during the follow-up and smaller sample size in the Changrob study. It was also shown that 6 tryptophan-rich antigens are non-immunogenic, among which 2 (PVX_112675 and PVX_092990) were found to be highly immunogenic and capable of inducing long-lived antibody responses that lasted for at least 5 years post-infection in Korean, Myanmar and Chinese individuals [403]. Various reasons could account for such difference, including the use of Korean strain *P. vivax* isolates, instead of Sal-1, as template for PCR amplification. Most importantly, it is possible that the exposure levels varied greatly between the Thai patients

and the participants from other studies, leading to contrasting results in the level of immunogenicity and antibody longevity of the same *P. vivax* antigens. To expand the current scope covered by this work, some further investigations could be done to determine the source of differences in reactivity between immunogenic and non-immunogenic antigens defined in this Chapter. For instance, other antibody-based assays could be used to verify the immunogenicity of each antigen in this population. Alternatively, the use of monoclonal antibodies could validate and compare the presence and/or accessibility of critical epitopes in these antigens.

Our data indicates that cytophilic antibodies (IgG1 and IgG3) are the dominant IgG subclass response induced by our large panel of *P. vivax* antigens, at least following symptomatic *P. vivax* infections in this low-transmission region. This is consistent with previous research highlighting IgG1 and IgG3 as the key subclasses during malaria, regardless of the *Plasmodium* species or geographical location [220, 224, 412, 413]. It has previously been proposed that *P. falciparum* infection initially induces non-cytophilic followed by cytophilic antibodies [414], but this was not what I observed following symptomatic *P. vivax* infections in individuals from western Thailand (who presumably had limited past exposure, supported by their self-reported malaria history). In comparison to previously published studies mostly utilising cross-sectional cohorts, our longitudinal data

and relatively frequent sampling allowed us to demonstrate that the dominance of IgG subclasses remains constant over time following *P. vivax* infection, at least in the absence of any boosting infections. No evidence of subclass switch was observed, which is proposed to occur with an increase in exposure and age [224], in this low-transmission region. However, in our positive control pool consisting of hyperimmune individuals from PNG, I did observe the presence of both IgG1 and IgG3 against most *P. vivax* antigens, compared to IgG1 alone for our Thai volunteers, suggesting that with increasing exposure and in higher transmission levels this switch may indeed occur. Similar observations were made in the studies focussing on PNG children where IgG1 and IgG3 were the dominant IgG subclass responses [219, 230]. Interestingly, the subclass switch was hypothesised to contribute to the longevity of total IgG upon exposure to malaria antigens [294, 415], but was not observed in our study where the study site is of relatively low transmission.

IgM antibodies have been identified as a short-lived response due to the general notion that IgM undergoes class-switch to IgG after a short period of time exposed to a pathogen [416]. In the context of *P. vivax* infections, Park and colleagues reported *P. vivax* MSP1-specific IgM responses that had lasted for less than 3 months [417]. However, our findings indicate that IgM responses can actually be long-lived (for more than 9 months), consistent with more recently

published reports [418-420]. Whilst the underlying mechanism for induction and maintenance of long-lived IgM is unclear, IgM-producing long-lived plasma cells have been shown to reside in the spleen in a mouse model [419]. These cells undergo somatic hypermutation upon antigenic stimulation, independent of GC and T cell help, suggesting an affinity maturation process that is unique and distinct from that of IgG [253, 419]. Nevertheless, our study is the first to address *P. vivax*-specific IgM kinetics in detail and to demonstrate that IgM can be maintained for at least 9 months in the absence of boosting infections. The direct comparison between total IgG and IgM kinetics also provides unique insights into the antigen-specific difference in the temporal dynamics between the two antibody responses. However, caution is warranted when interpreting these results as evidence in other disease models has shown that IgM can potentially be cross-reactive to highly IgG-immunogenic epitopes [421, 422].

I also measured IgG antibodies following a PCR-positive but asymptomatic *P. vivax* infection in a similar region of western Thailand. Defining antibody responses in asymptomatic individuals is challenging given that case detection and recruitment become more dependent on molecular surveillance tools that are less accessible than microscopy in field-settings. Yet it is important to assess longevity of naturally acquired immune responses following asymptomatic infections given the high proportion of *P. vivax* infections that are asymptomatic.

I was able to utilise samples previously collected as part of an observational longitudinal cohort study, in which most infections were asymptomatic [265], to address this question. Between 2015 and 2016, more than 90% of *Plasmodium* cases were found to sub-microscopic and asymptomatic in western Thailand [109, 423], highlighting the prevalence of the asymptomatic repertoire in our setting. Data from the Mueller laboratory has previously shown that total IgG responses against a panel of 11 *P. vivax* antigens are induced following asymptomatic *P. vivax* infections [424]. Our current results confirm these findings, against a larger panel of *P. vivax* antigens, and I was able to further extend these results to show that these responses can be maintained for an extended period of time following clearance of the infection (up to 14 months). Whilst there have been previous studies assessing antibody longevity following *P. vivax* infections [239, 242, 411, 425], ours is the first to do so to a large panel of *P. vivax* antigens with much more frequent sampling after an infection. This enables us to establish an antibody kinetic profile of higher resolution. Furthermore, previous work has often failed to exclude mixed infection cases from antibody measurement. I created a more stringent selection system to ensure the antibody profiles are *P. vivax*-specific. More importantly, the malaria-naïve control panels in our study are exceptionally larger than most previously published work, allowing more accurate prediction of seroprevalence in the target population. Lastly, I show that some newly identified *P. vivax* antigens in

our panel can be highly immunogenic and even induce long-lived antibody responses. This finding will broaden our current scope of 'antigenic candidates' and facilitate exploration of untraditional targets.

Our study has some limitations. First, antibody levels measured at enrolment (week 0) are already elevated above the baseline measured in malaria-naïve control panels. This may be due to a delay in care seeking, or because some individuals in our study have had past exposure to malaria. Second, it is currently impossible to determine whether the symptomatic infections detected at week 0 in our individuals are new infections from mosquito bites or due to relapses from previous infections. The source of infection may play a role in antibody boosting and maintenance. Third, due to the longer interval between sampling (4 weeks), there is the possibility of missed infections present in the asymptomatic cohort, which could contribute to the greater variation observed between individuals, especially towards the end of the study after adjusted for time of infection as the sample size reduced. Additionally, the IgM profile was not obtained in this cohort and thus further investigations on IgM responses following *P. vivax* asymptomatic infections will be required.

Chapter 5. Establishment of an ELISpot assay for protein-specific memory B cell measurements

5.1 Introduction

In the previous Chapters, I have established that antibody kinetic pattern and longevity were antigen-dependent in western Thailand with low transmission. It was speculated that such differences in the antibody response profile could be due to a differential capacity of each *P. vivax* antigen in inducing effective antigen-specific MBC responses. To verify this, I aimed to develop an enzyme-linked immunosorbent spot (ELISpot) assay to enumerate the number of antigen-specific MBCs over time in the same cohort.

The ELISpot assay has been an important tool for the quantification of immune cells. The assay was first described in 1983 and was used to visualise murine enzyme-bound ASCs in petri dishes [426]. Since then, as the technology has progressed, the assay has also evolved to cater to the need of higher sensitivity, clearer enzyme-bound activity and a higher capacity for processing larger number of samples with the use of specialised 96-well plates [427]. Despite this, the concept and basic setup remain relatively unchanged. Firstly, a capture antibody specific for the target analyte – be it total IgG or a cytokine – is used to coat the membrane of a 96-well ELISpot plate [428]. Subsequently, cells are transferred into the wells and incubated with the membrane bound capture antibodies. During incubation, immune cells secreting the analyte will be bound

and immobilised whilst producing more analytes [428]. This leaves a circular gradient of residual on the membrane, diffusing out from the centre of the cell. Finally, analyte production is terminated by multiple washes and removal of immune cells [428]. The residual of analytes is then visualised using either enzyme- or fluorochrome-labelled detection antibodies [429]. For the purpose of this Chapter, the setup of ELISpot assay is illustrated in Figure 2.3.

The ELISpot assay has been widely used to monitor cellular immune responses. Another commonly used method for this purpose is flow cytometry. Flow cytometry has been known to provide detailed phenotypic characterisation of the cell population of interest, and has been used to detect antigen-specific MBCs. However, this technique requires more cells and usually involves a tetramer enrichment step for antigen-specific detection [430]. Compared to flow cytometry, the ELISpot assay requires approximately 10-fold less cellular material for detection [431]. Given that the biological materials are often precious, the usage of flow cytometry for detection of human antigen-specific MBCs has been limited. On the other hand, ELISpot offers functional analysis and also excellent sensitivity in detecting rare antigen-specific cell populations [432-434]. In order to differentiate antigen-specific MBCs into ASCs, these cells must be re-stimulated with antigens or mitogenic stimuli that act to induce differentiation [435, 436]. These factors provide molecular signals that further

promote the production of target proteins or clonal expansion of target cell populations, resulting in an augmentation of sensitivity and robustness. Due to the extensive applications of the ELISpot assay since the early 1990s, the standardised data analysis procedures have been very well established, allowing the generation of highly reproducible results [437]. These strengths have made the ELISpot assay a popular choice of method in clinical trials and diagnostic fields with a wide range of applications [438, 439]. It was therefore decided that ELISpot was a more suitable assay than flow cytometry for our research questions and purpose.

For the detection of antigen-specific MBC responses against *Plasmodium* antigens, the protocols and reagents used are relatively similar between studies. As mentioned previously, the *in vitro* re-stimulation step is critical to differentiate resting MBCs into ASCs. Four of the most common reagents include protein A from *Staphylococcus aureus*, lectin purified from *Phytolacca americana* (pokeweed mitogen (PWM)) and CpG oligodeoxynucleotide (CpG ODN) and IL-10. Numerous studies have investigated the use and effect of the re-stimulation cocktail recipe containing a combination of protein A, PWM and CpG ODN with a slight variation in the relative proportion of each component [440-443]. *Staphylococcus* protein A and PWM have similar molecular mechanisms in inducing strong B cell responses. They both lead to activation and polyclonal

expansion of B cells via activation of TLR2 and are therefore commonly used together to provide a reliable source of B cell-specific stimuli [429, 444-446]. However, other studies have conversely shown that protein A and PWM can be competitive against each other, reducing the effects of the re-stimulating cocktail [446]. A critical component of the re-stimulation cocktail is CpG ODN, a synthetic DNA sequence containing unmethylated CpG motifs [447]. CpG ODN and its capacity of activating B cells via binding to primarily TLR9 has been well-established [448, 449]. The interaction between CpG ODN and TLR9 not only activates B cells but also promotes the differentiation of B cells into high affinity IgG-secreting plasma cells [449, 450]. To further facilitate B cell activation, IL-10 is frequently used in the re-stimulation cocktail. IL-10 is known to support B cell differentiation and survival whilst directly suppressing T cell stimulation [451, 452]. Another re-stimulation combination comprising of the TLR7/8 agonist R848 and IL-2 for B cell saturation has also been reported but its usage is not as common [242, 243, 453]. Therefore, one of the aims of this Chapter was to verify if the re-stimulation cocktail containing protein A, PWM and CpG ODN could successfully induce the differentiation of ASCs from the MBCs in Thai PBMC samples. In addition, I aimed to verify this protocol for *P. vivax* antigens, which has not been addressed in the past.

In this Chapter, I describe the process of optimising a MBC ELISpot assay to detect antigen-specific MBCs in *P. vivax*-infected and malaria-naïve individuals. The original protocol was developed by Weiss et al. to detect *P. falciparum*-specific MBC responses [440, 454]. PBMC samples collected from Melbourne malaria-naïve and Thai *P. vivax*-infected symptomatic individuals were used for optimisation. Optimisation was performed and focussed on the following aspects of the assay: a) re-stimulation duration for Thai PBMCs, b) concentration of tetanus toxoid (TT) and *P. vivax* antigens used for membrane coating and c) the number of PBMCs required to accurately detect antigen-specific MBCs. PBMC samples collected from malaria-naïve donors in Melbourne were randomly selected for the purpose of this optimisation. PBMC samples from Thai symptomatic individuals were down-selected by Dr Rhea Longley, and all had a relatively high number of cells before cryopreservation ($> 3\times10^6$ cells/mL).

5.2 Results

5.2.1 Sample recovery rate and the proportion of viable cells remaining

To assess the quality of PBMC samples and the number of cells available for the assay, I first examined the viability of PBMCs recovered after the cryopreservation procedure. The total number of cells obtained before freezing and after thawing were compared. Generally, the recovery rate was similar between Melbourne (mean = 79.26%, median = 78.03%) and Thai samples (mean = 78.03%, median = 87%) (Figure 5.1). However, the recovery rate was more variable in Thai than Melbourne samples, even for the same individual or time point (Figure 5.1B).

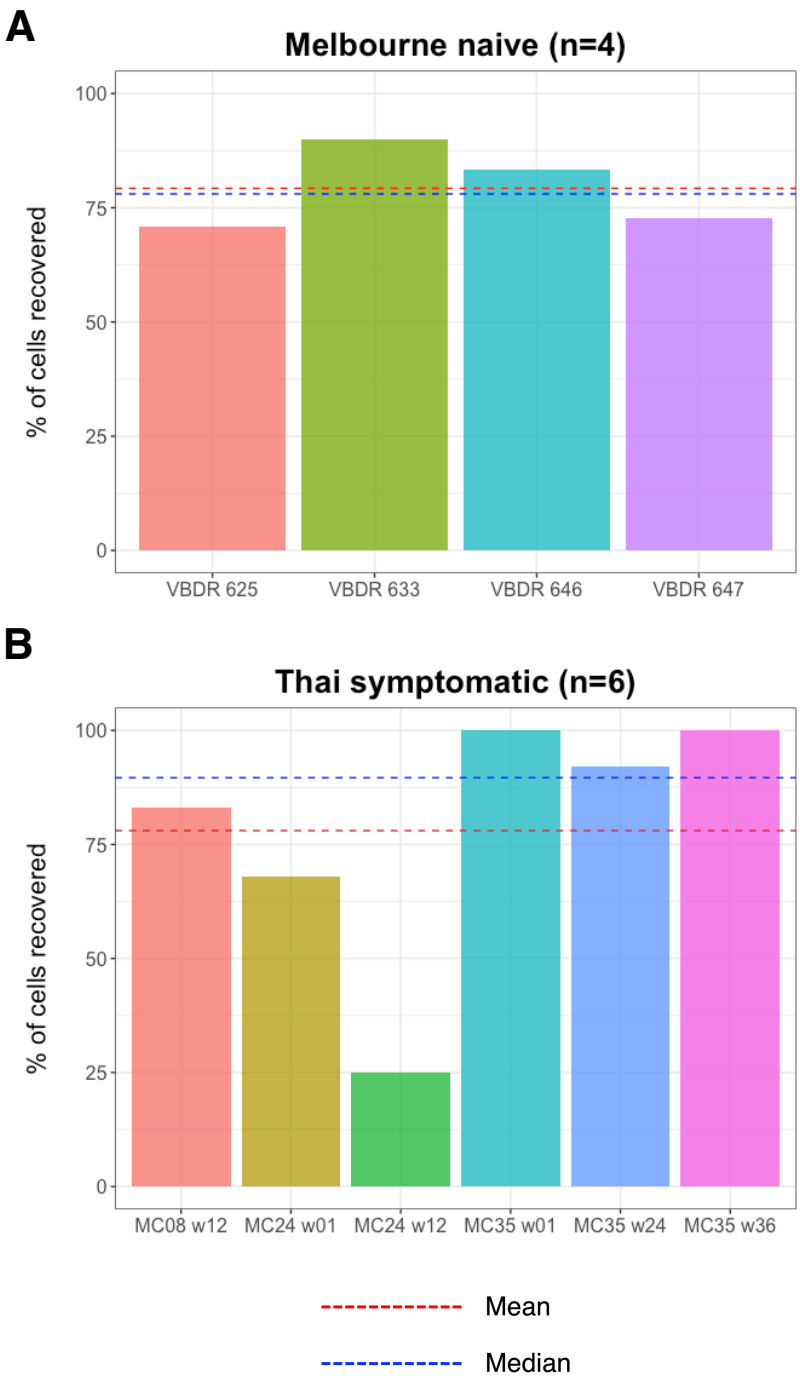


Figure 5.1 Percentage of PBMCs recovered after cryopreservation. The number of viable cells was calculated before freezing and after thawing PBMC samples from **A**) Melbourne malaria-naïve (n=4) and **B**) Thai *P. vivax*-infected symptomatic individuals (n=6). The results represent the proportion of cells recovered. Dotted lines in red correspond to the mean values whilst blue correspond to medians.

Subsequently, to validate the re-stimulation cocktail and the protocol Melbourne PBMC samples were restimulated for 6 days and the percentage of viable cells remaining and the number of IgG^+ ASCs per one million PBMCs were calculated and graphed. The percentage of viable cells remaining in cell culture after re-stimulation was calculated using the following formula:

$$\frac{\text{Total number of viable cells after 6-day incubation}}{\text{Starting number of viable cells recovered}} \times 100\%$$

Results were then compared between cell cultures incubated with the re-stimulation cocktail and those incubated with only the human B cell medium and no added B cell activators (Figure 5.2A). In Melbourne PBMC samples, the total number of cells remaining in the cell culture declined to an average of 45.77% (range = 13.83 – 109.09%) of the total cells recovered from cryopreservation after incubation with the re-stimulation cocktail for 6 days. A more substantial reduction was observed in cells incubated with human B cell medium in the absence of B cell activators, with a reduction to 30.95% (range = 9 – 72.73%) of total cells recovered. A paired t test was performed (where VBDR 647 was excluded) to determine the presence of statistical significance between samples stimulated with and without the B cell activators and an insignificant result was obtained ($p=0.19$). Despite this, these results show that the cell

culture was able to maintain the viability of approximately 30 – 40% of the cells revived which was also largely dependent on the presence of the B cell activators.

The impact of incubation reagents on cell culture composition became more evident when I compared the number of IgG^+ ASCs (Figure 5.2B), rather than the total number of cells recovered. The total number of IgG^+ ASCs was obtained from a 4-fold serial dilution of incubated cells on three anti-IgG antibody coated wells (ie. the positive control). Cell cultures stimulated with B cell mitogens had more IgG^+ ASCs (mean = 4866.67, range = 3166.67 – 8041.67) than the cultures without B cell mitogens (mean = 119.45, range = 75 – 216.67). The result of a paired t test again showed that there was no significant difference in the means between the two groups ($p=0.06$). However, the trend was more evident in the mean number of IgG^+ ASCs than the total number of cells recovered. This finding shows that the re-stimulation cocktail is able to promote the differentiation of MBCs into IgG^+ ASCs.

These results also indicated that this protocol performed well on Melbourne malaria-naïve PBMC samples with an incubation time of six days.

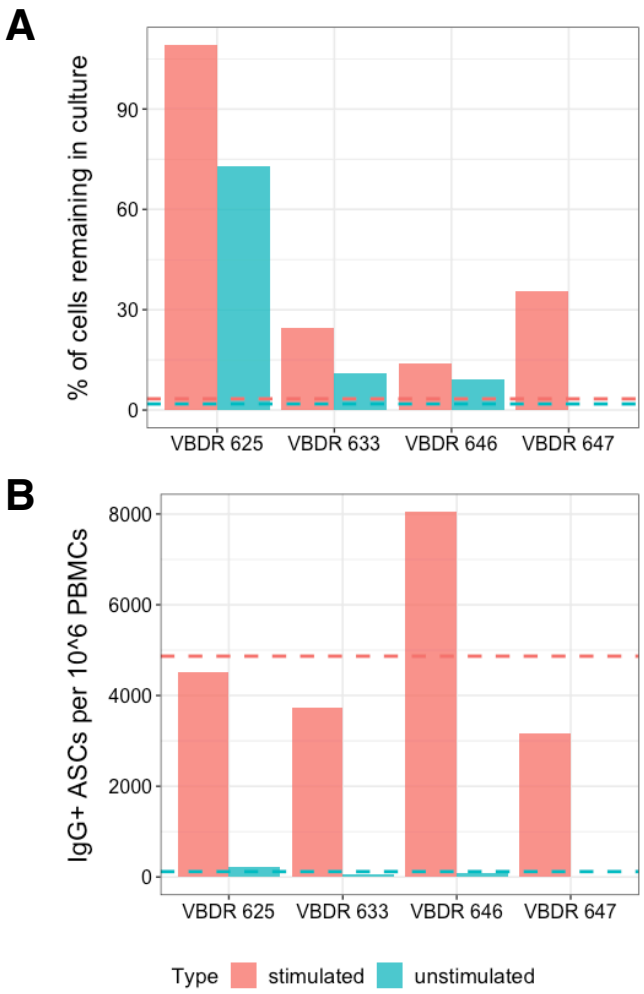


Figure 5.2 Effect of the re-stimulation cocktail on cell numbers. The purpose of the re-stimulation is to promote the differentiation of MBCs into ACSs to allow detection of antigen-specific ASCs in the ELISPOT. Therefore, a re-stimulation cocktail comprising multiple polyclonal activators and a humoral response enhancer was incubated with PBMC samples from Melbourne donors for six days. Stimulated cells are coloured in coral. In contrast, unstimulated cells in teal were also set up by incubating PBMCs with human B cell medium containing no additional B cell response activators. The influence of re-stimulation was examined by the extent of **A)** the percentage of viable cells remaining and **B)** the number of ASCs after 6 days of culture. Dotted lines correspond to the mean values of stimulated (coral) and unstimulated (teal) cell cultures. Sample ID VBDR 647 was only stimulated with the re-stimulation cocktail and hence no unstimulated results were produced.

5.2.2 Optimisation of re-stimulation duration for Thai PBMCs

Next, I optimised the duration of the re-stimulation for Thai PBMCs. According to past literature focussing on MBC responses against malaria, the incubation period for B cell re-stimulation typically varies within the range of 3 – 10 days [239, 242, 454]. In the previous Section, I have established that for Melbourne samples, a 6-day incubation period with the re-stimulation cocktail can efficiently differentiate MBCs into ASCs. Based on the unpublished data from the Hansen Laboratory, PBMC samples collected from rural and less developed field sites usually require longer re-stimulation time compared to the ones from metropolitan areas due to the poorer quality facilities for isolation and storage resulting in poorer quality cells. For example, the Thai PBMCs used in this study were stored on dry ice at the field site for up to one week before being transferred to liquid nitrogen in the main laboratory in Bangkok. The delay in appropriate storage of these Thai samples could be the primary cause of lower quality in the PBMCs which potentially required longer duration of polyclonal stimulation than those PBMCs collected in Melbourne. I therefore set up three trials – 6, 7 and 8 days of incubation – to determine the effect of variable re-stimulation duration on the proportion of viable cells remaining after re-stimulation and the number of ASCs detected. Following re-stimulation, each PBMC sample was diluted to three concentrations via a 4-fold serial dilution to establish the anti-

IgG positive control: 4×10^4, 1×10^4 and 2.5×10^3 cells per well. The spots counted were converted into the number of ASCs per 10^6 PBMCs and subsequently averaged (calculation for conversion is outlined in Table 2.3).

In Figure 5.3A, it is shown that the 6-day re-stimulation was most efficient in retaining the total number of viable cells (14.04% of cells recovered from cryopreservation), followed by 8 (12.5%) and 7-day (10.77%%) trials. However, the 7-day re-stimulation resulted in more than twice the number of IgG^+ ASCs per one million PBMCs compared to 6 and 8-day trials (Figure 5.3B). These results suggest that a 7-day re-stimulation duration is the most efficient for expanding IgG^+ ASCs for Thai PBMCs compared to 6 and 8-day re-stimulation durations (with the caveat that there were not enough cells from a single individual to perform 6, 7 and 8-day trials). Hence, for the following experiments involving Thai PBMC samples, cell cultures were re-stimulated for 7 days.

By comparing with the Melbourne PBMCs (13.83 – 109.09%), it was evident that the Thai PBMCs (10.77 – 14.04%) were less efficient in retaining the total number of viable cells following re-stimulation.

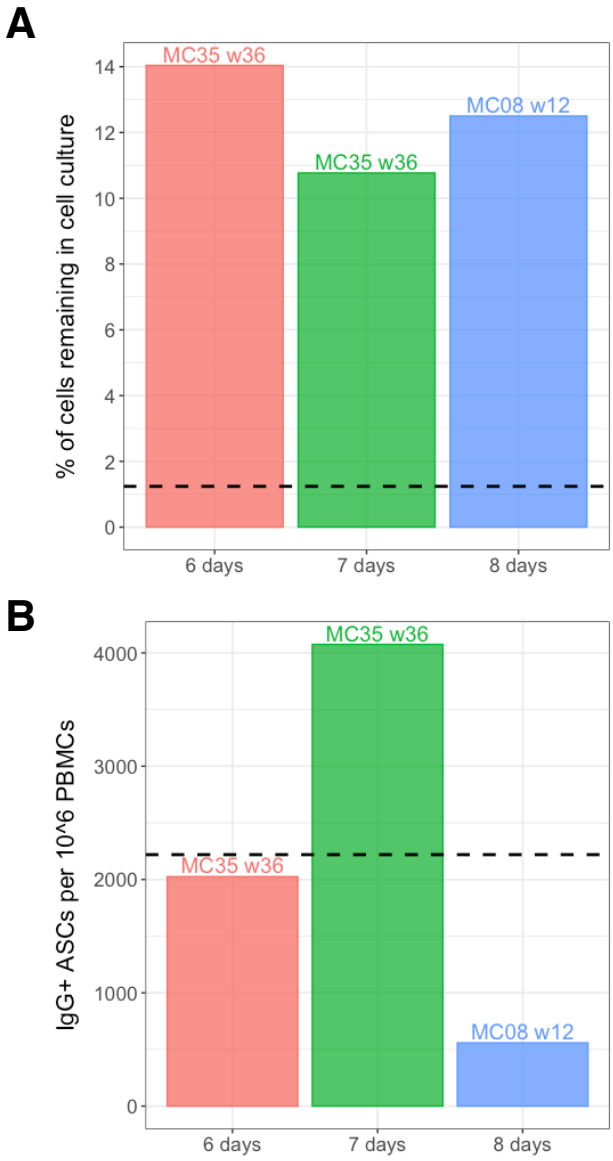


Figure 5.3 Effect of the re-stimulation duration on retention of viable cells and ASC differentiation from Thai PBMCs. To determine the optimal re-stimulation duration to maximise B cell responses in Thai PBMCs, cells were cultured with the re-stimulation cocktail for 6, 7 or 8 days. The influence of re-stimulation duration was examined by the extent of **A**) the percentage of viable cells remaining and **B**) the number of IgG^+ ASCs after re-stimulation. Dotted lines correspond to the mean values across the three trials.

5.2.3 Optimisation of antigen concentrations for antigen-specific IgG^+ ASC responses

The purpose of this optimisation trial was to explore the optimal concentrations of *P. vivax* antigens in order to achieve clear and robust ELISpot results. In addition, I aimed to examine the antigen-specific MBC responses against a common vaccine target for comparison.

As a pilot experiment, two *P. vivax* antigens were chosen as the target of antigen-specific MBC responses: $MSP1_{19}$ (PVX_099980) and hypothetical protein (PVX_090970). The two antigens were selected based on the following criteria: a) similar magnitude of total IgG responses following clinical *P. vivax* infection in the Thai symptomatic cohort based on my previous findings, b) similar level of malaria-naïve baseline, c) similar level of antigenic sequence diversity (see Chapter 6) and most importantly d) distinct total IgG kinetic profiles; long- and short-lived. As shown in Chapter 4, $MSP1_{19}$ exhibited a strong total IgG antibody response that was maintained above the malaria-naïve baseline for more than 9 months following *P. vivax* infection in the Thai symptomatic cohort (Figure 5.4). Similarly, the hypothetical protein was able to elicit a strong total IgG response in this cohort. However, this response was relatively short-lived compared to $MSP1_{19}$ (Figure 5.4). Hence, $MSP1_{19}$ and the hypothetical protein were used as

targets and the antigen-specific MBC responses were quantified in four individuals. More detailed results on the total IgG antibody kinetic profile of these two targets in the Thai symptomatic cohort are shown in Section 4.2.1, Chapter 4. For comparison, an irrelevant protein control was included. TT was selected for this purpose because it is a universally recommended vaccine, meaning most individuals should have MBC responses against this protein.

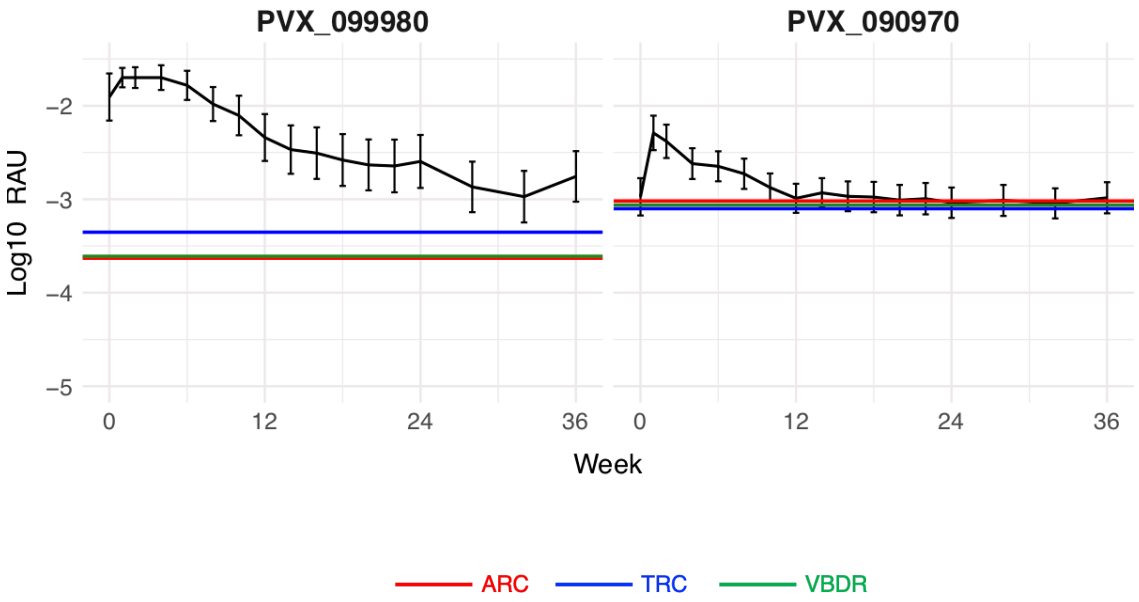


Figure 5.4 Total IgG kinetic profiles against two *P. vivax* antigens in 34 Thai patients with symptomatic *P. vivax* infections. Antigen-specific IgG antibody responses were measured for 9 months following a symptomatic *P. vivax* infection among 34 Thai individuals. PVX_099980 ($MSP1_{19}$) has a relatively long-lived total IgG profile whilst PVX_090970 (hypothetical protein) short-lived. Negative control panels consisted of malaria-naïve individuals from 3 sources: Australian Red Cross (ARC, n = 100), Thai Red Cross (TRC, n = 72) and Volunteer Blood Donor Registry (VBDR, n = 102). Data are expressed as median ± 95% CI.

I first confirmed the assay was performed successfully based on the results of the positive control. Similar to what I observed in the previous trials, the number of IgG^+ ASCs per one million PBMCs following re-stimulation varied greatly between samples (Figure 5.5). In this trial, three Thai individuals on average had a higher number of IgG^+ ASCs per one million PBMCs (mean = 6513.89, range = 3550 – 9183.33) than the only Melbourne donor tested (3741.67).

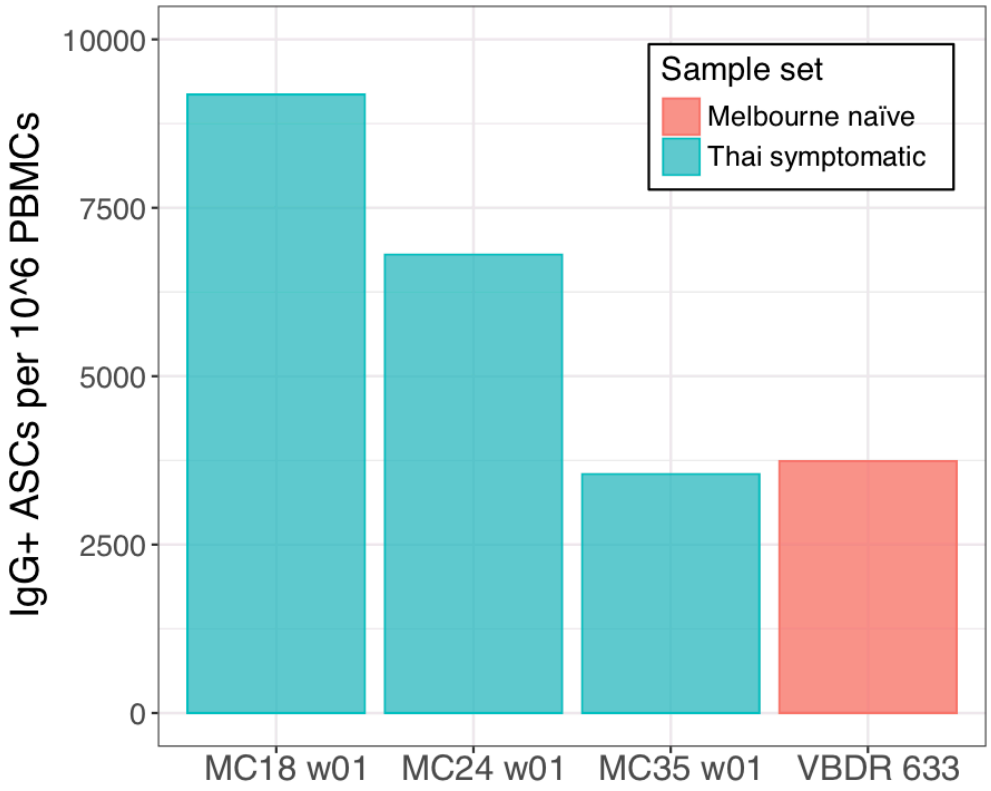


Figure 5.5 Validation of total IgG⁺ ASCs responses in four samples used for optimisation of antigen concentration. PBMC samples were incubated with the re-stimulation cocktail for 7 days and then the number of IgG⁺ ASCs was determined by ELISpot. The results are expressed per million PBMCs.

Next, I calculated the number of antigen-specific ASCs per one million PBMCs for TT, $MSP1_{19}$ and hypothetical protein at 10 or 15μg/mL as described below. For this optimisation trial, each PBMC sample following re-stimulation was diluted at 5×10^4 (50k) and 1×10^5 (100k) cells/well (this was later optimised as described in Section 5.2.4). The number of spots detected was then converted into the number of antigen-specific IgG^+ ASCs per 10^6 PBMCs (detailed method for calculation is outlined in Table 2.4).

TT was coated at 10μg/mL and tested in the three Thai individuals. On average, a total of 66.67 TT-specific ASCs per one million PBMCs were detected in Thai individuals (range = 50 – 90) (Figure 5.6A). This result showed that these Thai individuals were previously vaccinated against TT. Furthermore, TT at 10μg/mL was sufficient to detect antigen-specific MBC responses in this population and hence could be used as an irrelevant/positive protein control for future experiments.

$MSP1_{19}$, the *P. vivax* protein with a long-lived IgG profile, was tested at two different concentrations: 10 and 15μg/mL (Figure 5.6B). In the Thai individuals, an average of 65.83 (range = 50 – 87.5) antigen-specific ASCs per one million PBMCs was detected against 10μg/mL $MSP1_{19}$. Surprisingly, less antigen-specific ASCs were observed when the concentration of $MSP1_{19}$ increased to

15μg/mL (mean = 53.33, range = 25 - 70). Additionally, some level of variability in the number of antigen-specific ASCs was shown. This variation appeared to be dependent on the individual and the concentration of the antigen.

Lastly, a *P. vivax* hypothetical protein was used as a representative antigen with a short-lived IgG profile. It was tested at two different concentrations: 10 and 15μg/mL (Figure 5.6C). In contrast to $MSP1_{19}$, for the hypothetical protein more antigen-specific ASCs per one million PBMCs were detected at the higher concentration of 15μg/mL (mean = 69.17, range = 45 – 102.5) than 10μg/mL (mean = 43.06, range = 10 – 84.17). The variability between individuals appeared to be more prominent when the antigen was diluted at 10μg/mL compared to 15μg/mL.

As the results showed that 10μg/mL was sufficient to detect antigen-specific MBC responses against TT and $MSP1_{19}$, this concentration was selected for all subsequent experiments. Additionally, the use of TT [242, 454, 455] and *Plasmodium* antigens [242, 442] at a concentration no more than 10μg/mL was supported by multiple past studies. The decision was also made due to the limited availability of both TT and the two *P. vivax* antigens at the time of the experiment. An alternative approach would be to use individually optimised protein concentrations for each unique protein.

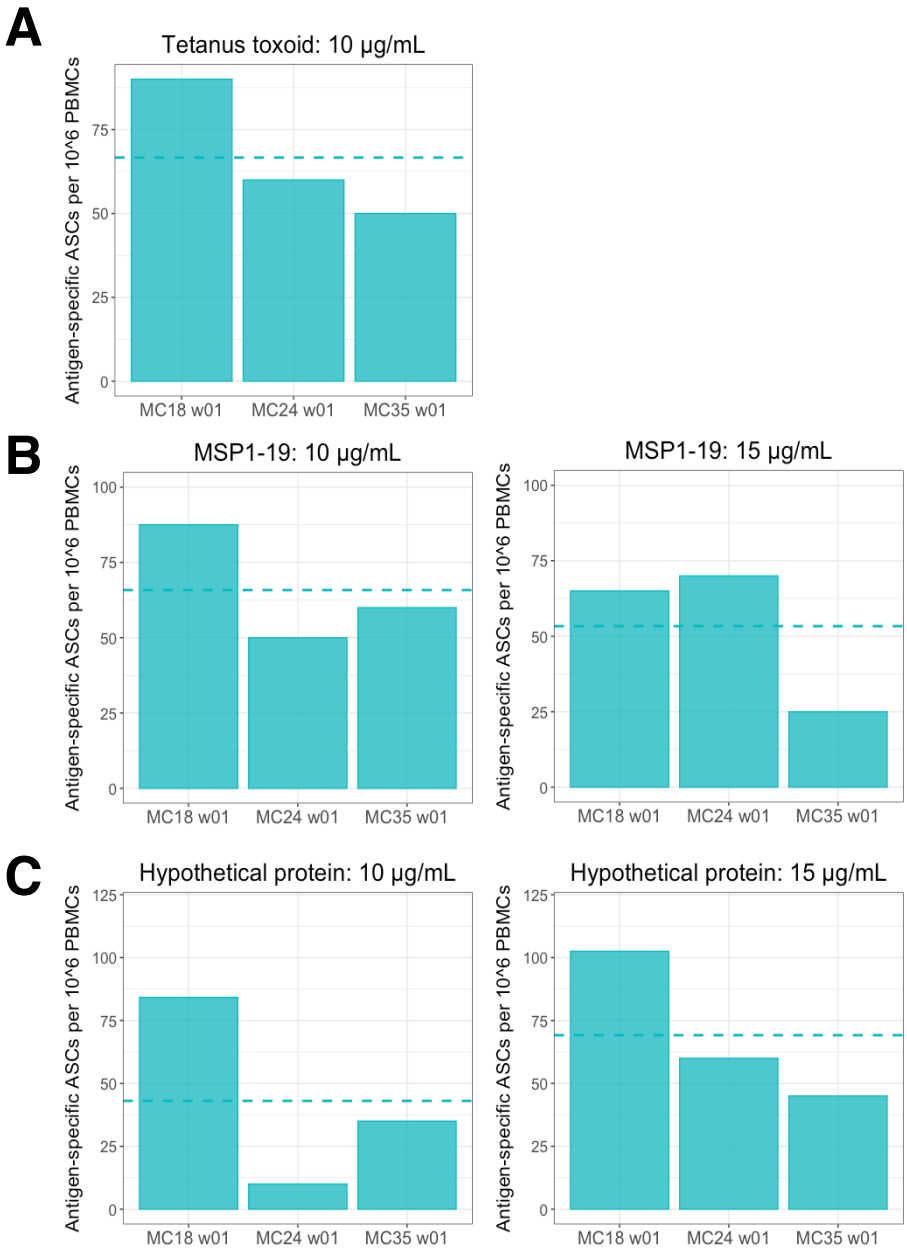


Figure 5.6 Frequency of antigen-specific ASCs against three antigens at different concentrations. PBMC samples were incubated with the re-stimulation cocktail and then added to ELISpot plates that were previously coated with **A**) tetanus toxoid, **B**) *P. vivax* $MSP1_{19}$ (PVX_099980) or **C**) hypothetical protein (PVX_090970) at different concentrations. All antigens were diluted in PBS to achieve the target concentrations. The dotted line in teal in each panel corresponds to the mean number of antigen-specific IgG^+ ASCs across the three Thai PBMCS samples.

5.2.4 Optimisation of cell concentrations for antigen-specific IgG^+ ASC responses

Following the optimisation of antigen concentration, the concentration of cells also required optimisation. This is due to the fact that a low cell concentration may not produce enough signal to reach the detection limit of an ELISpot assay. On the other hand, a high cell concentration may cause overcrowding of cells and produce unclear signals on the ELISpot membrane.

In the previous Section, the ELISpot assay was performed using 5×10^4 (50k) and 1×10^5 (100k) cells/well (Section 5.3). Whilst these cell numbers per well are lower than that usually used in published studies, I was still able to detect antigen-specific MBC responses. Prior studies have used cell concentrations in the range of 2.5×10^5 to 1×10^6 cells/well [242, 245, 456, 457], meaning the cell dilutions I used for antigen-specific ASC detection were 2.5 to 10 times lower than what other authors did. This prompted me to perform this trial, aiming to increase the cell concentrations and explore the differences in resultant responses. The newly proposed cell concentrations were 2.5×10^5 (250k) and 5×10^5 (500k) cells/well. The same two *P. vivax* antigens – $MSP1_{19}$ and hypothetical protein – were used in this trial. Both antigens were used at a concentration of 10μg/mL.

Figure 5.7 shows the difference in $MSP1_{19}$ and hypothetical protein-specific ASC frequency between PBMC samples diluted at four different concentrations: 50k, 100k, 250k and 500k cells per well. Due to sample availability, no Thai PBMC sample could be tested at all four cell concentrations at the same time. The allocation of different cell concentrations tested for each sample is shown in Table 5.1.

Table 5.1 Cell concentrations tested in each Thai PBMC sample for optimisation.

Sample ID	Concentrations tested (cells/well)
MC18 w01	50k
	100k
MC35 w01	50k
	100k
MC24 w01	50k
MC35 w24	250k
	500k
MC30 w12	250k

At cell concentrations 50k and 100k cells per well, the frequency of antigen-specific ASCs was calculated from singlets (or the average of duplicates if enough cells were available; calculation method was shown in Table 2.4 in detail). For $MSP1_{19}$, seeding wells with fewer cells resulted in the detection of a higher number of antigen-specific ASCs per million PBMCs. The average number of $MSP1_{19}$-specific ASCs per million PBMCs at 50k, 100k, 250k and 500k cells per well were 80, 52.5, 60 and 12, respectively (Figure 5.7A). For the hypothetical protein, the frequency of ASCs at the four cell concentrations (from low to high) was 27.3, 42.5, 42 and 12 (Figure 5.7B).

These findings indicated that using only 50k and 100k cells/well allowed the detection of antigen-specific ASCs in the Thai PBMCs. Based on these results, it was determined that 50k cells/well was the optimal cell concentration for *P. vivax* $MSP1_{19}$ and 100k cells/well for the hypothetical protein. This decision also fits in line with the fact that the majority of the Thai samples tend to have a lower total number of PBMCs available.

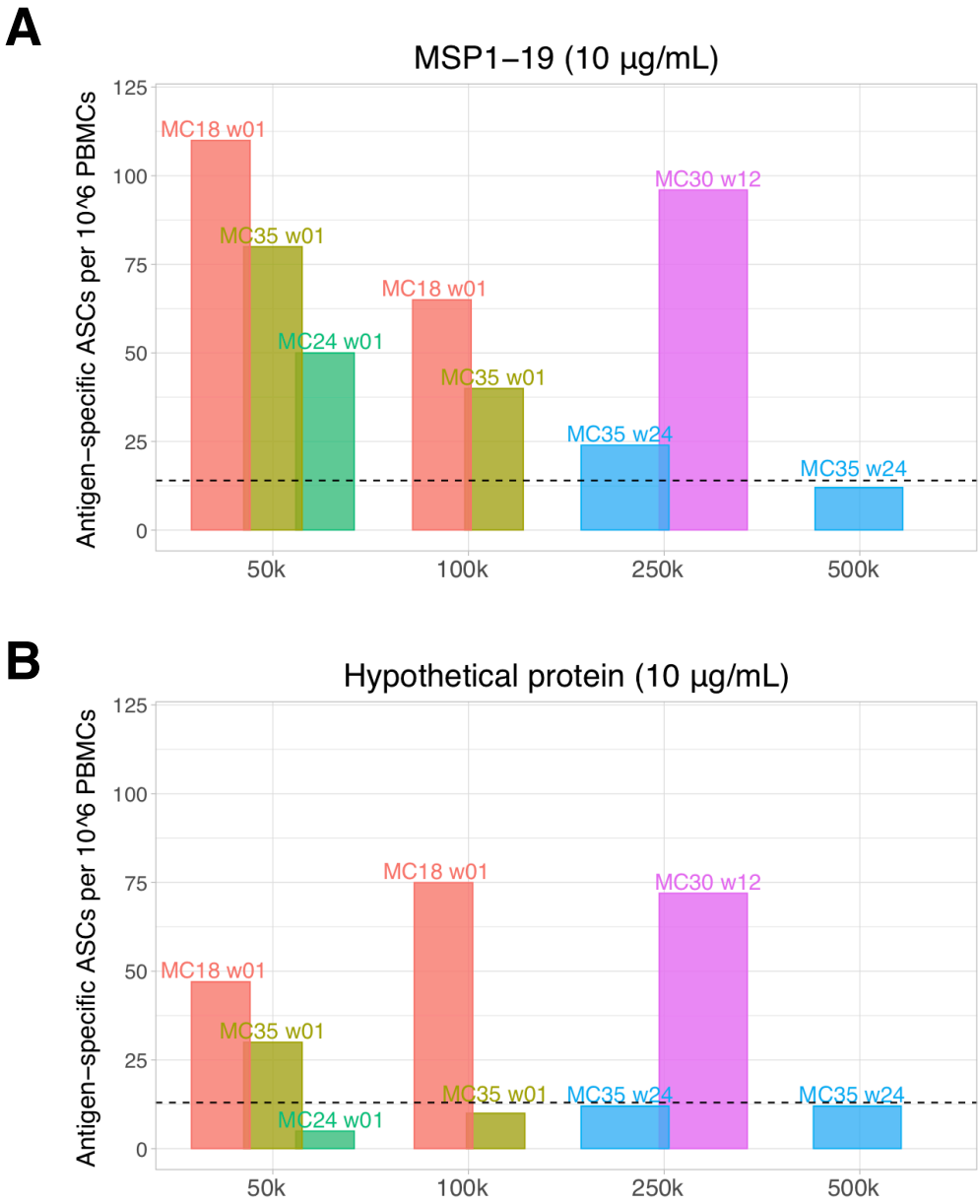


Figure 5.7 Frequency of antigen-specific ASCs against two *P. vivax* antigens with different cell concentrations. PBMC samples were incubated with re-stimulation cocktail and were subsequently diluted at four concentrations: 50k, 100k, 250k and 500k cells per well. Membrane of wells were previously coated with *P. vivax* **A)** $MSP1_{19}$ (PVX_099980) or **B)** hypothetical protein (PVX_090970) at a concentration of 10µg/mL. The black dotted lines correspond to the antigen-specific results of the Melbourne malaria-naïve individual.

5.3 Discussion

The ELISpot assay has been widely used to monitor the frequency and function of immune cells due to its high sensitivity and relatively easy setup. In this Chapter, I describe the process of optimising several aspects of the assay to suit the nature of our samples and research questions. First, I found that all of our PBMC samples were successfully revived from cryopreservation and could be re-stimulated with B cell activators to promote the differentiation of MBCs into ACSs. Furthermore, I optimised the re-stimulation duration, antigen and cell concentrations to suit the PBMCs collected under field conditions in Thailand. Due to limited cell availability, I chose durations and concentrations that were deemed sufficient, rather than performing an extensive comparison of all possibilities for all individuals (as there were not enough cells available to do so).

Based on my results, MBCs from PBMC samples from western Thailand most efficiently differentiated into ASCs after seven days of re-stimulation. In previous studies where Thai PBMC samples were used, the re-stimulation duration ranged from three to six days [239, 242, 243]. For PBMC samples from Peru with a similar level of malaria transmission, the re-stimulation duration used was six days [441]. Interestingly, the two studies reporting the shortest duration

(ie. three days) utilised a re-stimulation cocktail comprising of R848 and IL-2 as the polyclonal activator and promoter of B cell proliferation, respectively [242, 243]. This suggests that the composition of the re-stimulation cocktail may have a strong impact on the efficiency of ASCs differentiation from MBCs. Additionally, a re-stimulation cocktail comprising of R484 and IL-2 is potentially more efficient in B cell saturation than our current recipe. However, the effects of various re-stimulation cocktail compositions have not been compared, to my knowledge. This is possibly due to the fact that the data on the increase in ASC population following re-stimulation is often unavailable in published studies. Here I present a thorough investigation on the effect of the most commonly used B cell re-stimulation recipe (containing protein A, PWM, CpG ODN and IL-10), which successfully induced differentiation of resting MBCs into IgG^+ ASCs and hence provides valuable information for future experiments of a similar kind. It is worth noting that in this Chapter only one sample was tested at each of six, seven and eight-day trials due to sample availability. Further testing could have been undertaken to confirm the duration of PBMC re-stimulation for the Thai and Melbourne samples.

Antigen-specific MBC responses against malaria have been explored in other studies, most of which focussed on *P. falciparum* instead of *P. vivax*. Apical membrane antigen 1 (AMA1) and MSP1 (along with its other smaller fragments

such as $MSP1_{19}$ and $MSP1_{42}$) are some of the most commonly used *Plasmodium* antigens for investigation on antigen-specific MBC responses in malaria [239, 440-442, 454, 456, 458]. Here, I demonstrate that *P. vivax* $MSP1_{19}$-specific ASCs can be induced and detected in Thai symptomatic individuals at an average of 60 and 53 per one million re-stimulated PBMCs when coated at concentrations of 10 and 15μg/mL, respectively (range = 12 – 110; regardless of cell concentrations). This value is within the range of results reported from studies with larger sample sizes. For instance, Min et al. showed a range of 0 – 65 *P. vivax* MSP1-specific ASCs per one million PBMCs in southern Thailand [242]. Similarly, Clark et al. found a wide range of *P. falciparum* MSP1-specific ASC frequency between 7 to 352 [441]. In the present study, a considerable level of variability in antigen-specific MBC responses was also observed between donors. This is also consistent with previous literature [455]. This is most likely due to the limited sample size in each of our trials and the fact that samples were collected at different time points post-infection. Additionally, the size [440, 458] and breadth [459] of the *P. falciparum*-specific MBC compartment is known to increase with age, suggesting age should also be taken into consideration when interpreting the results. Therefore, as a potential future direction, other concentrations of the *P. vivax* antigens and a larger sample size could be trialled in our western Thailand population to verify the results reported from this Chapter and past literature.

Controls are the key components in a reliable assay. For detection of antigen-specific MBC responses in malaria, it is essential to include a non-malarial antigen as the irrelevant antigen control for comparison and ideally as a control. Antigens derived from several prevalent diseases that the general public is commonly exposed to and/or vaccinated against have been considered. These include pertussis, diphtheria and tetanus. In this experiment, I used TT at a concentration of 10μg/mL (in three Thai individuals). It was found that the average numbers of TT-specific ASCs per one million stimulated PBMCs is 66.67 at 10μg/mL. As reported from studies where 5μg/mL of TT was used as a control, approximately 5 – 100 TT-specific ASCs per one million stimulated PBMCs were detected [242, 454, 455]. No study has reported the use of 10μg/mL TT. For studies where other commonly used vaccine antigens were used, the results were highly variable [239, 245, 456, 458-460]. It is likely that the frequency of ASCs specific to common vaccine antigens is dependent on vaccination history [461, 462] and the timing/use of booster vaccinations in the area [245]. Therefore, it is not surprising that I observed significant variation in the TT-specific MBC response, and even use of other common vaccine antigens would most likely result in variable results across individuals. However, testing TT at higher concentrations and the use of other common vaccine antigens as controls in this assay could be further explored as an alternative irrelevant protein control.

To summarise, I successfully established the ELISpot assay for the detection of malaria antigen-specific MBC responses via multiple optimisation trials. The results of these trials enabled us to determine the B cell re-stimulation duration, antigen concentration for coating and cell dilutions to achieve optimal assay sensitivity whilst taking sample conservation into account. Despite the limited availability of the PBMCs per sample and the target antigens, the outcome of this work provides the fundamentals and opportunity for further optimisation of this assay. Upon completion of the optimisation, this protocol can be used to run the Thai symptomatic cohort from which participants' PBMCs were collected at the four time points since *P. vivax* infections (study design is described in Section 2.1.1). By establishing the kinetic pattern of antigen-specific MBC responses and correlating this information with the antibody kinetic profiles, I would be able to decipher the role of MBCs in modulating IgG antibody kinetics and longevity in the context of *P. vivax* malaria in a naturally infected population. These data could then lead to future projects where the phenotype of MBCs (i.e. such as atypical MBCs) could be further assessed by flow cytometry.

Chapter 6. Evaluation of the impact of antigen sequence diversity on antibody profiles

6.1 Introduction

The association between sequence diversity in *Plasmodium* antigens and naturally acquired immunity has gained attention only over the past decade due to the potential impact for vaccine efficacy. Given the low efficacies of recently developed malaria vaccines [463], the need to find and develop novel approaches to optimise current vaccine candidates has become clear. Genetic variability in *Plasmodium* parasites is generally assumed to confer protective advantage to the parasites as an approach to evade host immune responses [464]. A critical part of host immunity is antigen-specific antibody responses, elicited upon the contact of a parasite and APCs and ultimately the activation of antibody-producing B cells (Figure 1.3). Antibodies are strong facilitators of parasite clearance by promoting opsonic phagocytosis, activating complement pathways and inhibiting further parasitic transmission [210]. It is likely that high levels of genetic diversity in certain antigen sequences will confer the parasite with the ability to escape the allele-specific recognition of host antibody responses [316]. This is a hurdle for effective antibody recognition and rapid parasite removal. In clinical settings, high genetic variability was also shown to limit the efficacy of vaccines as most vaccines were designed to target a subset of genetic variants in the population [465]. Together, these findings highlight the importance of investigating genetic diversity in *P. vivax* and its association with antibody

responses. A significant impact on antibody responses due to parasite sequence diversity is not only important for vaccine design, but also for the use of antibody responses as markers of immunity or exposure. In this Chapter, I used population genetics to quantitatively determine the level of genetic diversity in our panel of *P. vivax* antigens which was then correlated with their corresponding antibody profiles. Based on the evidence outlined above, I hypothesised that higher genetic diversity in a *P. vivax* antigen might be associated with lower immunogenicity and shorter antibody longevity in individuals exposed to *P. vivax*. Furthermore, such associations were expected to be weak in the Thai symptomatic cohort as approximately 50% of these individuals had reported this clinical *P. vivax* infection as their first ever infection.

Population genetic analysis is a well-established tool to a) quantify and describe genetic variations within or between populations and b) explain such variations from an evolutionary point of view based on molecular evidence [466]. In an era where sequencing technologies and data sharing are fast advancing, population genetics has become a highly accessible and compatible tool for malaria epidemiology [467]. It has been applied extensively in the field of malaria research to assist in identifying the level of protein sequence diversity in populations and therefore infer better strategies for surveillance, control and elimination [468, 469].

Several common population genetic parameters are used in this work to quantify the level of genetic diversity of *P. vivax* antigens. Their definitions and interpretation are listed in Table 6.1. In addition, the length/size of the antigenic constructs was also included as longer sequences could have more available epitopes to elicit a detectable antibody response. Notably, I used SNPs as the only molecular marker to represent genetic diversity in this work with the potential of performing similar analyses on other markers such as InDels and short tandem repeats in the future.

In this Chapter, the above-mentioned population genetic parameters were generated using 'Vaxpack' R package developed by A/Prof Alyssa Barry's laboratory at WEHI following exclusion of low-quality and irrelevant DNA sequences. Subsequently, these population genetic parameters were correlated with each other and with several parameters that describe antigen-specific antibody kinetic profiles. By incorporating these parameters in our population genetic analysis along with antibody measurements, I highlight the immunological relevance of genetic diversity, which will help answer some key questions in the context of understanding how diversity in antigenic protein sequences could affect naturally acquired immunity and to what extent. I hypothesised that higher genetic diversity in a *P. vivax* antigen might be associated with lower immunogenicity and shorter antibody longevity in

individuals exposed to *P. vivax*. This could be due to the presence of highly variable epitopes and therefore difficulty in eliciting antigen-specific antibody and memory responses. Such associations were expected to be weak in the Thai symptomatic cohort as approximately 50% of these individuals had reported this clinical *P. vivax* infection as their first ever infection.

Table 6.1 Definition and general interpretation of population genetic parameters

Parameter	Abbreviation	Definition	Interpretation
Length		Size of construct in base pair	Potential association with number of epitopes
Number of segregating sites	S	Nucleotide polymorphisms across all samples	Definite number of polymorphisms
Nucleotide diversity	π	Pairwise nucleotide polymorphisms, reported as $\pi \times 10^{-3}$	Extent of diversity
Tajima's *D* [470]	*D*	A statistic based on estimated nucleotide diversity (θ_π), segregating sites (θ_S) and their variance (V) to test the presence and strength of balancing selection in shaping sequence diversity $d = \theta_\pi - \theta_S$ $D = \frac{d}{\sqrt{V_d(d)}}$	**Positive**: Balancing trait that maintains variations in populations (recent population contraction) **Zero (null)**: no variations **Negative**: Purifying trait that remove variations from populations (recent population expansion)
Total number of SNPs	SNPs		Describe the type and frequency of genetic polymorphisms and quantify protein-changing polymorphisms Greater the values, higher the level of diversity and more likely to cause a change in immune responses.
Number of synonymous or non-synonymous SNPs	SP or NS		
Proportion of non-synonymous SNPs	Proportion of NS	$\frac{Number\ of\ non-synonymous\ SNPs}{Total\ number\ of\ SNPs}$	
Number of haplotypes	h	Total number of unique combination of SNPs in an amino acid sequence	
Haplotype diversity [471]	Hd	Difference in diversity between two amino acid sequences based on sample size (n) and frequency (f) of each haplotype (*i*) $Hd = \left(\frac{n}{n-1}\right)(1 - \Sigma(f_i)^2)$	

6.2 Results

6.2.1 Summary statistics of population genetic parameters

A total of 325 parasite isolate samples were collected from 13 malaria-endemic countries and were then sequenced as part of the MalariaGEN *P. vivax* Genome Variation project, as described in Pearson et al., Nature Genetics, 2016 [346] and Hupalo et al 2016 [472]. The process of filtering isolate DNA sequences based on quality is described in Section 2.7.1 in Chapter 2. In brief, the sequences were mapped to the latest reference strain PvP01 [347]. This was followed by a series of filtering strategies to eliminate low-quality sequences from further analyses (based on sequencing depth, mapping quality, sample missingness and similarity between samples, etc.) to remove duplicates and samples with high complexity of infection (i.e. higher number of genetically distinct infections in a host). Finally, isolate sequences originating from Thailand were used for this project, given all antibody data was obtained from Thai individuals.

Amongst the 52 *P. vivax* antigens used for antibody kinetic measurements, 49 antigens were identified and functionally annotated on PvP01, as listed in Table 6.2. The three *P. vivax* antigens that were not identified are PVX_101590 (RBP2-

P2), AAY34130.1 (DBP region II, AH strain) and KMZ83376.1 (EBP region II). AAY34130.1 was not found on the reference strain PvP01 because it is an antigen specific to the strain AH. For PVX_101590, this could be due to the fact that it had not been fully characterised before PvP01 was assembled. KMZ83376.1 was annotated that it was found in a Brazilian *P. vivax* strain, suggesting that it may be absent in PvP01 originated from Indonesia. Following sample filters and hard filter (see Figure 2.4 in Chapter 2 for detail), 19 isolates from Thailand passed and were included in genetic diversity analysis.

To gain an overview of the data generated from population genetic analysis, I first visualised the distribution of sequence diversity measures across the 49 *P. vivax* antigens (Figure 6.1). Most parameters showed a slight to moderate level of positive skewness whilst the proportion of NS polymorphisms and Hd showed some degree of negative skewness (Figure 6.1). This distribution pattern indicates that most *P. vivax* antigens had a low to moderate level of sequence diversity amongst the parasitic population in Thailand. PVX_097715, a hypothetical protein, was identified as an outlier with exceptionally high level of diversity (including S, SNPs, π, *D*, NS, SP and Proportion of NS) and was the cause of the negative skew in the distribution of these parameters. The high values of π and *D* suggested that this antigen could contain a lot of SNPs that were commonly found in this population. However, further studies are required

to determine why this particular *P. vivax* antigen was more highly diverse compared to the other 48 antigens.

Table 6.2 Estimates of genetic diversity in *P. vivax* isolates (n=19) from Thailand for 49 candidate sero-surveillance antigens.

Antigen	Length (bp)	S	SNPs	$\pi \times 10^{-3}$	*D*	NS	SP	Proportion of NS	h	Hd
PVX_000930	333	0	0	0	0	0	0	0	0	0
PVX_001000	1878	15	15	2.24	-0.08	11	4	0.73	9	0.88
PVX_003555	1806	10	10	0.92	-1.49	3	7	0.3	4	0.3
PVX_003770	1032	82	85	25.73	0.54	79	6	0.93	15	0.97
PVX_082645	1068	8	8	1.53	-0.97	8	0	1	7	0.85
PVX_082650	1263	24	24	4.94	-0.36	12	12	0.5	5	0.53
PVX_082670	1167	6	6	1.04	-0.94	4	2	0.67	5	0.65
PVX_082700	1197	2	2	0.26	-1.10	0	2	0	1	0
PVX_082735	1404	13	13	2.28	-0.51	12	1	0.92	14	0.95
PVX_084340	1335	155	155	12.22	-2.64	125	30	0.81	3	0.21
PVX_084720	2658	10	10	0.70	-1.26	7	3	0.7	6	0.6
PVX_087885	720	2	2	0.55	-0.73	1	1	0.5	2	0.2
PVX_088820	780	5	5	0.92	-1.55	4	1	0.8	4	0.3
PVX_088860	1143	17	17	3.53	-0.65	15	2	0.88	14	0.97
PVX_088910	1590	9	9	2.02	0.86	9	0	1	12	0.94
PVX_090240	1023	33	37	11.98	1.19	31	6	0.84	16	0.98
PVX_090265	981	7	7	1.96	-0.14	6	1	0.86	5	0.67
PVX_090330	333	16	16	14.07	0.09	9	7	0.56	6	0.74
PVX_090970	705	2	2	0.43	-1.12	1	1	0.5	2	0.11
PVX_091710	2577	7	7	0.43	-1.49	5	2	0.71	6	0.71
PVX_092990	876	2	2	0.99	1.23	1	1	0.5	2	0.46

Antigen	Length (bp)	S	SNPs	$\pi \times 10^{-3}$	*D*	NS	SP	Proportion of NS	h	Hd
PVX_094255A	2004	7	7	0.73	-0.90	7	0	1	9	0.85
PVX_094255B[a]	3882	29	30	2.19	0.01	27	3	0.9	15	0.98
PVX_094255B[a]	2400	127	128	19.99	1.34	106	22	0.83	15	0.97
PVX_094830	711	3	3	1.038	-0.40	2	1	0.67	3	0.56
PVX_095055	1575	9	9	1.20	-0.94	6	3	0.67	8	0.84
PVX_096995	1242	7	7	1.18	-0.89	6	1	0.86	6	0.74
PVX_097625	1320	4	4	0.97	0.34	3	1	0.75	4	0.63
PVX_097680	2298	144	145	18.21	0.07	102	43	0.70	19	1
PVX_097715	1200	665	693	270.78	2.99	503	190	0.73	13	0.96
PVX_097720	2475	153	160	22.48	1.13	110	50	0.69	18	0.99
PVX_098582	3408	13	13	0.55	-1.82	10	3	0.77	8	0.81
PVX_098585	3033	42	43	3.50	-0.47	37	6	0.86	17	0.99
PVX_098915	1470	6	6	1.03	-0.37	1	5	0.17	2	0.52
PVX_099930	1095	1	1	0.10	-1.17	0	1	0	1	0
PVX_099980	324	1	1	0.34	-1.13	1	0	1	1	0
PVX_101530	981	87	93	29.03	0.60	65	28	0.7	10	0.88
PVX_110810[b]	987	20	20	6.75	0.64	19	1	0.95	9	0.85
PVX_112670	924	6	6	0.72	-1.98	3	3	0.5	2	0.11
PVX_112675	852	25	25	13.85	2.55	18	7	0.72	10	0.9
PVX_112680	846	4	4	1.20	-0.33	3	1	0.75	4	0.68
PVX_117385	981	4	4	0.61	-1.40	2	2	0.5	3	0.21
PVX_117880	534	1	1	0.21	-1.13	1	0	1	1	0
PVX_121897	759	0	0	0	0	0	0	0	0	0
PVX_121920	2928	29	29	2.68	-0.21	26	3	0.9	17	0.99
PVX_123685	1935	7	7	0.70	-1.09	5	2	0.71	6	0.75

Antigen	Length (bp)	S	SNPs	$\pi \times 10^{-3}$	*D*	NS	SP	Proportion of NS	h	Hd
PVX_125728	753	3	3	0.44	-1.68	3	0	1	4	0.3
PVX_125738	2361	19	19	1.84	-0.77	14	5	0.74	14	0.95
Summary										
Mean	1431.31	37.98	39.04	10.16	-0.36	29.43	9.61	0.69	7.5	0.62
Median	1167	9	9	1.20	-0.47	7	2	0.73	6	0.74
SD	824.71	99.90	103.86	38.70	1.11	75.92	28.37	0.28	5.5	0.35

[a]PVX_094255B (RBP2c-NB) were found to match two loci on the PvP01 reference strain due to the high similarity in DNA sequences. Data for PvP01 loci were recorded separately. [b] PVX_110810 represents PVX_110810A and B which have the same amino acid sequence (and hence the same values for all population genetic parameters) but were produced in different laboratories and were purified via different procedures. The results listed were subsequently correlated to antibody data specific to PVX_110810A and B. [c] π (nucleotide diversity) values were divided by 1000 for interpretation.

Abbreviations: S = number of segregating sites; SNPs = total number of SNPs; π = nucleotide diversity; *D* = Tajima's *D*; NS = number of non-synonymous SNPs; SP = number of synonymous SNPs; h = total number of haplotypes; Hd = haplotype diversity; SD = standard deviation.

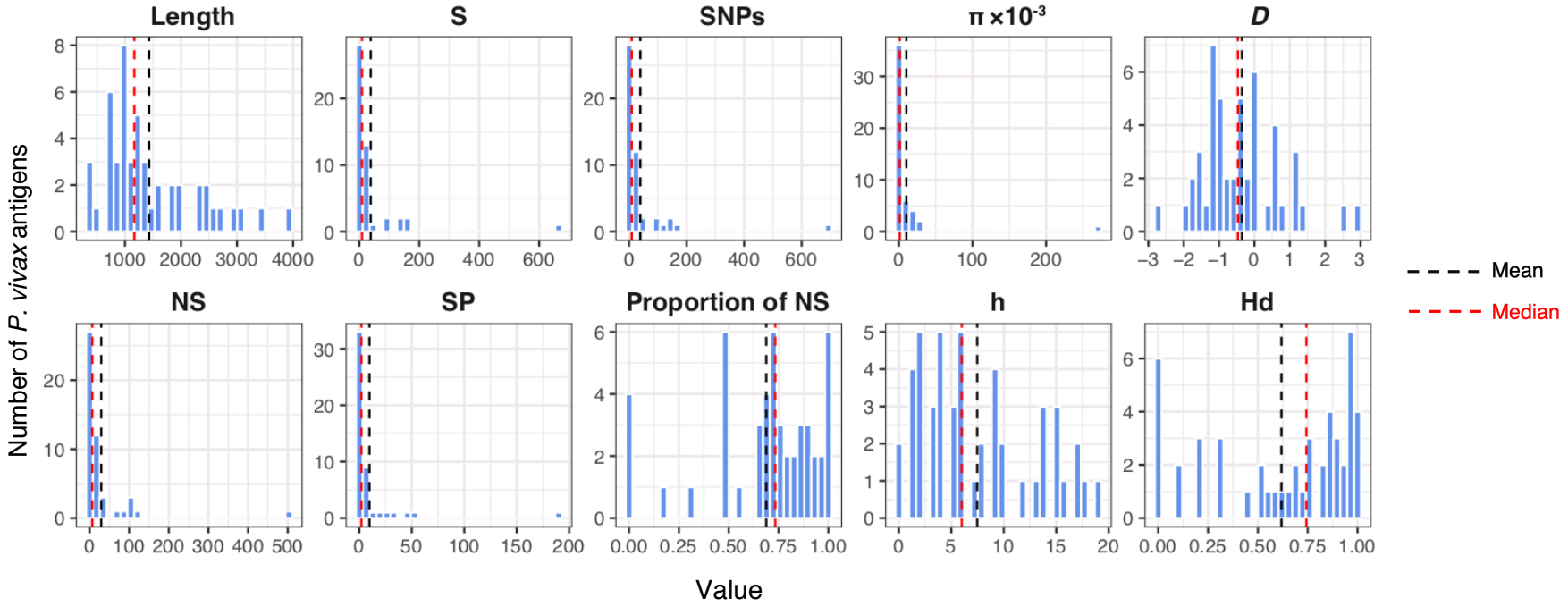


Figure 6.1 Frequency distribution of different population genetic parameters amongst the 49 candidate *P. vivax* sero-surveillance antigens. After mapping to reference PvP01, 49 of the 52 *P. vivax* antigens were found in a global sequencing dataset consisting of 325 parasitic isolates. 19 isolates from Thailand were down-selected and their sequence diversity was examined with population genetic analysis, generating 10 population genetic parameters. Dotted lines represent mean (black) and median (red). The x axis represents the value of the individual population genetic parameters and the y axis represents the number of *P. vivax* antigens (out of a total of 49).

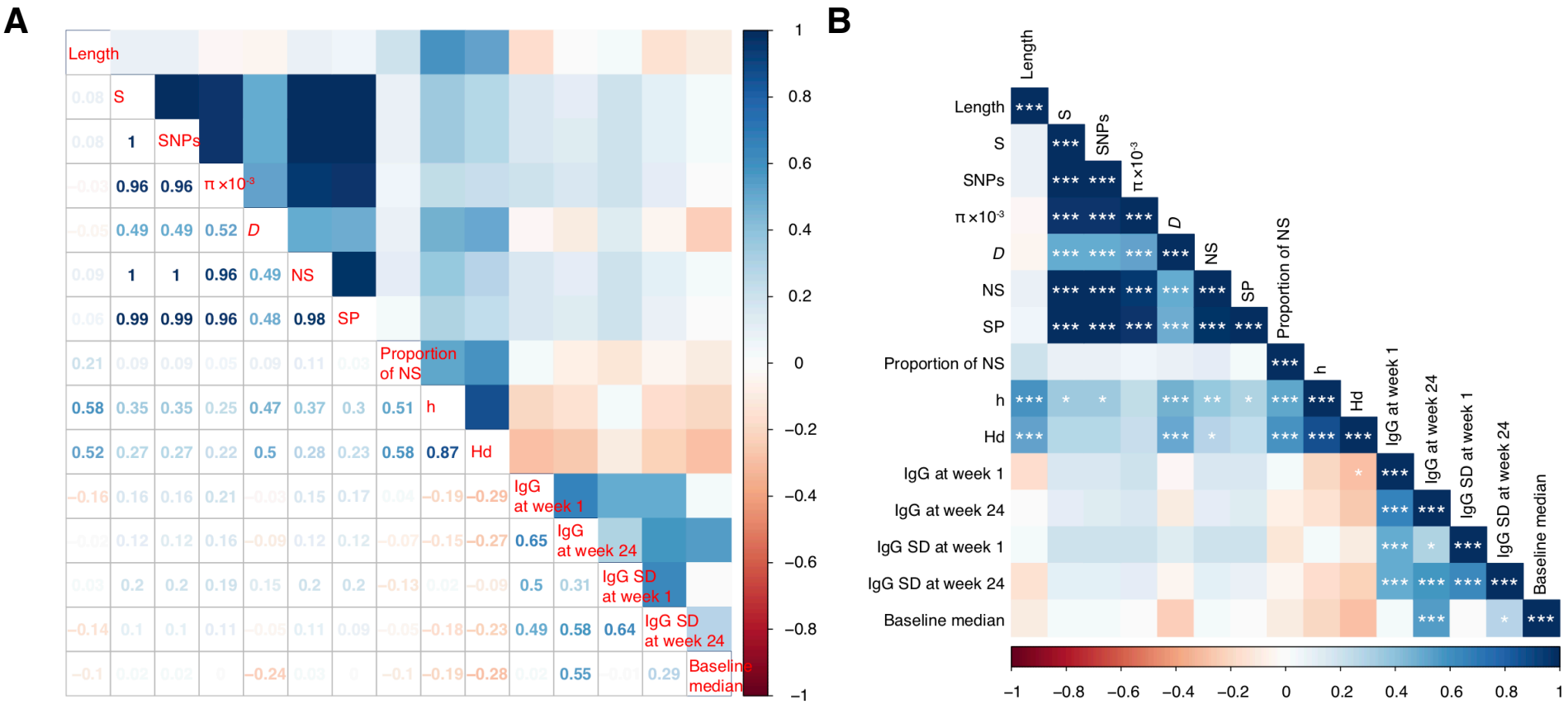
6.2.2 Impact of protein sequence diversity on total IgG and IgG subclass profiles in a symptomatic cohort

To assess the impact of high sequence diversity in *P. vivax* antigens on total IgG profiles, Pearson's correlation tests were performed between population genetic parameters and multiple IgG parameters. As outlined previously in Chapter 4, antigen-specific total IgG levels were measured in the longitudinal symptomatic Thai cohort whom were infected with *P. vivax* at enrolment and followed for nine months.

Five antigen-specific IgG parameters were generated from the antibody profile that described a few key features. These were the peak magnitude following initial infection (IgG at week 1), magnitude following a 6-month decay (IgG at week 24), SD of IgG responses at peak magnitude (IgG SD at week 1), after 6 months (IgG SD at week 24) and malaria-naïve baseline (Baseline median). The peak magnitude of the IgG response describes the immunogenicity of an antigen in this symptomatic population. SD was used as measurement of response variation between individuals. Lastly, antigen-specific IgG levels in almost 300 malaria-naïve individuals were also measured. The median of these measurements was calculated and utilised as a baseline to examine the effect of

protein sequence diversity on the background reactivity in these malaria-naïve populations.

Figure 6.2 shows the overall result of Pearson's correlation tests within and between population genetics and IgG parameters. More specifically, the R coefficients generated from the tests are shown in Figure 6.2A and the corresponding p values in Figure 6.2B. In Figure 6.2A, strong and positive correlations were observed between each pair of population genetic parameters (except for length) ($R=0.48 - 1$, $p<0.001$). In contrast, between population genetics and antibody parameters, the strength of correlation was weak, ranging between -0.29 and 0.21 (a mixture of both negative and positive correlations). A negative and statistically significant correlation between Hd and IgG magnitude at week 1 was observed ($R = -0.29$, $p = 0.046$) (Figure 6.2B and C), suggesting that in this symptomatic cohort, higher haplotype diversity was associated with lower total IgG magnitude 1-week post-infection. However, upon further investigation, an outlier existed (PVX_099980 ($MSP1_{19}$)) that exhibited a significantly higher IgG magnitude with a highly conserved antigenic sequence and hence no sequence diversity. Upon the removal of PVX_099980, the correlation with Hd was reduced and became statistically insignificant ($R = -0.14$, $p = 0.34$) (graph not shown).


A
B
Length
S
SNPs
π ×10-3
D
NS
SP
Proportion of NS
h
Hd
IgG at week 1
IgG at week 24
IgG SD at week 1
IgG SD at week 24
Baseline median
1
0.8
0.6
0.4
0.2
0
−0.2
−0.4
−0.6
−0.8
−1

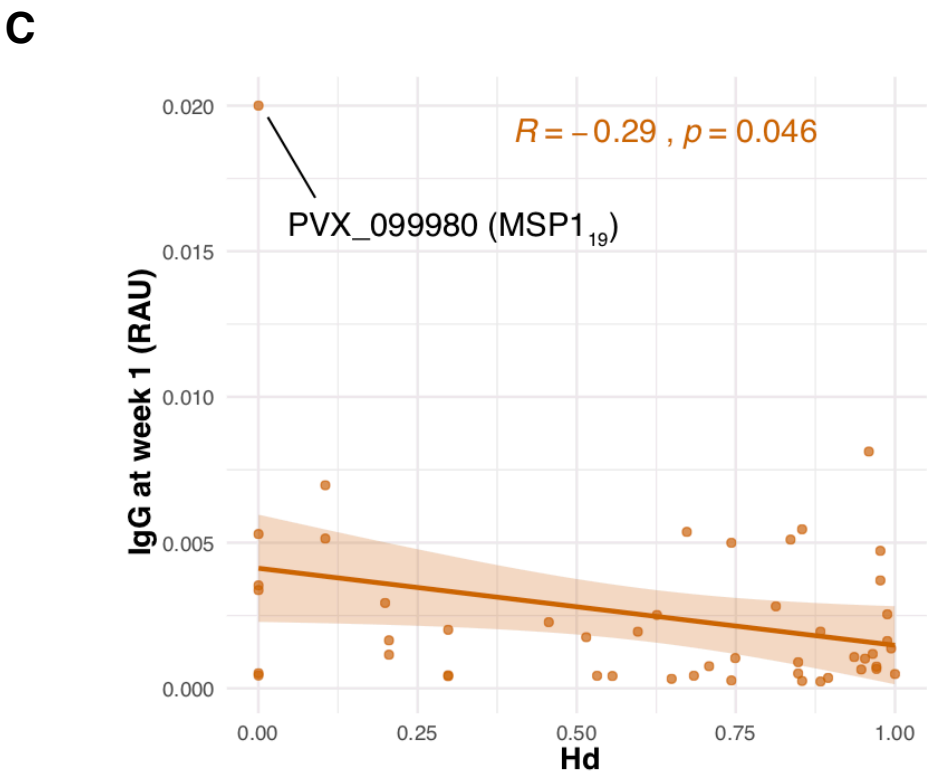


Figure 6.2 Correlations between protein sequence diversity and total IgG response in a symptomatic Thai cohort. Multiple population genetic parameters were generated and used to describe the sequence diversity in 49 *P. vivax* antigens. Antigen-specific total IgG responses in the symptomatic Thai cohort were measured and characterised using four IgG parameters (ie. median IgG responses at 1 and 24-week post-infection and IgG SD at 1 and 24-week post-infection). Pearson's correlation tests were performed to determine the strength of association between IgG response characteristics and antigenic sequence diversity. **A)** The R coefficients generated are summarised to indicate the strength of each pair of correlations, along with **B)** their corresponding p values to indicate statistical significance (p<0.05*, <0.01**, <0.001***). **C)** The correlation between Hd and IgG magnitude at week 1 was visualised separately to show the association in detail.

To determine if protein sequence diversity was associated with differential IgG subclass profiles, I visualised the distribution of population genetic parameters for each IgG subclass category established in the symptomatic Thai cohort (details described in Chapter 4). The four IgG subclass categories were established for 27 *P. vivax* antigens with total IgG responses 1-week post-infection >1 SD above the malaria-naïve baseline. The categories include: a) IgG1 only (n=13), b) IgG1 predominant & IgG3 sub-dominance (n=9), c) IgG1 predominant, IgG2 & IgG3 sub-dominance (n=2) and d) no obvious dominance (n=2). The categorisation was based on the major response(s) present at 2-week post-infection. Among the 27 antigens, I excluded three antigens which were not found in the reference strain PvP01 and therefore with no analysable population genetic data. Hence, the association was analysed using a total of 24 antigens.

As depicted in Figure 6.3, I found no evidence of an association between protein sequence diversity and IgG subclass profile following a symptomatic *P. vivax* infection. There was no clear grouping of *P. vivax* antigens within the same IgG subclass category for any particular population genetic parameter. For instance, the antigens inducing primarily IgG1 response (cyan and navy) were found to exhibit a wide range of most (if not all) population genetic parameters (Figure 6.3).This was most likely due to the fact that most of the antigens displayed

'IgG1 only' (n=11) or 'IgG1 & IgG3' (n=9) profiles. Antigens with 'IgG1, 2 & 3' and 'no obvious dominance' profiles were very rare in this cohort (n=2 and n=2, respectively). Despite the greater sample size, there was no clear division between antigens with 'IgG1 only' and 'IgG1 & 3' profiles.

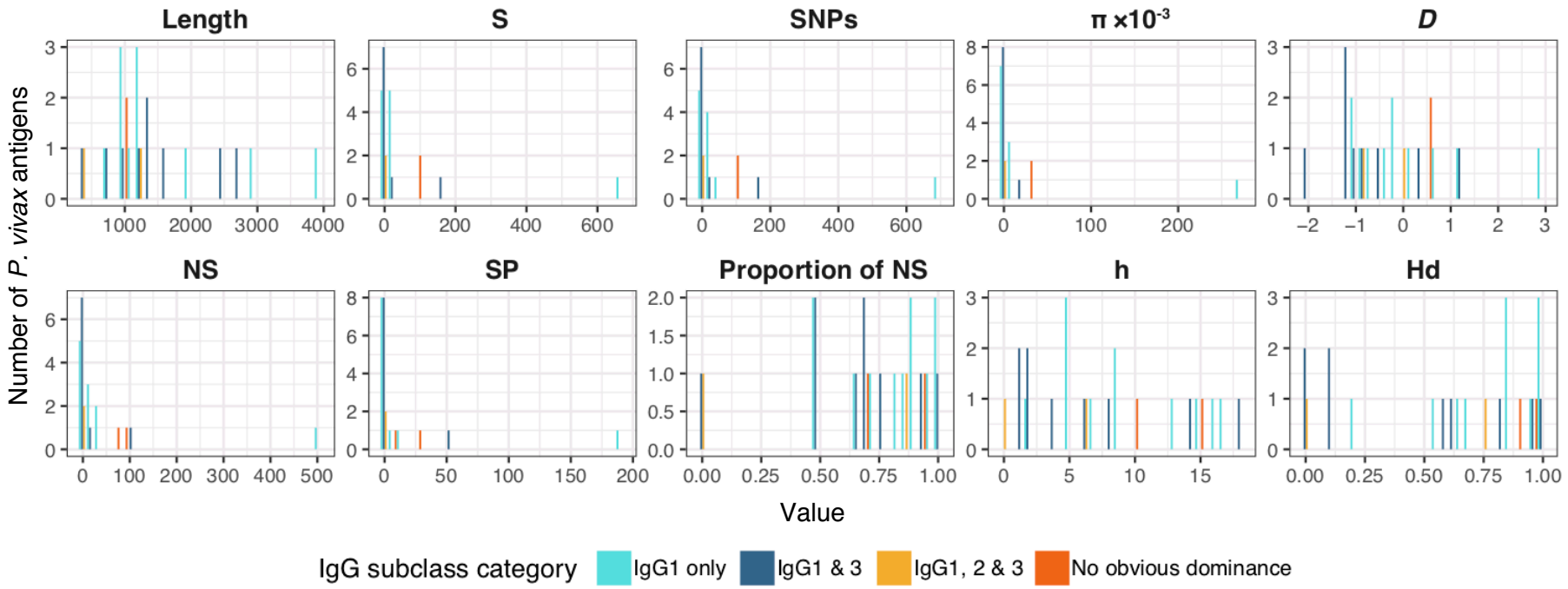


Figure 6.3 Distribution of data for population genetic parameters per IgG subclass category. IgG subclass responses were measured in the symptomatic Thai cohort against 27 *P. vivax* antigens with high immunogenicity (>1SD above malaria-naïve baseline), 24 of which were successfully mapped to reference PvP01. The IgG subclass profile was categorised based on the major response(s) at the peak of response (2-week post-infection). Amongst the 24 antigens, most exhibited an IgG1 dominant profile (n=11, cyan), followed by IgG1 predominant and IgG3 sub-dominant (n=9, navy), IgG1 predominant and IgG2 & 3 sub-dominant (n=2, gold), and no obvious dominance (n=2, orange). The association between sequence diversity and IgG subclass profile was visualised

by the distribution of data to reveal potential clusters. The x axis represents the value of the individual population genetic parameters and the y axis represents the number of *P. vivax* antigens (out of a total of 24).

6.2.3 Impact of protein sequence diversity on IgM profile in a symptomatic cohort

In the previous Section, I have established that the genetic diversity of an antigen sequence had very limited association with the total IgG and IgG subclass profiles in individuals with little past exposure (as manifested by the presence of clinical symptoms). IgG responses can be low or limited upon primary infections, but generally are of greater magnitude following repeated infections [174, 473]. It was hypothesised that the symptomatic individuals with limited past exposure could have less developed IgG responses leading to the weaker associations of IgG responses and genetic diversity of *P. vivax* antigen sequences. It has been reported that prominent IgM responses are often seen following the primary infection [212]. It is possible that the Thai symptomatic cohort with very limited past exposure could show stronger associations between IgM responses and the population genetic parameters. To assess this concept, I decided to investigate the associations between IgM responses and genetic diversity in the symptomatic cohort.

IgM antibody has been described as the early antibody responses against infections. In malaria, it was shown that during the early stage of an infection IgM contributed to the inhibition of RBC invasion and therefore was linked to

protection against symptoms [212]. Given that IgM and IgG potentially have distinctive roles in controlling the spread of *Plasmodium* parasites in the human hosts, it is possible that the protein sequence diversity of an antigen could have differential effects on how IgM and IgG antibodies recognise a target.

I first assessed the distribution of each population genetic parameter within the binary IgM immunogenicity category. An antigen was categorised as immunogenic if the peak response (1-week post-infection) was >2 SD above the malaria-naïve baseline. As depicted in Figure 6.4, non-IgM-immunogenic antigens were observed to show higher sequence diversity and a stronger sign of balancing selection than the IgM-immunogenic antigens. The values of S, SNPs, $\pi \times 10^{-3}$, *D* and proportion of non-synonymous SNPs were statistically higher ($p<0.05$) in non-IgM-immunogenic antigens (peak response was 2 SD below the malaria-naïve baseline) than the immunogenic antigens (peak response was 2 SD above the malaria-naïve baseline). This result indicates that high sequence diversity is associated with a lack of IgM antibody response following symptomatic infections.

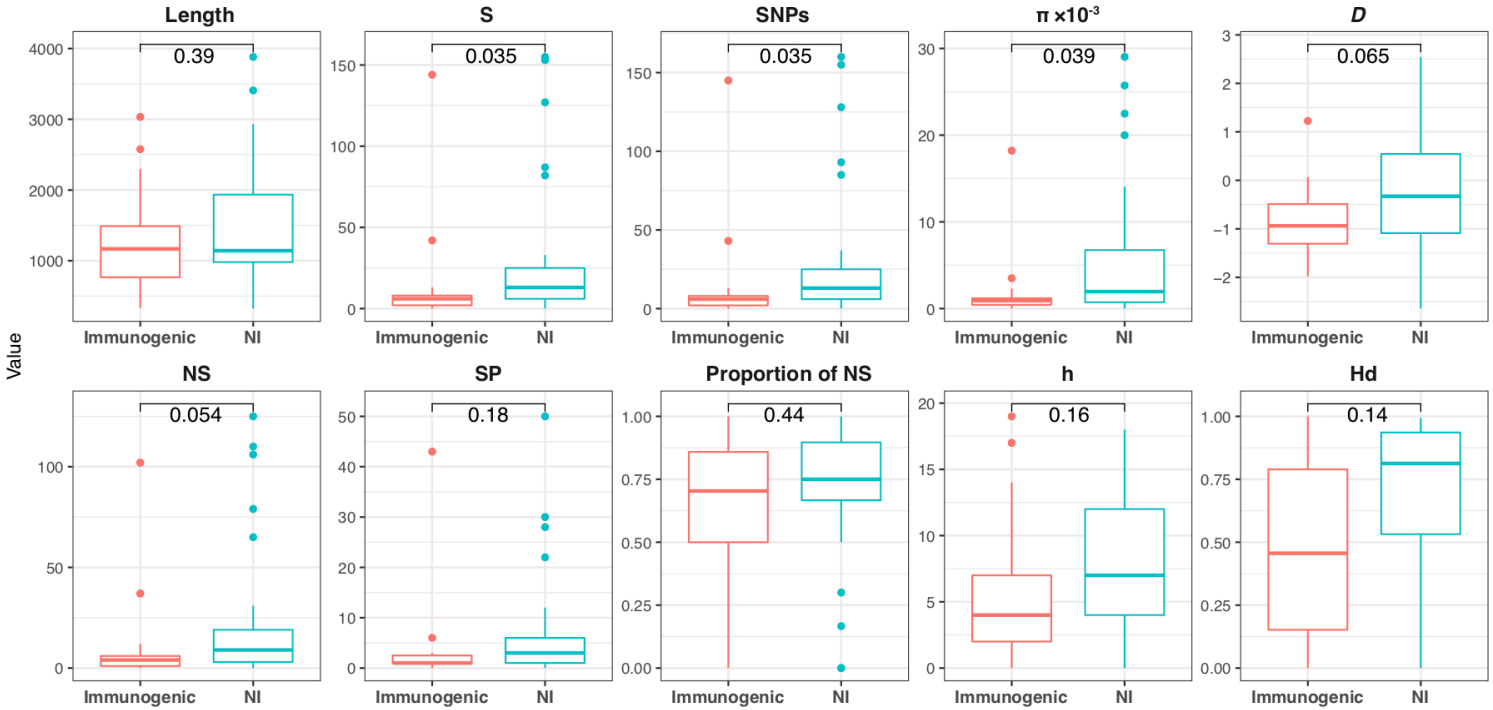


Figure 6.4 Distribution of population genetic parameters per IgM immunogenicity category. IgM responses against 52 *P. vivax* antigens at 1-week post-infection were measured in the symptomatic Thai cohort. Antigens with IgM responses >2SD above the malaria-naïve baseline were categorised as immunogenic (n=15) and ones without were non-immunogenic (NI) (n=37. The spread of each population genetic parameter was visualised to determine the association between antigenic sequence diversity and IgM immunogenic category. Mann-Whitney tests were performed and p values <0.05 were considered statistically significant.

Subsequently, I performed more in-depth Pearson's correlation tests between population genetics and IgM antibody parameters to quantify the strength of associations. I defined four IgM parameters: the magnitude at weeks 1 and 24, and the individual response variation at weeks 1 and 24.

At 1-week post-infection, higher protein sequence diversity was associated with lower IgM magnitude and SD (R range = -0.45 - 0) (Figure 6.5A). Compared to the level of associations for total IgG magnitude and SD in the same symptomatic Thai cohort (R range=-0.29 – 0.21), protein sequence diversity appeared to be more strongly correlated with IgM. Furthermore, several associations were found that were statistically significant ($p < 0.05$). These include associations between IgM peak response (IgM at week 1) and *D*, h and Hd (Figure 6.5B). Additionally, associations between IgM response variation at peak (IgM SD at week1) and $\pi \times 10^{-3}$ and NS were statistically significant (Figure 6.5B).

In contrast to 1-week post-infection which showed largely negative correlations, higher protein sequence diversity was associated with higher IgM magnitude and SD at 24-week post-infection (R range = 0 – 0.37) (Figure 6.5A). Interestingly, whilst IgG and IgM response magnitude at week 24 exhibited similar level of associations with sequence diversity, IgM SD at week 24 was more strongly correlated with sequence diversity than IgG SD at the same time point.

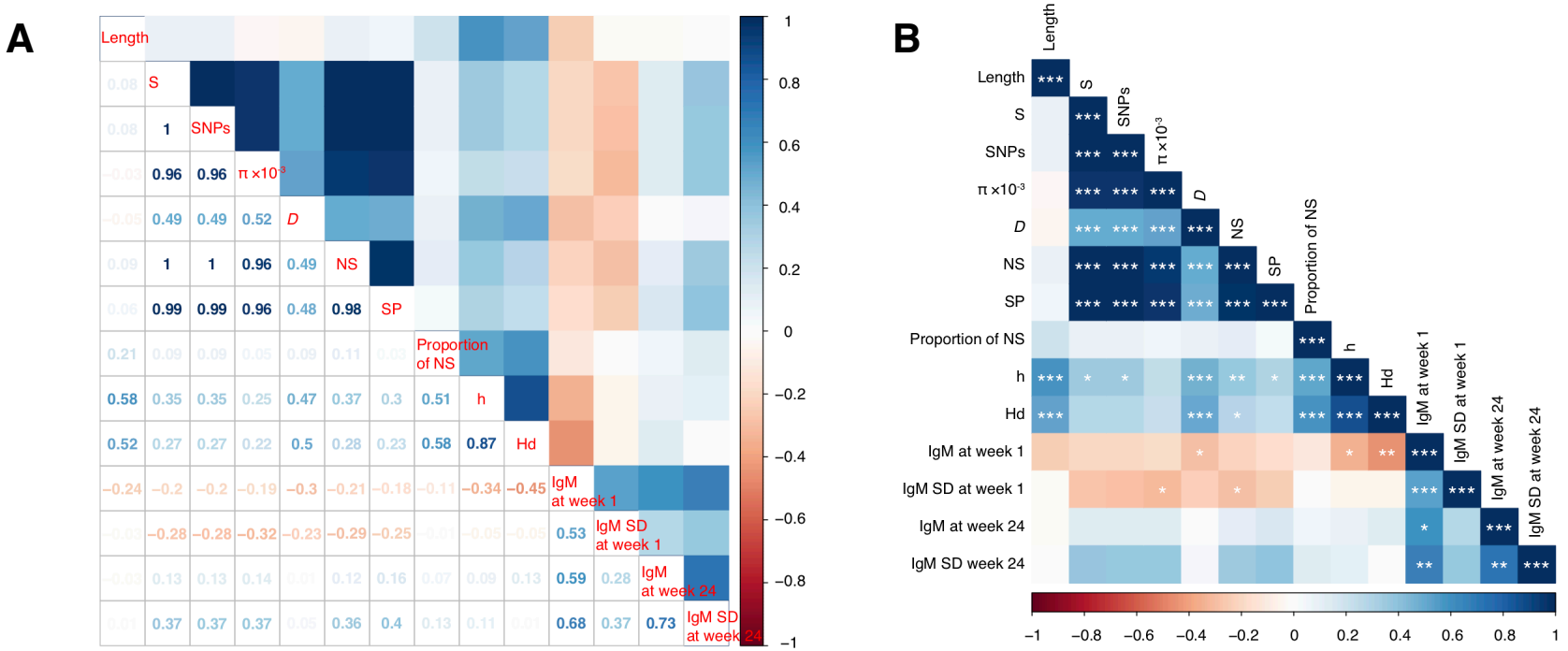


Figure 6.5 Heatmap for correlations between protein sequence diversity and IgM response in the symptomatic Thai cohort. Multiple population genetic parameters were generated and used to described sequence diversity in 49 *P. vivax* antigens. Antigen-specific IgM responses in the symptomatic Thai cohort were measured and characterised using two IgM parameters. Pearson's correlation tests were performed and **A)** the R coefficients generated are summarised to indicate the strength of each pair of correlation, along with **B)** their corresponding p values to indicate statistical significance ($p<0.05$*, <0.01**, <0.001***).

Upon further analysis, I found that a higher number of haplotypes was associated with reduced IgM peak magnitude (1-week post-infection) (Figure 6.6A). Similarly, increased haplotype diversity was also associated with reduced IgM peak magnitude (Figure 6.6B). These observations were most likely due to the influence of protein sequence diversity in the majority of the *P. vivax* antigens. This was demonstrated in Figure 6.6B in which antigens with greater haplotype diversity (shown as larger circles with lighter colours) mainly exhibited positive *D* values. Those with less haplotype diversity (smaller circles with darker colours), on the other hand, showed negative *D* values.

Unexpectedly, an increase in π and NS were associated with reduced IgM response variation between individuals (Figure 6.6C). However, once the outlier (identified as PVX_097715, a hypothetical protein) was removed, the associations no longer existed for both π ($R=-0.14$, $p=0.33$) and NS ($R=-0.057$, $p=0.7$).

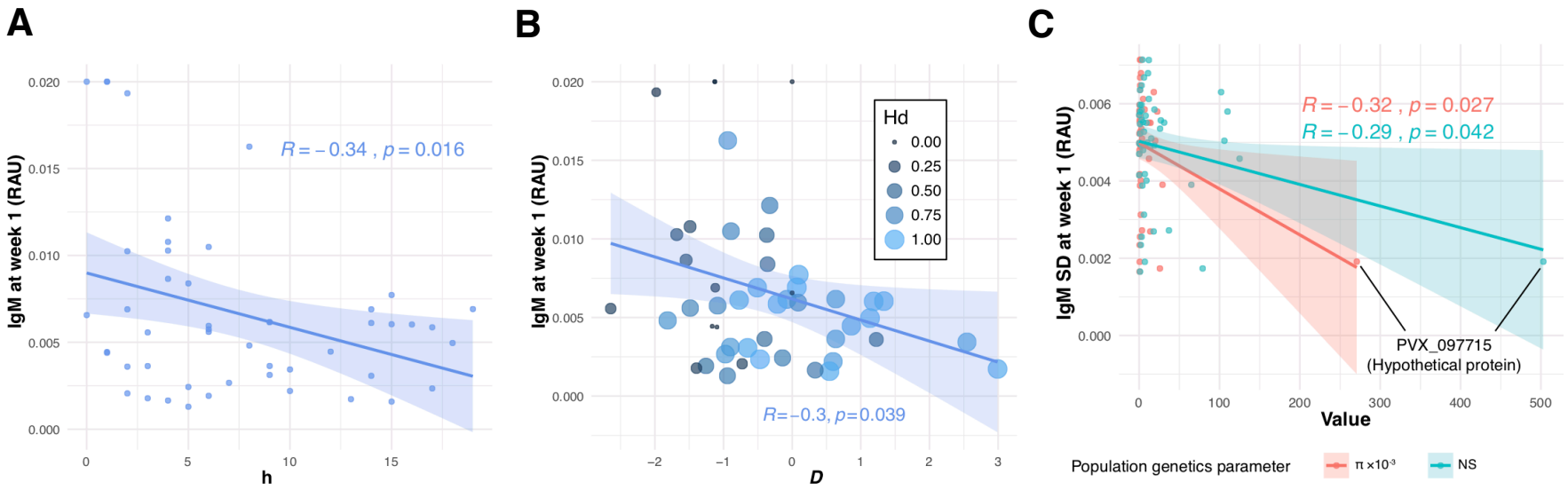


Figure 6.6 Significant correlations between population genetics and IgM parameters in the symptomatic Thai cohort. To further assess the statistically significant associations between multiple population genetic parameters and IgM responses in the symptomatic Thai cohort, IgM magnitude at peak (1-week post-infection) was plotted against **A)** number of haplotypes (h) and **B)** Tajima's *D* (*D*). In B), Hd of each antigen was indicated by colour and size: circles with lighter colour and larger size showed higher Hd value. Additionally, the detailed **C)** associations between nucleotide diversity (π) and number of non-synonymous SNPs (NS) were plotted against IgM response variation in SD. Pearson's correlation tests were performed, generating R coefficients and p values. P values <0.05 are considered significant.

6.2.4 Impact of protein sequence diversity on IgG profile in an asymptomatic cohort

The analyses so far were performed using the IgG profile following symptomatic infections in Thai individuals. It is like that the impact of protein sequence diversity on naturally acquired immunity would potentially be more evident in individuals with a higher level of past exposure who had been exposed to a higher number of genetically distinct infections and have thus obtained some level of immunity. Hence, I decided to investigate if the associations between protein sequence diversity and total IgG remain similar in asymptomatic individuals with (presumably) higher levels of past exposure. Therefore, correlation tests were again performed between population genetics and total IgG parameters for the asymptomatic Thai cohort. The same antigen-specific IgG parameters as used in the symptomatic cohort were generated for the asymptomatic cohort (IgG at week 1, IgG at week 24, IgG SD at week 1, IgG SD at week 24).

Figure 6.7A and B provide an overview of the results following correlation tests within and between population genetics and total IgG parameters in the asymptomatic cohort. Similar to the observations made in the symptomatic cohort, this aysmptomatic cohort showed strong and positive correlations between each pair of population genetic parameters (except for length) ($R=0.69 – 1$, $p<0.001$). In this asymptomatic cohort, the correlations between population genetics and total IgG

paramaters were slightly stronger compared to the symptomatic cohort (range of R coefficient = -0.27 – 0.47 compared to -0.29 - 0.21, respectively) (Figure 6.7A). There were also more positive correlations in the asymptomatic cohort than the symptomatic. Total IgG response variation between individuals (SD) at both 1- and 24-week post-infection was shown to be positively and significantly correlated to both Hd and *D* (Figure 6.7B). These associations were further examined and visualised in Figure 6.8.

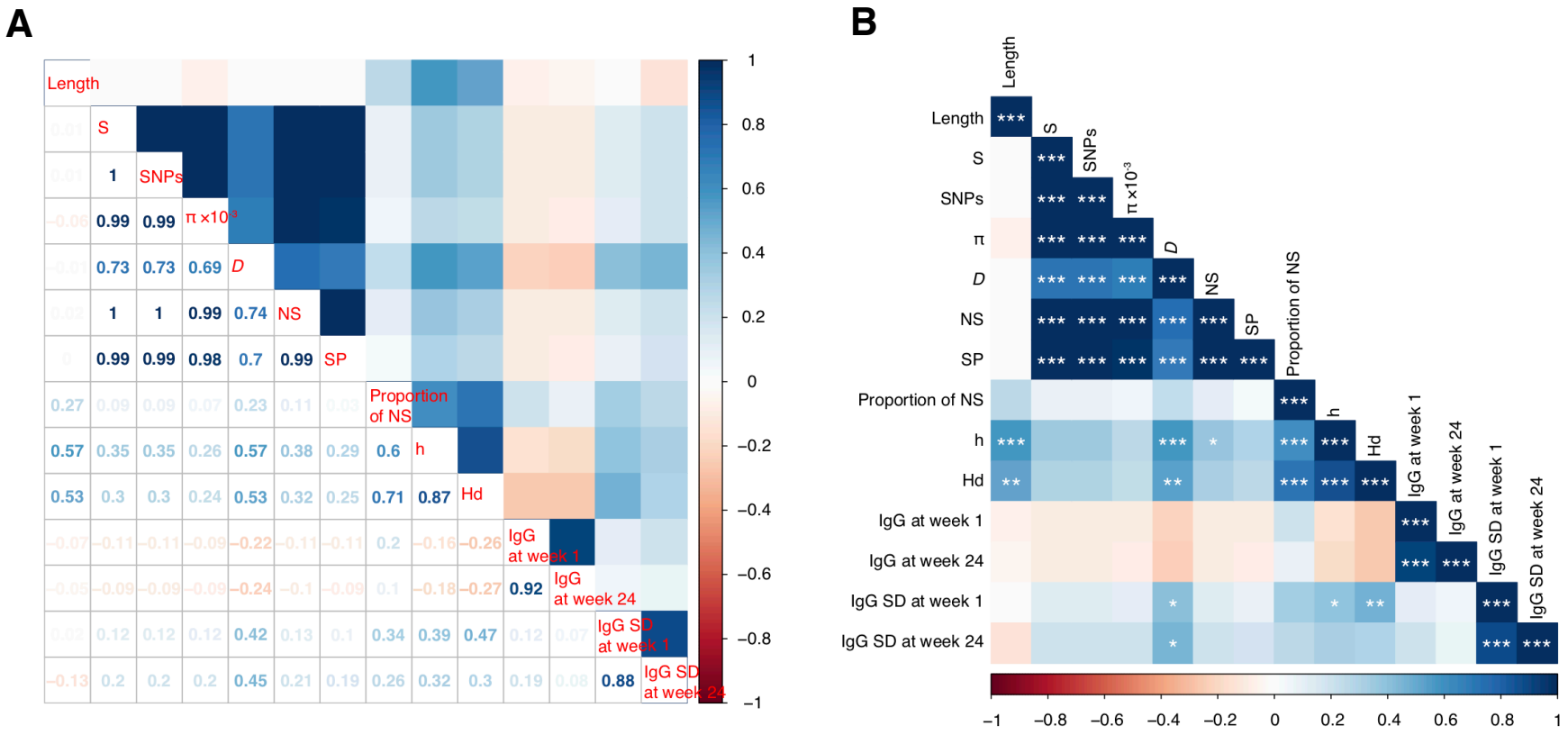


Figure 6.7 Heatmap for correlations between protein sequence diversity and total IgG response in the asymptomatic Thai cohort. Multiple population genetic parameters were generated and used to describe sequence diversity in 49 *P. vivax* antigens. Antigen-specific total IgG responses in the asymptomatic Thai cohort were measured and characterised using four IgG parameters. Pearson's correlation tests were performed and **A)** the R coefficients generated are summarised to indicate the strength of each pair of correlations, along with **B)** their corresponding p values to indicate statistical significance (p<0.05*, <0.01**, <0.001***).

It was observed that higher haplotype diversity was associated with increased total IgG response variation in the asymptomatic individuals ($R = 0.47$, $p = 0.0082$) (Figure 6.8A). Additionally, regardless of time since last infection (1- or 24-week post-infection), an increase in total IgG response variation is associated with antigens being under balancing selection as indicated by the greater *D* value (Figure 6.8B). It appears that most of the antigens were neutral based on the *D* values (bewteen -1 and 1) whilst a few outliers with evident signatures of balancing and purifying selections were present (Figure 6.2.5C). Amongst these outliers, antigens with higher Hd (indicated as larger circles with lighter colours) tended to have positive *D* values. In constrast, the antigens with lower Hd (smaller circles with darker colours) all exihibited *D* values under zero, regardless of time point (Figure 6.8C and D). These findings indicated that balancing selection played a role in shaping the protein sequence diversity of an antigen, which was associated with how antigen-specific antibodies recognised it.

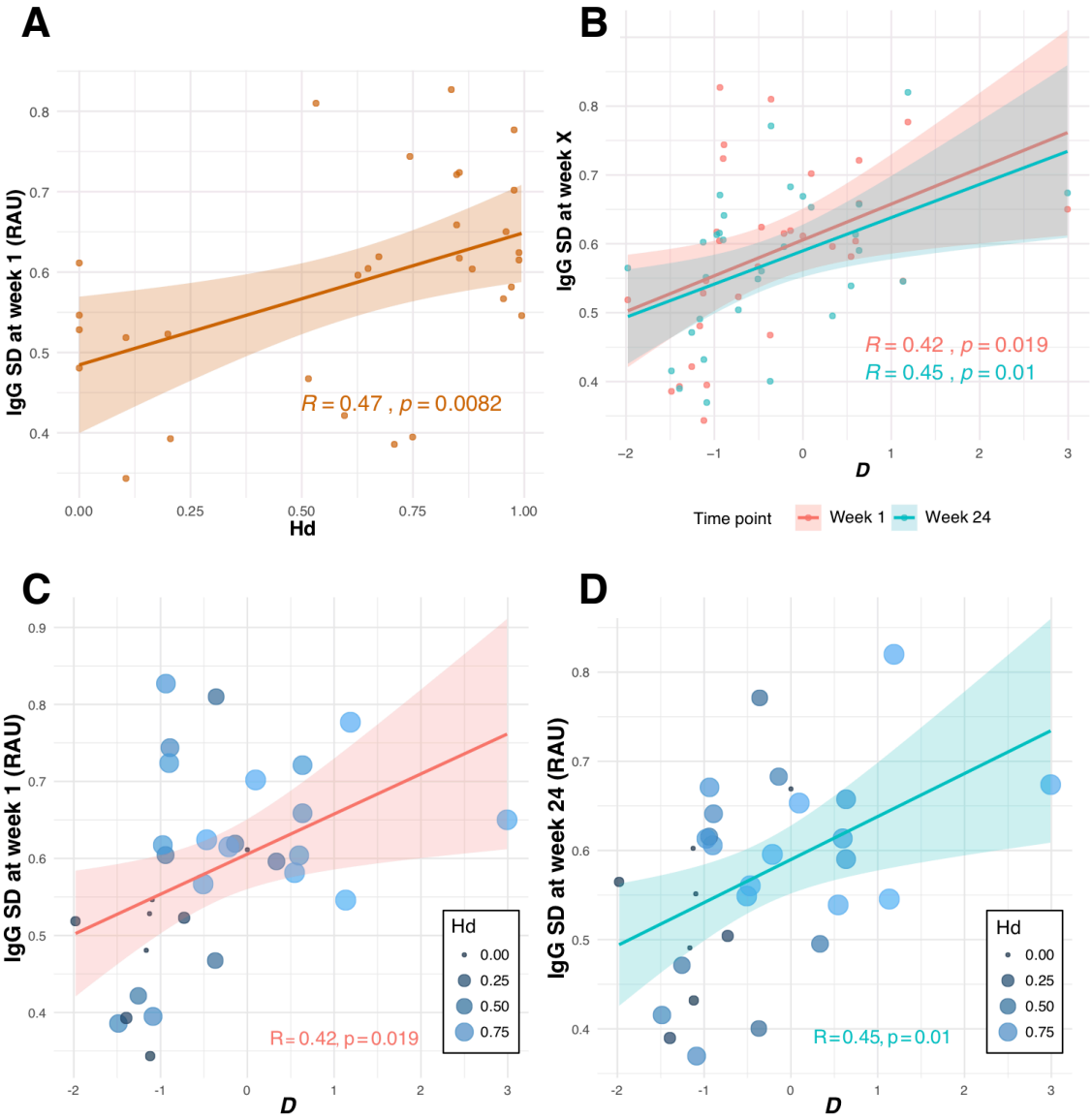


Figure 6.8 Significant correlations between haplotype diversity, balancing selection and total IgG response variation in the asymptomatic Thai cohort. To further assess the association between Tajima's *D* (*D*) and total IgG response variation in the asymptomatic Thai cohort, IgG SD was first plotted against **A)** Hd at 1-week post-infection and **B)** *D* with two time points separately. To further explain the source of haplotype diversity and its impact, IgG SD was also plotted against *D* with Hd of each antigen at **C)** week 1 and **D)** week 24, as indicated by circles of differing colours and sizes: circles with lighter colour and larger size showed higher Hd value. Pearson's correlation tests were performed, generating R coefficients and p values. P values <0.05 are considered significant.

6.3 Discussion

Population genetic analysis has been a useful tool to quantify diversity in *Plasmodium* antigens and has enabled estimation of the role of human immunity on shaping such diversity in a parasitic population. In the above Sections, I reported that high antigen sequence diversity was more strongly associated with IgM responses than IgG in the symptomatic cohort from western Thailand. Additionally, it was demonstrated that the impact of antigen sequence diversity on IgG responses was more evident in the asymptomatic cohort compared to the symptomatic one. In these two Thai cohorts, I also showed that the observed high protein sequence diversity was linked to strong signatures of balancing host selection which maintains genetic variations in the parasite population.

In this Chapter, I demonstrated the importance of sufficiently high past exposure in detecting the association between the genetic diversity of an antigen and the acquisition and development of complex antibody responses. The results support our hypothesis that the symptomatic individuals with little past exposure had less mature immunity, leading to limited or no associations between the strength of IgG responses and the different measures of antigen sequence diversity. This lack of associations could also be linked to the fact that the antibody measurements performed in the present study are all undertaken

using a single, specific allele of an antigen. Given that the symptomatic individuals would have exposure to less *P. vivax* antigen alleles, it is highly like that they may not had been previously infected with a parasite carrying the corresponding allele. The weak associations would thus be expected. A slight increase in the strength of associations for IgM magnitude is in line with IgM being the first antibody isotype produced following exposure to a pathogen [212] and with IgM showing a generally higher degree of cross-reactivity [418]. Additionally, the difference in the level of associations between IgM antibody parameters at weeks 1 and 24 could be reflective of the time-point-specific nature of how sequence diversity could be associated with antibody profiles. However, these speculations will require more data and further analyses to confirm. As individuals have gained further exposure against *Plasmodium* parasites (as presented by the asymptomatic cohort), the association of sequence diversity with IgG response variation became more significant. This finding again suggests that the asymptomatic individuals with more intensive past exposure would have experienced multiple *P. vivax* antigen alleles and therefore developed much larger antibody repertoires and generated greater inter-individual variations in the antibody responses upon re-encounter of specific alleles. It will be of great interest to verify this concept by examining the change in associations between sequence diversity and antibody response variation in

regions with higher malaria transmission where the whole populations have all been infected with many different alleles.

This work is also the first to describe the genetic diversity of a large panel of *P. vivax* antigens at a population level. Past studies mainly focussed on reporting the differential diversity between *P. falciparum* and *P. vivax* across geographically distinct populations. These studies have well established that *P. vivax* is more genetically diverse than *P. falciparum* in various populations with a wide range of malaria transmission levels [329, 331, 474, 475]. There are also a number of studies that focus on quantifying genetic diversity of individual molecular markers or *P. vivax* antigen-encoding genes [476-480]. However, that fact that these studies utilised datasets from various sources and different sample filtering strategies makes it difficult to draw further interpretations and conclusions. Additionally, some authors reported genetic diversity in other indices such as expected heterozygosity (H_E) and allelic richness (R_S). This is due to the fact that H_E and R_S are better suited to measuring genome-wide diversity instead of SNP diversity. Although H_E and R_S are analogous to Hd and h, respectively [481], it is difficult to directly compare their genetic diversity results to ours.

Nevertheless, some studies reported genetic diversity in *P. vivax* antigens using similar population genetic parameters. High level of nucleotide diversity (π) was reported in a number of *P. vivax* antigen-encoding gene families [329], some of which have been associated with merozoite invasion (*msp3*, *msp7*, *pvstp* and *pvrbp*)[482, 483], immune evasion (*P. vivax* virulence gene (*vir*)) [318] and protective antibody responses against malaria episodes in PNG children [213, 220]. These findings are comparable to those found in Thai isolates where *pvrbp* gene family members (including *pvrbp2a*, *pvrbp2b*, *pvrbp2d* and *pvrbp3*) involved in *P. vivax* blood stage infections exhibited significantly more NS than SP SNPs [484]. Similar to these findings, among our 24 *P. vivax* antigens with nucleotide diversity (defined as $\pi \times 10^{-3}$) greater than the median (1.20), I observed that most antigens (n=14, 58.33%) were associated with merozoite invasion into red blood cells. These include MSPs (n=5), RBPs (n=6), DBPs (n=2) and a microneme-derived protein (n=1). The annotation, stage of expression and estimates of genetic diversity for all *P. vivax* antigens are described in Tables 2.2 (Section 2.3.1 of Chapter 2) and 6.2 (Section 6.2.1 of this Chapter). Focusing on SNPs in *P. vivax* isolates from PNG, Arnott et al. reported their findings on genetic diversity in *P. vivax* AMA1 using population genetic parameters almost identical to ours (including S, π, NS, SP, h, Hd and Tajima's *D*). Compared to our Thai isolates (mean S=37.98; mean NS=29.43; mean $\pi \times 10^{-3}$ =10.16), PNG isolates appeared to have similar numbers of S (35) and NS (27.5) and value of

$\pi \times 10^{-3}$ (8.05) [477]. However, AMA1 in PNG exhibited more extensive level of diversity in h (44) and Hd (0.99) than the mean values generated with Thai isolates (h=7.5, Hd=0.62). This observation could be related to the higher transmission level in PNG compared to Thailand, which potentially suggests the role of high transmission level on increasing diversity within antigen protein sequences. However, since AMA1 was not included in our panel of *P. vivax* antigens, it is difficult to make a direct comparison on differences in genetic diversity of *P. vivax* antigens between PNG and Thailand.

In the present study, it was observed that stronger signatures of balancing selection were associated with increased levels of genetic diversity. Similarly, Arnott et al. demonstrated that specific domains of the AMA1 antigens with high level of diversity (indicated by relatively high $\pi \times 10^{-3}$ values) also exhibited significant and positive Tajima's *D*s [477]. It was stated by the authors that domains with strong positive Tajima's *D*s were likely to be a critical target of the host immune response, leading to more efficient protective effects. Similar observations were also made in a more recent study focussing on *P. vivax* reticulocyte binding antigen [485]. Nevertheless, whether or not balancing selection plays a diversifying role in the genomes of other organisms remains debatable. Balancing selection is known to maintain alleles at intermediate frequency, but is also shown to involve other mechanisms. It has been proposed

that the role of balancing selection is also dependent on the frequency [486] and evolutionary fitness of the alleles [487]. In this Chapter, it was found that a positive Tajima's *D* (indicating balancing selection) was strongly and positively associated with majority of the genetic diversity parameters (including S, $\pi \times 10^{-3}$, SNPs, SP, NS, h and Hd). For instance, high frequency of common SNPs is linked to high values of π and Hd (as they are influenced by allele frequency), resulting in the detection of positive Tajima's *D*. On the other hand, high frequency of mostly rare SNPs leads to lower π and Hd and therefore neutral or negative Tajima's *D*. Nevertheless, the positive correlation of key parameters such as $\pi \times 10^{-3}$ and Hd with Tajima's *D* clearly demonstrates the key role of balancing selection in maintaining genetic diversity in a large panel of *P. vivax* antigens.

This study has some minor limitations. Firstly, despite being the largest panel of *P. vivax* antigens investigated to-date, the present study will benefit greatly from incorporating even more antigens into the current panel. This will enable us to validate the observed associations, as the results of the correlations tests were susceptible to the effect of an outlier (as described in Sections 6.2.1, 6.2.2 and 6.2.3), especially in a population from Thailand where transmission and diversity are relatively low. A potential solution would be to perform similar analyses using isolate sequence data from regions with higher transmission

settings. Another limitation is that the current antibody parameters (signal magnitude and response variation at specific points) may not appropriately reflect the nature and details of the antibody kinetic profiles. Quantitative estimates generated from mathematical modelling of antigen-specific antibody kinetic profiles (such as estimated antibody half-lives) will greatly further our understandings on the association between genetic diversity and the decay of antibody responses. Lastly, future studies will need to address the source of high sequence diversity in PVX_097715 to allow validation of the results reported in this Chapter.

In summary, I report in the present study that high level of genetic diversity in 49 *P. vivax* antigens is likely to be the result of balancing selection, and is associated with increased IgG response variation between individuals and reduced IgM peak magnitude. Our results also indicate that transmission level and/or past exposure can affect the extent of impact of genetic diversity on antibody responses. A lack of research in this area poses a challenge to compare our results with other studies, which shows the novelty of this study. With an interest in optimising current strategies for developing highly efficacious vaccines and effective sero-surveillance tools, this study offers a feasible approach to investigate the level of genetic diversity in potential vaccine and/or serological marker candidates. Additionally, our findings provide unique

insights into the potential consequences involved in incorporating highly polymorphic antigens/haplotypes as vaccine candidates.

Chapter 7. General discussion and perspectives

7.1 Overview

For the past two decades, we as a global community have achieved several major milestones on the journey towards malaria elimination. These include an increase in the number of countries certified malaria-free by the WHO and also the ones moving towards zero indigenous malaria cases. In multiple Southeast Asian countries including Thailand, Cambodia, Lao, Myanmar and Viet Nam, the total number of malaria cases has reduced by 68% and the total number of deaths by 46% since 2010. However, in the 2019 World Malaria Report, the WHO has highlighted that the progress of elimination is slowing down [2]. Given that *P. vivax* is highly prevalent in regions with relatively low transmission such as Southeast Asia (accounting for approximately 50% of the total number of regional *P. vivax* cases) and Latin America (75%), a better understanding of this often neglected parasite will be a critical step towards more effective approaches to achieve elimination. Our understanding of *P. vivax* compared to *P. falciparum* is limited given the historical major focus of scientists on *P. falciparum*, due to the enormous burden it places on the African continent. Moreover, other challenges including *P. vivax*'s complex life cycle, the absence of continuous culture system, limited usage of radical cure and the large sub-patent repertoire resulted from *P. vivax* infections have led to little progress in *P. vivax*-focussed research and relevant applications.

The immunity elicited in response to malaria infections has been described to play a pivotal role in modulating parasite clearance and protection against clinical symptoms (Section 1.2). Numerous studies have demonstrated that multiple arms of malaria-specific immunity, especially antibody-mediated immunity, can be dampened as a major strategy for *Plasmodium* parasites to avoid recognition and hence prolong their survival in human hosts. Moreover, the serological profile of a population can be reflective of changes in transmission pattern and level of recent and past exposure. Taken together these findings indicate that anti-malarial antibody immune responses can be harnessed for novel surveillance tools based on infected individuals' immune status and for vaccines with greater efficacy. Nevertheless, previous studies have only addressed immune responses against a very limited number of traditional *P. vivax* antigens which have been intensively studied. The lack of appropriate longitudinal studies also forms a major hurdle to determine antibody longevity and immunological memory responses. Additionally, a clear majority of individuals living in low-transmission regions are asymptomatic [488-490]. These populations have been significantly under-addressed in the current studies that focus on only symptomatic individuals. In addition, it has been known the immune responses elicited against *Plasmodium* parasites are under the influence of multiple factors, including intrinsic host, environmental and antigenic factors (Section 1.3). Given that *P. vivax* is genetically more diverse

than *P. falciparum* and the level of diversity varies between geographic regions, the impact of antigenic factors, specifically antigen sequence diversity, on anti-malarial antibody responses is highly relevant in the era where novel approaches in designing surveillance tools and vaccines are urgently required. Therefore, to address these current knowledge gaps, I aimed to provide a deeper understanding and novel insights into the acquisition and development of antibody responses against *P. vivax* in a naturally exposed human population.

The first goal of this thesis was to optimise the bead-based multiplex platform Luminex® (Chapter 3) and subsequently establish antigen-specific total IgG antibody kinetic profiles against 52 *P. vivax* antigens for nine months in a symptomatic cohort in western Thailand with limited level of transmission (Chapter 4). Use of the multiplex platform enabled me to overcome a major limitation of prior studies that focussed on responses against only one or two antigens, whilst still being an appropriate assay for the small volumes of sample collected during field studies. The sampling interval was no more than four weeks during the entire nine-month study period, designed to give antibody kinetics of high resolution and over a long time period. Most prior studies have only followed up antibody responses for one-two months post-infection, or over longer time frames but without intermittent surveillance (meaning the presence of boosting infections could not be ruled out). Besides total IgG, IgG subclasses

1, 2, 3, 4 and IgM were also measured over time against a down-selected panel of antigens. As comparison to the symptomatic cohort, once-a-month measurement of IgG antibody responses was taken in a year-long asymptomatic cohort down-selected from a larger observational study in a nearby region. To further investigate the antigen-specific differences in antibody maintenance, optimisation of a MBC ELISpot assay to measure antigen-specific MBC responses was performed (Chapter 5) and will be used in future studies.

The second goal of this thesis was to determine how sequence diversity of *P. vivax* antigens affected antibody responses and to examine if such an effect differs between symptomatic and asymptomatic individuals (Chapter 6). 49 out of 52 *P. vivax* antigens were found and characterised on the reference strain and 19 *P. vivax* isolate sample sequences from Thailand were filtered and down-selected from a global dataset. Population genetic analysis was performed to quantify sequence diversity which was correlated to multiple antibody response parameters. This enabled us to investigate the association of antigen sequence diversity with the generation of antigen-specific antibody responses against malaria.

7.2 Establishment of *P. vivax*-specific antibody kinetic profiles and MBC ELISpot assay

7.2.1 Summary of findings

From the optimisaiton of Luminex® platform (Chapter 3), establishment of antibody kinetics following a *P. vivax* infection (Chapter 4) and optimisation of antigenic-specific MBC ELISpot assay (Chapter 5), the major findings are outlined below:

1) I successfully established a multiplex Luminex® assay to measure responses to 52 *P. vivax* proteins simultaneously using only 1µl plasma. This assay is highly robust and reproducible and has been adopted by other research groups.
2) I demonstrated that despite some antigen-specific variability, 52 *P. vivax* antigens from various life stages of the parasites shared highly similar antigen-specific antibody kinetic profiles: early peak at 1 to 2-week post-infection followed by a gradual exponential decay. This is the first time antibody responses have been described against such a large panel of *P. vivax* proteins in a longitudinal cohort.

3) In one of the first studies of antibody longevity following asymptomatic infections, I was able to show that IgG antibody responses are more long-lived following asymptomatic compared to symptomatic infections.
4) I demonstrated that nearly all proteins tested induced IgG subclasses 1 or 3 in Thai individuals with limited past exposure following a symptomatic *P. vivax* infection. This differs to that observed in PNG highly exposed adults.
5) I found that antigen-specific IgM responses could be longer lived than previously thought (lasting for at least nine months) following symptomatic infections in a low transmission region.
6) I successfully optimised and established an antigen-specific MBC ELISpot assay, which enabled me to quantify antigen-specific MBC responses in field samples with very limited cell numbers.

7.2.2 Study significance

Due to the unique biology of *P. vivax* parasites and several limitations of our current malaria elimination toolkit, *P. vivax* has been recognised as one of the biggest hurdles towards the 3rd Sustainable Development Goal set by WHO – eliminating malaria by 2030 [491]. These challenges include the presence of undetected asymptomatic reservoirs [44, 109, 423], restricted use of radical cure to clear hypnozoites [52, 53] and insufficient progress towards development of

efficacious vaccines [325, 465]. These scenarios have drawn the attention towards developing novel approaches for therapeutic and surveillance purposes. More recently, multiple studies have demonstrated that antibody responses could be used to reflect on the immune status and past or current exposure of a population [264] and the transmission level of a geographical region [108, 492]. Compared to these past studies, the findings shown in Chapter 4 represent the most thorough antigen-specific antibody kinetic profiles established for *P. vivax* with the highest resolution to-date. More specifically, these results have confirmed that antibody kinetics can be representative of past exposure, even in a region with low malaria transmission, as response to a number of antigens were relatively long-lasting (i.e 3 - 9 months or more) even following symptomatic infections. Furthermore, as our panel of *P. vivax* antigens also includes non-traditional antigenic targets that have not been studied previously (such as tryptophan-rich, hypothetical and unknown antigens), these observations have significantly broadened the scope of current malaria research. The data generated from this project were also used to infer selection of serological biomarkers for improved surveillance [112], demonstrating the significance of this approach in its applications and achieving global impact.

7.3 Population genetic analysis on *P. vivax* antigens and their associations with antibody profiles

7.3.1 Summary of findings

The major findings obtained following population genetic analysis to quantify antigenic sequence diversity and multiple correlation tests to determine its association with antibody responses (Chapter 6) are outlined below:

1) I have successfully defined genetic diversity in 49 *P. vivax* antigens. This reports the first analysis on a large panel of *Plasmodium* antigens at a population level.
2) I conducted the first major screen of how genetic diversity potentially associates with *P. vivax* naturally acquired immunity. I found that genetic diversity in *P. vivax* antigen sequences had little to no associations with IgG responses in the Thai symptomatic individuals.
3) In contrast, I demonstrated in the same symptomatic cohort that high antigen sequence diversity was linked to IgM immunogenicity. This association was slightly stronger than IgG.

4) In the asymptomatic cohort, I showed that the association of genetic diversity with IgG responses was much stronger compared to the symptomatic.
5) I reported host immunity with a balancing trait was associated with greater genetic diversity in an antigen.

7.3.2 Study significance

Investigation of the genetic diversity of antigens in the context of malaria has only come under the spotlight in the past few years, largely due to its implications in vaccine development. Such research has primarily focussed on a limited range of traditional *P. falciparum*-derived antigens [464, 471, 493]. In contrast, *P. vivax* remains relatively under-studied in this area despite being an emerging threat with an increased global burden [2]. In Chapter 6, I describe the process of quantifying genetic diversity of 49 *P. vivax* antigens including novel targets. This represents the largest panel of *P. vivax* antigens completed with corresponding antibody kinetic data. The high level of genetic diversity in these antigens can perhaps explain the non-sterilising nature of *P. vivax*-specific antibody immunity. The results in particular have demonstrated the absolute importance of including antibody data to showcase the immunological relevance of genetic diversity in malaria.

More importantly, the findings reported in Chapter 6 show that the associations of antigen genetic diversity with antibody responses could vary between antibody isotypes (IgG versus IgM) and between cohorts with differing levels of past exposure (symptomatic versus asymptomatic). These observations strongly indicated that such associations could appear less significant for individuals with less mature immunity and/or less past exposure. This is likely due to the fact that they had only been exposed to a limited variety of *P. vivax* antigen alleles and hence failed to efficiently elicit antibody responses against a specific allele upon encounter. Additionally, since IgM represents the antibody isotype that is produced on first encounter in a large amount within a short period of time, it was reasonable that IgM profiles were better associated with genetic diversity compared to IgG as demonstrated in Section 6.2.3. These speculations were further addressed and verified in Section 6.2.4 where genetic diversity showed strong and consistent associations with IgG profiles in the asymptomatic cohort with intensive past exposure. Together, I demonstrated the significance and possible implications of taking past exposure level into consideration when performing similar analyses at a population level.

During my investigation, the large panel of amino acid sequences also contributed significantly to the optimisation of the newly developed 'Vaxpack' by including more functional features. Moreover, this project provides evidence

of the role of human host immunity in identifying targets and in shaping the evolutionary fitness of *P. vivax* parasites. This information is critical for understanding host-pathogen interactions and for developing multivalent or chimeric vaccines that incorporate multiple targets [494]. Additionally, the findings I reported in this Chapter also help identifying antigenic targets that are better representative of the global and local populations for future sero-surveillance tools.

7.4 Future directions

The present study has demonstrated the antigen-specific nature of antibody responses in primarily a Thai symptomatic cohort, and has a number of major advantages over past work including the use of a large panel of *P. vivax* proteins and samples from longitudinal cohorts with intensive follow-up. I have now been able to use my results to determine areas of interest for further study.

7.4.1 Further defining antibody profiles in the asymptomatic Thai cohort

Firstly, we will aim to establish a more complete picture of antibody profiles in western Thailand. Particularly, we would like to further characterise antibody kinetics against our panel of *P. vivax* antigens in the Thai asymptomatic cohort.

In the present study, antigen-specific antibody kinetics in the asymptomatic cohort were only established against 33 antigens that were IgG-immunogenic in the symptomatic cohort (Chapter 4). However, it is possible that antigens that were not IgG-immunogenic in the symptomatic cohort could be IgG-immunogenic in the asymptomatic cohort. Additionally, IgG subclass and IgM kinetic profiles in the asymptomatic cohort were not measured. The results will provide critical insights into the role of humoral responses in modulating clinical symptoms. Furthermore, this knowledge can be potentially applied to identify asymptomatic individuals in *P. vivax*-endemic regions for timely interventions and prevention against further transmission.

7.4.2 Determining the role of antigen-specific MBCs in antibody longevity

A key area for further research will be to use the antigen-specific MBC assay I have established to determine the potential impact or role of MBCs in the antigen-specific longevity profiles. As described in Chapter 5, we hypothesise that atypical and/or impaired *P. vivax*-specific memory B cell populations could be a cause of short-lived antibody responses. This proposal was made based on the evidence reported from multiple prior studies, demonstrating that *P. vivax* infections could reduce the total number of B cells [495], alter the proportion of different B cell subsets [496] and induce long-term MBC and antibody responses

[239, 242, 244]. Besides MBC populations, plasma cells (PCs) and T_{FH} cells have been known to contribute to antibody production and antibody affinity maturation, respectively [174, 233, 497]. Evidence has shown that malaria infections significantly impaired the differentiation and function of T_{FH} cells, leading to less effective antibody responses and parasite clearance [177, 496, 498]. In contrast, the role of PCs remains controversial due to conflicting results on the change in frequency post-infection [237, 249, 441]. Therefore, it would be of interest to explore the association of the kinetic profiles of PC and T_{FH} populations with antibody longevity post-infection. This information can be used to develop approaches for prolonging the longevity of essential immune cells and antibody responses, optimising the process of selecting suitable serological marker and vaccine candidates.

7.4.3 Assessing the association of genetic diversity with quantitative measures of antibody responses and further analyses with populations from higher transmission settings

Another key finding from my thesis was that the genetic diversity of a *P. vivax* antigen in Thailand was statistically associated with measured antibody responses. However, such associations are the result of preliminary investigations using selected antibody parameters and could be due to multiple

direct or indirect factors. Hence, further analysis is required in order to further define *P. vivax*-specific antibody responses, specifically developing a quantitative measure of the acquisition and longevity of immunity would enable a better picture of the association between genetic diversity and immunity to be established. For this purpose, we will continue our work with Dr Michael White at the Institut Pasteur who will be generating a number of population-level parameters for each *P. vivax* antigen to describe the boost and decay of antibody levels. These parameters may include but are not limited to the half-lives of antibodies, short- and long-lived ASCs and the proportion of short- or long-lived ASCs. Analysing the association between genetic diversity and antibody responses using these parameters will be an important step in taking antigen diversity further into its application in diagnostics and vaccines.

To further extend the scope of my investigations described in Chapter 6, it will be of great interest to understand the impact of genetic diversity in *P. vivax* antigens on antibody responses in individuals living in regions with higher malaria transmission to compare with the current dataset. This will provide insights into the role of transmission level on shaping the effectiveness of *P. vivax*-specific immunity.

7.4.4 Examining the association of protein structure with antigen-specific antibody responses

Lastly, we are keen to investigate the association of protein structure with *P. vivax*-specific antibody responses. This concept stems from the studies showing that the structural location of polymorphisms and immunological targets (sites with strong signature of balancing selection) varied between *P. falciparum* antigens [499]. These findings suggest that the protein structure of a malarial antigen could alter the level of exposure of T or B cell epitopes, potentially resulting in differential induction of immune responses. With the use of easily accessible online structure-predicting tools such as I-TASSER [500], we anticipate that the answers to these questions will enable us to gain further knowledge of our *P. vivax* antigens in different transmission settings and therefore assist in identifying antigenic sequences that are most effective in inducing species-specific and robust immune responses.

7.5 Concluding remarks

The aims of this thesis are to outline the process involved to optimise relevant experimental designs, and to describe multiple kinetic patterns and associated factors of *P. vivax*-specific naturally acquired antibody immunity in a region of low transmission settings. This work was driven by the fact that strategies

targeting at *P. vivax* will be of great importance for eliminating the residual malaria transmission, yet research focussing on the acquisition and maintenance of *P. vivax*-specific antibody immunity remains insufficient. Using a large panel of *P. vivax* antigens, I was able to show the detailed antibody kinetic profiles in the infected populations. The complexity of genetic diversity in our antigens and how it contributes to host antibody immunity were also shown. Together, these findings highlight the importance of serology and antigen sequence diversity in maximising global impact of our current tools, which ultimately accelerates the overall progress towards malaria elimination.

References

1. WHO, W.H.O., *World Malaria Report 2018*. 2018.
2. WHO, W.H.O., *World Malaria Report 2019*. 2019.
3. McCarthy, J.S., et al., *Experimentally induced blood-stage Plasmodium vivax infection in healthy volunteers.* The Journal of infectious diseases, 2013. **208**(10): p. 1688-1694.
4. Yazdani, S., et al., *Immune responses to asexual blood-stages of malaria parasites.* Current molecular medicine, 2006. **6**(2): p. 187-203.
5. Derbyshire, E.R., M.M. Mota, and J. Clardy, *The Next Opportunity in Anti-Malaria Drug Discovery: The Liver Stage.* PLOS Pathogens, 2011. **7**(9): p. e1002178.
6. Pham, T.-T., et al., *Release of endothelial activation markers in lungs of patients with malaria-associated acute respiratory distress syndrome.* Malaria journal, 2019. **18**(1): p. 395-395.
7. Dondorp, A.M., et al., *Abnormal blood flow and red blood cell deformability in severe malaria.* Parasitology today, 2000. **16**(6): p. 228-232.
8. Katrak, S., et al., *Clinical consequences of submicroscopic malaria parasitaemia in Uganda.* Malaria Journal, 2018. **17**(1): p. 67.
9. Miller, L.H., et al., *The pathogenic basis of malaria.* Nature, 2002. **415**(6872): p. 673.
10. Chaparro-Narváez, P.E., et al., *Clinical and epidemiological aspects of complicated malaria in Colombia, 2007–2013.* Malaria Journal, 2016. **15**(1): p. 269.
11. Singh, R., et al., *A comparative study of clinical profiles of vivax and falciparum malaria in children at a tertiary care centre in Uttarakhand.* Journal of clinical and diagnostic research: JCDR, 2013. **7**(10): p. 2234.
12. Goyal, J.P. and A.M. Makwana, *Comparison of clinical profile between P. vivax and P. falciparum malaria in children: a tertiary care centre perspective from India.* Malaria research and treatment, 2014. **2014**.
13. Müller, I., et al., *Three different Plasmodium species show similar patterns of clinical tolerance of malaria infection.* Malaria Journal, 2009. **8**(1): p. 158.
14. Sharp, P. and P. Harvey, *Malaria and growth stunting in young children of the highlands of Papua New Guinea.* Papua and New Guinea medical journal, 1980. **23**(3): p. 132-140.
15. Briand, V., et al., *Fetal growth restriction is associated with malaria in pregnancy: a prospective longitudinal study in Benin.* The Journal of infectious diseases, 2016. **214**(3): p. 417-425.
16. Cates, J.E., et al., *Malaria, malnutrition, and birthweight: A meta-analysis using individual participant data.* PLOS Medicine, 2017. **14**(8): p. e1002373.
17. Gallup, J.L. and J.D. Sachs, *The economic burden of malaria.* The American journal of tropical medicine and hygiene, 2001. **64**(1_suppl): p. 85-96.
18. Medica, D.L. and P. Sinnis, *Quantitative dynamics of Plasmodium yoelii sporozoite transmission by infected anopheline mosquitoes.* Infection and immunity, 2005. **73**(7): p. 4363-4369.
19. Mullard, A., *Malaria medicine box expands.* Nature Reviews Drug Discovery, 2018. **17**: p. 693.

20. Imwong, M., et al., *Relapses of Plasmodium vivax infection usually result from activation of heterologous hypnozoites.* The Journal of infectious diseases, 2007. **195**(7): p. 927-933.
21. Cowman, A.F. and B.S. Crabb, *Invasion of Red Blood Cells by Malaria Parasites.* Cell, 2006. **124**(4): p. 755-766.
22. Malleret, B., et al., *Plasmodium vivax: restricted tropism and rapid remodeling of CD71-positive reticulocytes.* Blood, 2015. **125**(8): p. 1314-1324.
23. Srivastava, A., et al., *Host Reticulocytes Provide Metabolic Reservoirs That Can Be Exploited by Malaria Parasites.* PLOS Pathogens, 2015. **11**(6): p. e1004882.
24. Reilly, H.B., et al., *Quantitative dissection of clone-specific growth rates in cultured malaria parasites.* International journal for parasitology, 2007. **37**(14): p. 1599-1607.
25. White, N.J., *Malaria parasite clearance.* Malaria Journal, 2017. **16**(1): p. 88.
26. White, M.T., et al., *Plasmodium vivax and Plasmodium falciparum infection dynamics: re-infections, recrudescences and relapses.* Malaria Journal, 2018. **17**(1): p. 170.
27. Beier, J.C., *Malaria parasite development in mosquitoes.* Annual review of entomology, 1998. **43**(1): p. 519-543.
28. Vaughan, J.A., *Population dynamics of Plasmodium sporogony.* Trends in parasitology, 2007. **23**(2): p. 63-70.
29. Aly, A.S.I., A.M. Vaughan, and S.H.I. Kappe, *Malaria parasite development in the mosquito and infection of the mammalian host.* Annual review of microbiology, 2009. **63**: p. 195-221.
30. Howes, R.E., et al., *Global epidemiology of Plasmodium vivax.* The American journal of tropical medicine and hygiene, 2016. **95**(6_Suppl): p. 15-34.
31. Guerra, C.A., et al., *The international limits and population at risk of Plasmodium vivax transmission in 2009.* PLoS neglected tropical diseases, 2010. **4**(8): p. e774.
32. Battle, K.E., et al., *Mapping the global endemicity and clinical burden of Plasmodium vivax, 2000–17: a spatial and temporal modelling study.* The Lancet, 2019.
33. Kittichai, V., et al., *Substantial population structure of Plasmodium vivax in Thailand facilitates identification of the sources of residual transmission.* PLOS Neglected Tropical Diseases, 2017. **11**(10): p. e0005930.
34. Quah, Y.W., et al., *Molecular epidemiology of residual Plasmodium vivax transmission in a paediatric cohort in Solomon Islands.* Malaria Journal, 2019. **18**(1): p. 106.
35. Mendis, K., et al., *The neglected burden of Plasmodium vivax malaria.* The American journal of tropical medicine and hygiene, 2001. **64**(1_suppl): p. 97-106.
36. Baird, J.K., *Neglect of Plasmodium vivax malaria.* Trends in parasitology, 2007. **23**(11): p. 533-539.
37. Mueller, I., et al., *Key gaps in the knowledge of Plasmodium vivax, a neglected human malaria parasite.* The Lancet infectious diseases, 2009. **9**(9): p. 555-566.
38. Snow, R.W., et al., *Relation between severe malaria morbidity in children and level of Plasmodium falciparum transmission in Africa.* The Lancet, 1997. **349**(9066): p. 1650-1654.
39. WHO, W.H.O., *Severe falciparum malaria.* Transactions of the Royal Society of Tropical Medicine and Hygiene, 2000. **94**: p. 1-90.
40. Price, R.N., et al., *Vivax malaria: neglected and not benign.* The American journal of tropical medicine and hygiene, 2007. **77**(6 Suppl): p. 79-87.

41. Rahimi, B.A., et al., *Severe vivax malaria: a systematic review and meta-analysis of clinical studies since 1900.* Malaria journal, 2014. **13**(1): p. 481.
42. Hulden, L. and L. Hulden, *Activation of the hypnozoite: a part of Plasmodium vivax life cycle and survival.* Malaria journal, 2011. **10**: p. 90-90.
43. Shanks, G.D. and N.J. White, *The activation of vivax malaria hypnozoites by infectious diseases.* The Lancet Infectious Diseases, 2013. **13**(10): p. 900-906.
44. Robinson, L.J., et al., *Strategies for Understanding and Reducing the Plasmodium vivax and Plasmodium ovale Hypnozoite Reservoir in Papua New Guinean Children: A Randomised Placebo-Controlled Trial and Mathematical Model.* PLOS Medicine, 2015. **12**(10): p. e1001891.
45. Chu, C.S. and N.J. White, *Management of relapsing Plasmodium vivax malaria.* Expert review of anti-infective therapy, 2016. **14**(10): p. 885-900.
46. White, N.J., *Why Do Some Primate Malarias Relapse?* Trends in parasitology, 2016. **32**(12): p. 918-920.
47. Bahk, Y.Y., et al., *Epidemiological Characteristics of Re-emerging Vivax Malaria in the Republic of Korea (1993-2017).* The Korean journal of parasitology, 2018. **56**(6): p. 531-543.
48. White, N.J., *Determinants of relapse periodicity in Plasmodium vivax malaria.* Malaria Journal, 2011. **10**(1): p. 297.
49. Ashley, E.A., et al., *Plasmodium vivax Relapse Rates Following Plasmodium falciparum Malaria Reflect Previous Transmission Intensity.* The Journal of Infectious Diseases, 2019. **220**(1): p. 100-104.
50. Rénia, L. and Y.S. Goh, *Malaria Parasites: The Great Escape.* Frontiers in immunology, 2016. **7**: p. 463-463.
51. Roth, A., et al., *A comprehensive model for assessment of liver stage therapies targeting Plasmodium vivax and Plasmodium falciparum.* Nature communications, 2018. **9**(1): p. 1837-1837.
52. Recht, J., E.A. Ashley, and N.J. White, *Use of primaquine and glucose-6-phosphate dehydrogenase deficiency testing: Divergent policies and practices in malaria endemic countries.* PLoS neglected tropical diseases, 2018. **12**(4): p. e0006230-e0006230.
53. Avalos, S., et al., *G6PD deficiency, primaquine treatment, and risk of haemolysis in malaria-infected patients.* Malaria journal, 2018. **17**(1): p. 415-415.
54. Ding, X.C., et al., *Defining the next generation of Plasmodium vivax diagnostic tests for control and elimination: Target product profiles.* PLoS neglected tropical diseases, 2017. **11**(4): p. e0005516-e0005516.
55. Miller, L.H., et al., *The resistance factor to Plasmodium vivax in blacks: the Duffy-blood-group genotype, FyFy.* New England Journal of Medicine, 1976. **295**(6): p. 302-304.
56. Horuk, R., et al., *A receptor for the malarial parasite Plasmodium vivax: the erythrocyte chemokine receptor.* Science, 1993. **261**(5125): p. 1182-1184.
57. Ménard, D., et al., *Plasmodium vivax clinical malaria is commonly observed in Duffy-negative Malagasy people.* Proceedings of the National Academy of Sciences, 2010. **107**(13): p. 5967-5971.

58. Gunalan, K., et al., *Plasmodium vivax infections of Duffy-negative erythrocytes: historically undetected or a recent adaptation?* Trends in parasitology, 2018. **34**(5): p. 420-429.
59. Mendes, C., et al., *Duffy negative antigen is no longer a barrier to Plasmodium vivax–molecular evidences from the African West Coast (Angola and Equatorial Guinea).* PLoS neglected tropical diseases, 2011. **5**(6): p. e1192.
60. Mercereau-Puijalon, O. and D. Ménard, *Plasmodium vivax and the Duffy antigen: A paradigm revisited.* Transfusion Clinique et Biologique, 2010. **17**(3): p. 176-183.
61. Gruszczyk, J., et al., *Cryo-EM structure of an essential Plasmodium vivax invasion complex.* Nature, 2018. **559**(7712): p. 135-139.
62. Prajapati, S.K. and O.P. Singh, *Insights into the invasion biology of Plasmodium vivax.* Frontiers in cellular and infection microbiology, 2013. **3**: p. 8-8.
63. Baro, B., et al., *Plasmodium vivax gametocytes in the bone marrow of an acute malaria patient and changes in the erythroid miRNA profile.* PLoS neglected tropical diseases, 2017. **11**(4): p. e0005365-e0005365.
64. Obaldia, N., et al., *Bone Marrow Is a Major Parasite Reservoir in Plasmodium vivax Infection.* mBio, 2018. **9**(3): p. e00625-18.
65. Carlton, J.M., B.J. Sina, and J.H. Adams, *Why Is Plasmodium vivax a Neglected Tropical Disease?* PLOS Neglected Tropical Diseases, 2011. **5**(6): p. e1160.
66. Lim, C., et al., *Reticulocyte Preference and Stage Development of Plasmodium vivax Isolates.* The Journal of infectious diseases, 2016. **214**(7): p. 1081-1084.
67. Kho, S., et al., *High Risk of Plasmodium vivax Malaria Following Splenectomy in Papua, Indonesia.* Clinical Infectious Diseases, 2018. **68**(1): p. 51-60.
68. Elizalde-Torrent, A., et al., *Sudden spleen rupture in a Plasmodium vivax-infected patient undergoing malaria treatment.* Malaria Journal, 2018. **17**(1): p. 79.
69. Kim, K.M., B.K. Bae, and S.B. Lee, *Spontaneous splenic rupture in Plasmodium vivax malaria.* Annals of surgical treatment and research, 2014. **87**(1): p. 44-46.
70. Siqueira, A.M., et al., *Spleen rupture in a case of untreated Plasmodium vivax infection.* PLoS neglected tropical diseases, 2012. **6**(12).
71. Jiménez, B.C., et al., *Spontaneous splenic rupture due to Plasmodium vivax in a traveler: case report and review.* Journal of travel medicine, 2007. **14**(3): p. 188-191.
72. Ozsoy, M., et al., *Splenic complications in malaria: report of two cases from Turkey.* Journal of medical microbiology, 2004. **53**(12): p. 1255-1258.
73. Bi, Y., et al., *Impact of climate variability on Plasmodium vivax and Plasmodium falciparum malaria in Yunnan Province, China.* Parasites & Vectors, 2013. **6**(1): p. 357.
74. Brooker, S., et al., *Spatial clustering of malaria and associated risk factors during an epidemic in a highland area of western Kenya.* Tropical medicine & international health, 2004. **9**(7): p. 757-766.
75. Bhattacharya, S., et al., *Climate change and malaria in India.* Current science, 2006. **90**(3): p. 369-375.
76. McKenzie, F.E., G.M. Jeffery, and W.E. Collins, *Gametocytemia and fever in human malaria infections.* The Journal of parasitology, 2007. **93**(3): p. 627.

77. Adapa, S.R., et al., *Plasmodium vivax readiness to transmit: implication for malaria eradication.* BMC systems biology, 2019. **13**(1): p. 5-5.
78. Liu, Z., J. Miao, and L. Cui, *Gametocytogenesis in malaria parasite: commitment, development and regulation.* Future microbiology, 2011. **6**(11): p. 1351-1369.
79. Zollner, G.E., et al., *Population dynamics of sporogony for Plasmodium vivax parasites from western Thailand developing within three species of colonized Anopheles mosquitoes.* Malaria journal, 2006. **5**: p. 68-68.
80. Balabaskaran Nina, P., et al., *Dynamics of Plasmodium vivax sporogony in wild Anopheles stephensi in a malaria-endemic region of Western India.* Malaria journal, 2017. **16**(1): p. 284-284.
81. Ghosh, A.K., et al., *Malaria Parasite Invasion of the Mosquito Salivary Gland Requires Interaction between the Plasmodium TRAP and the Anopheles Saglin Proteins.* PLOS Pathogens, 2009. **5**(1): p. e1000265.
82. Bassat, Q., et al., *Key knowledge gaps for Plasmodium vivax control and elimination.* The American journal of tropical medicine and hygiene, 2016. **95**(6_Suppl): p. 62-71.
83. Choi, L., J. Pryce, and P. Garner, *Indoor residual spraying for preventing malaria in communities using insecticide-treated nets.* The Cochrane database of systematic reviews, 2019. **5**(5): p. CD012688-CD012688.
84. Tizifa, T.A., et al., *Prevention Efforts for Malaria.* Current tropical medicine reports, 2018. **5**(1): p. 41-50.
85. Levitz, L., et al., *Effect of individual and community-level bed net usage on malaria prevalence among under-fives in the Democratic Republic of Congo.* Malaria journal, 2018. **17**(1): p. 39-39.
86. Pryce, J., M. Richardson, and C. Lengeler, *Insecticide-treated nets for preventing malaria.* Cochrane Database of Systematic Reviews, 2018(11).
87. Sherrard-Smith, E., et al., *Systematic review of indoor residual spray efficacy and effectiveness against Plasmodium falciparum in Africa.* Nature communications, 2018. **9**(1): p. 4982-4982.
88. N'Guessan, R., et al., *Reduced efficacy of insecticide-treated nets and indoor residual spraying for malaria control in pyrethroid resistance area, Benin.* Emerging infectious diseases, 2007. **13**(2): p. 199-206.
89. Alout, H., et al., *Consequences of insecticide resistance on malaria transmission.* PLoS pathogens, 2017. **13**(9): p. e1006499-e1006499.
90. Kleinschmidt, I., et al., *Implications of insecticide resistance for malaria vector control with long-lasting insecticidal nets: a WHO-coordinated, prospective, international, observational cohort study.* The Lancet infectious diseases, 2018. **18**(6): p. 640-649.
91. Battle, K.E., et al., *The global public health significance of Plasmodium vivax*, in *Advances in parasitology*. 2012, Elsevier. p. 1-111.
92. St Laurent, B., et al., *Host attraction and biting behaviour of Anopheles mosquitoes in South Halmahera, Indonesia.* Malaria journal, 2017. **16**(1): p. 310-310.
93. Sinka, M.E., et al., *The dominant Anopheles vectors of human malaria in the Asia-Pacific region: occurrence data, distribution maps and bionomic précis.* Parasites & Vectors, 2011. **4**(1): p. 89.

94. Mueller, I., A.R. Shakri, and C.E. Chitnis, *Development of vaccines for Plasmodium vivax malaria.* Vaccine, 2015. **33**(52): p. 7489-7495.
95. Bennett, J.W., et al., *Phase 1/2a Trial of Plasmodium vivax Malaria Vaccine Candidate VMP001/AS01B in Malaria-Naive Adults: Safety, Immunogenicity, and Efficacy.* PLoS neglected tropical diseases, 2016. **10**(2): p. e0004423-e0004423.
96. Wu, Y., et al., *Phase 1 trial of malaria transmission blocking vaccine candidates Pfs25 and Pvs25 formulated with montanide ISA 51.* PloS one, 2008. **3**(7): p. e2636.
97. Malkin, E.M., et al., *Phase 1 vaccine trial of Pvs25H: a transmission blocking vaccine for Plasmodium vivax malaria.* Vaccine, 2005. **23**(24): p. 3131-3138.
98. Casares, S., T.-D. Brumeanu, and T.L. Richie, *The RTS,S malaria vaccine.* Vaccine, 2010. **28**(31): p. 4880-4894.
99. Alonso, P.L., et al., *Duration of protection with RTS,S/AS02A malaria vaccine in prevention of Plasmodium falciparum disease in Mozambican children: single-blind extended follow-up of a randomised controlled trial.* The Lancet, 2005. **366**(9502): p. 2012-2018.
100. RTS, S., *Efficacy and safety of RTS, S/AS01 malaria vaccine with or without a booster dose in infants and children in Africa: final results of a phase 3, individually randomised, controlled trial.* The Lancet, 2015. **386**(9988): p. 31-45.
101. van den Berg, M., et al., *RTS,S malaria vaccine pilot studies: addressing the human realities in large-scale clinical trials.* Trials, 2019. **20**(1): p. 316.
102. Baird, J.K., et al., *Diagnosis and treatment of Plasmodium vivax malaria.* The American journal of tropical medicine and hygiene, 2016. **95**(6_Suppl): p. 35-51.
103. Choi, L., et al., *Rapid diagnostic tests for Plasmodium vivax malaria in endemic countries.* Cochrane Database of Systematic Reviews, 2019(2).
104. Elliott, S.R., et al., *Research priorities for the development and implementation of serological tools for malaria surveillance.* F1000prime reports, 2014. **6**: p. 100-100.
105. Folegatti, P.M., et al., *A systematic review on malaria sero-epidemiology studies in the Brazilian Amazon: insights into immunological markers for exposure and protection.* Malaria Journal, 2017. **16**(1): p. 107.
106. Greenhouse, B., et al., *Priority use cases for antibody-detecting assays of recent malaria exposure as tools to achieve and sustain malaria elimination.* Gates open research, 2019. **3**: p. 131-131.
107. Kerkhof, K., et al., *Geographical patterns of malaria transmission based on serological markers for falciparum and vivax malaria in Ratanakiri, Cambodia.* Malaria Journal, 2016. **15**(1): p. 510.
108. Longley, R.J., et al., *Naturally acquired antibody responses to more than 300 Plasmodium vivax proteins in three geographic regions.* PLOS Neglected Tropical Diseases, 2017. **11**(9): p. e0005888.
109. Baum, E., et al., *Common asymptomatic and submicroscopic malaria infections in Western Thailand revealed in longitudinal molecular and serological studies: a challenge to malaria elimination.* Malaria journal, 2016. **15**(1): p. 333.
110. Niang, M., et al., *Unexpected high circulation of Plasmodium vivax in asymptomatic children from Kédougou, southeastern Senegal.* Malaria journal, 2017. **16**(1): p. 497-497.

111. Pereira, V.A., et al., *Evaluating seroprevalence to circumsporozoite protein to estimate exposure to three species of Plasmodium in the Brazilian Amazon.* Infectious Diseases of Poverty, 2018. **7**(1): p. 46.
112. Longley, R.J., et al., *Development and validation of serological markers for detecting recent exposure to Plasmodium vivax infection.* bioRxiv, 2018: p. 481168.
113. Cutts, J.C., et al., *Immunological markers of Plasmodium vivax exposure and immunity: a systematic review and meta-analysis.* BMC medicine, 2014. **12**: p. 150-150.
114. Slater, A.F., *Chloroquine: mechanism of drug action and resistance in Plasmodium falciparum.* Pharmacology & therapeutics, 1993. **57**(2-3): p. 203-235.
115. Douglas, N.M., et al., *Artemisinin combination therapy for vivax malaria.* The Lancet. Infectious diseases, 2010. **10**(6): p. 405-416.
116. Wellems, T.E. and C.V. Plowe, *Chloroquine-Resistant Malaria.* The Journal of Infectious Diseases, 2001. **184**(6): p. 770-776.
117. John, G.K., et al., *Primaquine radical cure of Plasmodium vivax: a critical review of the literature.* Malaria Journal, 2012. **11**(1): p. 280.
118. Nkhoma, E.T., et al., *The global prevalence of glucose-6-phosphate dehydrogenase deficiency: a systematic review and meta-analysis.* Blood Cells, Molecules, and Diseases, 2009. **42**(3): p. 267-278.
119. Baird, J.K., *Point-of-care G6PD diagnostics for Plasmodium vivax malaria is a clinical and public health urgency.* BMC medicine, 2015. **13**: p. 296-296.
120. Walsh, D.S., et al., *Randomized trial of 3-dose regimens of tafenoquine (WR238605) versus low-dose primaquine for preventing Plasmodium vivax malaria relapse.* Clinical infectious diseases, 2004. **39**(8): p. 1095-1103.
121. Nasveld, P. and S. Kitchener, *Treatment of acute vivax malaria with tafenoquine.* Transactions of the Royal Society of Tropical Medicine and Hygiene, 2005. **99**(1): p. 2-5.
122. Lacerda, M.V., et al., *Single-dose tafenoquine to prevent relapse of Plasmodium vivax malaria.* New England Journal of Medicine, 2019. **380**(3): p. 215-228.
123. White, M.T., et al., *Mathematical modelling of the impact of expanding levels of malaria control interventions on Plasmodium vivax.* Nature Communications, 2018. **9**(1): p. 3300.
124. Chu, C.S. and D.O. Freedman, *Tafenoquine and G6PD: a primer for clinicians.* Journal of travel medicine, 2019. **26**(4): p. taz023.
125. Eisele, T.P., *Mass drug administration can be a valuable addition to the malaria elimination toolbox.* Malaria Journal, 2019. **18**(1): p. 281.
126. Sutanto, I., et al., *Negligible Impact of Mass Screening and Treatment on Mesoendemic Malaria Transmission at West Timor in Eastern Indonesia: A Cluster-Randomized Trial.* Clinical infectious diseases : an official publication of the Infectious Diseases Society of America, 2018. **67**(9): p. 1364-1372.
127. Aidoo, E.K., et al., *Reactive case detection of Plasmodium falciparum in western Kenya highlands: effective in identifying additional cases, yet limited effect on transmission.* Malaria Journal, 2018. **17**(1): p. 111.

128. Martin, T.C.S. and J.M. Vinetz, *Asymptomatic Plasmodium vivax parasitaemia in the low-transmission setting: the role for a population-based transmission-blocking vaccine for malaria elimination.* Malaria journal, 2018. **17**(1): p. 89-89.
129. Aitken, E.H., A. Alemu, and S.J. Rogerson, *Neutrophils and Malaria.* Frontiers in immunology, 2018. **9**.
130. Prame Kumar, K., A.J. Nicholls, and C.H.Y. Wong, *Partners in crime: neutrophils and monocytes/macrophages in inflammation and disease.* Cell and Tissue Research, 2018. **371**(3): p. 551-565.
131. Joos, C., et al., *Clinical Protection from Falciparum Malaria Correlates with Neutrophil Respiratory Bursts Induced by Merozoites Opsonized with Human Serum Antibodies.* PLOS ONE, 2010. **5**(3): p. e9871.
132. Leoratti, F.M.d.S., et al., *Neutrophil Paralysis in Plasmodium vivax Malaria.* PLOS Neglected Tropical Diseases, 2012. **6**(6): p. e1710.
133. Bhattacharya, S.K., et al., *Vivax malaria and bacteraemia: a prospective study in Kolkata, India.* Malaria Journal, 2013. **12**(1): p. 176.
134. Tan, L.K.K., et al., *Acute lung injury and other serious complications of Plasmodium vivax malaria.* The Lancet Infectious Diseases, 2008. **8**(7): p. 449-454.
135. Bansal, G.P., C.S. Weinstein, and N. Kumar, *Insight into phagocytosis of mature sexual (gametocyte) stages of Plasmodium falciparum using a human monocyte cell line.* Acta tropica, 2016. **157**: p. 96-101.
136. Chua, C.L.L., et al., *Monocytes and macrophages in malaria: protection or pathology?* Trends in parasitology, 2013. **29**(1): p. 26-34.
137. Ortega-Pajares, A. and S.J. Rogerson, *The Rough Guide to Monocytes in Malaria Infection.* Frontiers in immunology, 2018. **9**: p. 2888-2888.
138. Kalantari, P., *The Emerging Role of Pattern Recognition Receptors in the Pathogenesis of Malaria.* Vaccines, 2018. **6**(1): p. 13.
139. Antonelli, L.R., et al., *The CD14+ CD16+ inflammatory monocyte subset displays increased mitochondrial activity and effector function during acute Plasmodium vivax malaria.* PLoS pathogens, 2014. **10**(9): p. e1004393.
140. Angulo, I. and M. Fresno, *Cytokines in the Pathogenesis of and Protection against Malaria.* Clinical and Diagnostic Laboratory Immunology, 2002. **9**(6): p. 1145.
141. Arango Duque, G. and A. Descoteaux, *Macrophage cytokines: involvement in immunity and infectious diseases.* Frontiers in immunology, 2014. **5**: p. 491-491.
142. Collin, M. and V. Bigley, *Human dendritic cell subsets: an update.* Immunology, 2018. **154**(1): p. 3-20.
143. Yap, X.Z., et al., *Dendritic Cell Responses and Function in Malaria.* Frontiers in Immunology, 2019. **10**: p. 357.
144. Jangpatarapongsa, K., et al., *Plasmodium vivax parasites alter the balance of myeloid and plasmacytoid dendritic cells and the induction of regulatory T cells.* European journal of immunology, 2008. **38**(10): p. 2697-2705.

145. Gonçalves, R.M., et al., *CD4+ CD25+ Foxp3+ regulatory T cells, dendritic cells, and circulating cytokines in uncomplicated malaria: do different parasite species elicit similar host responses?* Infection and immunity, 2010. **78**(11): p. 4763-4772.
146. Pinzon-Charry, A., et al., *Apoptosis and dysfunction of blood dendritic cells in patients with falciparum and vivax malaria.* The Journal of Experimental Medicine, 2013. **210**(8): p. 1635.
147. Amorim, K.N., et al., *Dendritic cells and their multiple roles during malaria infection.* Journal of immunology research, 2016. **2016**.
148. Cooper, M.A., T.A. Fehniger, and M.A. Caligiuri, *The biology of human natural killer-cell subsets.* Trends in immunology, 2001. **22**(11): p. 633-640.
149. Dickinson, A., et al., *Graft-versus-Leukemia Effect Following Hematopoietic Stem Cell Transplantation for Leukemia.* Frontiers in Immunology, 2017. **8**.
150. Kurioka, A., et al., *CD161 Defines a Functionally Distinct Subset of Pro-Inflammatory Natural Killer Cells.* Frontiers in immunology, 2018. **9**: p. 486-486.
151. Wolf, A.-S., S. Sherratt, and E.M. Riley, *NK Cells: Uncertain Allies against Malaria.* Frontiers in immunology, 2017. **8**: p. 212-212.
152. Park, J.Y., et al., *IL-15-induced IL-10 increases the cytolytic activity of human natural killer cells.* Molecules and cells, 2011. **32**(3): p. 265.
153. Lee, A.J. and A.A. Ashkar, *The dual nature of type I and type II interferons.* Frontiers in immunology, 2018. **9**.
154. D'Ombrain, M.C., et al., *Association of early interferon-γ production with immunity to clinical malaria: a longitudinal study among Papua New Guinean children.* Clinical Infectious Diseases, 2008. **47**(11): p. 1380-1387.
155. Burrack, K.S., G.T. Hart, and S.E. Hamilton, *Contributions of natural killer cells to the immune response against Plasmodium.* Malaria journal, 2019. **18**(1): p. 321-321.
156. Ribeiro-Dias, F. and C.E. Tosta, *Dynamics and kinetics of natural killer cell cytotoxicity in human malaria as evaluated by a novel stepwise cytotoxicity assay.* Revista da Sociedade Brasileira de Medicina Tropical, 2006. **39**(4): p. 357-364.
157. Chaves, Y.O., et al., *Immune response pattern in recurrent Plasmodium vivax malaria.* Malaria Journal, 2016. **15**(1): p. 445.
158. Farber, D.L., et al., *Immunological memory: lessons from the past and a look to the future.* Nature Reviews Immunology, 2016. **16**(2): p. 124-128.
159. Broere, F. and W. van Eden, *T cell subsets and T cell-mediated immunity*, in *Nijkamp and Parnham's Principles of Immunopharmacology*. 2019, Springer. p. 23-35.
160. Seder, R.A., et al., *Protection Against Malaria by Intravenous Immunization with a Nonreplicating Sporozoite Vaccine.* Science, 2013. **341**(6152): p. 1359.
161. Kaech, S.M., E.J. Wherry, and R. Ahmed, *Vaccines: effector and memory T-cell differentiation: implications for vaccine development.* Nature Reviews Immunology, 2002. **2**(4): p. 251.
162. Nlinwe, O.N., et al., *T-cell responses against Malaria: Effect of parasite antigen diversity and relevance for vaccine development.* Vaccine, 2018. **36**(17): p. 2237-2242.
163. John, C.C., et al., *Gamma Interferon Responses to Plasmodium falciparum Liver-Stage Antigen 1 and Thrombospondin-Related Adhesive Protein*

and Their Relationship to Age, Transmission Intensity, and Protection against Malaria. Infection and Immunity, 2004. **72**(9): p. 5135.

164. Bucci, K., et al., *Influence of age and HLA type on interferon-gamma (IFN-γ) responses to a naturally occurring polymorphic epitope of Plasmodium falciparum liver stage antigen-1 (LSA-1).* Clinical & Experimental Immunology, 2000. **122**(1): p. 94-100.
165. Chelimo, K., et al., *Interferon-gamma responses to Plasmodium falciparum liver-stage antigen-1 and merozoite-surface protein-1 increase with age in children in a malaria holoendemic area of western Kenya.* Malaria Journal, 2003. **2**(1): p. 37.
166. Junqueira, C., et al., *Cytotoxic CD8(+) T cells recognize and kill Plasmodium vivax-infected reticulocytes.* Nature medicine, 2018. **24**(9): p. 1330-1336.
167. Muxel, S.M., et al., *The Spleen CD4+ T Cell Response to Blood-Stage Plasmodium chabaudi Malaria Develops in Two Phases Characterized by Different Properties.* PLOS ONE, 2011. **6**(7): p. e22434.
168. Xu, H., et al., *The mechanism and significance of deletion of parasite-specific CD4(+) T cells in malaria infection.* The Journal of experimental medicine, 2002. **195**(7): p. 881-892.
169. Boyle, M.J., et al., *The Development of Plasmodium falciparum-Specific IL10 CD4 T Cells and Protection from Malaria in Children in an Area of High Malaria Transmission.* Frontiers in immunology, 2017. **8**: p. 1329-1329.
170. Ourives, S.S., et al., *Analysis of the lymphocyte cell population during malaria caused by Plasmodium vivax and its correlation with parasitaemia and thrombocytopaenia.* Malaria Journal, 2018. **17**(1): p. 303.
171. Jangpatarapongsa, K., et al., *Immunity to malaria in Plasmodium vivax infection: a study in central China.* PloS one, 2012. **7**(9): p. e45971-e45971.
172. Hojo-Souza, N.S., et al., *CD4+ T cells apoptosis in Plasmodium vivax infection is mediated by activation of both intrinsic and extrinsic pathways.* Malaria journal, 2015. **14**: p. 5-5.
173. Borges, Q.I., C.J.F. Fontes, and A.S. Damazo, *Analysis of lymphocytes in patients with Plasmodium vivax malaria and its relation to the annexin-A1 and IL-10.* Malaria journal, 2013. **12**: p. 455-455.
174. Ly, A. and D.S. Hansen, *Development of B Cell Memory in Malaria.* Frontiers in immunology, 2019. **10**: p. 559-559.
175. Hansen, D.S., et al., *Emerging concepts in T follicular helper cell responses to malaria.* International Journal for Parasitology, 2017. **47**(2): p. 105-110.
176. Lee, S.K., et al., *B cell priming for extrafollicular antibody responses requires Bcl-6 expression by T cells.* The Journal of experimental medicine, 2011. **208**(7): p. 1377-1388.
177. Obeng-Adjei, N., et al., *Circulating Th1-Cell-type Tfh Cells that Exhibit Impaired B Cell Help Are Preferentially Activated during Acute Malaria in Children.* Cell Reports, 2015. **13**(2): p. 425-439.
178. Yap, X.Z., L.S.P. Hustin, and R.W. Sauerwein, *T(H)1-Polarized T(FH) Cells Delay Naturally-Acquired Immunity to Malaria.* Frontiers in immunology, 2019. **10**: p. 1096-1096.
179. Lawand, M., J. Déchanet-Merville, and M.-C. Dieu-Nosjean, *Key Features of Gamma-Delta T-Cell Subsets in Human Diseases and Their Immunotherapeutic Implications.* Frontiers in immunology, 2017. **8**: p. 761-761.

180. Balato, A., D. Unutmaz, and A.A. Gaspari, *Natural Killer T Cells: An Unconventional T-Cell Subset with Diverse Effector and Regulatory Functions.* Journal of Investigative Dermatology, 2009. **129**(7): p. 1628-1642.
181. Fergusson, J.R., V.M. Fleming, and P. Klenerman, *CD161-expressing human T cells.* Frontiers in immunology, 2011. **2**: p. 36-36.
182. Slauenwhite, D. and B. Johnston, *Regulation of NKT Cell Localization in Homeostasis and Infection.* Frontiers in immunology, 2015. **6**: p. 255-255.
183. Zhao, Y., C. Niu, and J. Cui, *Gamma-delta (γδ) T cells: friend or foe in cancer development?* Journal of Translational Medicine, 2018. **16**(1): p. 3.
184. Arora, G., et al., *NK cells inhibit Plasmodium falciparum growth in red blood cells via antibody-dependent cellular cytotoxicity.* eLife, 2018. **7**: p. e36806.
185. Mise, N., et al., *Antibody-dependent cellular cytotoxicity toward neuroblastoma enhanced by activated invariant natural killer T cells.* Cancer science, 2016. **107**(3): p. 233-241.
186. Dantzler, K.W. and P. Jagannathan, *γδ T Cells in Antimalarial Immunity: New Insights Into Their Diverse Functions in Protection and Tolerance.* Frontiers in immunology, 2018. **9**: p. 2445-2445.
187. Wu, L. and L. Van Kaer, *Natural killer T cells in health and disease.* Frontiers in bioscience (Scholar edition), 2011. **3**: p. 236-251.
188. Ribot, J.C., et al., *γδ-T cells promote IFN-γ-dependent Plasmodium pathogenesis upon liver-stage infection.* Proceedings of the National Academy of Sciences of the United States of America, 2019. **116**(20): p. 9979-9988.
189. Perera, M.K., et al., *Transient increase in circulating gamma/delta T cells during Plasmodium vivax malarial paroxysms.* The Journal of experimental medicine, 1994. **179**(1): p. 311-315.
190. Deroost, K. and J. Langhorne, *Gamma/delta T cells and their role in protection against malaria.* Frontiers in immunology, 2018. **9**.
191. Cohen, S., I. McGregor, and S. Carrington, *Gamma-globulin and acquired immunity to human malaria.* Nature, 1961. **192**(4804): p. 733-737.
192. Karrer, U., et al., *Immunodeficiency of alymphoplasia mice (aly/aly) in vivo: structural defect of secondary lymphoid organs and functional B cell defect.* European journal of immunology, 2000. **30**(10): p. 2799-2807.
193. Wang, L.D., et al., *Selection of B lymphocytes in the periphery is determined by the functional capacity of the B cell antigen receptor.* Proceedings of the National Academy of Sciences of the United States of America, 2004. **101**(4): p. 1027.
194. Srinivasan, L., et al., *PI3 kinase signals BCR-dependent mature B cell survival.* Cell, 2009. **139**(3): p. 573-586.
195. Okada, T., et al., *Antigen-Engaged B Cells Undergo Chemotaxis toward the T Zone and Form Motile Conjugates with Helper T Cells.* PLOS Biology, 2005. **3**(6): p. e150.
196. Nikbakht, N., S. Shen, and T. Manser, *Cutting edge: macrophages are required for localization of antigen-activated B cells to the follicular perimeter and the subsequent germinal center response.* The Journal of Immunology, 2013. **190**(10): p. 4923-4927.
197. Keitany, G.J., et al., *Blood Stage Malaria Disrupts Humoral Immunity to the Pre-erythrocytic Stage Circumsporozoite Protein.* Cell Reports, 2016. **17**(12): p. 3193-3205.

198. Takemori, T., et al., *Generation of memory B cells inside and outside germinal centers.* European journal of immunology, 2014. **44**(5): p. 1258-1264.
199. Coffey, F., B. Alabyev, and T. Manser, *Initial clonal expansion of germinal center B cells takes place at the perimeter of follicles.* Immunity, 2009. **30**(4): p. 599-609.
200. Berek, C., A. Berger, and M. Apel, *Maturation of the immune response in germinal centers.* Cell, 1991. **67**(6): p. 1121-1129.
201. Jacob, J., et al., *Intraclonal generation of antibody mutants in germinal centres.* Nature, 1991. **354**(6352): p. 389-392.
202. Lindhout, E., et al., *Direct evidence that human follicular dendritic cells (FDC) rescue germinal centre B cells from death by apoptosis.* Clinical & Experimental Immunology, 1993. **91**(2): p. 330-336.
203. Wang, X., et al., *Follicular dendritic cells help establish follicle identity and promote B cell retention in germinal centers.* The Journal of experimental medicine, 2011. **208**(12): p. 2497-2510.
204. Victora, G.D., et al., *Germinal center dynamics revealed by multiphoton microscopy with a photoactivatable fluorescent reporter.* Cell, 2010. **143**(4): p. 592-605.
205. Shulman, Z., et al., *Dynamic signaling by T follicular helper cells during germinal center B cell selection.* Science, 2014. **345**(6200): p. 1058-1062.
206. Han, S., et al., *Cellular interaction in germinal centers. Roles of CD40 ligand and B7-2 in established germinal centers.* J Immunol, 1995. **155**(2): p. 556-67.
207. Zotos, D., et al., *IL-21 regulates germinal center B cell differentiation and proliferation through a B cell-intrinsic mechanism.* The Journal of experimental medicine, 2010. **207**(2): p. 365-378.
208. Klein, U., K. Rajewsky, and R. Küppers, *Human immunoglobulin (Ig)M+IgD+ peripheral blood B cells expressing the CD27 cell surface antigen carry somatically mutated variable region genes: CD27 as a general marker for somatically mutated (memory) B cells.* The Journal of experimental medicine, 1998. **188**(9): p. 1679-1689.
209. Elgueta, R., et al., *Molecular mechanism and function of CD40/CD40L engagement in the immune system.* Immunological reviews, 2009. **229**(1): p. 152-172.
210. Irani, V., et al., *Molecular properties of human IgG subclasses and their implications for designing therapeutic monoclonal antibodies against infectious diseases.* Molecular Immunology, 2015. **67**(2, Part A): p. 171-182.
211. McCaffery, J.N., et al., *A multi-stage Plasmodium vivax malaria vaccine candidate able to induce long-lived antibody responses against blood stage parasites and robust transmission-blocking activity.* Frontiers in cellular and infection microbiology, 2019. **9**.
212. Boyle, M.J., et al., *IgM in human immunity to Plasmodium falciparum malaria.* Science Advances, 2019. **5**(9): p. eaax4489.
213. He, W.-Q., et al., *Antibodies to Plasmodium vivax reticulocyte binding protein 2b are associated with protection against P. vivax malaria in populations living in low malaria transmission regions of Brazil and Thailand.* PLOS Neglected Tropical Diseases, 2019. **13**(8): p. e0007596.

214. Bouharoun-Tayoun, H., et al., *Mechanisms underlying the monocyte-mediated antibody-dependent killing of Plasmodium falciparum asexual blood stages.* The Journal of experimental medicine, 1995. **182**(2): p. 409-418.
215. Ismail, H.A., et al., *Subclass responses and their half-lives for antibodies against EBA175 and PfRh2 in naturally acquired immunity against Plasmodium falciparum malaria.* Malaria journal, 2014. **13**(1): p. 425.
216. Anchang-Kimbi, J.K., et al., *IgG isotypic antibodies to crude Plasmodium falciparum blood-stage antigen associated with placental malaria infection in parturient Cameroonian women.* African health sciences, 2016. **16**(4): p. 1007-1017.
217. Dobano, C., et al., *Differential patterns of IgG subclass responses to Plasmodium falciparum antigens in relation to malaria protection and RTS, S vaccination.* Frontiers in immunology, 2019. **10**: p. 439.
218. Versiani, F.G., et al., *High levels of IgG3 anti ICB2-5 in Plasmodium vivax-infected individuals who did not develop symptoms.* Malaria Journal, 2013. **12**(1): p. 294.
219. França, C.T., et al., *Plasmodium vivax reticulocyte binding proteins are key targets of naturally acquired immunity in young Papua New Guinean children.* PLoS neglected tropical diseases, 2016. **10**(9): p. e0005014.
220. França, C.T., et al., *Identification of highly-protective combinations of Plasmodium vivax recombinant proteins for vaccine development.* Elife, 2017. **6**: p. e28673.
221. Hill, D.L., et al., *Opsonising Antibodies to P. falciparum Merozoites Associated with Immunity to Clinical Malaria.* PLOS ONE, 2013. **8**(9): p. e74627.
222. Osier, F.H.A., et al., *Opsonic phagocytosis of Plasmodium falciparummerozoites: mechanism in human immunity and a correlate of protection against malaria.* BMC Medicine, 2014. **12**(1): p. 108.
223. Hill, D.L., et al., *Merozoite Antigens of Plasmodium falciparum Elicit Strain-Transcending Opsonizing Immunity.* Infection and Immunity, 2016. **84**(8): p. 2175.
224. Weaver, R., et al., *The association between naturally acquired IgG subclass specific antibodies to the PfRH5 invasion complex and protection from Plasmodium falciparum malaria.* Scientific reports, 2016. **6**: p. 33094-33094.
225. Kana, I.H., et al., *Cytophilic Antibodies Against Key Plasmodium falciparum Blood Stage Antigens Contribute to Protection Against Clinical Malaria in a High Transmission Region of Eastern India.* The Journal of Infectious Diseases, 2018. **218**(6): p. 956-965.
226. Boyle, M.J., et al., *Human antibodies fix complement to inhibit Plasmodium falciparum invasion of erythrocytes and are associated with protection against malaria.* Immunity, 2015. **42**(3): p. 580-590.
227. Reiling, L., et al., *Targets of complement-fixing antibodies in protective immunity against malaria in children.* Nature communications, 2019. **10**(1): p. 610-610.
228. Cole-Tobian, J.L., et al., *Strain-specific duffy binding protein antibodies correlate with protection against infection with homologous compared to heterologous plasmodium vivax strains in Papua New Guinean children.* Infection and immunity, 2009. **77**(9): p. 4009-4017.

229. Matos, A.d.S., et al., *Antibody Responses Against Plasmodium vivax TRAP Recombinant and Synthetic Antigens in Naturally Exposed Individuals From the Brazilian Amazon.* Frontiers in Immunology, 2019. **10**(2230).
230. He, W.-Q., et al., *Antibody responses to Plasmodium vivax Duffy binding and Erythrocyte binding proteins predict risk of infection and are associated with protection from clinical Malaria.* PLoS neglected tropical diseases, 2019. **13**(2): p. e0006987.
231. Gupta, E.D., et al., *Naturally Acquired Human Antibodies Against Reticulocyte-Binding Domains of Plasmodium vivax Proteins, PvRBP2c and PvRBP1a, Exhibit Binding-Inhibitory Activity.* The Journal of Infectious Diseases, 2017. **215**(10): p. 1558-1568.
232. Ceravolo, I.P., et al., *Naturally acquired inhibitory antibodies to Plasmodium vivax Duffy binding protein are short-lived and allele-specific following a single malaria infection.* Clinical & Experimental Immunology, 2009. **156**(3): p. 502-510.
233. Khodadadi, L., et al., *The Maintenance of Memory Plasma Cells.* Frontiers in Immunology, 2019. **10**(721).
234. Roth, K., et al., *Tracking plasma cell differentiation and survival.* Cytometry Part A, 2014. **85**(1): p. 15-24.
235. Kinyanjui, S.M., et al., *IgG antibody responses to Plasmodium falciparum merozoite antigens in Kenyan children have a short half-life.* Malaria Journal, 2007. **6**(1): p. 82.
236. Akpogheneta, O.J., et al., *Duration of naturally acquired antibody responses to blood-stage Plasmodium falciparum is age dependent and antigen specific.* Infection and immunity, 2008. **76**(4): p. 1748-1755.
237. Sullivan, R.T., et al., *B cell sub-types following acute malaria and associations with clinical immunity.* Malaria Journal, 2016. **15**(1): p. 139.
238. White, M.T., et al., *Dynamics of the Antibody Response to Plasmodium falciparum Infection in African Children.* The Journal of Infectious Diseases, 2014. **210**(7): p. 1115-1122.
239. Wipasa, J., et al., *Long-Lived Antibody and B Cell Memory Responses to the Human Malaria Parasites, Plasmodium falciparum and Plasmodium vivax.* PLOS Pathogens, 2010. **6**(2): p. e1000770.
240. Wang, Q., et al., *Naturally Acquired Antibody Responses to Plasmodium vivax and Plasmodium falciparum Merozoite Surface Protein 1 (MSP1) C-Terminal 19 kDa Domains in an Area of Unstable Malaria Transmission in Southeast Asia.* PLOS ONE, 2016. **11**(3): p. e0151900.
241. Kano, F.S., et al., *The Presence, Persistence and Functional Properties of Plasmodium vivax Duffy Binding Protein II Antibodies Are Influenced by HLA Class II Allelic Variants.* PLoS neglected tropical diseases, 2016. **10**(12): p. e0005177-e0005177.
242. Min, H.M.K., et al., *Immunogenicity of the Plasmodium vivax merozoite surface protein 1 paralog in the induction of naturally acquired antibody and memory B cell responses.* Malaria journal, 2017. **16**(1): p. 354-354.
243. Changrob, S., et al., *Persistence of long-lived memory B cells specific to Duffy binding protein in individuals exposed to Plasmodium vivax.* Scientific reports, 2018. **8**(1): p. 8347.

244. Kochayoo, P., et al., *The acquisition of long-lived memory B cell responses to merozoite surface protein-8 in individuals with Plasmodium vivax infection.* Malaria Journal, 2019. **18**(1): p. 188.
245. Dorfman, J.R., et al., *B cell memory to 3 Plasmodium falciparum blood-stage antigens in a malaria-endemic area.* Journal of infectious diseases, 2005. **191**(10): p. 1623-1630.
246. Weiss, G.E., et al., *The Plasmodium falciparum-Specific Human Memory B Cell Compartment Expands Gradually with Repeated Malaria Infections.* PLOS Pathogens, 2010. **6**(5): p. e1000912.
247. Weiss, G.E., et al., *A positive correlation between atypical memory B cells and Plasmodium falciparum transmission intensity in cross-sectional studies in Peru and Mali.* PloS one, 2011. **6**(1): p. e15983-e15983.
248. Portugal, S., et al., *Malaria-associated atypical memory B cells exhibit markedly reduced B cell receptor signaling and effector function.* eLife, 2015. **4**: p. e07218.
249. Lugaajju, A., et al., *Development of Plasmodium falciparum specific naïve, atypical, memory and plasma B cells during infancy and in adults in an endemic area.* Malaria journal, 2017. **16**(1): p. 37-37.
250. Ubillos, I., et al., *Chronic exposure to malaria is associated with inhibitory and activation markers on atypical memory B cells and marginal zone-like B cells.* Frontiers in immunology, 2017. **8**: p. 966.
251. Pérez-Mazliah, D., et al., *Plasmodium-specific atypical memory B cells are short-lived activated B cells.* eLife, 2018. **7**: p. e39800.
252. Muellenbeck, M.F., et al., *Atypical and classical memory B cells produce Plasmodium falciparum neutralizing antibodies.* The Journal of experimental medicine, 2013. **210**(2): p. 389-399.
253. Krishnamurty, A.T., et al., *Somatically Hypermutated Plasmodium-Specific IgM⁺ Memory B Cells Are Rapid, Plastic, Early Responders upon Malaria Rechallenge.* Immunity, 2016. **45**(2): p. 402-414.
254. Cook, J., et al., *Using serological measures to monitor changes in malaria transmission in Vanuatu.* Malaria Journal, 2010. **9**(1): p. 169.
255. Dewasurendra, R.L., et al., *Effectiveness of a serological tool to predict malaria transmission intensity in an elimination setting.* BMC infectious diseases, 2017. **17**(1): p. 49-49.
256. Kattenberg, J.H., et al., *Characterization of Plasmodium falciparum and Plasmodium vivax recent exposure in an area of significantly decreased transmission intensity in Central Vietnam.* Malaria Journal, 2018. **17**(1): p. 180.
257. Surendra, H., et al., *Analysis of serological data to investigate heterogeneity of malaria transmission: a community-based cross-sectional study in an area conducting elimination in Indonesia.* Malaria Journal, 2019. **18**(1): p. 227.
258. Keffale, M., et al., *Serological evidence for a decline in malaria transmission following major scale-up of control efforts in a setting selected for Plasmodium vivax and Plasmodium falciparum malaria elimination in Babile district, Oromia, Ethiopia.* Transactions of The Royal Society of Tropical Medicine and Hygiene, 2019. **113**(6): p. 305-311.

259. Hodgson, S.H., et al., *Changes in serological immunology measures in UK and Kenyan adults post-controlled human malaria infection.* Frontiers in microbiology, 2016. **7**: p. 1604.
260. Perraut, R., et al., *Serological signatures of declining exposure following intensification of integrated malaria control in two rural Senegalese communities.* PLOS ONE, 2017. **12**(6): p. e0179146.
261. Pires, C.V., et al., *Blood-stage Plasmodium vivax antibody dynamics in a low transmission setting: A nine year follow-up study in the Amazon region.* PLOS ONE, 2018. **13**(11): p. e0207244.
262. Achan, J., et al., *Serologic Markers of Previous Malaria Exposure and Functional Antibodies Inhibiting Parasite Growth Are Associated With Parasite Kinetics Following a Plasmodium falciparum Controlled Human Infection.* Clinical Infectious Diseases, 2019.
263. White, L.J., et al., *The role of simple mathematical models in malaria elimination strategy design.* Malaria Journal, 2009. **8**(1): p. 212.
264. Fowkes, F.J., P. Boeuf, and J.G. Beeson, *Immunity to malaria in an era of declining malaria transmission.* Parasitology, 2016. **143**(2): p. 139-153.
265. Longley, R.J., et al., *Acquisition and longevity of antibodies to Plasmodium vivax preerythrocytic antigens in Western Thailand.* Clin. Vaccine Immunol., 2016. **23**(2): p. 117-124.
266. Doolan, D.L., C. Dobaño, and J.K. Baird, *Acquired immunity to malaria.* Clinical microbiology reviews, 2009. **22**(1): p. 13-36.
267. Marsh, K. and S. Kinyanjui, *Immune effector mechanisms in malaria.* Parasite Immunology, 2006. **28**(1-2): p. 51-60.
268. Commons, R.J., et al., *The effect of chloroquine dose and primaquine on Plasmodium vivax recurrence: a WorldWide Antimalarial Resistance Network systematic review and individual patient pooled meta-analysis.* The Lancet. Infectious diseases, 2018. **18**(9): p. 1025-1034.
269. Askling, H.H., et al., *Malaria risk in travelers.* Emerging infectious diseases, 2005. **11**(3): p. 436-441.
270. Baird, J.K., *Age-dependent characteristics of protection v. susceptibility to Plasmodium falciparum.* 1998.
271. Lawpoolsri, S., et al., *Epidemiological profiles of recurrent malaria episodes in an endemic area along the Thailand-Myanmar border: a prospective cohort study.* Malaria journal, 2019. **18**(1): p. 124-124.
272. Aguirre-Gamboa, R., et al., *Differential Effects of Environmental and Genetic Factors on T and B Cell Immune Traits.* Cell Reports, 2016. **17**(9): p. 2474-2487.
273. Torcia, M.G., et al., *Functional deficit of T regulatory cells in Fulani, an ethnic group with low susceptibility to Plasmodium falciparum malaria.* Proceedings of the National Academy of Sciences of the United States of America, 2008. **105**(2): p. 646-651.
274. Neil-Dunne, I., et al., *Gravidity-Dependent Production of Antibodies That Inhibit Binding of Plasmodium falciparum-Infected Erythrocytes to Placental Chondroitin Sulfate Proteoglycan during Pregnancy.* Infection and Immunity, 2001. **69**(12): p. 7487.
275. Mor, G. and I. Cardenas, *The immune system in pregnancy: a unique complexity.* American journal of reproductive immunology (New York, N.Y. : 1989), 2010. **63**(6): p. 425-433.

276. Wyss, K., et al., *Obesity and Diabetes as Risk Factors for Severe Plasmodium falciparum Malaria: Results From a Swedish Nationwide Study.* Clinical infectious diseases : an official publication of the Infectious Diseases Society of America, 2017. **65**(6): p. 949-958.
277. Djimde, M., et al., *Relationship between weight status and anti-malarial drug efficacy and safety in children in Mali.* Malaria Journal, 2019. **18**(1): p. 40.
278. Alexandre, M.A.A., et al., *The association between nutritional status and malaria in children from a rural community in the Amazonian region: a longitudinal study.* PLoS neglected tropical diseases, 2015. **9**(4): p. e0003743-e0003743.
279. Menendez, C., et al., *The impact of placental malaria on gestational age and birth weight.* The Journal of infectious diseases, 2000. **181**(5): p. 1740-1745.
280. Jacobson, R.M., et al., *Studies of twins in vaccinology.* Vaccine, 2007. **25**(16): p. 3160-3164.
281. De Craen, A., et al., *Heritability estimates of innate immunity: an extended twin study.* Genes and immunity, 2005. **6**(2): p. 167.
282. Evans, D.M., et al., *A major quantitative trait locus for CD4–CD8 ratio is located on chromosome 11.* Genes & Immunity, 2004. **5**(7): p. 548-552.
283. Gelder, C.M., et al., *Associations between human leukocyte antigens and nonresponsiveness to influenza vaccine.* The Journal of infectious diseases, 2002. **185**(1): p. 114-117.
284. Mentzer, A.J., et al., *Searching for the human genetic factors standing in the way of universally effective vaccines.* Philosophical Transactions of the Royal Society B: Biological Sciences, 2015. **370**(1671): p. 20140341.
285. Scepanovic, P., et al., *Human genetic variants and age are the strongest predictors of humoral immune responses to common pathogens and vaccines.* Genome medicine, 2018. **10**(1): p. 59-59.
286. O'Connor, D., et al., *Common Genetic Variations Associated with the Persistence of Immunity following Childhood Immunization.* Cell reports, 2019. **27**(11): p. 3241-3253. e4.
287. Timmann, C., et al., *Genome-wide association study indicates two novel resistance loci for severe malaria.* Nature, 2012. **489**(7416): p. 443.
288. Marchant, A., et al., *Predominant influence of environmental determinants on the persistence and avidity maturation of antibody responses to vaccines in infants.* The Journal of infectious diseases, 2006. **193**(11): p. 1598-1605.
289. Brodin, P., et al., *Variation in the human immune system is largely driven by non-heritable influences.* Cell, 2015. **160**(1-2): p. 37-47.
290. Ntumngia, F.B., et al., *The role of the human Duffy antigen receptor for chemokines in malaria susceptibility: current opinions and future treatment prospects.* Journal of receptor, ligand and channel research, 2016. **9**: p. 1-11.
291. Maestre, A., et al., *Acquired antibody responses against Plasmodium vivax infection vary with host genotype for duffy antigen receptor for chemokines (DARC).* PloS one, 2010. **5**(7): p. e11437-e11437.
292. Kano, F.S., et al., *Susceptibility to Plasmodium vivax malaria associated with DARC (Duffy antigen) polymorphisms is influenced by the time of exposure to malaria.* Scientific Reports, 2018. **8**(1): p. 13851.

293. Gai, P.P., et al., *Duffy antigen receptor for chemokines gene polymorphisms and malaria in Mangaluru, India.* Malaria Journal, 2019. **18**(1): p. 328.
294. Tongren, J.E., et al., *Target antigen, age, and duration of antigen exposure independently regulate immunoglobulin G subclass switching in malaria.* Infection and immunity, 2006. **74**(1): p. 257-264.
295. Mackinnon, M.J., et al., *Heritability of Malaria in Africa.* PLOS Medicine, 2005. **2**(12): p. e340.
296. Stresman, G.H., *Beyond temperature and precipitation: ecological risk factors that modify malaria transmission.* Acta Tropica, 2010. **116**(3): p. 167-172.
297. Rossati, A., et al., *Climate, environment and transmission of malaria.* Le infezioni in medicina: rivista periodica di eziologia, epidemiologia, diagnostica, clinica e terapia delle patologie infettive, 2016. **24**(2): p. 93-104.
298. Phillips, R., *Current status of malaria and potential for control.* Clinical microbiology reviews, 2001. **14**(1): p. 208-226.
299. Abiodun, G.J., et al., *Modelling the influence of temperature and rainfall on the population dynamics of Anopheles arabiensis.* Malaria Journal, 2016. **15**(1): p. 364.
300. Hunsperger, E.A., et al., *Evaluation of commercially available anti-dengue virus immunoglobulin M tests.* Emerging infectious diseases, 2009. **15**(3): p. 436-440.
301. Kohanteb, J. and S. Ardehali, *Cross-reaction of sera from patients with various infectious diseases with Leishmania infantum.* Medical Principles and Practice, 2005. **14**(2): p. 79-82.
302. Fairlie-Clarke, K.J., et al., *Antibody isotype analysis of malaria-nematode co-infection: problems and solutions associated with cross-reactivity.* BMC Immunology, 2010. **11**(1): p. 6.
303. Helmby, H., *Schistosomiasis and malaria: another piece of the crossreactivity puzzle.* Trends in Parasitology, 2007. **23**(3): p. 88-90.
304. Naus, C.W.A., et al., *Serological responses among individuals in areas where both schistosomiasis and malaria are endemic: cross-reactivity between Schistosoma mansoni and Plasmodium falciparum.* The Journal of infectious diseases, 2003. **187**(8): p. 1272-1282.
305. Woodberry, T., et al., *Antibodies to Plasmodium falciparum and Plasmodium vivax Merozoite Surface Protein 5 in Indonesia: Species-Specific and Cross-Reactive Responses.* The Journal of Infectious Diseases, 2008. **198**(1): p. 134-142.
306. Muh, F., et al., *Cross-species analysis of apical asparagine-rich protein of Plasmodium vivax and Plasmodium knowlesi.* Scientific reports, 2018. **8**(1): p. 5781.
307. Igonet, S., et al., *Cross-reactivity Studies of an Anti-Plasmodium vivax Apical Membrane Antigen 1 Monoclonal Antibody: Binding and Structural Characterisation.* Journal of Molecular Biology, 2007. **366**(5): p. 1523-1537.
308. Bansal, G.P., et al., *Antibodies elicited during natural infection in a predominantly Plasmodium falciparum transmission area cross-react with sexual stage-specific antigen in P. vivax.* Acta Tropica, 2017. **170**: p. 105-111.
309. Yadava, A., et al., *Cross-Species Immunity Following Immunization With a Circumsporozoite Protein–Based Vaccine for Malaria.* The Journal of Infectious Diseases, 2012. **205**(9): p. 1456-1463.

310. Gnidehou, S., et al., *Cross-Species Immune Recognition Between Plasmodium vivax Duffy Binding Protein Antibodies and the Plasmodium falciparum Surface Antigen VAR2CSA.* The Journal of infectious diseases, 2018. **219**(1): p. 110-120.
311. Lopez-Perez, M., et al., *IgG Responses to the Plasmodium falciparum Antigen VAR2CSA in Colombia Are Restricted to Pregnancy and Are Not Induced by Exposure to Plasmodium vivax.* Infection and immunity, 2018. **86**(8): p. e00136-18.
312. Belachew, E.B., *Immune response and evasion mechanisms of Plasmodium falciparum parasites.* Journal of immunology research, 2018. **2018**.
313. del Portillo, H.A., et al., *A superfamily of variant genes encoded in the subtelomeric region of Plasmodium vivax.* Nature, 2001. **410**(6830): p. 839.
314. Luo, Z., S.A. Sullivan, and J.M. Carlton, *The biology of Plasmodium vivax explored through genomics.* Annals of the New York Academy of Sciences, 2015. **1342**(1): p. 53.
315. Carlton, J.M., et al., *Comparative genomics of the neglected human malaria parasite Plasmodium vivax.* Nature, 2008. **455**(7214): p. 757.
316. Ferreira, M.U., M. da Silva Nunes, and G. Wunderlich, *Antigenic diversity and immune evasion by malaria parasites.* Clin. Diagn. Lab. Immunol., 2004. **11**(6): p. 987-995.
317. Bernabeu, M., et al., *Functional analysis of Plasmodium vivax VIR proteins reveals different subcellular localizations and cytoadherence to the ICAM-1 endothelial receptor.* Cellular microbiology, 2012. **14**(3): p. 386-400.
318. Requena, P., et al., *Plasmodium vivax VIR Proteins Are Targets of Naturally-Acquired Antibody and T Cell Immune Responses to Malaria in Pregnant Women.* PLOS Neglected Tropical Diseases, 2016. **10**(10): p. e0005009.
319. Liu, E.W., et al., *Protein-Specific Features Associated with Variability in Human Antibody Responses to Plasmodium falciparum Malaria Antigens.* The American journal of tropical medicine and hygiene, 2018. **98**(1): p. 57-66.
320. Guy, A.J., et al., *Proteome-wide mapping of immune features onto Plasmodium protein three-dimensional structures.* Scientific Reports, 2018. **8**(1): p. 4355.
321. Lucas, A. and G. McFadden, *Secreted Immunomodulatory Viral Proteins as Novel Biotherapeutics.* The Journal of Immunology, 2004. **173**(8): p. 4765.
322. Hewitson, J.P., J.R. Grainger, and R.M. Maizels, *Helminth immunoregulation: the role of parasite secreted proteins in modulating host immunity.* Molecular and biochemical parasitology, 2009. **167**(1): p. 1-11.
323. Osier, F.H.A., et al., *Allelic Diversity and Naturally Acquired Allele-Specific Antibody Responses to Plasmodium falciparum Apical Membrane Antigen 1 in Kenya.* Infection and Immunity, 2010. **78**(11): p. 4625.
324. Wright, G.J. and J.C. Rayner, *Plasmodium falciparum erythrocyte invasion: combining function with immune evasion.* PLoS pathogens, 2014. **10**(3): p. e1003943-e1003943.
325. Barry, A.E. and A. Arnott, *Strategies for designing and monitoring malaria vaccines targeting diverse antigens.* Frontiers in immunology, 2014. **5**: p. 359-359.
326. Stanisic, D.I., A.E. Barry, and M.F. Good, *Escaping the immune system: how the malaria parasite makes vaccine development a challenge.* Trends in parasitology, 2013. **29**(12): p. 612-622.

327. Guy, A.J., et al., *Insights into the Immunological Properties of Intrinsically Disordered Malaria Proteins Using Proteome Scale Predictions.* PLOS ONE, 2015. **10**(10): p. e0141729.
328. Lipsitch, M. and J.J. O'Hagan, *Patterns of antigenic diversity and the mechanisms that maintain them.* Journal of the Royal Society, Interface, 2007. **4**(16): p. 787-802.
329. Neafsey, D.E., et al., *The malaria parasite Plasmodium vivax exhibits greater genetic diversity than Plasmodium falciparum.* Nature genetics, 2012. **44**(9): p. 1046-1050.
330. Koepfli, C., et al., *Plasmodium vivax Diversity and Population Structure across Four Continents.* PLOS Neglected Tropical Diseases, 2015. **9**(6): p. e0003872.
331. Jennison, C., et al., *Plasmodium vivax Populations Are More Genetically Diverse and Less Structured than Sympatric Plasmodium falciparum Populations.* PLOS Neglected Tropical Diseases, 2015. **9**(4): p. e0003634.
332. Silva, J.C., et al., *A New Method for Estimating Species Age Supports the Coexistence of Malaria Parasites and Their Mammalian Hosts.* Molecular Biology and Evolution, 2015. **32**(5): p. 1354-1364.
333. Takala, S.L. and C.V. Plowe, *Genetic diversity and malaria vaccine design, testing and efficacy: preventing and overcoming 'vaccine resistant malaria'.* Parasite immunology, 2009. **31**(9): p. 560-573.
334. Longley, R.J., et al., *High Efficacy of Primaquine Treatment for Plasmodium vivax in Western Thailand.* The American journal of tropical medicine and hygiene, 2016. **95**(5): p. 1086-1089.
335. Wampfler, R., et al., *Strategies for Detection of Plasmodium species Gametocytes.* PLOS ONE, 2013. **8**(9): p. e76316.
336. Lifeblood, A.R.C., *Eligibility.*
337. HealthDirect, *Blood donation.* 2018, March.
338. Cross, T.T.R., *Blood donation.*
339. Tsuboi, T., et al., *Wheat Germ Cell-Free System-Based Production of Malaria Proteins for Discovery of Novel Vaccine Candidates.* Infection and Immunity, 2008. **76**(4): p. 1702.
340. França, C.T., et al., *An Antibody Screen of a Plasmodium vivax Antigen Library Identifies Novel Merozoite Proteins Associated with Clinical Protection.* PLOS Neglected Tropical Diseases, 2016. **10**(5): p. e0004639.
341. Krogh, A., et al., *Predicting transmembrane protein topology with a hidden Markov model: application to complete genomes.* Journal of molecular biology, 2001. **305**(3): p. 567-580.
342. Pierleoni, A., P.L. Martelli, and R. Casadio, *PredGPI: a GPI-anchor predictor.* BMC bioinformatics, 2008. **9**(1): p. 392.
343. Mitchell, A.L., et al., *InterPro in 2019: improving coverage, classification and access to protein sequence annotations.* Nucleic acids research, 2019. **47**(D1): p. D351-D360.
344. Bahl, A., et al., *PlasmoDB: the Plasmodium genome resource. A database integrating experimental and computational data.* Nucleic acids research, 2003. **31**(1): p. 212-215.
345. Wootton, J.C., *Non-globular domains in protein sequences: automated segmentation using complexity measures.* Computers & chemistry, 1994. **18**(3): p. 269-285.
346. Pearson, R.D., et al., *Genomic analysis of local variation and recent evolution in Plasmodium vivax.* Nature genetics, 2016. **48**(8): p. 959-964.

347. Auburn, S., et al., *A new Plasmodium vivax reference sequence with improved assembly of the subtelomeres reveals an abundance of pir genes.* Wellcome open research, 2016. **1**: p. 4-4.
348. Houser, B., *Bio-Rad's Bio-Plex® suspension array system, xMAP technology overview.* Archives of physiology and biochemistry, 2012. **118**(4): p. 192-196.
349. Reslova, N., et al., *xMAP technology: applications in detection of pathogens.* Frontiers in microbiology, 2017. **8**: p. 55.
350. Oliver, K.G., J.R. Kettman, and R.J. Fulton, *Multiplexed analysis of human cytokines by use of the FlowMetrix system.* Clinical chemistry, 1998. **44**(9): p. 2057-2060.
351. Carson, R.T. and D.A. Vignali, *Simultaneous quantitation of 15 cytokines using a multiplexed flow cytometric assay.* Journal of immunological methods, 1999. **227**(1-2): p. 41-52.
352. de Mast, Q., et al., *Increased serum hepcidin and alterations in blood iron parameters associated with asymptomatic P. falciparum and P. vivax malaria.* haematologica, 2010. **95**(7): p. 1068-1074.
353. Rodrigues-da-Silva, R.N., et al., *Alterations in cytokines and haematological parameters during the acute and convalescent phases of Plasmodium falciparum and Plasmodium vivax infections.* Memorias do Instituto Oswaldo Cruz, 2014. **109**(2): p. 154-162.
354. Tomaz, F.M.M.B., et al., *Humoral immune responses against the malaria vaccine candidate antigen Plasmodium vivax AMA-1 and IL-4 gene polymorphisms in individuals living in an endemic area of the Brazilian Amazon.* Cytokine, 2015. **74**(2): p. 273-278.
355. Ambrosino, E., et al., *A multiplex assay for the simultaneous detection of antibodies against 15 Plasmodium falciparum and Anopheles gambiae saliva antigens.* Malaria journal, 2010. **9**(1): p. 317.
356. Turner, L., et al., *Antibodies against PfEMP1, RIFIN, MSP3 and GLURP are acquired during controlled Plasmodium falciparum malaria infections in naïve volunteers.* PLoS One, 2011. **6**(12): p. e29025.
357. Wu, L., et al., *Optimisation and standardisation of a multiplex immunoassay of diverse Plasmodium falciparum antigens to assess changes in malaria transmission using sero-epidemiology.* Wellcome Open Research, 2019. **4**.
358. Fernandez-Becerra, C., et al., *Naturally-acquired humoral immune responses against the N- and C-termini of the Plasmodium vivax MSP1 protein in endemic regions of Brazil and Papua New Guinea using a multiplex assay.* Malaria journal, 2010. **9**(1): p. 29.
359. Kerkhof, K., et al., *Implementation and application of a multiplex assay to detect malaria-specific antibodies: a promising tool for assessing malaria transmission in Southeast Asian pre-elimination areas.* Malaria journal, 2015. **14**(1): p. 338.
360. Powell, R.L., et al., *A multiplex microsphere-based immunoassay increases the sensitivity of SIV-specific antibody detection in serum samples and mucosal specimens collected from Rhesus Macaques infected with SIVmac239.* BioResearch open access, 2013. **2**(3): p. 171-178.
361. Varela, M.L., et al., *Optimization of a magnetic bead-based assay (MAGPIX®-Luminex) for immune surveillance of exposure to malaria using multiple Plasmodium antigens and sera from different endemic settings.* Malaria journal, 2018. **17**(1): p. 324.

362. Lammie, P.J., et al., *Development of a new platform for neglected tropical disease surveillance.* International journal for parasitology, 2012. **42**(9): p. 797-800.
363. De Jager, W., et al., *Simultaneous detection of 15 human cytokines in a single sample of stimulated peripheral blood mononuclear cells.* Clin. Diagn. Lab. Immunol., 2003. **10**(1): p. 133-139.
364. Staples, E., et al., *Optimising the quantification of cytokines present at low concentrations in small human mucosal tissue samples using Luminex assays.* Journal of immunological methods, 2013. **394**(1-2): p. 1-9.
365. Opalka, D., et al., *Simultaneous quantitation of antibodies to neutralizing epitopes on virus-like particles for human papillomavirus types 6, 11, 16, and 18 by a multiplexed luminex assay.* Clin. Diagn. Lab. Immunol., 2003. **10**(1): p. 108-115.
366. Wong, J., et al., *Rapid detection of antibodies in sera using multiplexed self-assembling bead arrays.* Journal of immunological methods, 2009. **350**(1-2): p. 171-182.
367. Dias, D., et al., *Optimization and Validation of a Multiplexed Luminex Assay To Quantify Antibodies to Neutralizing Epitopes on Human Papillomaviruses 6, 11, 16, and 18.* Clinical and Diagnostic Laboratory Immunology, 2005. **12**(8): p. 959.
368. Sivashanmugam, A., et al., *Practical protocols for production of very high yields of recombinant proteins using Escherichia coli.* Protein science : a publication of the Protein Society, 2009. **18**(5): p. 936-948.
369. Schlieker, C., B. Bukau, and A. Mogk, *Prevention and reversion of protein aggregation by molecular chaperones in the E. coli cytosol: implications for their applicability in biotechnology.* Journal of Biotechnology, 2002. **96**(1): p. 13-21.
370. Fahrner, R.L., H.V. Iyer, and G.S. Blank, *The optimal flow rate and column length for maximum production rate of protein A affinity chromatography.* Bioprocess Engineering, 1999. **21**(4): p. 287-292.
371. Harper, S. and D.W. Speicher, *Purification of proteins fused to glutathione S-transferase.* Methods in molecular biology (Clifton, N.J.), 2011. **681**: p. 259-280.
372. Harbers, M., *Wheat germ systems for cell-free protein expression.* FEBS Letters, 2014. **588**(17): p. 2762-2773.
373. Morita, E.H., et al., *A wheat germ cell-free system is a novel way to screen protein folding and function.* Protein science, 2003. **12**(6): p. 1216-1221.
374. Rui, E., et al., *Plasmodium vivax: comparison of immunogenicity among proteins expressed in the cell-free systems of Escherichia coli and wheat germ by suspension array assays.* Malaria journal, 2011. **10**(1): p. 192.
375. Pinkevych, M., et al., *The dynamics of naturally acquired immunity to Plasmodium falciparum infection.* PLoS computational biology, 2012. **8**(10).
376. Day, K.P. and K. Marsh, *Naturally acquired immunity to Plasmodium falciparum.* Parasitology today, 1991. **7**(3): p. 68-71.
377. Cooper, E.L. and M.J. Ma, *Understanding nutrition and immunity in disease management.* Journal of traditional and complementary medicine, 2017. **7**(4): p. 386-391.

378. Bittencourt, N.C., et al., *Genetic sequence characterization and naturally acquired immune response to Plasmodium vivax Rhoptry Neck Protein 2 (PvRON2).* Malaria journal, 2018. **17**(1): p. 401.
379. Longley, R.J., J. Sattabongkot, and I. Mueller, *Insights into the naturally acquired immune response to Plasmodium vivax malaria.* Parasitology, 2016. **143**(2): p. 154-170.
380. Torres, K.J., et al., *Antibody response dynamics to the Plasmodium falciparum conserved vaccine candidate antigen, merozoite surface protein-1 C-terminal 19kD (MSP1-19kD), in Peruvians exposed to hypoendemic malaria transmission.* Malaria journal, 2008. **7**(1): p. 173.
381. Almeida, A.P.M.M., et al., *Long-lasting humoral and cellular immune responses elicited by immunization with recombinant chimeras of the Plasmodium vivax circumsporozoite protein.* Vaccine, 2014. **32**(19): p. 2181-2187.
382. Morais, C.G., et al., *Antibodies to Plasmodium vivax apical membrane antigen 1: persistence and correlation with malaria transmission intensity.* The American journal of tropical medicine and hygiene, 2006. **75**(4): p. 582-587.
383. Vatakis, D. and M. McMillan, *The signal peptide sequence impacts the immune response elicited by a DNA epitope vaccine.* Clin. Vaccine Immunol., 2011. **18**(10): p. 1776-1780.
384. Kovjazin, R. and L. Carmon, *The use of signal peptide domains as vaccine candidates.* Human vaccines & immunotherapeutics, 2014. **10**(9): p. 2733-2740.
385. Haase, S. and T.F. de Koning-Ward, *New insights into protein export in malaria parasites.* Cellular microbiology, 2010. **12**(5): p. 580-587.
386. Hiller, N.L., et al., *A host-targeting signal in virulence proteins reveals a secretome in malarial infection.* Science, 2004. **306**(5703): p. 1934-1937.
387. Naik, R.S., et al., *Glycosylphosphatidylinositol anchors of Plasmodium falciparum: molecular characterization and naturally elicited antibody response that may provide immunity to malaria pathogenesis.* The Journal of experimental medicine, 2000. **192**(11): p. 1563-1576.
388. Cheng, Y., et al., *Immunological characterization of Plasmodium vivax Pv32, a novel predicted GPI-anchored merozoite surface protein.* Malaria journal, 2018. **17**(1): p. 273.
389. Shi, Q., et al., *Enhanced protection against malaria by a chimeric merozoite surface protein vaccine.* Infection and immunity, 2007. **75**(3): p. 1349-1358.
390. Balam, S., et al., *Plasmodium falciparum merozoite surface protein 2: epitope mapping and fine specificity of human antibody response against non-polymorphic domains.* Malaria journal, 2014. **13**(1): p. 510.
391. De Silva, H.D., et al., *The antibody response to Plasmodium falciparum Merozoite Surface Protein 4: comparative assessment of specificity and growth inhibitory antibody activity to infection-acquired and immunization-induced epitopes.* Malaria journal, 2011. **10**(1): p. 266.
392. Chaudhry, S., et al., *Comparative analysis of low complexity regions in Plasmodia.* Scientific reports, 2018. **8**(1): p. 1-9.
393. Toll-Riera, M., et al., *Role of low-complexity sequences in the formation of novel protein coding sequences.* Molecular biology and evolution, 2012. **29**(3): p. 883-886.
394. Mendes, T., et al., *Repeat-enriched proteins are related to host cell invasion and immune evasion in parasitic protozoa.* Molecular biology and evolution, 2013. **30**(4): p. 951-963.

395. Ehrenstein, M.R. and C.A. Notley, *The importance of natural IgM: scavenger, protector and regulator.* Nature Reviews Immunology, 2010. **10**(11): p. 778-786.
396. Irion, A., H.-P. Beck, and T. Smith, *Assessment of positivity in immuno-assays with variability in background measurements: a new approach applied to the antibody response to Plasmodium falciparum MSP2.* Journal of immunological methods, 2002. **259**(1-2): p. 111-118.
397. Murungi, L.M., et al., *A threshold concentration of anti-merozoite antibodies is required for protection from clinical episodes of malaria.* Vaccine, 2013. **31**(37): p. 3936-3942.
398. Fodjo, B.A., et al., *Antibody responses to the full-length VAR2CSA and its DBL domains in Cameroonian children and teenagers.* Malaria journal, 2016. **15**(1): p. 532.
399. Priest, J.W., et al., *Specificity of the IgG antibody response to Plasmodium falciparum, Plasmodium vivax, Plasmodium malariae, and Plasmodium ovale MSP119 subunit proteins in multiplexed serologic assays.* Malaria Journal, 2018. **17**(1): p. 417.
400. Muthui, M.K., et al., *Immune Responses to Gametocyte Antigens in a Malaria Endemic Population-The African falciparum Context: A Systematic Review and Meta-Analysis.* Frontiers in immunology, 2019. **10**: p. 2480-2480.
401. Siddiqui, A.A., et al., *Expression, purification, and characterization of the immunological response to a 40-kilodalton Plasmodium vivax tryptophan-rich antigen.* Infection and immunity, 2008. **76**(6): p. 2576-2586.
402. Zeeshan, M., H. Bora, and Y.D. Sharma, *Presence of memory T cells and naturally acquired antibodies in Plasmodium vivax malaria-exposed individuals against a group of tryptophan-rich antigens with conserved sequences.* The Journal of infectious diseases, 2013. **207**(1): p. 175-185.
403. Wang, B., et al., *Immunoprofiling of the tryptophan-rich antigen family in Plasmodium vivax.* Infection and immunity, 2015. **83**(8): p. 3083-3095.
404. Ling, I., S. Ogun, and A. Holder, *The combined epidermal growth factor-like modules of Plasmodium yoelii Merozoite Surface Protein-1 are required for a protective immune response to the parasite.* Parasite immunology, 1995. **17**(8): p. 425-433.
405. Mirahmadi, H., et al., *High-Level Expression of Immunogenic Recombinant Plasmodium vivax Merozoite Surface Protein (Pvmsp-142 kDa) in pGEX 6P1 Vector.* Iranian journal of public health, 2015. **44**(1): p. 89.
406. Galinski, M.R., et al., *A reticulocyte-binding protein complex of Plasmodium vivax merozoites.* Cell, 1992. **69**(7): p. 1213-1226.
407. Rodriguez, L.E., et al., *Intimate molecular interactions of P. falciparum merozoite proteins involved in invasion of red blood cells and their implications for vaccine design.* Chemical reviews, 2008. **108**(9): p. 3656-3705.
408. Restrepo-Montoya, D., et al., *Identification of Plasmodium vivax proteins with potential role in invasion using sequence redundancy reduction and profile hidden Markov models.* PLoS One, 2011. **6**(10).
409. López, C., et al., *The in vitro antigenicity of Plasmodium vivax Rhoptry Neck Protein 2 (PvRON2) B-and T-Epitopes selected by HLA-DRB1 binding profile.* Frontiers in cellular and infection microbiology, 2018. **8**: p. 156.

410. Hietanen, J., et al., *Gene models, expression repertoire, and immune response of Plasmodium vivax reticulocyte binding proteins.* Infection and immunity, 2016. **84**(3): p. 677-685.
411. Changrob, S., et al., *Immunogenicity of glycosylphosphatidylinositol-anchored micronemal antigen in natural Plasmodium vivax exposure.* Malaria journal, 2017. **16**(1): p. 348.
412. Morais, C.G., et al., *IgG isotype to C-terminal 19 kDa of Plasmodium vivax merozoite surface protein 1 among subjects with different levels of exposure to malaria in Brazil.* Parasitology research, 2005. **95**(6): p. 420-426.
413. Saavedra-Langer, R., et al., *IgG subclass responses to excreted-secreted antigens of Plasmodium falciparum in a low-transmission malaria area of the Peruvian Amazon.* Malaria journal, 2018. **17**(1): p. 328.
414. Ferreira, M.U., et al., *The IgG-subclass distribution of naturally acquired antibodies to Plasmodium falciparum, in relation to malaria exposure and severity.* Annals of Tropical Medicine & Parasitology, 1998. **92**(3): p. 245-256.
415. Stanisic, D.I., et al., *Immunoglobulin G subclass-specific responses against Plasmodium falciparum merozoite antigens are associated with control of parasitemia and protection from symptomatic illness.* Infection and immunity, 2009. **77**(3): p. 1165-1174.
416. Ho, F., et al., *Distinct short-lived and long-lived antibody-producing cell populations.* European journal of immunology, 1986. **16**(10): p. 1297-1301.
417. Park, J.-W., et al., *Naturally acquired antibody responses to the C-terminal region of merozoite surface protein 1 of Plasmodium vivax in Korea.* Clin. Diagn. Lab. Immunol., 2001. **8**(1): p. 14-20.
418. Skountzou, I., et al., *Influenza virus-specific neutralizing IgM antibodies persist for a lifetime.* Clin. Vaccine Immunol., 2014. **21**(11): p. 1481-1489.
419. Bohannon, C., et al., *Long-lived antigen-induced IgM plasma cells demonstrate somatic mutations and contribute to long-term protection.* Nature communications, 2016. **7**(1): p. 1-13.
420. Zenklusen, I., et al., *Immunization of malaria-preexposed volunteers with PfSPZ vaccine elicits long-lived IgM invasion-inhibitory and complement-fixing antibodies.* The Journal of infectious diseases, 2018. **217**(10): p. 1569-1578.
421. MacNeil, A., Z. Reed, and P.E. Rollin, *Serologic cross-reactivity of human IgM and IgG antibodies to five species of Ebola virus.* PLoS neglected tropical diseases, 2011. **5**(6).
422. Papa, A., D. Karabaxoglou, and A. Kansouzidou, *Acute West Nile virus neuroinvasive infections: Cross-reactivity with dengue virus and tick-borne encephalitis virus.* Journal of medical Virology, 2011. **83**(10): p. 1861-1865.
423. Baum, E., et al., *Submicroscopic and asymptomatic Plasmodium falciparum and Plasmodium vivax infections are common in western Thailand-molecular and serological evidence.* Malaria journal, 2015. **14**(1): p. 95.
424. Longley, R.J., et al., *Asymptomatic Plasmodium vivax infections induce robust IgG responses to multiple blood-stage proteins in a low-transmission region of western Thailand.* Malaria journal, 2017. **16**(1): p. 178.

425. McLean, A.R., et al., *Antibody responses to Plasmodium falciparum and Plasmodium vivax blood-stage and sporozoite antigens in the postpartum period.* Scientific reports, 2016. **6**(1): p. 1-10.
426. Czerkinsky, C.C., et al., *A solid-phase enzyme-linked immunospot (ELISPOT) assay for enumeration of specific antibody-secreting cells.* Journal of Immunological Methods, 1983. **65**(1): p. 109-121.
427. Lima-Junior, J.d.C., F.N. Morgado, and F. Conceição-Silva, *How Can Elispot Add Information to Improve Knowledge on Tropical Diseases?* Cells, 2017. **6**(4): p. 31.
428. Kalyuzhny, A.E., *Chemistry and Biology of the ELISPOT Assay*, in *Handbook of ELISPOT: Methods and Protocols*, A.E. Kalyuzhny, Editor. 2005, Humana Press: Totowa, NJ. p. 15-31.
429. Crotty, S., et al., *Tracking human antigen-specific memory B cells: a sensitive and generalized ELISPOT system.* Journal of Immunological Methods, 2004. **286**(1): p. 111-122.
430. Cossarizza, A., et al., *Guidelines for the use of flow cytometry and cell sorting in immunological studies.* European Journal of Immunology, 2017. **47**(10): p. 1584-1797.
431. Lehmann, P.V. and W. Zhang, *Unique strengths of ELISPOT for T cell diagnostics*, in *Handbook of ELISPOT*. 2012, Springer. p. 3-23.
432. Gajewski, T.F., *Monitoring specific T-cell responses to melanoma vaccines: ELISPOT, tetramers, and beyond.* Clinical and diagnostic laboratory immunology, 2000. **7**(2): p. 141-144.
433. Clay, T.M., et al., *Assays for Monitoring Cellular Immune Responses to Active Immunotherapy of Cancer.* Clinical Cancer Research, 2001. **7**(5): p. 1127.
434. Karlsson, A., et al., *Comparison of the ELISPOT and cytokine flow cytometry assays for the enumeration of antigen-specific T cells.* Journal of immunological methods, 2004. **283**: p. 141-53.
435. McCutcheon, M., et al., *A sensitive ELISPOT assay to detect low-frequency human T lymphocytes.* Journal of Immunological Methods, 1997. **210**(2): p. 149-166.
436. Power, C.A., et al., *A valid ELISPOT assay for enumeration of ex vivo, antigen-specific, IFNγ-producing T cells.* Journal of Immunological Methods, 1999. **227**(1): p. 99-107.
437. Calarota, S.A. and F. Baldanti, *Enumeration and characterization of human memory T cells by enzyme-linked immunospot assays.* Clinical & developmental immunology, 2013. **2013**: p. 637649-637649.
438. Janetzki, S., et al., *Evaluation of Elispot assays: influence of method and operator on variability of results.* Journal of Immunological Methods, 2004. **291**(1): p. 175-183.
439. Ranieri, E., I. Popescu, and M. Gigante, *CTL elispot assay*, in *Cytotoxic T-Cells*. 2014, Springer. p. 75-86.
440. Weiss, G.E., et al., *The Plasmodium falciparum-specific human memory B cell compartment expands gradually with repeated malaria infections.* PLoS pathogens, 2010. **6**(5): p. e1000912.
441. Clark, E.H., et al., *Plasmodium falciparum malaria in the Peruvian Amazon, a region of low transmission, is associated with immunologic memory.* Infection and immunity, 2012. **80**(4): p. 1583-1592.

442. Ayieko, C., et al., *Changes in B cell populations and merozoite surface protein-1-specific memory B cell responses after prolonged absence of detectable P. falciparum infection.* PLoS One, 2013. **8**(6): p. e67230.
443. Ndungu, F.M., et al., *Long-lived P lasmodium falciparum specific memory B cells in naturally exposed S wedish travelers.* European journal of immunology, 2013. **43**(11): p. 2919-2929.
444. Bekeredjian-Ding, I., et al., *Staphylococcus aureus Protein A Triggers T Cell-Independent B Cell Proliferation by Sensitizing B Cells for TLR2 Ligands.* The Journal of Immunology, 2007. **178**(5): p. 2803.
445. Keener, A.B., et al., *Staphylococcus aureus Protein A Disrupts Immunity Mediated by Long-Lived Plasma Cells.* Journal of immunology (Baltimore, Md. : 1950), 2017. **198**(3): p. 1263-1273.
446. Bekeredjian-Ding, I., et al., *Poke Weed Mitogen Requires Toll-Like Receptor Ligands for Proliferative Activity in Human and Murine B Lymphocytes.* PLOS ONE, 2012. **7**(1): p. e29806.
447. Krieg, A.M., et al., *CpG motifs in bacterial DNA trigger direct B-cell activation.* Nature, 1995. **374**(6522): p. 546.
448. Hartmann, G., *CpG: unraveling the key to B-cell function.* Blood, 2003. **101**(11): p. 4230.
449. Henn, A.D., et al., *Modulation of single-cell IgG secretion frequency and rates in human memory B cells by CpG DNA, CD40L, IL-21, and cell division.* The Journal of Immunology, 2009. **183**(5): p. 3177-3187.
450. Richard, K., S.K. Pierce, and W. Song, *The agonists of TLR4 and 9 are sufficient to activate memory B cells to differentiate into plasma cells in vitro but not in vivo.* Journal of immunology (Baltimore, Md. : 1950), 2008. **181**(3): p. 1746-1752.
451. Itoh, K. and S. Hirohata, *The role of IL-10 in human B cell activation, proliferation, and differentiation.* The Journal of Immunology, 1995. **154**(9): p. 4341-4350.
452. Akdis, C.A. and K. Blaser, *Mechanisms of interleukin-10-mediated immune suppression.* Immunology, 2001. **103**(2): p. 131-136.
453. Jahnmatz, M., et al., *Optimization of a human IgG B-cell ELISpot assay for the analysis of vaccine-induced B-cell responses.* Journal of immunological methods, 2013. **391**(1-2): p. 50-59.
454. Weiss, G.E., et al., *High efficiency human memory B cell assay and its application to studying Plasmodium falciparum-specific memory B cells in natural infections.* Journal of immunological methods, 2012. **375**(1-2): p. 68-74.
455. Ampomah, P., et al., *Kinetics of B cell responses to Plasmodium falciparum erythrocyte membrane protein 1 in Ghanaian women naturally exposed to malaria parasites.* The Journal of Immunology, 2014. **192**(11): p. 5236-5244.
456. Elias, S.C., et al., *Analysis of human B-cell responses following C h A d63-MVA MSP 1 and AMA 1 immunization and controlled malaria infection.* Immunology, 2014. **141**(4): p. 628-644.
457. Crompton, P.D., et al., *The TLR9 ligand CpG promotes the acquisition of Plasmodium falciparum-specific memory B cells in malaria-naive individuals.* The Journal of Immunology, 2009. **182**(5): p. 3318-3326.

458. Lyke, K.E., et al., *Antigen-specific B memory cell responses to Plasmodium falciparum malaria antigens and Schistosoma haematobium antigens in co-infected Malian children.* PloS one, 2012. **7**(6): p. e37868.
459. Nogaro, S.I., et al., *The breadth, but not the magnitude, of circulating memory B cell responses to P. falciparum increases with age/exposure in an area of low transmission.* PloS one, 2011. **6**(10): p. e25582.
460. Marcellini, V., et al., *Protection against pertussis in humans correlates to elevated serum antibodies and memory B cells.* Frontiers in immunology, 2017. **8**: p. 1158.
461. Weinberger, B., et al., *Recall responses to tetanus and diphtheria vaccination are frequently insufficient in elderly persons.* PloS one, 2013. **8**(12): p. e82967.
462. Jahnmatz, M., et al., *Pertussis-specific memory B-cell and humoral IgG responses in adolescents after a fifth consecutive dose of acellular pertussis vaccine.* Clin. Vaccine Immunol., 2014. **21**(9): p. 1301-1308.
463. Draper, S.J., et al., *Malaria Vaccines: Recent Advances and New Horizons.* Cell host & microbe, 2018. **24**(1): p. 43-56.
464. Franks, S., et al., *Genetic Diversity and Antigenic Polymorphism in Plasmodium falciparum: Extensive Serological Cross-Reactivity between Allelic Variants of Merozoite Surface Protein 2.* Infection and Immunity, 2003. **71**(6): p. 3485.
465. Ouattara, A., et al., *Designing malaria vaccines to circumvent antigen variability.* Vaccine, 2015. **33**(52): p. 7506-7512.
466. Casillas, S. and A. Barbadilla, *Molecular Population Genetics.* Genetics, 2017. **205**(3): p. 1003-1035.
467. Greenhouse, B. and D.L. Smith, *Malaria genotyping for epidemiologic surveillance.* Proceedings of the National Academy of Sciences, 2015. **112**(22): p. 6782.
468. Hedrick, P.W., *Population genetics of malaria resistance in humans.* Heredity, 2011. **107**(4): p. 283-304.
469. Arnott, A., A.E. Barry, and J.C. Reeder, *Understanding the population genetics of Plasmodium vivax is essential for malaria control and elimination.* Malaria Journal, 2012. **11**(1): p. 14.
470. Tajima, F., *Statistical method for testing the neutral mutation hypothesis by DNA polymorphism.* Genetics, 1989. **123**(3): p. 585.
471. Barry, A.E., et al., *Contrasting population structures of the genes encoding ten leading vaccine-candidate antigens of the human malaria parasite, Plasmodium falciparum.* PloS one, 2009. **4**(12): p. e8497-e8497.
472. Hupalo, D.N., et al., *Population genomics studies identify signatures of global dispersal and drug resistance in Plasmodium vivax.* Nature genetics, 2016. **48**(8): p. 953-958.
473. Stavnezer, J., J.E.J. Guikema, and C.E. Schrader, *Mechanism and regulation of class switch recombination.* Annual review of immunology, 2008. **26**: p. 261-292.
474. Ferreira, M.U., et al., *Population structure and transmission dynamics of Plasmodium vivax in rural Amazonia.* The Journal of infectious diseases, 2007. **195**(8): p. 1218-1226.

475. Gray, K.-A., et al., *Population genetics of Plasmodium falciparum and Plasmodium vivax and asymptomatic malaria in Temotu Province, Solomon Islands.* Malaria Journal, 2013. **12**(1): p. 429.
476. Brito, C.F.A.d. and M.U. Ferreira, *Molecular markers and genetic diversity of Plasmodium vivax.* Memórias do Instituto Oswaldo Cruz, 2011. **106**: p. 12-26.
477. Arnott, A., et al., *Distinct patterns of diversity, population structure and evolution in the AMA1 genes of sympatric Plasmodium falciparum and Plasmodium vivax populations of Papua New Guinea from an area of similarly high transmission.* Malaria journal, 2014. **13**: p. 233-233.
478. Bahk, Y.Y., et al., *Genetic Diversity of Plasmodium vivax Causing Epidemic Malaria in the Republic of Korea.* The Korean journal of parasitology, 2018. **56**(6): p. 545-552.
479. Roesch, C., et al., *Genetic diversity in two Plasmodium vivax protein ligands for reticulocyte invasion.* PLOS Neglected Tropical Diseases, 2018. **12**(10): p. e0006555.
480. Kaur, H., et al., *Exploration of genetic diversity of Plasmodium vivax circumsporozoite protein (Pvcsp) and Plasmodium vivax sexual stage antigen (Pvs25) among North Indian isolates.* Malaria Journal, 2019. **18**(1): p. 308.
481. Arnott, A., et al., *High genetic diversity of Plasmodium vivax on the north coast of Papua New Guinea.* The American journal of tropical medicine and hygiene, 2013. **89**(1): p. 188-194.
482. Beeson, J.G., et al., *Merozoite surface proteins in red blood cell invasion, immunity and vaccines against malaria.* FEMS microbiology reviews, 2016. **40**(3): p. 343-372.
483. Zhu, X., et al., *Tryptophan-rich domains of Plasmodium falciparum SURFIN(4.2) and Plasmodium vivax PvSTP2 interact with membrane skeleton of red blood cell.* Malaria journal, 2017. **16**(1): p. 121-121.
484. Kosaisavee, V., et al., *Genetic Diversity in New Members of the Reticulocyte Binding Protein Family in Thai Plasmodium vivax Isolates.* PLOS ONE, 2012. **7**(3): p. e32105.
485. Camargo-Ayala, P.A., et al., *On the Evolution and Function of Plasmodium vivax Reticulocyte Binding Surface Antigen (pvrbsa).* Frontiers in genetics, 2018. **9**: p. 372-372.
486. Bronson, P.G., et al., *A sequence-based approach demonstrates that balancing selection in classical human leukocyte antigen (HLA) loci is asymmetric.* Human molecular genetics, 2012. **22**(2): p. 252-261.
487. Brandt, D.Y.C., et al., *The Effect of Balancing Selection on Population Differentiation: A Study with HLA Genes.* G3 (Bethesda, Md.), 2018. **8**(8): p. 2805-2815.
488. Mueller, I., et al., *Natural acquisition of immunity to Plasmodium vivax: epidemiological observations and potential targets*, in *Advances in parasitology*. 2013, Elsevier. p. 77-131.
489. Cheng, Q., J. Cunningham, and M.L. Gatton, *Systematic review of sub-microscopic P. vivax infections: prevalence and determining factors.* PLoS neglected tropical diseases, 2015. **9**(1): p. e3413-e3413.
490. Jiram, A.I., et al., *Evidence of asymptomatic submicroscopic malaria in low transmission areas in Belaga district, Kapit division, Sarawak, Malaysia.* Malaria Journal, 2019. **18**(1): p. 156.
491. Assembly, G.W., *Sustainable Development Goals (SDGs).* Transforming our world : the 2030 Agenda for Sustainable Development, 2015. **2030**.

492. Kerkhof, K., et al., *Geographical patterns of malaria transmission based on serological markers for falciparum and vivax malaria in Ratanakiri, Cambodia.* Malaria journal, 2016. **15**(1): p. 510.
493. Barry, A.E., et al., *The stability and complexity of antibody responses to the major surface antigen of Plasmodium falciparum are associated with age in a malaria endemic area.* Molecular & cellular proteomics : MCP, 2011. **10**(11): p. M111.008326-M111.008326.
494. Early, A.M., et al., *Host-mediated selection impacts the diversity of Plasmodium falciparum antigens within infections.* Nature Communications, 2018. **9**(1): p. 1381.
495. Kassa, D., et al., *Characterization of peripheral blood lymphocyte subsets in patients with acute Plasmodium falciparum and P. vivax malaria infections at Wonji Sugar Estate, Ethiopia.* Clin. Vaccine Immunol., 2006. **13**(3): p. 376-379.
496. Figueiredo, M.M., et al., *T follicular helper cells regulate the activation of B lymphocytes and antibody production during Plasmodium vivax infection.* PLoS pathogens, 2017. **13**(7): p. e1006484.
497. Taylor, J.J., K.A. Pape, and M.K. Jenkins, *A germinal center–independent pathway generates unswitched memory B cells early in the primary response.* The Journal of Experimental Medicine, 2012. **209**(3): p. 597.
498. Ryg-Cornejo, V., et al., *Severe Malaria Infections Impair Germinal Center Responses by Inhibiting T Follicular Helper Cell Differentiation.* Cell Reports, 2016. **14**(1): p. 68-81.
499. Guy, A.J., et al., *Structural patterns of selection and diversity for Plasmodium vivax antigens DBP and AMA1.* Malaria Journal, 2018. **17**(1): p. 183.
500. Zhang, Y., *I-TASSER: Fully automated protein structure prediction in CASP8.* Proteins: Structure, Function, and Bioinformatics, 2009. **77**(S9): p. 100-113.